Inaugural-Dissertation zur Erlangung der Doktorwürde
(Dr. rer. biol. vet.)
der Tierärztlichen Fakultät der Ludwig-Maximilians-Universität München

Analysis and comparison of dynamic mRNA expression changes in the equine and porcine endometrium during the estrous cycle

von: Simone Mariella Gebhardt

aus München

München 2017

Aus dem Veterinärwissenschaftlichen Department der Tierärztlichen Fakultät
der Ludwig-Maximilians-Universität München

Lehrstuhl für Molekulare Tierzucht und Biotechnologie

Arbeit angefertigt unter der Leitung von: Univ.-Prof. Dr. Eckhard Wolf

Mitbetreuung durch: Priv.-Doz. Dr. Stefan Bauersachs

Gedruckt mit Genehmigung der Tierärztlichen Fakultät
der Ludwig-Maximilians-Universität München

Dekan:	Univ.-Prof. Dr. Reinhard K. Straubinger, PhD
Berichterstatter:	Univ.-Prof. Dr. Eckhard Wolf
Korreferent/en:	Univ.-Prof. Dr. Rolf Mansfeld

Tag der Promotion: 29.07.2017

CONTENTS

In the course of this study following results have been published:

Biol Reprod. 2012 Oct 17. 'Exploration of Global Gene Expression Changes During the Estrous Cycle in Equine Endometrium.' Gebhardt S, Merkl M, Herbach N, Wanke R, Handler J, Bauersachs S. PMID: 2307716

ABBREVIATIONS

A	
AA	Arachidonic acid
ABCA1	ATP-binding cassette, sub-family A
ACTB	Actin, beta
ADB	Annotation data base
ANOVA	Analysis of variance
ANXA3,7	Annexin A3, and Annexin A7
Approx.	Approximately
Aqua dest.	Distilled water
B	
BAALC	Brain and acute leukemia, cytoplasmic
BfB	Bundesmonopolverwaltung für Branntwein
BLAT	BLAST-like alignment tool
BLAST	Basic local alignment search tool
BOE	Bovine oviduct and endometrium
Bp	Base pair
BSA	Bovine serum albumin
Bta	*Bos taurus*
BV	Blood vessel
C	
C	Cytosine
cAMP	Cyclic adenosinmonophosphat
CCNE1	Cyclin E1
CDH16	Cadherin 16
CDK4	Cyclin-dependent kinase 4
cDNA	Complementary DNA
CL	Corpus luteum
COL1A1	Collagen, type 1, alpha 1
COX	Cyclooxygenase
cRNA	Complementary RNA
C_T	Cycle threshold
CTP	Cytidine triphosphate
CXCR4	Chemokine (C-X-C motif) receptor 4
Cy3	Cyanine 3
D	
D	Days
DAVID	Database for annotation, visualization and integrated discovery
DEG	Differentially expressed gene
DNA	Deoxyribonucleic acid

dNTP	Deoxynucleic triphosphate
DTT	Dithiothreitol
E	
E2	Estradiol
Eca	*Equus caballus*
eCG	Equine chorionic gonadotropin
ECM	Extracellular matrix
EDTA	Ethylendiamine tetraacetic acid
e.g.	For example
EIA	Enzyme immunoassay
ELFA	Enzyme linked fluorescence assay
EP1-4	G-protein-coupled receptors 1-4
ERGIC1	Endoplasmic reticulum-golgi intermediate compartment 1
ERP29	Endoplasmic reticulum protein 29
ESR	Estrogen receptor
EtBr	Ethidium bromide
EtOH	Ethanol
F	
FDR	False discovery rate
FGFR1	Fibroblast growth factor receptor 1
FSH	Follicle stimulating hormone
G	
G	Guanine
GADPH	Glyceraldehyde 3 phosphate dehydrogenase
GE	Glandular epithelium
GnRH	Gonadotropin releasing hormone
H	
h	Hour
H_2O	Water
H3F3A	H3 histone, family 3A
hCG	Human chorionic gonadotropin
HCL	Hydrogen chloride
H&E	Hematoxylin and eosin stain
HKG	House keeping gene
Hsa	*Homo sapiens*
I	
ID	Identifier
i.e.	That is
IFNτ	Interferon τ
IGF	Insulin like growth factor
INHBA	Inhibin, beta A

IU	International unit
i.v.	Intravenous
K	
KEGG	Kyoto Encyclopedia of Genes and Genomes
L	
LE	Luminal epithelium
LH	Luteinizing hormone
LIMMA	Linear models of microarray data
M	
M	Mare
Max.	Maximal
MCM7	Minichromosome maintenance complex component 7
MeV	Multi experiment viewer
$MgCl_2$	Magnesium chloride
Min.	Minutes
M-MLV RT	Moloney Murine Leukemia Virus Reverse Transcriptase
mRNA	Messenger RNA
MRP	Maternal recognition of pregnancy
N	
NaOAc	Sodium acetate
NaOH	Sodium hydroxide
NCBI	National center for biotechnology information
NK	Natural killer cells
NO	Nitrogen oxide
Nt	Nucleotide
O	
OD	Optical density
OXT	Oxytocin
OXTR	Oxytocin receptor
P	
P4	Progesterone
PBS	Phosphate buffered saline
PCR	Polymerase chain reaction
PG	Prostaglandin
PGE2	Prostaglandin E2
PGF	Placental growth factor
PGF2a	Prostaglandin F2-alpha
PGR	Progesterone receptor
PGRMC1	Progesterone membrane component 1
PLA2	Phospholipase A2
PLK2	Polo-like kinase 2

PRL	Prolactin
PyroP	Pyrophosphate
Q	
qPCR	Quantitative real-time RT-PCR
R	
RER	Rough endoplasmatic reticulum
RIA	Radioimmunoassay
RIN	RNA intensity number
RNA	Ribonucleic acid
RNase out	RNase inhibitor
RNA-Seq.	RNA sequencing
RPL7	Ribosomal protein L7
RPS27a	Ribosomal protein S27a
RT	Room temperature
S	
S	Sow
SAM	Significance analysis of microarrays
SE	Surface epithelium
Sec.	Second
SERPING1	Serpin peptidase inhibitor, clade G (C1 inhibitor), member 1
sGE	Superficial ductal glandular epithelium
SLC25A22	Solute carrier family 25 (mitochondrial carrier: glutamate), member
SNRPA	Small nuclear ribonucleoprotein polypeptide A
SOTA	Self organizing tree algorithm
SPP1	Secreted phosphoprotein 1
ssDNA	Single strand deoxyribonucleic acid
Ssc	*Sus scrofa*
StAR	Steroidogenic acute regulatory protein
T	
T	Thymine
TIMP3	TIMP metallopeptidase inhibitor 3
TXA2	Thromboxane A2
U	
U	Uracil
UBB	Ubiquitin B
UCSC	University of California, Santa Cruz
V	
Vsn	Variance stabilization and normalization

I. INTRODUCTION

1. The role of the endometrium in reproduction

The endometrium is the inner mucous lining of the mammalian uterus which has been of main interest in research of female reproduction over the last decades. During the 1970's it has been established that the endometrium influences the action of the corpus luteum (CL) via a local or a systemic uteroovarian pathway (Johnson et al., 2003) several studies unraveled the role of prostaglandin F_2-alpha (PGF2a) as luteolysin in this process (McCracken, 1973). Further on, in the 1980's it was discovered that the presence of significant amounts of PGF2a in the blood and uterine lumen during the estrous cycle, pregnancy and pseudopregnancy provoked by estrogen injections, is a result of its retrograde transfer in the area of the mesometrium (Koziorowski, 1988, Krzymowski, 1982). However, the physiological functions of the uterus were found to depend upon proper integration of endocrine and paracrine signals by the different cell types and tissue layers (Bigsby, 1991, Cunha et al., 1985). To date it is known that the endometrium plays an important morphological, functional and regulatory role during the sexual cycle: transport of sperm, uterine clearance (horse and pig), preparation for pregnancy, i.e., uterine secretions for support of conceptus growth and development, and preparation for conceptus implantation.

1.1. Morphological changes of the endometrium throughout the estrous cycle

During the sexual cycle, the ovarian cycle and the uterine cycle run in parallel and their interplay is mainly regulated by the ovarian steroid hormones estradiol (E2) and progesterone (P4). The ovarian cycle is responsible for follicular development, rupture of the follicle and development and regression of the corpus luteum (CL) whereas the uterine cycle is characterized by the morphological and functional changes of the endometrium (Loeffler et al., 2013). These changes start after puberty in sexually mature females and are influenced by numerous factors including nutrition, environment, lactation stage, age and individual genetic background. Non-seasonal polyestrous mammals (cat, cow and pig) cycle several times throughout a year whereas seasonal polyestrous mammals (horse, sheep, goat and doe) only show regularly returning estrous cycles in specific phases during the year, e.g., mares are so called "long-day breeders" with ovulatory activity being related to days with 'long' daylight. Goats and sheep only cycle when day times are short and therefore are called "short-day breeders". Typical characteristics of the estrous cycle as length of cycle, hormonal regulation, reproductive behavior and the anatomy of participating female reproductive organs show similarities but also extreme differences between mammalian species. According to the steroid hormone concentrations the estrous cycle is divided into four main phases: preestrus (late luteal phase, early estrus or follicular phase), estrus (ovulatory phase), metestrus (early luteal phase) and diestrus (mid luteal phase).

1.1.1. Morphological changes of the equine endometrium throughout the estrous cycle

During estrus the mitotic activity of the luminal epithelial (LE) cells is extremely high, the nuclei are enlarged and oval-shaped and the LE appears cylindrical. At this time during the cycle, high E2 concentration and low P4 concentration contribute to the increasing uterine wall edema. The edematization eases the tissue and therefore proliferative glands appear less packed. At this time in cycle the connective tissue is enriched with body liquid and clearly vascularized. Secretory products as well as cell debris are commonly found in the lumen of the glands during this time in the cycle. The increased secretory activity together with infiltration of the luminal epithelium by granulocytes and macrophages is important for uterine clearance after breeding

(Tunon, 1995). In addition, uterine granulocytes show tendency of arranging in groups close to the lumen and single erythrocytes are found in the Stratum compactum (Schoon et al., 1992). Gerstenberg and coworkers (Gerstenberg, 1999) observed a sudden marked and highly significant increase in the proliferation rate of the epithelial cells within the secretory portions of the endometrial glands between day 3 and day 7 after ovulation. In addition, Vogel and Humke (Vogel et al., 1973) found that equine uterine glands are changing their shape and size throughout the cycle. At estrus, uterine glands are transforming from an elongated to a coiled shape and the end of the glands becomes aciniformed. During the luteal phase the number of secretory endometrial cells rapidly declines and only few are present (Aurich, 2011). Following estrus, the edematization of the endometrium decreases and the density of the uterine glands increases (Soede et al., 2011). According to Vogel and Humke (Vogel et al., 1973), the glands become more and more aciniformed and start to build clusters during postestrum and elongate during interestrum. Unfortunately, in this population there is no exact time definition given for the phase 'postestrum' and 'interestrum'. At diestrus the uterine cells show cubical orientation. According to Riegel (Riegel J., 2002) the height of the equine epithelium is at maximum during this time of the estrous cycle. During late luteal phase, the proliferation rate in all types of cells (luminal epithelium, gland neck epithelium, superficial stroma, deep gland epithelium and deep stroma) and the superficial strata (luminal epithelium and stratum compactum) decreases to basal values (Gerstenberg, 1999).

1.1.2. Morphological changes of the porcine endometrium throughout the estrous cycle

During the estrous cycle the porcine endometrium exhibits distinct morphological changes in foldings at the luminal side. At estrus primary folds are high while during diestrus there are additionally secondary and tertiary folds developed. However, the height of the foldings clearly decreases during this process but increases again at preestrus (Fabian, 1960). In addition, the changes in the height of the luminal epithelia throughout the estrous cycle have been reported differently in literature. A maximum height was reported by Corner (Corner, 1921) and Steinbach (Steinbach et al., 1970) on day 4 and by Mehlhorn (Mehlhorn et al., 1975) on day 5 of the estrous cycle. Fabian (Fabian, 1960) observed a maximum height of the luminal epithelia not before day 7 / 8. However, a change in height from 50-62 µm at metestrus compared to 34-41 µm at estrus was found by Sidler (Sidler et al., 1986). A minimum height of 12-16 µm on day 12 of the reproductive cycle was shown by latter group and verified by Corner (Corner, 1921) and Fabian (Fabian, 1960). In contrast, other research groups (Mehlhorn et al., 1975, Prehn, 1963) observed a minimum height around day 17 of the cycle. Stroband (Stroband et al., 1986) did not detect significant local changes in the height at all. This extreme divergence could be explained by the disagreement in the onset of the estrous cycle and methodical differences in tissue preparation. At estrus the luminal epithelial cells are highly prismatic and change their shape to iso-prismatic during the luteal phase. The columnar cells are irregularly arranged and their nuclei are situated at different levels in the cells, giving the epithelium a stratified appearance. Mitotic cells are increased during this time. Following estrus the number of mitotic cells among the luminal secretory cells decreases. Besides the cells of the luminal epithelium, the small secretory cells in the glandular epithelium show mitotic activity around day 5 and the presence of clear secretory vesicles continues up to day 16 during the estrous cycle (Stroband et al., 1986). In addition to secretory cells, Kaeoket (Kaeoket et al., 2001) observed different types of cells of the immune system (e.g. lymphocytes, neutrophils, eosinophils and macrophages) in the connective tissue of subepithelial and glandular layers of the porcine endometrium at different stages of the estrous cycle. According to the latter, highest number of lymphocytes in the surface and glandular epithelia is at early diestrus. In addition, macrophages were only found at preestrus and estrus, except for a few cells in the glandular epithelium at

early diestrus. The edematization of the stroma decreases after estrus, remains unidentified during diestrus and starts again at the beginning of estrus.

1.2. Anatomy and physiology of the uterus and the endometrium

1.2.1. Uterus

The uterus, as the major female hormone-responsive reproductive organ is divided into the body (corpus uteri), the uterine tubes (cornua uteri) and the cervix. At one end, the cervix opens into the vagina while the other end is connected to one or both uterine tubes/horns depending on the species. The development of the uterus starts from the paired paramesonephric ducts during early fetal life and their degree of fusion is variable for different types of uteri amongst species. Women and higher primates exhibit a single completely fused uterus (uterus simplex) with a connection between the isthmus and the uterine body but no uterine horns. Lagomorphs, some rodents and marsupials possess two uteri (uterus duplex). These species exhibit two large horns, two cervices but no uterine body. In mammals like horse, swine (Figure I-1) and ruminants, the fusion of the paired paramesonephric ducts is only partial with a homogenous uterine body but the uterus remains paired and develops two uterine horns (uterus biscornis) (Loeffler et al., 2013). The equine uterine tubes reach a length of about 18-30 cm whereas the fusion in the sow is very short and results in even longer uterine horns that can reach a length up to 60-90 cm.

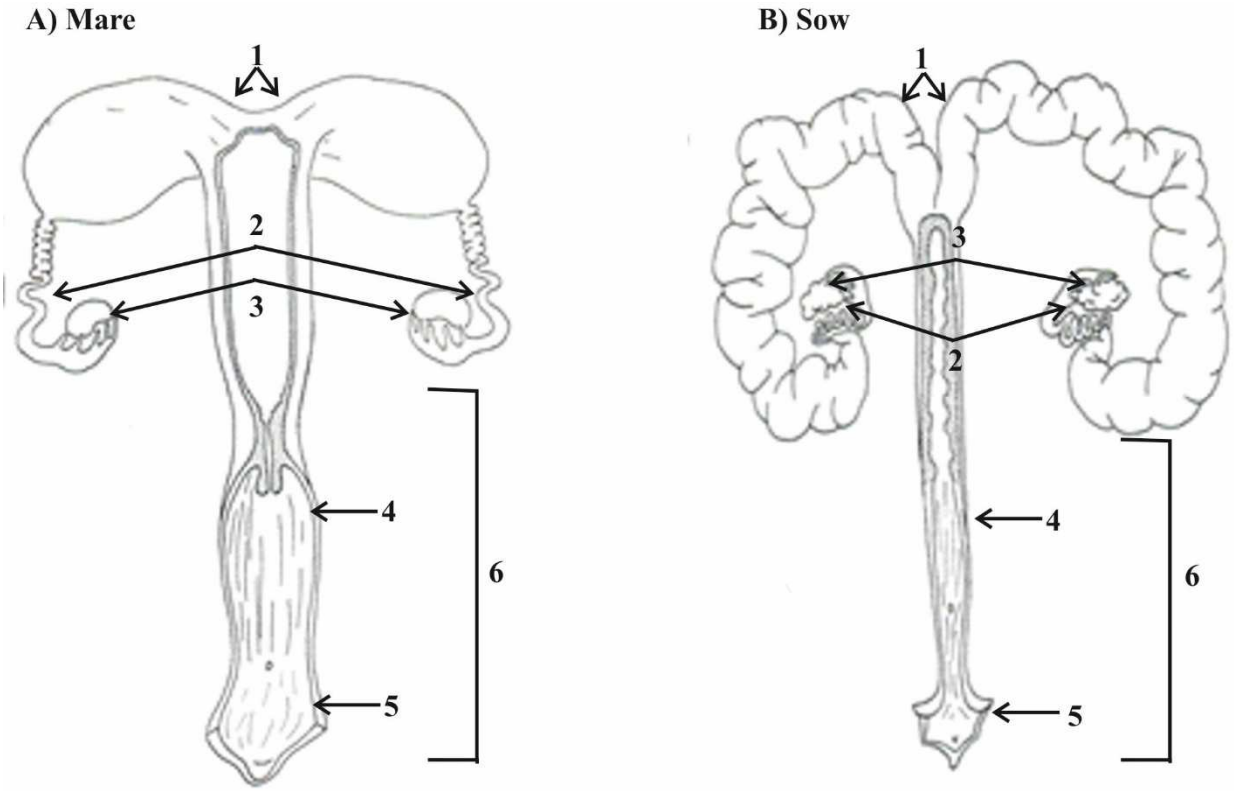

Figure I-1: Graphical illustration of the reproductive tract of the mare (A) and sow (B). 1-uterine tubes, 2-fallopian tubes, 3-ovary, 4-cervix, 5-vagina, 6-uterine body. Graphic copied from 'Embryologie der Haustiere' (Rüsse, 1998) and edited using CorelDrawX7 software.

Besides the different types of uteri, mammals are additionally separated into groups regarding different types of placentation (the formation of the placenta which requires close synchrony between the state of uterine receptivity and the stage of embryonic development) and different types of developed placentae. Most domestic animals (except carnivores) exhibit a non-invasive placentation which means that epithelial cells are remained intact on the uterine lumen surface, no induction of endometrial stromal cell decidualization occurs and the trophoblast does not

invade maternal tissue but rather expands to cover a large maternal surface (Croy et al., 2009). The different types of placenta development are divided i) regarding the degree of rearranging the layers in between the maternal and fetal vascular system, ii) interdigitation between maternal and fetal tissues and iii) based on placental shape and distribution of contact sites between fetal membranes and endometrium. In domestic animals, the number of maternal layers in the placental barrier results in two main placental classes: the epitheliochorial and the endotheliochorial placenta. Ruminants, pigs and horses develop an epitheliochorial placenta and carnivores establish the endotheliochorial (attachment of the chorion to the maternal endothelial vessels) placenta type (Hyttel et al., 2010). In addition, the mare and the sow exhibit a Semiplacenta diffusa (surface of the allantochorion is involved in formation of the placenta) while the porcine chorioallantonic surface area is increased by foldings and therefore referred to as being 'folded', the equine placenta is referred to as being villous because chorion villi a gathered in numerous microcotyledones (Hyttel et al., 2010).

1.2.2. Endometrium

The uterine wall is arranged in three layers: the perimetrium (overlay of serosa–exterior), the myometrium (smooth musculature–medial) and the endometrium (mucosa–interior). The basic composition of the endometrial tissue is similar between mammalian groups and consists of the luminal epithelium (LE) which provides a defensive barrier and is also the site of embryo attachment, glandular epithelium (GE) which secretes paracrine and autocrine factors, stroma cells which regulate growth, morphogenesis, cytodifferentiation, and function of the epithelium, blood vessels (BV or endothelial cells) and a variety of immune cells such as macrophages, lymphocytes, and mast cells (Spencer et al., 1995a). However, there are differences between species in shape and constitution of the endometrium.

The equine endometrium is arranged in 12-15 longitudinal folds which are supported by collagenous connective tissue cores (Morel, 2008). It comprises a single-layered cylindrical LE (with fractionally ciliated respiratory cells) which is attached to a basal lamina and the Lamina propria. Furthermore, the Lamina propria differentiates into a subepithelial narrow Stratum compactum (Str. comp.) and a wide Stratum spongiosum (Str. spong.). Whereas the Str. comp. shows high density of spindle-shaped stroma cells, the Str. spong. mainly exhibits blood vessels and arborescent, tubular uterine glands (Kenney, 1978). Equine uterine glands develop from the endometrial mucosa, penetrate into the submucosa and become more and more coiled during the cycle. They secrete material into the lumen of the uterus.

In direction towards the lumen, the porcine endometrium is folded and anatomically differentiated into a simple luminal epithelium and the subjacent Lamina propria. As in other domesticated mammals, the porcine LE is highly prismatic and single-layered. It is called Epithelium simplex columnare (Leiser et al., 1988). In the area of more apical parts of the uterine glands and around the openings of the glands in the porcine LE ciliated cells are common and found (Stroband et al., 1986). Branched tubular uterine glands are embedded in the Lamina propria which consists of squamous connective tissue. The amount of uterine glands is higher in the deep endometrial stroma (Kaeoket et al., 2001).

2. Endocrine/paracrine hormone actions on the uterus during the estrous cycle

In general, female mammals share the same endocrine regulatory system including the release of the gonadotropin releasing hormone (GnRH) from the hypothalamus in pulses and the secretion of the pituitary follicle stimulating hormone (FSH) and the luteinizing hormone (LH). This system elapses hierarchically starting with the hypothalamus on the top, the pituitary gland

in the middle, the ovaries on the basis. Their communication occurs through a very complex network and is finalized by characteristic actions of the ovarian steroid hormones on the uterus. Regular estrous cycles, as well as establishment and maintenance of pregnancy, require integration of both endocrine and paracrine signals from the ovary, conceptus, and uterus itself. Within the uterus, different cell types communicate with one another in a classical paracrine manner (Spencer et al., 1995a).

2.1. Steroid hormone metabolism and synthesis

Steroid hormones have influences on metabolism, inflammation, immune functions, salt and water balance, development of sexual characteristics and the ability to withstand illness and injury. Their synthesis is derived from cholesterol in the adrenal gland and their actions on the uterus are mainly mediated through their respective receptors which show species-specific expression in the uterus and interact in a complex pattern.

2.1.1. Progesterone (P4)

Progesterone plays a crucial role in the expression of genes needed for several functions regarding female mammalian reproduction at the level of the endometrium; regulation of the endometrial luteolytic mechanism, anti-luteolytic effects of interferon-tau (IFNτ) and maintenance of pregnancy (Spencer, 2004). During its biosynthesis the rate determining step is exhibited by the transport of cholesterol from the outer to the inner mitochondrial membrane. This transport is regulated by the enzyme steroidogenic acute regulatory protein (StAR) which shows the affinity to bind cholesterol (Tuckey et al., 2002). At the inner mitochondrial membrane the side chain between the 20^{th} and the 22^{nd} carbon atom of cholesterol is cleaved and pregnenolone is synthesized. The enzyme performing this reaction is cytochrome P450scc which is located in mitochondria and controlled by the anterior pituitary hormones. Pregnenolone can further be converted to i) progesterone or to ii) 17-hydroxypregnenolone which is converted into estradiol.

Under the influence of P4, the amount of endometrial glandular structures greatly increases and become more tortuous. Throughout the estrous cycle P4 concentration rises to a peak at diestrus. For example, in mares P4 concentration is highest around day 8 during the cycle and decreases rapidly afterwards, whereas in the pig P4 concentration is highest on day 12. Thus, determination of P4 concentration in peripheral blood plasma is a common and confident way to analyze estrous cycle manners which are species dependent.

In all mammalian uteri the progesterone receptor (PGR) is expressed in the endometrial epithelium and stroma during the early luteal phase, allowing direct regulation of a number of genes by progesterone via activation of the PGR (Spencer, 2004). During this time in cycle P4 from the newly formed CL which is along with the luteinized granulosa cells in the ovary the main source of progesterone, stimulates accumulation of phospholipids in LE and superficial ductal glandular epithelium (sGE) that can liberate arachidonic acid for synthesis and secretion of PGF2a. During following diestrus, progesterone levels further increase and act via PGR to block the expression of estrogen receptor alpha (ERa) and oxytocin receptor (OXTR) in the endometrial LE and sGE (McCracken, 1980). This interactive network has especially been studied and analyzed in the ovine uterus. Progesterone signaling through its nuclear transcription factor is essential for normal uterine function. Although deregulation of the receptor of progesterone (PGR)-mediated signaling is known to underscore uterine dysfunction and a number of endometrial pathologies, the early molecular mechanisms of this deregulation are unclear. Paradoxically, progesterone is involved first in suppressing and then inducing the development of the endometrial luteolytic mechanism during the estrous cycle. The timing of PGR down-regulation in the LE and superficial GE by progesterone appears to determine when

the luteolytic mechanism develop in the endometrium. Thereby the expression of *ESR1* and *OXTR* in the LE and sGE increase which causes by the induction of oxytocin increasingly PGF2a release (Spencer**,** 2004). This hypothesis is strongly supported by the finding that exogenous progesterone administration during metestrus decreased the interestrus interval in sheep and cattle (Garrett et al.**,** 1988, Woody et al.**,** 1967).

2.1.2. Estradiol-17ß (E2)

Estradiol is a member of the estrogen family which comprises the main key steroid hormones in female reproduction and which has several functions during the estrous cycle; suppressing the secretion of FSH in a negative feedback mechanism and aiding that way during the selection of the dominant follicle, preventing multifollicular development in the mid-late follicular phase in monoovulatory species (e.g. horse), and triggering of the LH surge by initiating a positive feedback mechanism when its concentration rises to a critical level. It is further known that E2 secreted by the ovary induces proliferation of endometrial cells in human (Jabbour et al.**,** 2006), rodents (Zhang et al.**,** 2006) and sheep (Johnson et al.**,** 1997). Additionally, it also induces the expression of growth factors throughout the estrous cycle in the bovine endometrium and promotes the proliferation of bovine endometrial epithelial cells by stimulating the production of a variety of growth factors in stromal cells (Arai et al.**,** 2013, Xiao et al.**,** 1998). E2 stimulates the edematization of the mucosa inducing the LH surge and increasing blood circulation and has an influence on the contraction of smooth musculature. In rodents and humans, estrogens produced from the developing follicles stimulate endometrial growth (Groothuis et al.**,** 2007).

The synthesis of estradiol is carried out by the interplay of theca cells and granulosa cells in the ovary. Therefore, the luteinizing hormone binds its receptor on the surface of the theca cells and stimulates the production of androgens. Then the androgens (androstendion, testosterone and dehydroepiandrosteron) are transported to the adjacent granulosa cells and are aromatized to estrogens which is triggered by the binding of the follicle stimulating hormone to its receptors. The aromatization of estrogens as well as synthesis of androgens is stimulated by the second messenger cyclic adenosinmonophosphat (cAMP). Some estrogens are also produced in smaller amounts by other tissues such as the liver, adrenal glands and fat cells (Nelson et al.**,** 2001).

Furthermore, estrogen is known to stimulate the expression of several steroid hormone receptors in the uterus. The highly regulated uterine estrogen receptor alpha (ESR1), progesterone receptor (PGR), and oxytocin receptor (OXTR) expression is caused by estrogen levels that peak from an ovulatory Graafian follicle at the time of estrus (Spencer et al.**,** 1995a). It has been shown that *PGR* mRNA and protein have relatively high endometrial levels during estrus (Hartt**,** 2005) in sheep and horse. Throughout the estrous cycle, E2 concentration is highest during the estrus phase and decreased during the luteal phase.

2.2. Prostaglandin metabolism and synthesis

Prostaglandins (PG) are a group of local paracrine mediators that are traditionally synthesized from an intermediate arachidonic acid (AA) released from plasma membrane phospholipids (Figure I-2).

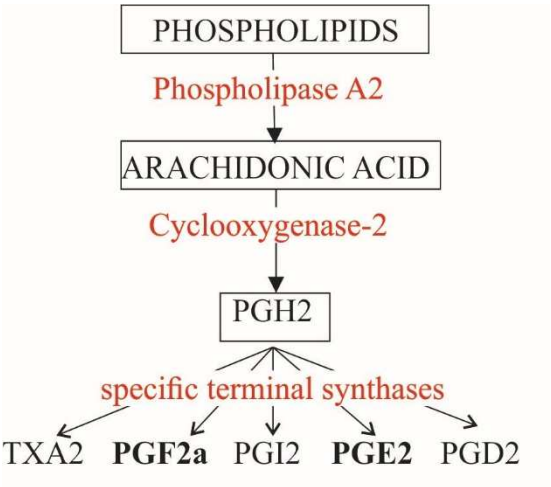

Figure I-2: Cyclooxygenase pathway of prostaglandin synthesis showing main steps and main enzymes. Arachidonic acid is first created from phospholipids via phospholipase A2 (PLA2) and then enzymatically catalyzed by the enzyme cyclooxygenase-2 (COX-2), also known as prostaglandin-endoperoxide synthase 2 (PTGS2) and oxygenated to yield endoperoxide-containing prostaglandin G2 (PGG2). The enzyme also reduces hydroperoxyl in PGG2 to hydroxyl to form PGH2 via a separate peroxidase. A cell specific isomerase catalyzes the reaction of PGH2 to different PG's and Tromboxane A2. PGG2-prostaglandin G2, PGH2-prostaglandin H2, PGE2-prostaglandin E2, PGF2a-prostaglandin F_2 alpha, TXA2-thromboxane A2. Illustration was created using CorelDraw X7 software.

Systematic studies of these substances have begun in the 1930's and revealed plenty of different types of prostaglandins with different functions; actions in the central nervous system, inflammation, pain, immunity, vascular homeostasis and reproduction (Narumiya et al., 1999). According to the literature the F and E types of prostaglandins are implicated in many aspects of reproductive function (Narumiya et al., '99). In connection with the topic of this study the metabolism and synthesis of prostaglandin F2a (PGF2a) and prostaglandin E2 (PGE2) are of major interest. PGF2a is involved in many physiological functions including contraction of uterine, bronchial, vascular and arterial smooth muscles (Watanabe, 2002), regulation of ocular pressure (Crawford et al., 1987), renal filtration (Weber, 1980), stimulation of hair growth (Sasaki et al., 2005) and regulation of the ovarian cycle through the induction of luteolysis (McCracken J., 1999). The onset of luteolysis (in some species) is known to be induced in the late luteal phase when oxytocin (OXT) is released in high-frequency bursts from the posterior pituitary. Pituitary OXT, supplemented with additional OXT released from the corpus luteum e.g. in sheep, then acts to stimulate the release of luteolytic pulses of PGF2a by the uterus (Boerboom et al., 2004). In addition E2 was found to stimulate the synthesis of PGF2a by the uterus in the guinea pig (Blatchley et al., 1971), the rat (Castracane et al., 1975) and in sheep (Caldwell et al., 1972) and further on it became apparent in studies of the sheep uterus that E2 together with P4 controls the release of PGF2a by regulation of the endometrial oxytocin receptor (McCracken J., 1999).

OXTR is a typical member of the rhodopsin-type (class I) G protein coupled receptor family and is differentially expressed in various tissues. In the uterus or hypothalamus, OXTR regulation correlates with the pattern of sex steroids, in particular estradiol (Goff, 2004). The complex interaction between sex hormones and their endometrial receptors in the pulsatile release of endometrial PGF2a has been summarized by Spencer and coworkers (Spencer, 2004) in the sheep but is still not completely clarified yet.

In domestic animals, the endometrium also secretes prostaglandin E2 (PGE2) which in contrast to PGF2a is known to have luteoprotective effects. Uterine PGE2 production increases in early pregnancy (in sheep and pigs) and its infusion can protect the corpus luteum from the luteolytic effect of endogenous and exogenous PGF2a (McCracken J., 1999). PGE2 mediates its effect

by binding to either of four subtypes of G-protein-coupled receptors (PTGER1-4), also known as EP1-4), which are encoded by four individual genes (Narumiya et al., 1999). In addition, uterine blood vessels are relaxed by estrogens, PGE2, nitrogen oxide (NO), LH, numerous cytokines and constricted by progesterone, PGF2a, OXT, noradrenalin and the central sympathetic nervous system (Krzymowski et al., 2008). The most intensive blood flow in the uterine artery was noted by several research groups (Ford et al., 1979, Ford et al., 1977) in the follicular phase, before and at the time of ovulation. Blood flow in the uterus also depends on the phase of the cycle. The rhythmic changes in uterine blood flow during the cycle in each species appear to be temporally associated with the daily estrogen/progesterone ratios observed in systemic blood. The higher the E2/P4 ratio is, the greater is the quantity of blood flowing through the uterine vascular bed (Ford, 1982).

2.3. Endocrine regulation of the equine estrous cycle

The average equine estrous cycle is about 22 days (D) in length and the four different phases are divided into estrus (ovulatory phase-around D0), early luteal phase, mid luteal phase (diestrus–around D8) and late luteal phase (reviewed in (Aurich, 2011)) (Figure I-3). As the mare is a monotocous animal, only one follicle is selected as dominant follicle and therefore only one follicle ovulates during an estrous cycle. The pre-ovulatory follicle continues growing from selection onwards, until reaching a diameter of 44-55 mm two days before ovulation (Ginther et al., '08).

2.3.1. Estrus and early luteal phase

Throughout the equine estrous cycle, ovulatory phase starts around day 16 and ceases after a period of 5-7 days. The ovulatory process of the equine follicle involves a specific and unique pattern of gene regulation in theca and mural granulose cells which includes differences in the expression of a variety of factors (Sayasith et al., '07). As in ruminants, the high level of LH during this stage primarily stimulates the further development of the dominant follicle, which produces high amounts of estradiol responsible for the LH surge in a positive feedback loop preceeding ovulation. Progesterone levels immediately start to increase in the course of the formation of the new CL, while estradiol decreases to basal levels (da Costa et al., '05) following ovulation.

2.3.2. Diestrus and late luteal phase

The CL is a temporary endocrine gland which mainly produces progesterone and does not appear at the outer surface of the ovaries. It is pear–shaped and the thinner end shows the fossa ovarii. In the event of fertilization it persists until day 150 and is called corpus luteum graviditatis. During normal estrous cycle the CL is degenerated and called corpus luteum albicans. The structures of the equine CL are formed by luteal (small and large luteal cells) and non-luteal cells. As in other domesticated animals, CL function is under the control of LH and P4. Functional luteolysis in the mare starts around day 14 after ovulation (Zavy et al., '78) while blood concentration of P4 decreases and overlaps with a decreasing P450scc expression. Structural luteolysis develops later and more slowly (Ginther et al., '05, '07). In the connection with the theme of luteolysis oxytocin plays an important role by stimulating the pulsatile release of prostaglandin F2a from the endometrium (Aurich, '11) which causes regression of the CL during late luteal phase. In turn, endometrial PGF2a stimulates secretion of oxytocin from the CL and hypothalamus, creating a positive feedback loop that increases the magnitude of the PGF2a spike. In the mare, oxytocin has been proven to be produced by hypothalamic neurons and secreted from the posterior pituitary but also in the endometrium (Aurich, '11). So far, expression of a number of genes involved in prostaglandin synthesis and signaling has been investigated during the estrous cycle and early pregnancy (Boerboom et al., 2004, Merkl et al.,

2010). In cyclic mares increased capacity of prostaglandin production during the late luteal phase has been observed, e.g., increased expression of prostaglandin-endoperoxide synthase 2 (PTGS2), also known as cyclooxygenase 2 (COX2), in uterine epithelial cells on day 15 of the cycle, whereas the increase of endometrial PTGS2 expression is inhibited in pregnant mares (Boerboom et al., 2004)

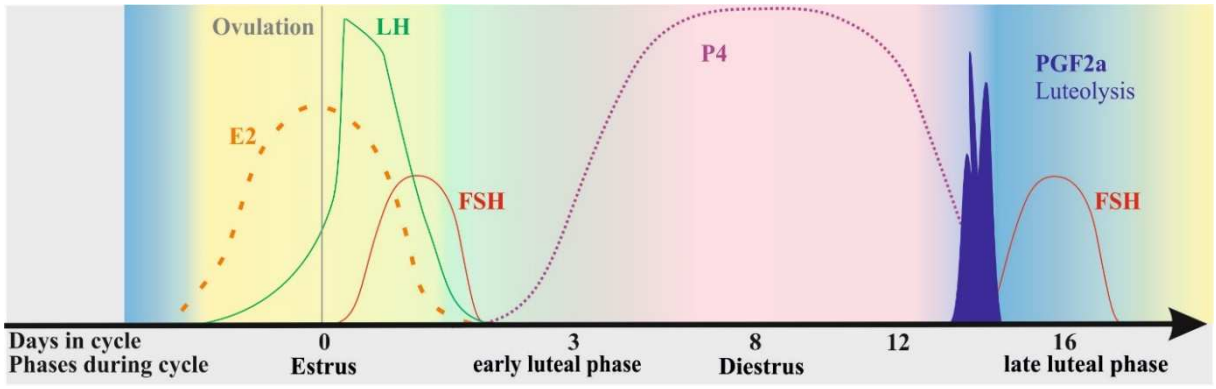

Figure I-3: Summary of the endocrine hormone signaling throughout the equine estrous cycle. Cycle length shown is 21 days. E2-estradiol, P4-progesterone, LH-luteinizing hormone, FSH-follicle stimulating hormone, PGF2a-prostaglandin F_2 alpha. Graphic was edited by the use of CorelDraw X7 software.

2.4. Endocrine regulation of the porcine estrous cycle

The estrous cycle in gilts spans an ordinary period of 21 days (D) but can vary in its length from 18 to 24 days. The pig is polytocous and may therefore ovulate 15 to 30 follicles in one estrous phase depending on age, breed, nutritional status and other factors. During the estrous cycle functional changes of the female genitals are periodically repeated, which constitute requirements for individual fertility. According to the changes in steroid hormone concentrations and corresponding endometrial changes, the porcine estrous cycle can be divided into four stages; preestrus, estrus (around D0), metestrus and diestrus (around D12) (Figure I-4).

2.4.1. Estrus and metestrus

FSH is involved in the maintenance of a pool of medium sized follicles, but these follicles need to be selected by LH for final maturation and ovulation. The selection process of follicles continues during a large part of the follicular phase, but seems finalized on the first day of estrus, which is defined as the period of time when the female is receptive to the male and will stand for mating. The length of the period of estrus varies among species and is defined as the period around ovulation in which sows show receptive behavior. In comparison to the mare the estrus phase in the pig is much shorter. In the presence of a boar, estrus lasts 40–60 h on average, but varies from less than 24 h to more than 96 h for individual sows (Soede et al., 2011). During estrus, spontaneous ovulation takes place which varies from about 1–3 h in spontaneously ovulating sows and up to 6 h in induced sows (Soede, 1997). Ovulation appears at approximately two-thirds of the estrus period about 30±3 h (mean±SD) after the LH surge. During this period, estrogen production from the pre-ovulatory follicles reaches its maximum, which induces the preovulatory LH surge (and a small FSH surge) via positive feedback causing an immediate decrease in peripheral concentrations of 17β-estradiol. The LH surge also initiates the follicular changes that result in ovulation and luteinization of the follicle wall, triggering progesterone production (Soede et al., 2011). After rupture of preovulatory follicles at ovulation, extensive remodeling and reorganization of tissue take place, resulting in the formation of fully functional corpora lutea in the mid-luteal phase (Soede et al., 2011).

2.4.2. Luteal phase and luteolysis

The developing corpora lutea (*pl*. corpus luteum) produce increasing quantities of P4 that reach peak values by days 10-12 after ovulation also suppressing secretion of gonadotropins and independent of LH input from the pituitary (Peltoniemi et al., 1995). In non-pregnant pigs, luteolysis occurs around day 15 after ovulation, and is caused by uterine prostaglandin F_2 alpha (PGF2a) which is taken to the CL by the narrow contact between the Vena uterine and the Ateria ovarica. Other than in cattle, uterine prostaglandin secretion increases earlier than day 15, but it is only by days 12–13 that corpora lutea of pigs become sensitive to prostaglandins. In case of pregnancy, the conceptus secretes estrogens between days 10 and 15 which show anti-luteolytic effects by redirecting PGF2a secretion (Waclawik, 2011) and are debated together with prolactin as pregnancy recognition signal in pigs. Other than that, the action of oxytocin in controlling PGF2a secretion has not been defined in the pig yet. In pigs, luteal OXT may not be responsible for initiation of luteolysis, but is more likely involved in the control of pulsatile release of PGF2a, especially the height and frequency of the peaks of this hormone during luteolysis (Kotwika et al., 1999). In addition, OXT stimulates the synthesis and secretion of PGE2 (PG which has the opposite action to PGF2a on the CL) by endometrial luminal epithelial (LE) cells only during early pregnancy but not on the corresponding days of the estrous cycle (Waclawik et al., 2010).

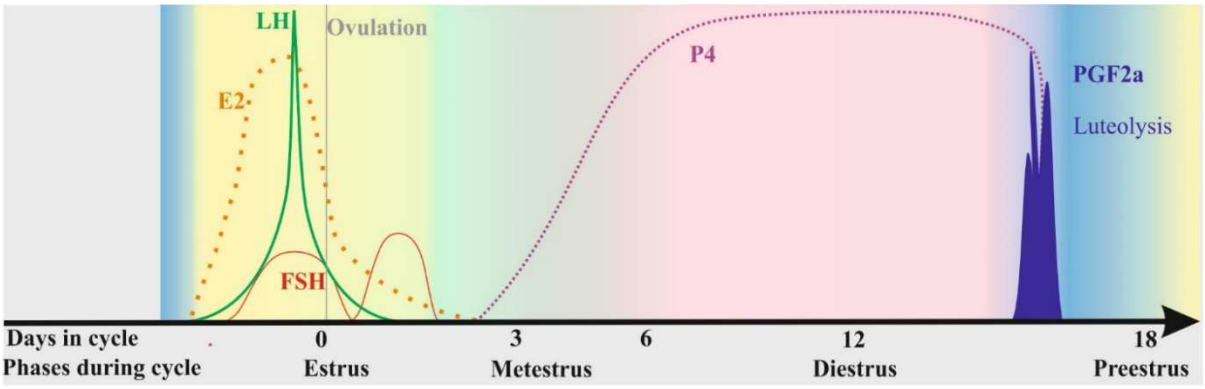

Figure I-4: Summary of the endocrine hormone signaling throughout the porcine estrous cycle. Cycle length shown is 21 days. E2-estradiol, P4-progesteron, LH-luteinizing hormone, FSH-follicle stimulating hormone, PGF2a-prostaglandin F_2 alpha. Graphic was established using CoralDrawX7 software.

3. Approaches for the study of transcriptome changes

Since most physiological processes are associated with complex changes in RNA expression profiles, transcriptome analysis is a powerful strategy for a holistic description of cellular changes at the molecular level. A number of analytical approaches, such as DNA microarrays and RNA sequencing (RNA-Seq) have been developed for systematic analyses of mammalian transcriptomes (Bauersachs et al., 2012). Microarrays have been used in two main ways: i) comparison of data established from healthy and diseased tissue with the aim to study changes in gene expression, to state characteristics of diseases and to identify novel therapeutic ways and ii) to study the actions of hormones, cytokines and drugs etc. on tissues of interest. With the development of microarray technology, global approaches have been pursued to identify gene expression changes in the endometrium involved in the regulation of the reproductive cycle. The tremendous number of studies of gene expression changes in the endometrium (of different domestic mammalian species) during the estrous cycle (Bauersachs et al., 2005, Forde et al., 2011, Mitko, 2008) and in comparison of the estrous cycle and early pregnancy (Hakhuyan et al., 2009, Klein, 2010, Krzymowski, 2004, Merkl et al., 2010, Samborski et al., 2013) that were published within a short time frame elucidates scientific importance. Results of these studies demonstrate clearly that the morphological and functional changes of the

endometrium throughout the estrous cycle still have to be further investigated (reviewed in (Krzymowski et al., 2008)), which was the objective of this study.

4. Scientific importance and aim of the present study

Infertility is a serious problem with common aspects in several species. The reasons for subfertility or infertility principally relate to events prior to insemination (impaired oocyte and/or follicle development) or after insemination (failure of the fertilized oocyte to undergo normal development, increased early embryo mortality and inadequate physiological development of the uterine endometrium, i.e. reduced receptivity). In addition, subfertility or infertility is a major problem resulting in economic losses in livestock breeding and food industry. Overcoming these problems requires a better understanding of the biochemical and cellular processes that drive the coordinated physiological regulation of ovarian, oocyte, embryo and uterine function at this important time. Reproductive success depends on the functionality of biological processes: maturation and selection of gametes, fertilization, pre-and post-implantation embryonic development, fetal growth regulation, birth and early postnatal development of offspring. Altogether, these processes are based on a functional and faultless reproductive cycle. The challenge is to understand the complexity of key mechanisms that are characteristic for successful reproduction in domestic animals and to use that knowledge to enhance fertility and reproductive health or to establish acceptable methods for control of fertility, as there is only limited scientific knowledge.

The scientific aim of this thesis was to analyze gene expression changes in equine and porcine endometrium and to understand the interaction of the variety of differentially expressed genes in relation to common and species-specific characteristics in distinct events during the estrous cycle.

In addition, similarly and inversely correlated gene expression profiles in equine and porcine endometrium during the estrous cycle were analyzed. This comparison was performed to understand the interaction and relation of identified common and species-specific gene expression changes throughout the reproductive cycle between equine and porcine endometrium. A comparison of these genes to gene expression changes in bovine endometrium throughout the cycle (Mitko, 2008) was performed to get additional insights into the complex regulation of the reproductive cycle among species.

II. MATERIALS AND METHODS

1. Materials

1.1. Chemicals

Name	Company
2-Propanol	Merck
Agarose LE	Metaphor
Boric acid	Roth
Bromphenol blue	Serva
Chloroform	Merck
DNA low ladder (N3233)	New England Biolabs
Eosin – Phloxin	Merck
Ethanol (30-96%)	BfB and Roth
Ethidium bromide (10 mg/ml)	Roth
Ethylene diaminetetraacetate (EDTA)	Merck
Equine chorionic gonadotropin (Intergonan)	MSD Animal Health Innovation GmbH
Heparin sodium salt	SIGMA
Histofluid	Superior
Human chorionic gonadotropin (Ovogest)	MSD Animal Health Innovation GmbH
Hydrochloric acid (HCl)	Roth
Mayer's Hemalaun	AppliChem
Nuclease-free Water	Millipore
RNAlater	Life Technologies GmbH
Saccharose	Merck
Sodium acetate	Merck
Sodium hydroxide	Riedel-de-Haen
Tris (tris(hydroxymethyl)aminomethane) (Tris Base)	Roth
TRIzol® Reagent	Invitrogen
Urea	Roth
Xylol	SAV LP

Table II-I: Used chemicals (name and company) in this study.

1.2. Buffers

Name	Composition
1% acidic alcohol:	1 ml concentrated HCl + 400 ml 70 % Ethanol
2.5x HSE – Buffer:	2.4 g Urea + 5 g Saccharose + 1 ml 0.5 M EDTA (pH 8.0) + 1 ml 1 % Bromphenol blue + 10 ml H_20
1x PBS + Heparin (10 units/ml):	0.024 g Heparin + 0.5 ml PBS
10x TBE – Buffer:	108 g Tris Base + 55 g Boric acid + 40 ml 0.5 M EDTA (pH 8.0) + 1l H_2O

TE – Buffer (pH 7.2):	5 ml Tris – HCl (1 mol/l, pH 7.2) + 1 ml EDTA (0.5 mol/l, pH 8.0) + 500 ml H_20
TE – Buffer (pH 8.0):	5 ml Tris – HCl (1 mol/l, pH 8.0) +1 ml EDTA (0.5 mol/l, pH 8.0) + 500 ml H_20

Table II-II: Buffers used in this study (composition and pH-value).

1.3. Kits

Name	Company
DNA 1000 Assay	Agilent Technologies
Gene expression Hybridization kit	Agilent Technologies
Quick Amp Labeling (One-color) kit	Agilent Technologies
Low Input Quick Amp Labeling (One-color)	Agilent Technologies
RNA 6000 Nano Assay	Agilent Technologies
RNA Spike–in (One–color)	Agilent Technologies
RNeasy Mini (50 colums)	Qiagen
Sprint RT Complete-Double PrePrimed	Clontech
FastStart SYBR Green Master	Roche

Table II-III: All Kits used in this study (Name and company).

1.4. Oligonucleotides (primer for qPCR)

Gene Symbol [1]	Entrez Gene ID [2]	Target Accession number [3]	Primersequences [4] (1st – forward, 2nd – reverse)
Equus caballus			
ABCA1	100054241	ENSECAT00000011043	GCCCGCCTGAAAGGGCTCTC
			CCCCACAAAGGCCAACGCCA
ACTB	100033878	NM_001081838	TGATATCGCCGCGCTCGTGG
			ATGCCCACCATCACGCCCTG
ANXA3	100059394	ENSECAT00000019790	ATCTGGGTTGGACACCGGGGG
			GTGCGTTCGACCGCTCAGTCA
CDH16	100052822	ENSECAT00000010631	CGGTGCTTGTGGAGGCCCAG
			GCGGGGTGTGCAGAGGTGTC
CDK4	100051005	ENSECAT00000027031	CCCGGACCGATCCCGAGTGTA
			GTCCCATAGGCGCCGACACC
COL1A1	100033877	ENSECAT00000020087	AAGGCGATGCTGGTCCCCCTG
			AGCCTCACCACGATCGCCACT
CXCR4	100050974	ENSECAT00000003720	CGGCTGGAGAGCGAGCGGTTA
			ATTCTCCTCCCGGAAGCAGGGC
ERGIC1	100069822	ENSECAT00000007756	CGTGCCCACGGTGTACGAGG
			AGGCTGCCGTCTCTCCGTGT
ERP29	100057258	ENSECAT00000000362	CCAAGGGCGCCCCTCTGGATA
			TCCCCACCTCTGCCACCAAGAG
GADPH	100033897	ENSECAT00000023721	GCAATGCCTCCTGCACCACCA
			TCCCAGAGGGGCCATCCACG
H3F3A	100054462	XM_001489242	CCAGAGCGCAGCTATTGGTGCT
			CTCCACGTATGCGGCGTGCTAG
INHBA	100034076	BM735205	GTGGGCAAAGTGGGGGAGAACG
			GCCAGACTTCTGCACGCTCCA

MCM7	100053690	ENSECAT00000021201	CTGCACCGTCATTGCCGCAG
			TGTCTGACGTGGCTGCCGAC
PGRMC1	100058718	DN509190	TTCCGGAGCCCTCCCTAGCG
			GCTGGTCCCCGCGCACTATC
RN18S	100861557	AJ311673.1	GCGTGTGCCTACCCTACGCC
			GCGACGGGCGGTGTGTACAA
RPL7	100033932	CD535100	TGATCGCGCACGACGTGGAT
			GGTGGTGCAGGTCTTCCTGTGG
RPS27a	100052644	ENSECAT00000019995	GTGTTGAGACTTCGTGGTGGTGCT
			GCACTCCCGACGAAGGCGAC
SERPING1	100066476	ENSECAT00000011379	TCCCCATTCAGCATCGCCAGC
			GGGTACGAGAGGACGCTCTCCA
SNRPA	100050337	ENSECAT00000021045	TGGGTGATCTGGACCCTTTGGCAT
			TTGTGCACCCCGTTTGCCCT
SLC25A22	100147341	ENSECAT00000012473	GGGGGCCACGCTGCTCAG
			GGTGCAGTCCAGGATCCCCGA
SPP1	100053029	ENSECAT00000018317	TCCTAGCACCACAGACCGTGTCC
			TGGCTTTCGTTGGACTGACTTGGG
UBB	100033924	NM_001081862.1	CGTCTCAGGGGTGGCTGTTAGC
			TGGGGCTAATGGCTGGAGTGCA
Sus scrofa			
ABCA1	100152112	ENSSSCT00000005966	ACTCAGCAGCAGTTTGTGGCCC
			TCCAGGCTGGGGTACTTGCCA
ANXA7	100156638	ENSSSCT00000011272	TCCCCGGCTCCATCTTGCCA
			TCCCCGGCTCCATCTTGCCA
BAALC	100170128	NM_001129969	TTGAGCCCCGCTACTACGAGAGC
			CACCATTGGCAGACACGCCATCT
CCNE1	100523248	TC469751	GCCGAGGGAGAAGAAGGAAAGG
			AAGGCTGATTGCCACACTGGCT
CDK4	100144492	NM_001123097	GCCCAGTGCAGTCGGTGGT
			GTGCTGCAGGGCTCGGAAGG
COL1A1	397571	ENSSSCT00000019137	GTCCCAGCGCCAGAGTCCCT
			CGGGGGCCAGTGTCTCCCTT
CXCR4	396659	NM_213773	AACCTCTGCCCAGCACGCAC
			GTCCACCCCGCTTTCCCTTGG
FGFR1	100153248	XM_001928678	GGAATCGCCGAGCCCAGTGAG
			GTGACCAGGCTCCACACCTCCA
H3F3A	396970	NM_213930	CTTCCAGCGTCTGGTGCGGG
			CTCCACGTATGCGGCGTGCT
PGF	100156404	ENSSSCT00000002642	CGAGTGCAGACCTCTGCGGGA
			GTGCCAGCAGGGAGGTAACTGAG
SERPING1	100144304	NM_001123194	TTCACCTGTGTCCACCAGGCCC
			GGGCTGCTCCCATACAGGCTCT
SNRPA	768109	NM_001077222	CACCAATGCCCTGCGCTCCA
			GTCCCGCTCCACGAAGGTGC
SPP1	397087	NM_214023	GAGGGCAGCACTGACAGCCG
			GAAGGGCAGAGGCGAAGCCC
TIMP-3	396775	ENSSSCT00000000163	CTCGGGCTTGTCGTGCTCCTG
			GGCCCCTCCTTCACCAGCTTCT

UBB	396966	XM_001925271	TGTGGCGCAGGCAGTTTCGTG GTCACTGGGCTCCACTTCCAGGG

Table II-IV: Oligonucleotides for qPCR analysis.1 Official Gene Symbol, 2 Gene Identifier supplied by NCBI, 3 Target Accession number supplied by databases (microarray), 4 reverse and forward primer sequences from PrimerBLAST (http://www.ncbi.nlm.nih.gov/tools/primer-blast/).

1.5. Equipment and consumables

Name	Company
Benchtop microcentrifuge	Roth
Bioanalyzer 2100	Agilent Technologies
Camera (universal camera DP72)	Olympus
Centrifuge (GS-15R)	Beckmann
Centrifuge 5417R	Eppendorf
Dialyzing membrane	Millipore
Eppendorf reaction vials (0.5ml, 1.5ml and 2ml)	Eppendorf
Gasket slides	Agilent Technologies
Gibco BRL Horizontal Gel	Invitrogen
Glass coverslips	Menzel
Gloves (gentle Skin)	Meditrade
Gloves (nitrile)	Kimberly Clark
High-speed stirrer (DIAX 900)	Heidolph
Hybridization chambers (stainless, G2534A)	Agilent Technologies
Incubator	Memmert
Magnetic stirr plate (RCT)	IKA
MicroAmo ™adhesive Film (48 – well fast optical)	ABI Biosystems
MicroAmo ™Reaction Plate (48 – well optical)	ABI Biosystems
Microaray Scanner (G2505C)	Agilent Technologies
Microscope (BX41)	Olympus
Microtome (HM 360)	Microm
Microwave (8521)	Privileg
Nanodrop (1000)	PEQLAB
PCI – Gel Imager	INTAS
Pipette set	Gilson
Pipette tip (10 ml)	TPP
Pipette tips (low – bind filtered)	Biozym
Pipetus – akku	Hirschmann Laborgeräte
Scalpel/dissecting instruments	Specialized trade for veterinary equipment
Shaker (Vibrax)	IKA
StepOne ™ (RT – PCR)	ABI Biosystems
Thermocycler T1	Biometra
Thermomixer (5436)	Eppendorf
UV Crosslinker	Spectrolinker
Vials (5ml)	Sarstedt
Vortexer (Vortex Genie2 Si)	Scientific industries inc
Water bath	Bachofer
Weighing machine (LA 1205)	Sartorius

Table II-V: Used equipment and consumables (Name and company).

1.6. Software and databases

Name	Company and web address
Bioanalyzer 2100 Expert B02.08	Agilent Technologies
Bowtie	http://bowtie-bio.sourceforge.net/index.shtml
DAVID (Database for Annotation, Visualization and Integrated Discovery)	http://david.abcc.ncifcrf.gov/
Ensembl	http://www.ensembl.org/index.ht
Feature extraction software 10.7.3.1	Agilent Technologies
Geneplotter (graphics related functions of Bioconductor)	http://www.bioconductor.org/
KEGG (Kyoto Encyclopedia of Genes and Genomes)	http://www.genome.jp/kegg/
LIMMA (linear models of microarray data)	http://www.bioconductor.org/
MeV (Multi experiment viewer, V4.7.1, V4.8.1)	http://www.tm4.org/mev/
Microsoft Office 2013	Microsoft Corp.
Nanodrop 1000 V3.7.1	PEQLAB
NCBI (National centre of biotechnology information) BLAST (Basic local alignment search tool)	http://blast.ncbi.nlm.nih.gov/Blast.cgi
newCAST™ software	Visiopharm
PrimerBLAST	http://www.ncbi.nlm.nih.gov/tools/ primer-blast/
RefSeq (NCBI Reference Sequence Database)	http://www.ncbi.nlm.nih.gov/ref
SAM (significance analysis of microarray (Mirosoft Excel add-in))	http://www.bioconductor.org/
Siggenes (SAM and Efron's empirical Bayes approaches)	http://www.bioconductor.org/
StepOne TM V2.0	ABI Biosystems
UCSC Genome Browser (University of California Santa Cruz)	http://genome.ucsc.edu/cgi-
Vsn (Variance stabilization and calibration for microarray data)	http://www.bioconductor.org/
WikiPathways	http://wikipathways.org/index.php/ WikiPathways

Table II-VI: Name, company and web address of all databases and saftware used in this study.

2. Methods

2.1. Housing of animals

2.1.1. Housing of mares

The mares used for this study were provided from and housed in the facilities of the Bavarian principal and state stud of Schwaiganger, Germany.

2.1.2. Housing of sows

Management of experimental animals was performed by Dr. Barbara Kessler und Christian Erdle (Chair for Molecular Animal Breeding and Biotechnology, LMU Munich, Oberschleissheim). After treatment, the animals were transferred to the experimental slaughterhouse in Grub, Germany.

2.2. Sample collection

2.2.1. Collection of equine endometrial biopsy samples

The collection of samples was performed in context of routine analysis of the mare's fertility (evaluation of breeding fitness). Endometrial biopsy samples were collected from five normal cycling mares (M1, M2, M3, M4 and M5, Bavarian Warmblood). Follicular development and ovulation were monitored routinely by daily transrectal palpation and ultrasound examination. Mares were treated with 1500 IU human chorionic gonadotropin (hCG) i.v. to induce ovulation when mares developed an ovarian follicle of approximately 35 mm in diameter accompanied by prominent endometrial edema. Samples were obtained by transcervical biopsy and taken at five different days (D) (D0, D3, D8, D12, and D16) during the estrous cycle. No more than two biopsies were taken during the same cycle with an interval of at least 15 days. Samples were cut into six plane–parallel slices and every second slice was transferred into embedding capsules with their right cut surface facing downwards, covered with a foam sponge to avoid distortion of tissue samples, and fixed by immersion in 4 % buffered formaldehyde. The remaining pieces of the biopsy samples were immediately transferred into vials containing 4 ml RNAlater for mRNA expression analysis. The vials were cooled on ice and incubated overnight at 4°C. Samples were removed from RNAlater the day after and sample weight was recorded before storage at -80°C until further processing. Additionally, blood samples were collected in EDTA tubes from the jugular vein on each time point chosen to determine peripheral plasma progesterone concentrations. Blood samples were centrifuged at 2000 *g*, 4 ° C for 10 min. and plasma was decanted and stored at -20 ° C until assay. The collection of the biopsy and blood samples was performed by Dr. vet. med. M. Merkl. Sample collection procedures and progesterone assay protocol are recorded in the dissertation of Dr. vet. med. M. Merkl.

2.2.2. Collection of porcine endometrial biopsy samples

All animals have been purchased from a fattening farm at the age of 6 month and are about a cross-breeding between the German landrace and the Piétrain. The collection of samples has been notified to the legal authorities. The animals were treated with a single injection (750 IU) of equine chorionic gonadotropin (eCG) and, 72 h later, a single injection with 750 IU of human chorionic gonadotropin (hCG) to synchronize ovulation (Samborski et al**.,** 2013). The eCG stimulates follicular development due to its FSH-like activity, and hCG causes ovulation because of its LH-like activity (Youngs**,** 2001). Samples were obtained from six different normal cycling gilts on each of the five different days (D0, D3, D6, D12 and D18; in total n=30, S1101-S1130) during the estrous cycle. For precise biopsy sample collection on D0, the animals were treated 21 days ahead. Immediately after slaughtering the reproductive tract was removed from the animal. The uteri were bisected through the corpus and, starting from the corpus, the uterine tubes were opened longitudinally along the anti-mesometrial side. Three sets of endometrial biopsy samples were taken from each uterine tube (left and right): proximal (i.e. close to the ovaries = front), intermedial (middle) and distal (towards the corpus = back). The biopsy samples (altogether 90 for each uterine tube) were immediately transferred into vials containing 3 ml RNAlater for mRNA expression analysis. The vials were cooled on ice and incubated overnight at 4 ° C. Samples were removed from RNAlater and their weight was ascertained and stored at -80 ° C until further processing. Additionally, blood samples were collected in EDTA tubes from each animal to determine peripheral plasma progesterone concentrations. Blood samples were centrifuged at 4000 g, 4 ° C for 10 min. and plasma was decanted and stored at -20 ° C until assay. For additional characterization of cycle stages the number and size of corpora lutea and follicles in the ovary (left and right) were counted and documented in the 'sample collecting protocol' (see Supplemental Material-Table VIII-II) as well as shape and composition of the uteri.

2.3. Determination of plasma progesterone concentrations

2.3.1. Equine blood samples

Progesterone (P4) concentrations in peripheral blood plasma were measured by mini VIDAS® and VIDAS® Progesterone kits, a system based on the enzyme linked fluorescent assay (ELFA) technique. A detection limit of 0.25 ng/ml and a correlation coefficient of 0.89 related to radioimmunoassay (RIA) are certified for the assay by the manufacturer. The measurements were performed by Dr. vet. med. M. Merkl for equine blood samples and procedures can be read in the dissertation of Dr. vet. med. M. Merkl.

2.3.2. Porcine blood samples

For porcine blood samples the progesterone concentrations in peripheral blood plasma were measured with a system based on a sensitive enzyme immunoassay (EIA) for progesterone determination in unextracted bovine plasma using the secondary antibody technique (Prakash et al., 1987). The analysis was run in the laboratory of Prof. Susanne E. Ulbrich for porcine blood samples.

2.4. Quantitative Stereology

For qualitative histological and quantitative stereological analyses, formalin-fixed slices of each biopsy samples were embedded in paraffin with their right cut surface facing downwards. Histological sections were cut at a nominal thickness of 3 µm with a rotary microtome, transferred onto glass slides and stained with hematoxylin & eosin (H&E). H&E stain is a very popular staining method in histology that tinges different structures in histological slices. It is divided into two single stain reactions: Hemalaun and eosin staining. Haematoxylin is a natural dye of the Logwood (*Haematoxylum campechianum*) and has to be concentrated to Haemalaun to develop its staining character. Haemalaun dyes acidic respectively basophile structures blue especially the nucleus with its DNA and the rough endoplasmic reticulum (rER) with its ribosomes. The second stain reaction is performed with Eosin, which is a synthetic dye that colors acidophilic respectively alkaline structures red, for example cell plasma proteins. Quantitative stereological analyses were carried out with the newCAST™ software.

2.4.1. H&E–Staining protocol

Formalin–fixed slices had to be arranged in the same orientated direction during the cutting process with the microtome. The slices were put in an incubator at 37 ° C over night. To dissolve paraffin from tissue, the slices were transferred in xylene for 20 min. For removing of extra staining, the slices were processed through a descending alcohol line–up starting from 96 % to 70 % of concentrated ethanol. Then the slices were washed in water and stained for 5 min. in Mayer's Hemalaun. Afterwards, the slices were rinsed in the tap for 2 – 3 min. Before the second staining with Eosin–Phloxin the slices were put in an acidic alcohol solution (1%) for a couple of minutes. Acidic alcohol is used as differentiation solution in histology and cytology to remove excess stain and define nuclei. Adjacent eosin staining lasted until lightly tinged. Then, the slices were put through an ascending alcohol line–up starting from 70 % to 96 % of concentrated ethanol and afterwards put in distilled water for 5 min. The slices were dried out and covered with glass cover slips using Histofluid.

2.4.2. Tissue composition

Slides were displayed on a monitor at a 400 x final magnification by a camera (universal camera) coupled to a microscope (standard laboratory microscope) and images were superimposed by an adjustable point counting grid. Approximately 2000 points were evaluated

per biopsy sample to determine volume densities of luminal epithelium (LE), glandular epithelium (GE), blood vessels (BV) and remaining tissue. This estimation was used to quantify cell and tissue morphology of all equine endometrial biopsy samples on all five days during the cycle. The volume densities (Vv) of the different tissue compartments were obtained by dividing the number of points hitting a compartment (P(compartment), e.g. points hitting blood vessels, P(blood vessels)) by the total number of points hitting the biopsy sample (P(sample)) considering the number of points in the counting grid used Vv (compartment/sample)=P(compartment)/P(sample)*points used in grid.

2.5. Isolation of total RNA

Total RNA was isolated for microarray analysis and quantitative real-time RT-PCR (qPCR). For a meaningful analysis of obtained RNA expression data, it is necessary to perform isolation of RNA under standardized conditions. To prevent degradation of RNA by ubiquitous RNases, working areas were cleaned with ethanol anytime before use. Every step was performed using gloves and RNase-free equipment.

All endometrial biopsy samples (25 equine samples and 90 porcine samples) were homogenized with Trizol–method according to the manufacturer's instruction. TRIzol reagent contains phenol which dissolves hydrophobic protein areas and guanidine isothiocyanate which denaturates hydrophilic proteins, respectively. Afterwards, phase separation - into three different phases was induced by adding chloroform. The upper aqueous phase contains RNA, the interphase contains DNA agglutinated to denatured DNA-binding proteins (most likely histones) and the lower organic phase contains dissolved proteins and precipitated proteins at the bottom. This is a common method of total RNA extraction from cells and tissues based on the original publication of Chomczynski (Chomczynski et al., 2006). It takes slightly longer than column-based methods like RNAeasy but it has higher capacity and can yield more RNA. Along with lysis buffers containing chaotropic salts it is generally considered the method that gives the best quality of RNA with many tissue samples. In the next step the aqueous phase was then precipitated with isopropanol and samples were clarified with ethanol and diluted in RNase-free water.

2.5.1. Homogenization

While handling TRIzol reagent, safety precautions had to be taken. According to their weight all samples were added to TRIzol reagent as follows: 1 ml of TRIzol per 50 to 100 mg sample weight. Using an applicator, the tissue sample was transferred to the reaction tube containing TRIzol and lysed with high-speed homogenizer for 60 s until the solution was homogenous. The homogenizer was cleaned and inspected for resting tissue each time of use. Cleaning was performed with 0.5 N NaOH solution and desalted water and the homogenizer was dried with a paper towel. NaOH solution destroys RNases and also RNA due to the alkaline environment. Samples were put on ice or stored at -20 ° C until further processing.

2.5.2. Phase separation

Homogenized samples were thawed at RT for 10 minutes and shortly centrifuged. Chloroform was added for phase separation according to the volume of TRIzol used (0.2 ml $CHCl_3$ per 1 ml TRIzol) and the solution was mixed per hand for 15 seconds. Following incubation for 10 min. at RT, the samples were centrifuged for 30 min. at 6 ° C and 25.000 *g*.

2.5.3. RNA-precipitation

The corresponding amount of isopropanol was placed in 2 ml reaction vials (0.5 ml isopropanol- per 1 ml TRIzol). After centrifugation the aqueous phase was transferred to the reaction vials

containing the appropriate amount of isopropanol and carefully mixed. The solution was incubated at RT for 10 min. and afterwards centrifuged for at least 30 min. with 25.000 g at 6 ° C. The supernatant was discarded. One ml of 75 % ethanol were added per 1 ml of original volume of TRIzol and centrifuged for 15 min. with 25.000 g at 6 ° C. Again the supernatant was discarded. After short centrifugation the remaining 75 %-EtOH was removed. The pellets were dried in the opened reaction vials close to the flame (Bunsen burner) and 100 µl of nuclease-free water was added for dissolving the purified RNA. The solution was put on ice for at least 30 min. Afterwards the samples were heated in a water bath at 58 ° C for 10 min and put back on ice. To remove any remaining contaminants from the Trizol isolation, an additional precipitation with sodium acetate (NaOAc) and isopropanol was performed. Therefore, 1 volume of isopropanol and 1/10 volume of NaOAc (3M) were added to the RNA solution and incubated at RT for 10 min. The samples were centrifuged at 6 ° C and 25.000 g for another 10 min. Then 500 µl 75 % EtOH were added to the pellet and again centrifuged at 6 ° C for 10 min with 25.000 g. The supernatant was decanted and the pellets were dried at flame. Afterwards, the pellets are dissolved in 100 µl water and put on ice for at least 30 min. Then the samples were heated for 10 min. at 58 ° C in a thermomixer and afterwards put back on ice.

2.5.4. Pooling of RNA isolated from porcine endometrial tissue samples

Isolated RNA samples were pooled together; every three (front-middle-back) samples of the left uterine tube of one animal in the same amount of RNA. Concentration (ng/µl) was measured as described in 2.5.5. The three samples were added to a total volume proportional to RNA volume: 2 µl of the sample with lowest RNA concentration were put in an reaction tube as major component while the volume of remaining two RNA samples were calculated. Due to divergent P4 concentrations six animals have been excluded for further processing.

$$\frac{\text{concentration of main sample (ng/µl)}}{\text{concentration of remaining sample (ng/µl)}} = \text{volume rate (same amount as µl added to tube)}$$

Equation II-1: Volume of RNA isolated from procine tissue needed for pooling. If the volume was lower than 1 µl, volumes were multiplied by factor 2 for accurate pipetting and total volume needed for further processing.

Sample ID[1]	Conc. RNA [ng/µl][2]	Volume RNA [µl][3]	Total Volume [µl][4]	Sample ID[1]	Conc. RNA [ng/µl][2]	Volume RNA [µl][3]	Total Volume [µl][4]
D0S19-f	2166	0.4		D6S17-f	2147	1	
D0S19-m	725	1.1		D6S17-m	1406	1.5	
D0S19-b	402	2	3.5	D6S17-b	1069	2	4.5
D0S20-f	1025	1.6		D6S18-f	2048	0.9	
D0S20-m	990	1.6		D6S18-m	1772	2	
D0S20-b	804	2	5.2	D6S18-b	2459	0.7	3.6
D0S21-f	1139	2		D12S2-f	1518	1.1	
D0S21-m	1318	1.7		D12S2-m	1049	1.6	
D0S21-b	1171	1.9	5.7	D12S2-b	840	2	4.7
D0S22-f	1202	2		D12S3-f	879	2	
D0S22-m	1871	1.3		D12S3-m	988	1.8	
D0S22-b	1839	1.3	4.6	D12S3-b	1221	1.4	5.2
D0S24-f	629	2		D12S5-f	1597	1.3	
D0S24-m	1499	0.8		D12S5-m	1204	1.7	
D0S24-b	910	1.4	4.2	D12S5-b	1030	2	5
D3S7-f	1471	2		D12S6-f	1199	2	
D3S7-m	2614	1.1		D12S6-m	1492	1.6	

D3S7-b	1465	2	5.1	D12S6-b	1455	1.6	5.3
D3S8-f	1299	1.9		D18S25-f	418	1.3	
D3S8-m	1258	2		D18S25-	537	1	
D3S8-b	1251	2	5.9	D18S25-b	280	2	4.4
D3S10-f	1140	2		D18S26-f	639	2	
D3S10-m	1893	1.2		D18S26-	713	1.8	
D3S10-b	1587	1.4	4.6	D18S26-b	701	1.8	5.6
D3S12-f	1885	2		D18S27-f	843	1.9	
D3S12-m	2191	1.7		D18S27-	813	2	
D3S12-b	2467	1.5	5.2	D18S27-b	870	1.9	5.8
D6S14-f	1574	1.3		D18S28-f	653	1	
D6S14-m	1021	2		D18S28-	341	2	
D6S14-b	1701	1.2	4.5	D18S28-b	348	2	5
D6S15-f	1381	1.6		D18S29-f	375	2	
D6S15-m	1444	1.6		D18S29-	2063	0.4	
D6S15-b	1129	2	5.2	D18S29-b	718	1	3.4
D6S16-f	1314	1.1		D18S30-f	1184	0.7	
D6S16-m	724	2		D18S30-	832	1	
D6S16-b	1364	1.1	4.2	D18S30-b	418	2	3.7

Table II-VII: Concentrations and pooling of RNA isolated from remaining 72 porcine tissue samples.[1] Sample identifier: D-day, S-sow, f-front, m-middle, b-back, [2] concentration meassured with Nanodrop 1000 UV-VIS, [3] calculated volume of RNA pooled together [4] total volume of all porcine RNA samples.

2.5.5. Spectrophotometrical analysis of nucleic acids

Quantity and purity of nucleic acids were measured with a NanoDrop 1000 UV-VIS Spectrophotometer and applicable Software (V3.7.1). The spectrophotometer measures the optical density of aqueous RNA/DNA solutions which can be influenced through attenuation, wavelength, chaotropic salts, phenol and proteins. Measurements are performed at different wavelength. Measurement at 260 nm is used for estimation of nucleic acid concentration (for RNA 1 OD= 40 ng/µl per 10 mm light path, for DNA 50 ng/µl). Two ratios of OD values are used for analysis of purity: 230/260-nm and 260/280-nm ratio. The 230/260 ratio indicates the presence of contaminants like chaotropic salts if lower than 2.1. Ratio 260/280-nm indicates contamination of RNA samples with DNA, proteins and phenol or of DNA samples with RNA, proteins and phenol, respectively. The 260/280-nm ratio for pure RNA is 2.0 and for DNA 1.8 (at neutral pH). Before initializing the instrument, the sample loading area was cleaned with nuclease-free water. Once the instrument was initialized, a sample type (using the drop down menu) was selected. Afterwards, the instrument was blanked with the reference solution (TE–buffer or nuclease-free water).

2.5.5.1. RNA

The sample loading area was cleaned each time between measurements with a laboratory wipe. 1.5 µl of the RNA sample were measured each time. A baseline being flat at 0 is requested. If the baseline deviates from 0 and is not a flat horizontal line any longer, the instrument has to be reblanked with nuclease-free water and then the sample can be measured again. The software provides different menus for RNA analysis: ‘Nucleic acid’ (for concentration of total RNA) and ‘Microarray’ (for analysis of fluorescently labeled cRNA to determine the µg cRNA yield and Cyanine 3 dye concentration to determine label incorporation).

2.5.5.2. DNA

Nucleic acid (ss-DNA) was used to measure the concentration of oligonucleotides (PCR primer) used for quantitative real- time PCR (qPCR). Due to the short nucleic sequences of oligonucleotides, the difference in weight between pyrimidine (thymine and cytosine) and purine (guanine and amine) bases must be considered. Therefore Dr. H. Blum developed a procedure by which at first only 85 % of recommended water volume by the company were added. The samples were then mixed on a vortexer and incubated for at least 24 hours in the fridge. Afterwards, the oligonucleotides were measured with a NanoDrop 1000 UV-VIS Spectrophotometer and applicable Software (V3.7.1). Considering the optical density, molecular weight and concentration (calculation by Dr. H. Blum) the volume of water to have a final concentration of 100 pmol/µl was added.

2.5.6. Microfluidics-based electrophoresis for sizing, quantification and quality control of nucleic acids

Quality and quantity (DNA fragments) of total RNA and DNA was determined electrophoretically with an Agilent 2100 Bioanalyzer.

2.5.6.1. Analysis of RNA samples

Agilent RNA kits are designed for the analysis of total RNA (eukaryotic and prokaryotic) and mRNA samples. RNA samples are analyzed by using electrophoretic separation on micro-fabricated fluidic chips and subsequently detected via laser-induced fluorescence measurement. RNA degradation is a gradual process reflected by a decrease in the 28S to 18S ribosomal RNA ratio and an increase in the baseline signal between the two ribosomal RNA peaks and the lower marker. The Bioanalyzer software automatically calculates the ratio of the 28S to 18S ribosomal RNA. Although ribosomal RNA ratios can be used for determining the level of sample degradation in gel electrophoresis, a more sophisticated analysis is performed by the Agilent 2100 Bioanalyzer software to more accurately described sample integrity. The RNA integrity number (RIN) provided by the Bioanalyzer software is based on a combination of different features that contribute information about RNA integrity to provide a more robust universal measure (see www.agilent.de). The integrity number follows a numeric range from 1 to 10 with 10 for optimal RNA integrity and 1 for complete degradation. Additionally, the Bioanalyzer 2100 estimates the RNA concentration. The complete RNA 6000 Nano kit guide can be found in the online help of the 2100 expert software. Samples were diluted to a final concentration of 250 ng/µl for best results. The RNA analysis was run according to the manufacturer's instructions.

2.5.6.2. Analysis of DNA samples

For comparative quantitative real-time RT-PCR (qPCR) it is important to confirm that the PCR produced specific DNA fragments. Confirmation was performed in two steps i) analysis of PCR product size(s) and ii) sequence analysis. The Agilent 2100 Bioanalyzer DNA 1000 kit was used to get high resolution (down to 5 bp) over the entire size range of the obtained qPCR products. Furthermore, the analysis with the Agilent 2100 Bioanalyzer DNA 1000 assay provides accurate quantification of the DNA fragments amplified in the qPCR reactions that was needed for subsequent sequence analysis of the products. The analysis of the PCR products was performed according to the manufacturer's instructions.

2.5.7. Agarose gel electrophoresis

Agarose gel electrophoresis was also used to analyze nucleic acids according to their molecular weight. The nucleic acids, which are stained with ethidium bromide, are exposed to ultraviolet

light. According to fluorescence intensities, brightness of the fragments and comparison to the ladder, quantity and size of DNA fragments are determined. This method is less expensive than analyzing DNA with a Bioanalyzer but needs far more time effort. Agarose gel electrophoresis was used to analyze qPCR products derived from test series, which was performed to find optimal annealing temperatures for obtaining PCR products. A "small DNA" agarose was used (2 %/1x TBE) for PCR products with a size of 100–200 bp. One gram of "small DNA" agarose was added to 45 ml of H_20 in an Erlenmeyer flask and dissolved by heating in a microwave. Evaporated water was refilled. With a magnetic stir bar (added before heating) on top of a magnetic stirrer, the agarose solution was mixed during cool-down below 50°C. In the meantime, 250 ml running buffer were prepared: 225 ml H_2O + 25 ml 10 x TBE/EtBr. Five milliliter of the EtBr/TBE (2 x) were added to the agarose and spilled on the gel chamber (setup with inserted comb). The gel rested until it was hardened (3 x polymerization time). Meanwhile, the samples were prepared: 2 µl sample +1.3 µl 2.5 x HSE buffer. The samples were gently mixed on a vortexter. Four µl of DNA low ladder (N3233) (1:10 dilution, 50 ng/µl) and 2 µl of prepared samples were put on the gel. At first, a field strength of 3 V/cm was applied which lasted for 10 min. and was then changed to 5 V/cm for the remaining 1.5 h. Afterwards the gel was put into the INTAS PCI–Gel–Imager and exposed with 254 nm ultraviolet light. The fluorescence was recorded by a digital camera.

2.5.8. Agilent microarray analysis

DNA microarrays simultaneously measure the expression of thousands of genes. They are produced on glass slides or other substrates and contain DNA sequences (e.g. cDNA fragments produced by PCR, short or long oligonucleotides) spotted or synthesized *in situ* on the surface in a known order. The probe features are placed on the slide surface with robotic arms or built one base at a time with photolithographic or other synthesis technologies. In case of Agilent microarrays, 60 nt oligonucleotide probes are synthesized in situ using a technology similar to inkjet printing. Nucleotides are specifically printed to defined positions corresponding to the microarray design and incorporated into the growing oligonucleotide sequence by the use of highly efficient coupling reagents. Each oligonucleotide sequence is assigned a so-called 'Probe ID' whose identity and location is stored in an annotation file provided by the company (Agilent Technologies, Germany). The microarray slides used in this study were 4x44k Horse Genome arrays (252132210082, 252132210083, 252132210084, 252132210085, 252132210088, 252132210089, 252132210102) and 4x44k Porcine Genome arrays (252644010216, 252644010217, 252644010218, 252644010219, 252644010220, 252644010221) with 4 array areas on each slide with 44,000 probes, respectively. In order to control labeling efficiency and detection sensitivity, probes designed against different mRNA spike-in control transcripts are replicated 30 times on the microarray. Furthermore, probes were included that were present 10 times on the array to allow intra-array reproducibility. Isolated RNA has to be converted into fluorescently labeled cRNA which can then hybridize to the respective complementary probes. For detection of hybridized cRNAs, the cRNA was labeled with cyanine 3 (Cy3), a widely used fluorescent marker.

2.5.8.1. Agilent Quick Amp Labeling Kit, one-color

The microarray analysis was run according to the manufacturer's instructions. The first step was to prepare the Agilent One-Color Spike in Mix provided by the company and the RNA samples. As starting material for the labeling reaction, 500 ng total RNA were prepared in 5.3 µl RNAse-free water.

2.5.8.2. Agilent Low RNA Input Quick Amp Labeling Kit, one-color

At first the Agilent One-Color Spike in Mix and the RNA samples were prepared for labeling reaction as provided by the company. Therefore 100 ng total RNA was diluted in 2.5 µl RNAse-free water.

2.5.8.3. cDNA synthesis

In the first step the RNA is reverse transcribed into double-stranded cDNA using a modified reverse transcriptase (Moloney Murine Leukemia Virus Reverse Transcriptase, M-MLV RT), an RNA-dependent DNA polymerase which needs a primer to start the cDNA synthesis. A T7 promoter primer was added to the total RNA samples. M-MLV RT is the preferred reverse transcriptase for long mRNA templates because the RNase H activity of M-MLV RT is weaker than the commonly used Avian Myeloblastosis Virus (AMV) reverse transcriptase. RNase H separates the DNA-RNA hybrid in a hydrolytic manner through a metallic ion. It is also responsible for the removing of RNA primers and therefore allows the completion of the synthesized dsDNA. Dithiothreitol (DTT) is applied to renaturate wrongly folded proteins. RNase–out inhibits degradation via RNases in this step.

2.5.8.4. Production of Cy3-labelled cRNA

The synthesis of the labelled cRNA is carried out using a T7 RNA polymerase. The polymerase synthesizes the cRNA starting at the T7 promoter sequence which was introduced with the T7 promoter primer during cDNA synthesis. In this step the Cyanine3–labelled CTP is incorporated. Since the reaction is, in principle, a so-called run-off transcription, the RNA polymerase can bind multiple times to the promoter and synthesize multiple cRNA copies from one cDNA template facilitating up to 1000-fold amplification of the original template mRNA. For example, in case of 100 ng total RNA as starting material, at least 3 µg cRNA are produced from 3 ng polyA$^+$ RNA (approx. 3% of total RNA). After amplification, the purification of cRNA was carried out with Qiagen RNeasy kit. The columns contain a silica gel membrane, which preferentially binds the RNA. After the last centrifugation step the purified cRNA is eluted with 30 µl of nuclease–free water and put on ice. For quantifying the cRNA, samples were measured with the Nanodrop 1000 (program ‘Microarray’) and specific activity (label incorporation) and yield of cRNA were calculated (Equation II-2).

cRNA yield:

(Concentration of cRNA (ng/µl)) * 30 µl (elution volume) / 1000 = µg of cRNA.

Specific activity:

(Concentration of Cy3) / (Concentration of cRNA) * 1000 = pmol Cy3 per µg cRNA

Equation II-2: Calculation of cRNA yield and specific activity. Cy3-Cyanine 3

For the ‘Agilent Quick Amp Labeling Kit, one-color ‘ the company suggests that if the cRNA yield is less than 1.65 µg and the specific activity less than 9.0 pmol Cy3 per µg cRNA the preparation should better be repeated. To continue to hybridization process the company suggest by using the ‘Agilent Low RNA Input Quick Amp Labeling Kit, one-color’ the cRNA yield should be no lesser than 1.65 µg and the specific activity no lesser than 6.0 pmol Cy3 per µg cRNA.

2.5.8.5. Hybridization to microarrays

Each gene transcript is represented on the slide by one or more single-stranded oligonucleotides. The labeled cRNA can bind to complementary probes via hydrogen bonds building a double helix. To optimize the kinetics of hybridization the cRNA strands have to be fragmented. In order to do so Blocking and Fragmentation buffer were added to each sample and the samples were then incubated for 30 min. at 6°C. The fragmentation process was stopped utilizing the provided Hybridization buffer. The hybridization processes are demonstrated in Figure II-1. The samples were then immediately loaded onto the gasket slides located in the hybridization chamber. Subsequently the microarray slides were placed on top of the gasket slides forming a 'Sandwich' and the hybridization chambers were carefully screwed according to the manufacturer's instructions. The hybridization assemblies were put into the hybridization oven and incubated at 65°C and 10 rpm for 17 hours. Before starting the washing process, Triton X-102 (0.005 %) detergent was added to the wash buffers provided by the company. Triton X-102 effectively removes background artifacts without affecting the stringency of the wash buffers (cited from agilent.com). Unhybridized cRNA strands were washed off carrying out 'washing procedures' as described in 'Agilent microarray hybridization chamber user guide' and 'Agilent protocol' (controlling temperature within preheated W2 buffer-step, stabilization and drying solution not used).

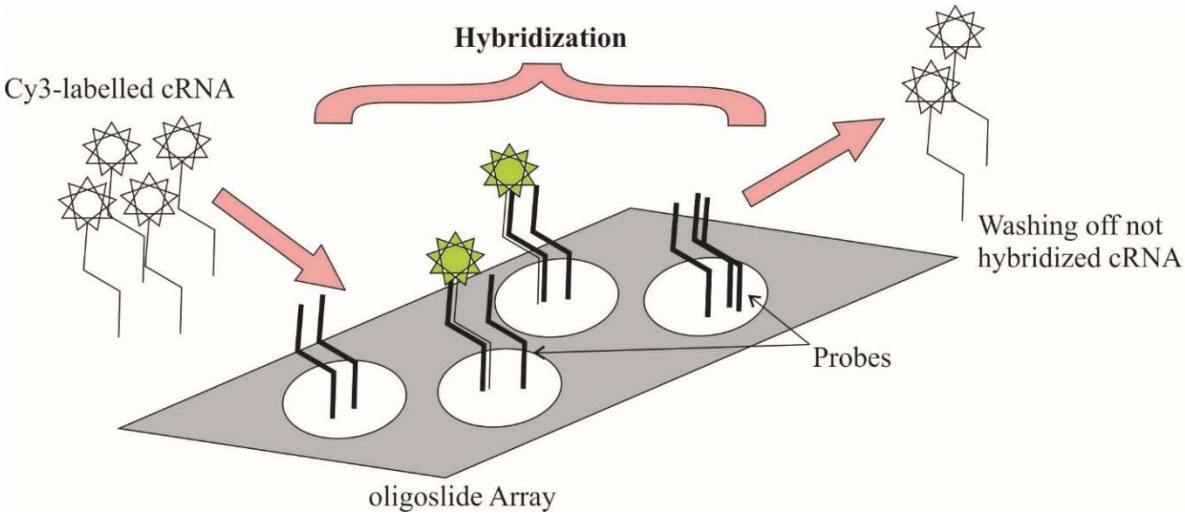

Figure II-1: Schematical illustration of microarray hybridization. Cy3-labelled cRNA is put on top of the oligonucleotide array (4x44k) and after hybridization process not hybridized cRNA is washed off. Microarrays are scanned with a 532 nm laser (green channel) for detection of Cy3-labelled probes. Graphic was established using CorelDraw X6 software.

2.5.8.6. Scanning of microarrays

The microarray scanner plays a pivotal role in the DNA microarray processing workflow and can profoundly affect the quality and reliability of microarray data (cited from agilent.com). High-throughput gene expression data from microarray experiments are collected by scanning the signal intensities of the corresponding spots on the array by dedicated fluorescence scanners. For the recent high-density microarray chips, the scanners used for imaging need to have high resolution lasers for dye excitation at different wavelengths and photomultiplier tubes (PMT) for signal detection (Schermer**,** 1999). The signal intensities are proportional to the amounts of hybridized cRNA and can be used to compare gene expression levels between different samples. The Agilent G2565CA Microarray Scanner features two lasers (SHG-YAG-Laser and Helium-Neon Laser) that can measure fluorescence intensity in the green channel (Cy3-532 nm) and in the red channel (Cy5 633 nm). It also provides an automatic PMT gain calibration prior to each scan and the dynamic range is $>10^5$ for a single scan in 20 bit scan mode (see Agilent G2565CA

Microarray Scanner System user guide on www.agilent.com). Immediately after the washing process the slides were put into slide holders provided by the company for scanning process. Scanning was performed at 3 µm scan resolution (20 bit, single pass).

2.5.9. Data analysis for microarrays

2.5.9.1. Feature extraction, filtering, normalization and statistical analysis

Processing of images generated by the scanner was performed with Feature Extraction Software 10.7.3.1 (Agilent Technologies). The computer algorithm converts the images into the numerical information that quantifies gene expression. At first, the identity of the position of the features that are arranged in a grid is found. Next, the software determines the pixels in the area of a feature which are part of the feature, and so their intensity will be counted towards a quantitative measurement of intensity at that feature. In Agilent Feature Extraction software this step is called 'variable circle segmentation' that fits a circle of variable size onto the region containing the feature. For determining if the feature intensity is significant compared to the background intensity, the 'well-above-background' test is processed. This test depends upon an estimation of background error after background subtraction which is performed via the calculation of a background surface fit. This is estimated by using negative control features and features in an intensity-range similar to the negative controls. Replicated probes were then leveled using 'intra-array variations'. The resulting processed signal intensities were subsequently filtered in MS Excel based on the 'Is well above background' flag. For the equine dataset the filter threshold was "detected in 4 of 5 samples in at least one of the five experimental groups". The filter threshold for the porcine dataset was "detection in 3 of 4, 4 of 5 and 5 of 6 samples in at least one of the five experimental groups", respectively. The processed signal intensities for the remaining features for the equine dataset were processed with the BioConductor package 'vsn' and for the porcine dataset scaled to the 75th percentile for inter-array normalization. For both data sets, a heatmap based on pair-wise distances (BioConducter package 'geneplotter') was generated for the quality control of the datasets. Significance analysis was performed using the SAM function of the 'siggenes' package (BioConducter, multiclass). For equine data the false discovery rate (FDR) was 1 % and for porcine data set 0.1%. The equine data discussed in this publication have been deposited in NCBIs Gene Expression Omnibus (GEO, http://www.ncbi.nlm.nih.gov/geo/) and are accessible through GEO Series accession number GSE39043.

In order to improve the annotation of the probes (assignment to known horse, pig and human genes) BLAT and BLAST analyses were performed using Ensembl and NCBI BLAST to obtain equine, porcine and human (putative orthologous genes), Entrez Gene identifiers and the corresponding gene information. Furthermore, for equine annotation the UCSC genome browser was used and porcine array annotation was additionally run using Bowtie, RefSeq, TIGR, and UniGene databases.

2.5.9.2. Cluster analysis and DAVID functional annotation clustering

In order to classify the obtained differentially expressed genes (DEGs) according to their gene expression profile during the equine and porcine estrous cycle, clustering with the 'Self-organizing tree algorithm' (SOTA, MeV 4.7.1, TM4 software site) was performed.

The correlation of obtained DEGs from equine and porcine gene expression analysis was estimated using MS Excel. At first the correlation coefficient was determined (=Correl r term), then the test statistic (t-value) was calculated and furthermore, to develop the significance of results, the *p*-value was defined ($p<0.05$).

Correl r: t-value:

$$r(X,Y)=\frac{\sum(x-\bar{x})(y-\bar{y})}{\sqrt{\sum(x-\bar{x})^2(y-\bar{y})^2}} \quad ; \quad t=\frac{r*\sqrt{(n-2)}}{\sqrt{(1-r^2)}} \quad ; \ \bar{x}, \bar{y} \text{ sample mean}$$

Equation II-3: Determination of significant correlated differentially expressed genes in both species.

Based on calculated significance standards (positive and negative correlation) the resulting list of DEGs was then further divided according to profile clustering from SOTA analysis. Functional classification of the DEGs was done for each expression cluster with the 'Functional annotation clustering' tool of the Database for Annotation, Visualization, and Integrated Discovery (DAVID) (Dennis et al., 2003). This analysis was performed on the basis of Entrez Gene IDs of the putative human orthologous genes. For significance statement and graphical illustration pattern throughout the equine and the porcine estrous cycle, and for positive and negative correlation analysis, the clustering was calculated in percentage using 'chart' in database software. In addition, the list of significant positive and negative correlated genes was compared to the list of differentially expressed genes in bovine endometrium (list was established by (Mitko, 2008)) to further compare gene expression patterns between different species.

2.5.10. Quantitative real–time RT-PCR (qPCR)

Amplification and simultaneous quantification of DNA was carried out by a technique called quantitative real-time reverse transcription polymerase chain reaction (qPCR). This method is based on the PCR, which is used to amplify a targeted cDNA molecule. The key feature is the detection of synthesized DNA as the reaction progresses in real time. The qPCR experiments were performed according to the StepOneTM Software V 2.1 – Protocol with SYBR Green reagent (SYBR Green I dye, Roche). The SYBR Green (fluorescence) reagent binds to the DNA whereby the fluorescence of the reagent increases. The threshold cycle (C_T), which inversely correlates with the target mRNA concentration, was measured as the cycle number at which the SYBR Green fluorescence signal appeared above the background threshold. C_T values of the target genes were normalized against the reference gene ubiquitin B (UBB). The reference gene was chosen based on corresponding literature and experience from previous studies. Additional reference genes were tested but did not show stable expression over all 5 times. All PCRs were performed in duplicates.

2.5.10.1. cDNA synthesis

The same RNA samples as for microarray analysis were used for quantitative real-time RT-PCR (qPCR). First-strand cDNA was synthesized starting from 1 µg total RNA with the Sprint^{TM} RT Complete-Double Pre Primed Kit. The total RNA was diluted in a total volume of 20 µl with distilled water and added to each well containing lyophilized reagents. The solution was gently mixed and put in a pre-warmed PCR-thermal cycler and incubated for 60 min. at 42 ° C. The reaction was terminated by heat inactivation at 70 ° C for 10 min. and 60 µl nuclease-free water was added to the cDNA samples.

2.5.10.2. Quantitative real-time PCR protocol

The quantitative real-time PCR experiments were performed in accordance to the StepOne TM Software V 2.1–Protocol type comparative Ct with SYBR Green reagent for both data sets. All PCRs were performed in duplicates in a reaction volume of 10 µl. Nine microliter of master mix solution + 1 µl of sample cDNA were put into one well on a 48 well PCR plate and covered with film (Table II-5). The plate was then gently mixed and centrifuged with Beckman centrifuge. The reaction process was continued with Step One equipment as followed: thermal

cycler profile initial denaturation at 95 ° C for 10 min followed by 40 cycles of denaturation, annealing and amplification (95°C 15 s, 60°C 1 min.). Melting curve analysis was performed with 95 ° C 15 s, 60 ° C 1 min., 95 ° C 15 s.

Component	Volume [µl] for 2 reactions
FastStart SYBR Green Master Mix (2x) (Roche)	11
Water	8.2
Forward Primer (10 pMol)	0.4
Reverse Primer (10 pMol)	0.4
Total Reaction mix Volume	20.0

Table II-VIII: Reaction mix for qPCR.Calculation was run using StepOne TM software V2.0.

2.5.11. Analysis of qPCR datasets

The threshold cycle (C_T), which inversely correlates with the target mRNA level, was measured as the cycle number at which the reporter fluorescent emission appeared above the background threshold. C_T values were normalized against the reference gene *UBB*. The further analysis of Ct–values for equine data was performed with the 'R' package LIMMA (linear models of microarray data) - a statistical analysis tool based on the F-tests. Additionally, for both datasets (equine and porcine), one–way ANOVA tests were run for analysis of significance ($P< 0.05$).

2.5.12. Analysis and purification of qPCR products

The size and the sequence of qPCR products were analyzed to confirm the amplification of target gene-specific DNA fragments. A microdialysis was used to purify qPCR products from PCR buffer components and remaining PCR primer, salts and free nucleotides. Therefore the PCR products were transferred onto a specific nuclear pore membrane (pore diameter 0.025 µm, diameter 45 mm) used as a filter. The TE buffer was diluted in a ratio of 1:4 (10 ml TE + 30 ml H_2O) with nuclease-free water and put into a petri dish. The dish was put on top of a magnetic stir plate with a magnetic stir bar. The membrane was marked and gently placed onto the diluted TE buffer. Approx. 20 µl of PCR reactions were pipetted on top of the membrane and left to dialyze for about 30–45 min. Afterwards the buffer was removed and samples were transferred from the membrane to fresh reaction vials and stored at -20 ° C until further processing. PCR products were analyzed with Agilent Bioanalyzer 2100 DNA 1000 Kit as described in 2.5.6.2.

2.5.13. „Sanger"-sequencing of purified qPCR products

The concentrations of qPCR products were measured with an Agilent Bioanalyzer 2100 as described in 2.5.6.2. Three pmol primer (forward or reverse) and 3 µl of the dialyzed qPCR product were mixed and the reaction volume was filled up with water to a total volume of 6 µl. DNA sequencing was performed on a capillary sequencer (Avant 3100) by the sequencing service of LAFUGA Genomics.

III. RESULTS

1. Peripheral plasma progesterone (P4) concentrations

1.1. Equine P4 concentrations

Table III-1 summarizes all P4 concentrations measured in each mare. For measurement of plasma progesterone (P4) concentrations, blood samples were collected in different cycles (when the corresponding biopsy was taken), except for samples on day 0.

Sample-ID	P4 concentration [ng/ml]	Sample-ID	P4 concentration [ng/ml]	Sample-ID	P4 concentration [ng/ml]
D0M1	1.2	D8M1	23.1	D16M1	1.2
D0M2	0.8	D8M2	30.0	D16M2	1.2
D0M3	1.4	D8M3	23.4	D16M3	1.2
D0M4	0.8	D8M4	21.1	D16M4	2.3
D0M5	1.0	D8M5	14.8	D16M5	3.7
D3M1	4.1	D12M1	11.0		
D3M2	6.3	D12M2	11.9		
D3M3	11.2	D12M3	12.3		
D3M4	5.0	D12M4	26.8		
D3M5	8.5	D12M5	14.7		

Table III-I: P4 concentration in each mare on five different times during estrous cycle.P4 concentrations in peripheral blood plasma were measured based on the ELFA technique. D-day, M-mare, P4-progesterone.

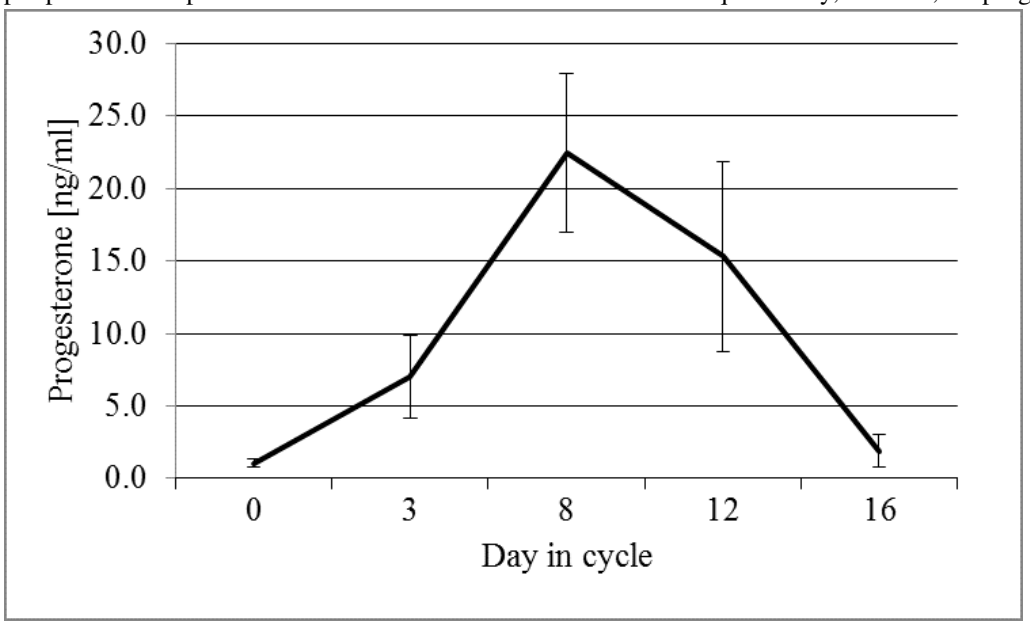

Figure III-1: Equine plasma progesterone (P4) concentrations. P4 concentrations are shown as means (ng/ml-vertical axis) with standard deviation measured in blood samples collected on each time (horizontal axis- day of the cycle) of biopsy collection. Diagramm was established in MS Excel.

Altogether, P4 concentrations were low on day 16 (1.2-3.7 ng/ml), basal on day 0 (0.8-1.4 ng/ml), rising on day 3 (4.1-11.2 ng/ml), highest on day 8 (14.8-30.0 ng/ml) and in average second highest on day 12 (11.0-26.8 ng/ml). Standard deviation of P4 concentrations was highest on days 8 and 12 (5.5 and 6.5), respectively. Results show similarity in P4 profiles between all mares on each times of the estrous cycle (calculated in mean) (Figure III-1).

1.2. Porcine P4 concentrations

Blood samples for measurement of plasma progesterone (P4) concentrations were collected from six different cycling gilts on each of the five different time points (when animals were slaughtered and endometrial tissue were taken) (Figure III-2 (means and standard deviation)). Twenty-four (labeled in grey in Table III-2) out of the 30 animals have been chosen for microarray analysis. For day 0 gilt number 23 (D0S23) was excluded because of two times higher concentrations than the remaining gilts as well as number S9 and S11 for day 3 (D3S9 and D3S11). For day 6 gilt number 13 (D6S13) was excluded because of only half as high P4 concentration. For day 12 gilts with the highest and lowest P4 concentrations were excluded (D12S21 and D12S24).

P4 concentrations showed lowest levels on day 0 (0.2-0.3 ng/ml) which are followed by increasing levels on day 3 (5.0–7.6 ng/ml) and rising till day 6 (11.2-18.1 ng/ml). Highest concentrations were reached on day 12 (25.0-35.7 ng/ml). For the samples taken on day 18, the concentration levels were decreasing (2.3-15.8 ng/ml) except for sample D18S28 (42.8 ng/ml). Standard deviation of P4 concentrations was highest on days 12 and 18 (11.9 and 14.9).

Sample-ID	P4 concentration [ng/ml]	Sample-ID	P4 concentration [ng/ml]	Sample-ID	P4 concentration [ng/ml]
D0S19	<0,2	D3S11	9.5	D12S3	34.2
D0S20	<0,2	D3S12	6.6	D12S4	14.3
D0S21	<0,2	D6S13	4.5	D12S5	25
D0S22	0.3	D6S14	11.2	D12S6	28
D0S23	0.6	D6S15	18	D18S25	2.3
D0S24	<0,2	D6S16	11.6	D18S26	3.4
D3S7	7	D6S17	16.8	D18S27	14.4
D3S8	7.6	D6S18	18.1	D18S28	42.8
D3S9	11.4	D12S1	50	D18S29	15.8
D3S10	5	D12S2	35.7	D18S30	8.1

Table III-II: P4 concentrations in each gilt on five different times during estrous cycle. Animals highlighted in grey were excluded for further processing. D-day, S-sow/gilt, P4-progesterone.

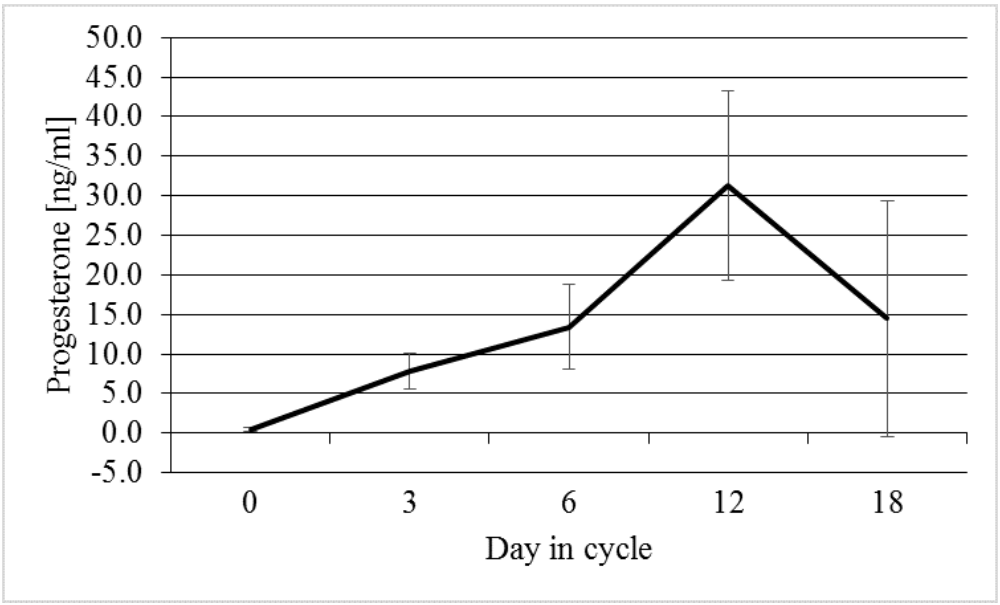

Figure III-2: Porcine plasma progesterone (P4) concentrations. Figure shows P4 concentrations for all 30 animals measured in blood samples as mean (ng/ml-vertical axis) taken at the time (horizontal axis-day of the cycle) of sample collection. Diagramm was created using MS Excel.

2. Endometrial samples

2.1. Equine endometrial samples

The volume percentage of luminal epithelium (LE), blood vessels (BV), glandular epithelium (GE) and the remaining tissue (Rest) was estimated in the endometrial biopsy samples using quantitative stereological techniques to verify similar percentages of endometrial cell types between biological replicates and to see if there are differences in percentages during the estrous cycle. The volume fractions were in a range from 0.5 % to 1.1 % for LE, from 1.4 % to 2.4 % for BV, from 30.1 % to 34.4 % for GE, and from 63.5 % to 68.1 % for the remaining tissue (Figure III-3). A trend (p=0.084) for higher volume percentage on days 12 and 16 was observed for GE. Standard deviations were higher for the observed proportions of LE and BV. Altogether, the analysis showed no statistically significant difference for all analyzed compartments between biological replicates and during the estrous cycle (Table III-3).

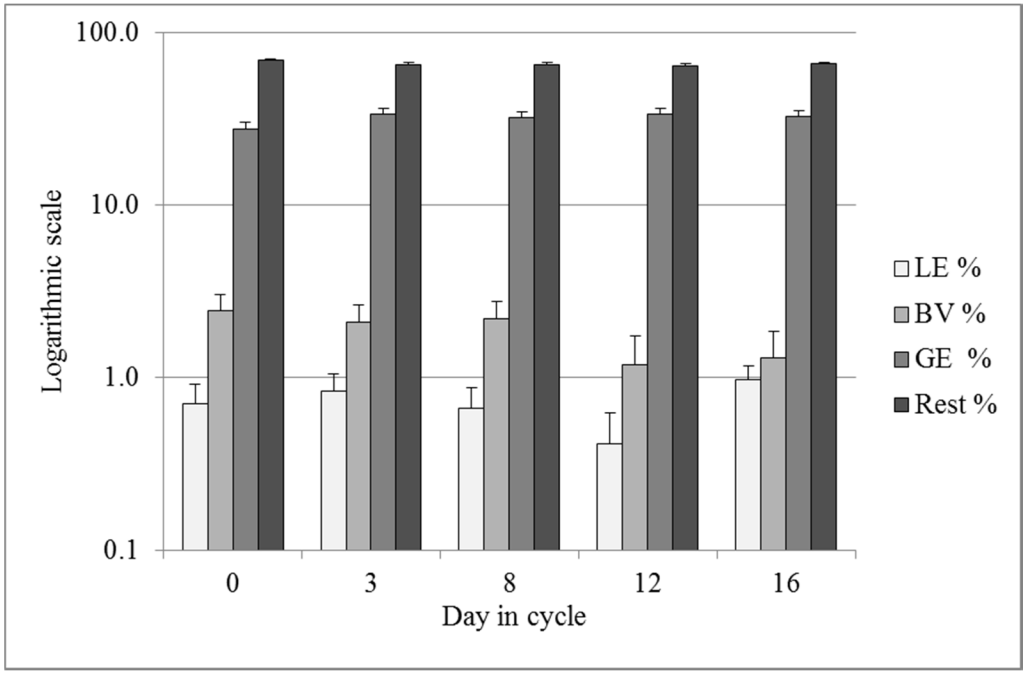

Figure III-3: Quantitative stereological analysis.Quantitative stereological analysis was performed for equine biopsy samples collected from five mares (N=5) on five different days (horizontal axis) during the estrous cycle. The volume fraction of sample tissue is calculated as mean (percentage) and presented in logarithmic scale (vertical-axis). LE-luminal epithelium, BV-blood vessels, GE-glandular epithelium, Rest-remaining tissue. Diagramme was established in MS Excel.

Sample-ID	LE [%]	BV [%]	GE [%]	Rest [%]
D16M1	1.5	1.1	31.2	66.2
D16M2	0.8	0.6	32.5	66.0
D16M3	1.2	2.1	35.0	61.7
D16M4	1.0	2.0	39.0	58.0
D16M5	0.8	1.3	32.3	65.5
D0M1	0.7	2.6	26.2	70.5
D0M2	1.1	2.5	27.7	68.7
D0M3	0.5	1.4	27.7	70.4
D0M4	0.5	2.9	33.1	63.4
D0M5	1.0	2.4	29.3	67.3
D3M1	1.1	1.5	25.1	72.2
D3M2	0.3	2.1	34.5	63.1

D3M3	0.9	2.3	30.2	66.6
D3M4	1.1	0.3	33.8	64.9
D3M5	0.8	1.9	30.8	66.5
D8M1	0.8	2.4	27.6	69.2
D8M2	0.3	1.2	24.9	73.7
D8M3	1.2	2.2	33.2	63.4
D8M4	0.3	2.2	32.6	64.9
D8M5	0.7	2.8	32.3	64.2
D12M1	0.2	0.6	30.4	68.8
D12M2	1.3	1.1	33.6	64.0
D12M3	0.2	1.2	30.5	68.1
D12M4	0.4	2.2	40.4	57.0
D12M5	0.5	2.3	37.2	60.0
ANOVA[1]	0.204	0.132	0.084	0.260

Table III-III: Results of quantitative stereology.LE: luminal epithelium; BV: blood vessels; GE: glandular epithelium; Rest: remaining tissue; %: volume percent, [1] ANOVA- Analysis of Variance of p-values.

2.2. Porcine endometrial samples

The endometrium of gilts slaughtered on day 0 showed no abnormality. Eleven early CLs in the left ovary from gilt number S9 and S11 were found on day 3 (D3S9 and D3S11) of the estrous cycle. In addition, the endometrium of D3S9 was very much vascularized and the uterus was also very, very small. In general, the uteri of all animals on day 3 were very small (just as one of animals on day 6 compared to others). The uterus of D6S13 hardly showed any vascularization. It was suspected that the stage of D6S13 did not correspond to day 6 but seemed more likely to be from day 0. P4 concentration reflected this statement. Sample collection protocol for day 12 (D12S01-S06) showed 'not OK' for D12S04. The left ovary contained only five CL's but very little ones figuring together like 'raspberry-shaped'. D12S01 showed 23 CL's in the right and 21 CL's in the left ovary. Therefore, the very high P4 concentration in D12S01 and the very low P4 concentration in D12S04 corresponded with the status of the ovaries. Sample collection on day 18 revealed very well developed uteri with a very gelatinous mucosa for animals D18S25-D18S27. Twenty-two CL's were counted in the left ovary of animal D18S28 in contrast to 9 CL's as in the remaining animals on day 18. This is in agreement with the almost three times higher P4 value in this animal compared to the animals D18S27 and D18S29. The P4 concentration was even 10 times higher than in the remaining animals on day 18.

2.3. Isolation of RNA

2.3.1. Isolated RNA from equine samples

Results of RNA isolation from all 25 equine biopsy samples showed stable values for 260/280 ratios but a tendency to higher rates for 260/230 ratios. The RIN values showed middle based position ranging from 6.8 to 9.4. The RIN of sample D3M5 was the lowest with 6.80 and D3M3 showed highest RIN value of 9.4 (Table III-4).

Sample ID	Concentration RNA [ng/µl]	260/280 nm	260/230 nm	RIN
D0M1	606	1.95	2.26	8.3
D0M2	939	1.97	2.33	7.6
D0M3	928	2.00	2.33	9.0
D0M4	718	1.94	1.92	8.1
D0M5	724	1.95	2.30	8 3

D3M1	1457	2.00	2.31	9.3
D3M2	1556	1.98	2.27	8.4
D3M3	188	1.99	2.17	8.6
D3M4	1997	1.99	2.29	9.4
D3M5	1717	2.00	2.20	6.8
D8M1	1073	1.99	2.25	9.0
D8M2	2081	1.94	2.12	8.2
D8M3	2053	1.98	2.21	8.9
D8M4	2133	1.98	2.15	8.9
D8M5	1876	1.99	2.17	6.9
D12M1	1204	1.99	2.29	8.2
D12M2	1035	1.98	2.25	8.3
D12M3	1446	2.00	2.25	7.1
D12M4	1426	2.00	2.23	8.6
D12M5	1698	1.98	2.14	8.9
D16M1	930	1.99	2.18	8.4
D16M2	745	1.93	2.02	7.6
D16M3	845	1.97	2.32	8.6
D16M4	912	1.93	2.05	8.1
D16M5	762	1.95	2.21	7.3

Table III-IV: Concentration, spectotrophomatrical analysis and RIN of equine RNA samples.RIN-RNA integrity number, D-day, M-mare.

2.3.1. Isolated RNA from porcine samples

In average the 90 porcine samples showed stable values for 260/280 ratios but, as with the equine samples, a tendency to higher rates for 260/230 ratios. The RIN values showed good ranges (from 7.9 to 10.0) (Table III-5).

Sample ID	Concentration RNA [ng/µl]	260/280 nm	260/230 nm	RIN
D12S1-f	1258	1.94	2.33	8.6
D12S1-m	953	1.92	2.24	9.0
D12S1-b	1079	1.98	2.00	9.5
D12S2-f	1518	2.04	1.88	9.7
D12S2-m	1049	2.04	1.26	9.4
D12S2-b	840	1.97	1.99	7.9
D12S3-f	879	1.99	1.85	9.5
D12S3-m	988	1.90	2.33	9.6
D12S3-b	1221	1.92	2.3	9.5
D12S4-f	1115	1.99	2.03	9.4
D12S4-m	233	2.01	1.52	9.8
D12S4-b	355	1.8	2.48	8.8
D12S5-f	1597	2.02	1.90	10
D12S5-m	1204	2.04	1.61	8.0
D12S5-b	1030	2.05	1.84	9.6
D12S6-f	1199	2.05	1.58	9.2
D12S6-m	1492	2.02	1.76	9.2
D12S6-b	1455	2.00	2.04	9.4
D3S7-f	1471	1.98	2.28	10
D3S7-m	2614	1.9	2.02	10
D3S7-b	1465	1.97	2.17	8.0

D3S8-f	1299	1.97	2.11	8.1
D3S8-m	1258	2.01	1.82	8.2
D3S8-b	1251	1.97	1.79	8.2
D3S9-f	2558	1.93	2.21	8.4
D3S9-m	2268	1.94	2.19	8.3
D3S9-b	2535	1.89	2.06	8.1
D3S10-f	1140	1.97	1.95	10
D3S10-m	1893	1.95	2.16	10
D3S10-b	1587	1.98	2.06	10
D3S11-f	1120	1.95	2.32	10
D3S11-m	2341	1.96	2.03	10
D3S11-b	1427	2.01	1.80	10
D3S12-f	1885	1.97	2.13	10
D3S12-m	2190	1.95	2.14	10
D3S12-b	2467	1.93	2.07	10
D6S13-f	1138	2.01	1.99	10
D6S13-m	1118	2.02	2.21	10
D6S13-b	748	1.98	1.22	10
D6S14-f	1574	1.98	1.97	9.7
D6S14-m	1021	2.06	1.94	9.6
D6S14-b	1701	1.95	2.06	9.8
D6S15-f	1381	2	1.86	9.6
D6S15-m	1444	2.02	1.99	9.1
D6S15-b	1129	2.01	1.64	9.3
D6S16-f	1314	2	2.18	10
D6S16-m	724	2.05	1.63	9.1
D6S16-b	1364	2.05	1.47	9.6
D6S17-f	2147	1.92	2.17	10
D6S17-m	1406	1.99	1.96	10
D6S17-b	1069	2	1.54	10
D6S18-f	2048	1.92	2.38	8.9
D6S18-m	1772	1.96	2.28	9.0
D6S18-b	2459	1.91	2.11	9.2
D0D19-f	2166	1.93	2.22	10
D0S19-m	725	2	1.95	10
D0S19-b	402	1.93	1.94	10
D0D20-f	1025	1.94	1.94	9.9
D0S20-m	989	1.98	2.13	9.7
D0S20-b	804	2.01	1.98	9.9
D0D21-f	1139	1.98	1.97	9.8
D0S21-m	1318	1.94	1.98	9.8
D0S21-b	1171	1.96	2.09	10
D0D22-f	1202	1.94	2.05	10
D0S22-m	1871	1.94	2.06	10
D0S22-b	1839	1.99	2.03	10
D0D23-f	1156	1.93	1.77	9.8
D0S23-m	1593	1.94	2.07	9.8
D0S23-b	2139	1.94	2.06	9.9
D0D24-f	629	1.87	2.15	9.8

D0S24-m	1499	1.95	1.95	9.8
D0S24-b	910	1.97	2.05	9.7
D18S25-f	417	1.89	2.3	9.5
D18S25-m	537	1.99	2.77	9.5
D18S25-b	280	1.91	1.8	9.4
D18S26-f	639	2.04	2.67	9.4
D18S26-m	713	1.99	2.7	9.4
D18S26-b	701	1.99	2.6	9.2
D18S27-f	842	1.94	2.02	9.0
D18S27-m	813	1.92	2.54	8.9
D18S27-b	870	1.94	2.03	9.5
D18S28-f	653	1.93	2.62	8.9
D18S28-m	341	1.82	2.35	8.8
D18S28-b	348	1.8	2.37	8.5
D18S29-f	375	1.8	2.34	8.5
D18S29-m	2063	1.92	2.22	9.3
D18S29-b	718	1.93	2.66	9.3
D18S30-f	1184	1.95	2.03	9.7
D18S30-m	832	1.95	2.04	9.8
D18S30-b	418	1.89	1.85	9.8

Table III-V: Concentration, spectotrophomatrical analysis and RIN of porcine RNA samples.RIN-RNA integrity number, D-day, S-sow, f-front, m-middle, b-back

3. Microarray data

3.1. Microarray analysis of equine endometrium during the estrous cycle

The 4x44 Horse Genome microarray was run according to manufacturer's protocol. Due to manufacturer's problems with quality of some components of the labeling kit, several kits had to be run with different lot numbers. The cRNA samples with best Cy3 incorporation and cRNA yield from same endometrial samples were pooled together for best results.

3.1.1. Heatmap

After data processing and normalization the microarray data set was initially analyzed with a heatmap based on pairwise distances (Figure III-4). Samples collected on day 8 as well as samples from day 12 clustered together in separate groups clearly distant from the samples collected on day 16, day 0, and day 3. Also the samples from day 0 and day 3 formed relatively homogeneous groups. Samples from day 16 were the most heterogeneous group, where 4 samples clustered together and one (D16M1) was more similar to samples from day 0.

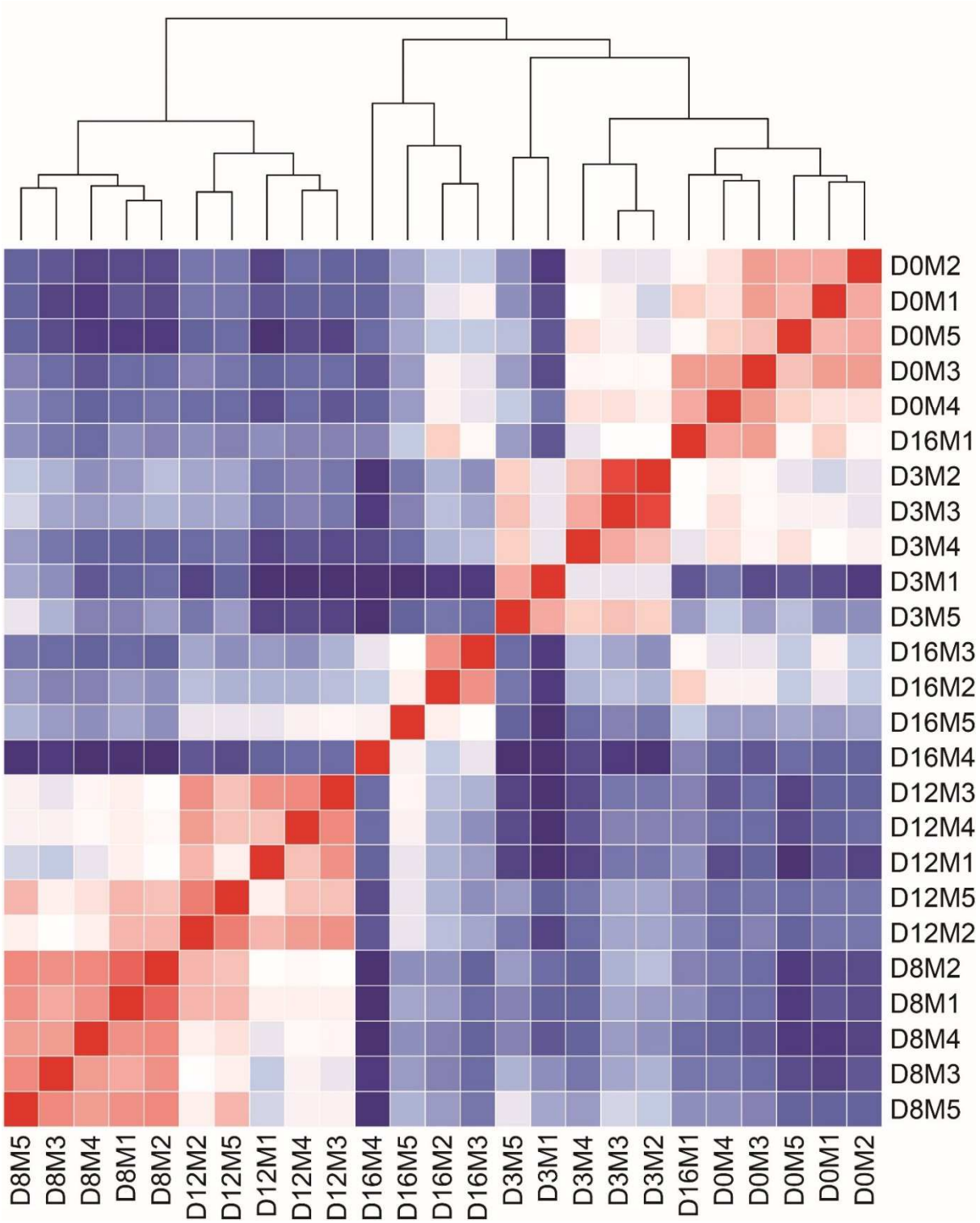

Figure III-4: Heatmap of pairwise distances from equine microarray data set. Pairwise distances were calculated based on the normalized signal intensities of the differentially expressed probes. Each column represents one sample and shows the distance to all samples (including itself) with red for distance = 0 and dark blue for the highest observed distance. Illustration was edited with CorelDraw X6 software and results have been published by Gebhardt and coworkers (Gebhardt et al., 2012). D-day, M-mare.

3.1.2. Clustering of similar mRNA expression profiles (MeV/SOTA)

For identification of differentially expressed genes and estimation of the false discovery rate (FDR), SAM (Significance Analysis of Microarrays, (Tusher, 2001)) was used which is a part

of the R package Siggenes. Statistical analysis of microarray data revealed almost 10,000 differential probes (siggenes, multiclass, FDR 1 %). These microarray probes represented approx. 4,996 different genes/transcripts which are listed in supplementary data. For classifying these genes according to their gene expression during the estrous cycle a clustering based on similarity in expression profiles (MeV, SOTA algorithm) was performed (Figure III-5- see next page).

This mRNA expression profiling analysis revealed eight major expression profiles. In cluster 1 (637 genes) the genes showed in average highest expression levels on day 0 and low levels during the luteal phase. Expression of some of these genes already increased on day 16. The genes in cluster 2 (582 genes) showed mRNA expression profiles with highest levels from day 0 to day 3 and low levels from day 8 to day 16. Expression of the majority of genes in cluster 3 (721 genes) peaked on day 3. For the genes in cluster 4 (501 genes) highest mRNA levels were found from day 3 to day 8. In cluster 5 (701 genes) the genes showed profiles that are similar to those in cluster 4 but with later increase and higher levels up to day 12. Cluster 6 (709 genes) displayed higher mRNA expression levels from day 8 to day 12 and lowest levels on the remaining days of the estrous cycle. The highest expression levels in cluster 7 (501 genes) were found on day 12 with a slight decrease to day 16 and lower levels on day 0, day 3 and day 8. Genes clustering together in in cluster 8 (644 genes) showed highest mRNA levels on day 16 and lowest levels on day 3 and day 8.

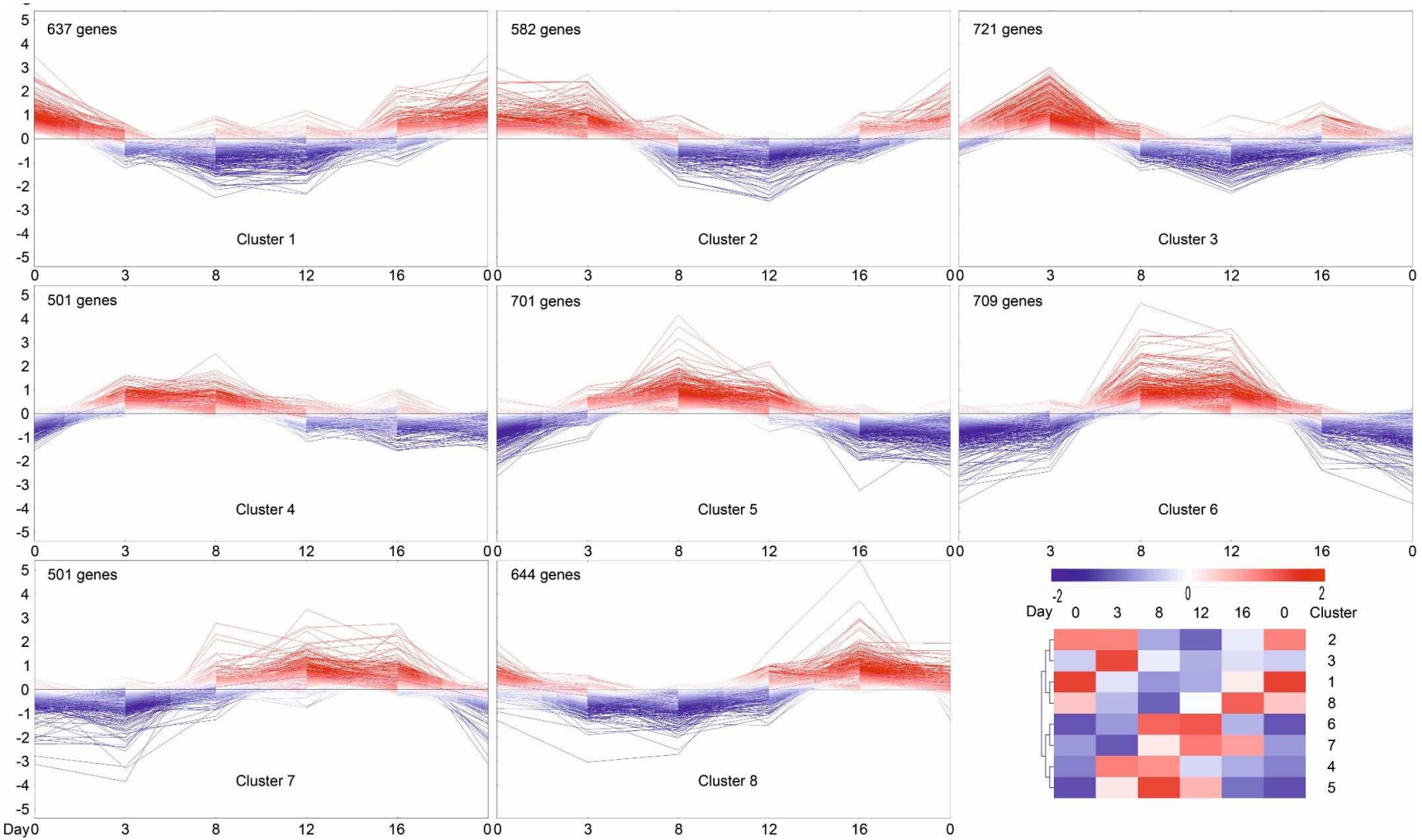

Figure III-5: Clustering based on similarity in gene expression profiles during the equine estrous cycle Relative gene expression levels during the estrous cycle were obtained for all differentially expressed genes by calculation of mean-centered expression values (vsn-normalized value of one time point minus mean of vsn-normalized values of all 5 time points, vsn-normalized values are in log2 scale). Self-organizing tree algorithm (SOTA) of MeV software (version 4.7.1) was used to obtain groups of genes with similar expression profiles. Vertical axis is in log2 scale and shows the deviation from the mean expression during the estrous cycle. Horizontal axis shows the day of the estrous cycle. The SOTA dendrogram (bottom right) shows the similarity between clusters and mean expression changes during the cycle. Figure was edited in CorelDraw X6 and previously published in Gebhardt et.al (Gebhardt et al., 2012).

3.1.3. Functional annotation clustering

In order to characterize molecular functions and assigned biological processes as over-represented during different phases of the estrous cycle, functional annotation clustering (DAVID) was performed for the individual clusters of genes with similar expression profiles obtained by SOTA clustering. This analysis resulted in a relatively large number of significant annotation clusters of related functional terms that represented distinct over-represented functions/processes for different cycle stages. For graphical illustration of these processes a diagram based on the frequency patterns (numbers of genes on different cycle stages) during the cycle was plotted (Figure III-6). The selected functional categories were clustered according to their frequency patterns during the estrous cycle. Total results of DAVID functional annotation charts (Category/Term, Genes, FDR, P-values, and Enrichment score) are provided in supplementary data.

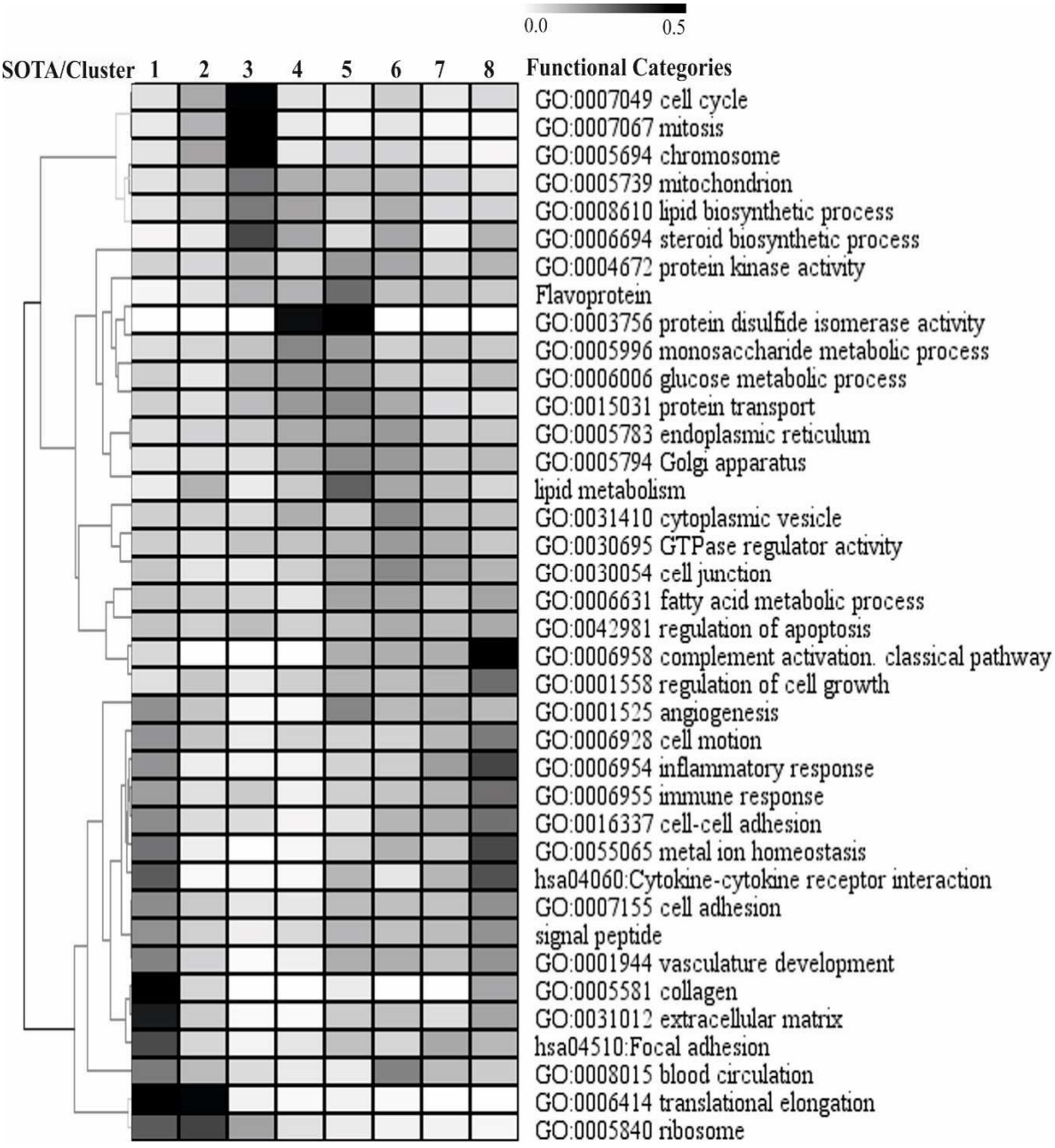

Figure III-6: Representation of selected functional categories/terms during the equine estrous cycle. Functional terms over-represented during distinct phases of the estrous cycle were selected from DAVID functional

annotation clustering analysis. Numbers of genes assigned to these functional terms (in rows) are shown for each SOTA cluster (in columns) as percentage of the number of all differentially expressed genes assigned to a term (white = 0 %; black = 50 %). SOTA cluster with highest RNA expression: 1- on day 0, 2-from day 0 to day 3, 3- on day 3, 4-from day 3 to day 8, 5- on day 8, 6- from day 8 to day 12, 7-from day 12 to day 16 and 8- on day 16. Graphic was edited using CorelDraw X6 software.

In Figure III-6 the genes in Cluster 1 (highest mRNA expression levels on day 0) represented processes related to functional categories like 'collagens', 'extracellular matrix (ECM)', 'focal adhesion' and 'translational elongation'. Highest numbers of genes were found for Cluster 2 (genes with highest expression levels from day 0 to day 3) as related to the categories 'translational elongation' and 'ribosome'. Specifically for cluster 3 (highest expression levels on day 3), categories related to 'cell cycle', 'mitosis', and 'chromosome' were highly overrepresented and showed highest numbers of genes. The category 'protein disulfide isomerase activity' showed a likewise distinctive pattern and was represented only in SOTA Clusters 4 and 5 (3 and 4 genes, respectively). Cluster 4 represents genes with highest expression from day 3 to day 8 and Cluster 5 genes with highest mRNA expression on day 8. Cluster 6 represented genes with highest mRNA levels from day 8 to day 12. Functions and processes, such as metabolic processes (lipids, fatty acid, glucose), secretory processes (vesicles, endoplasmic reticulum, Golgi) and cell junctions showed numerous genes with highest mRNA expression during the luteal phase (SOTA clusters 4, 5 and 6). Furthermore, the analysis of Cluster 7 (highest mRNA expression from day 12 to day 16) revealed overrepresentation of categories like' focal adhesion'. Cluster 8 (highest mRNA levels on day 16) showed over-representation for the functional terms 'immune response', 'complement activation, classical pathways', 'collagens' and 'regulation of cell growth'. Some functional categories showed a kind of biphasic pattern of their representation during the estrous cycle, such as 'angiogenesis' and 'blood circulation' with highest numbers of genes during estrus (on day 0) and during the luteal phase, respectively.

3.1.4. Genes involved in prostaglandin metabolism and signaling and in steroid hormone signaling

Genes involved in prostaglandin metabolism and signaling and in progesterone and estrogen signaling play an important regulatory role during the estrous cycle. Related genes were obtained from corresponding Gene Ontology categories (www.geneontology.org), a search in the Entrez Gene database (www.ncbi.nlm.nih.gov/gene) and in the literature, respectively. For steroid hormone signaling, only selected genes were used, e.g. classical and non-classical hormone receptors and related receptors and some genes encoding steroid hormone metabolic enzymes. Relative expression values of DEGs matching this candidate list were subjected to hierarchical clustering for gene expression during the estrous cycle in equine endometrium for a cluster analysis (Figure III-7).

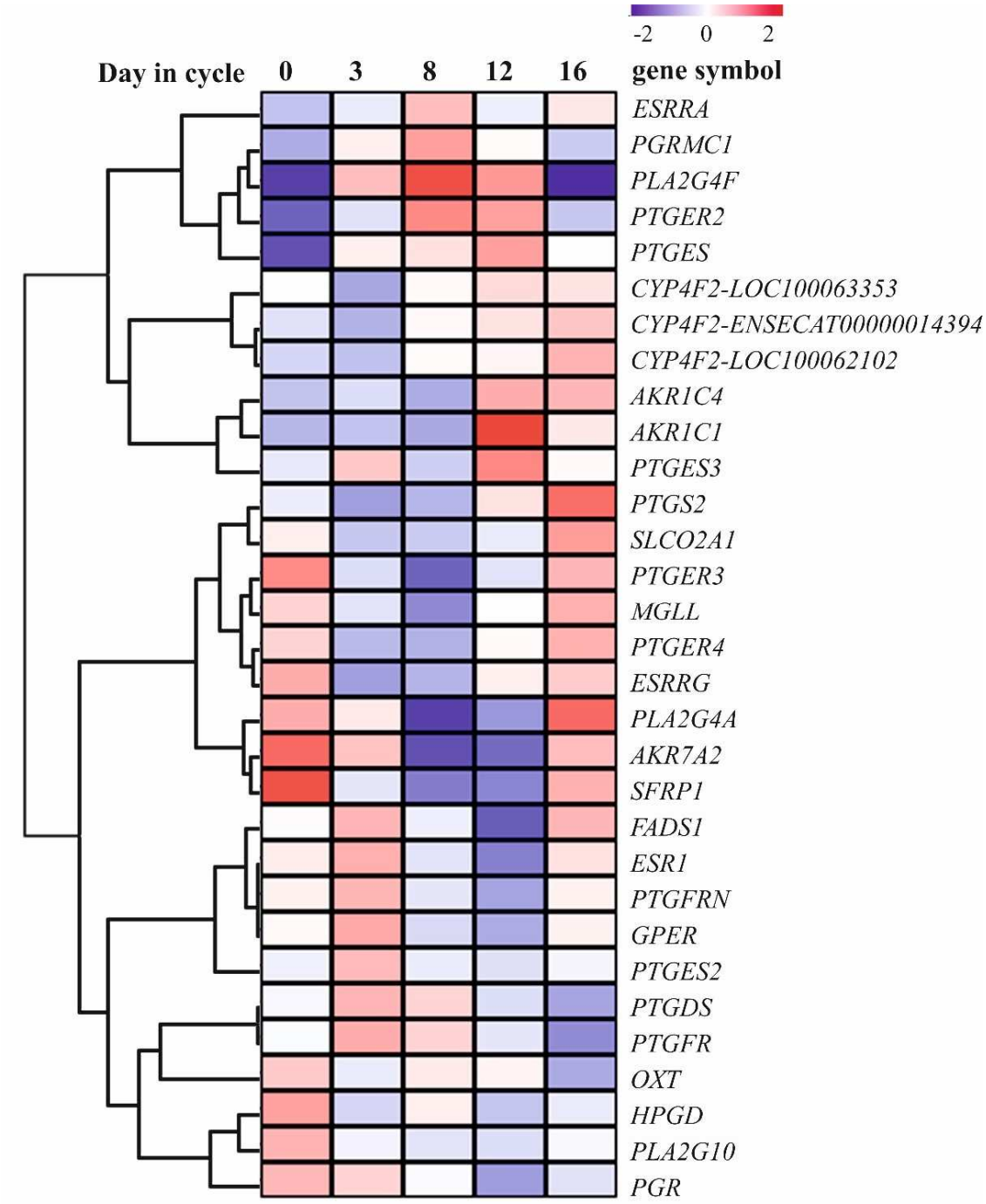

Figure III-7: Heatmap of genes related to prostaglandin metabolism and signaling and to steroid hormone signaling. Figure shows hierarchical clustering of gene expression during the estrous cycle in equine endometrium (MeV software, version 4.9.0). Color scale is from 4-fold lower (log2-fold=-2) than the mean (blue) to 4-fold higher (log2-fold=2) than the mean (red). Graphic was edited using CorelDraw X6 software.

These genes showed a variety of distinct expression profiles during the cycle. Estrogen-related receptor alpha (*ESRRA*) and gamma (*ESRRG*) mRNAs showed completely different expression changes during the cycle compared to the classical nuclear receptors, so did progesterone receptor membrane component 1 (*PGRMC1*). In contrast, Estrogen receptor 1 mRNA (*ESR1*) showed a very similar profile to G protein-coupled estrogen receptor 1 mRNA (*GPER*) with highest levels on day 3 and lowest on day 12, whereas progesterone receptor mRNA (*PGR*) had highest expression on day 0 decreasing to day 12. Messenger RNA levels of prostaglandin E synthases (*PTGES, PTGES2, PTGES3*) were in average highest during the luteal phase whereas PGE receptor mRNAs (*PTGER2, PTGER3, PTGER4*) showed completely different expression

profiles. Most of the genes involved in arachidonic acid metabolism had their highest mRNA levels at estrus. Prostaglandin D2 synthase 21kDa (*PTGDS)* mRNA showed highest levels on day 0 and on day 3. Additionally, oxytocin, prepropeptide (*OXT*) mRNA showed highest expression on day 0 and lowest on day 16. Interestingly, hydroxyprostaglandin dehydrogenase 15- (NAD) (*HPGD*) which is known to metabolize prostaglandins was also regulated during the estrous cycle with highest levels on day 3 and on day 0. Some of the results have been published by Gebhardt and coworkers (Gebhardt et al**.,** 2012).

3.1.5. Genes related to 'regulation of apoptosis'

A manageable number of genes related to the regulation of apoptotic functions were found as over-represented (18 genes in total) whereof one third was up-regulated during estrus phase (baculoviral IAP repeat containing 3, *BIRC3,* caspase 7, apoptosis-related cysteine peptidase *CASP7,* interleukin 1 receptor, type I, *IL1R1,* interferon regulatory factor 1, *IRF1,* mitogen-activated protein kinase kinase kinase 14, *MAP3K14,* and phorbol-12-myristate-13-acetate-induced protein 1, *PMAIP1*), three genes showed highest mRNA expression during early luteal phase (cytochrome c, somatic, *CYCS,* endonuclease G, *ENDOG,* and helicase, lymphoid specific, *HELLS*) and the remaining genes were up-regulated during the luteal phase (BCL2-like 1, *BCL2L1,* BCL2/adenovirus E1B interacting protein 3-like, *BNIP3L,* granzyme B (granzyme 2, cytotoxic T-lymphocyte-associated serine esterase 1), *GZMB,* insulin-like growth factor 1 receptor, *IGF1R,* interleukin-1 receptor-associated kinase 4 and 2, *IRAK4/2,* myelocytomatosis oncogene, *MYC,* and TNFRSF1A-associated via death domain, *TRADD*). For apoptosis signaling, candidate genes were found using www.wikipathways.com and compared to the list of DEGs found in equine endometrium (Table III-8).

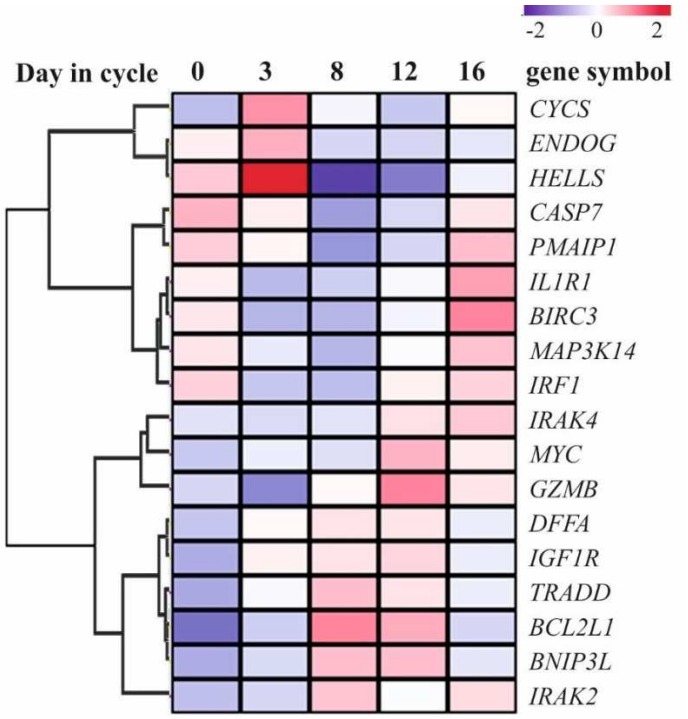

Figure III-8: Heatmap of expression profiles for genes related to 'regulation of apoptosis'. Relative expression values of differentially expressed genes matching the apoptosis candidate list were subjected to hierarchical clustering for gene expression during the estrous cycle in equine endometrium (MeV software, version 4.9.0). Color scale is from 4-fold lower (log2-fold=-2) than the mean (blue) to 4-fold higher (log2-fold=2) than the mean (red). Graphic was edited using CorelDraw X6 software.

3.1.6. Genes related to angiogenesis, blood circulation and vasculature development

The functional categories 'angiogenesis', 'blood circulation' and 'vasculature development' found as over-represented during the estrous cycle were obtained from corresponding Gene Ontology categories, search in Entrez Gene, WikiPathways, KEGG database and in literature. Relative expression values of differentially expressed genes matching this candidate list were subjected to hierarchical clustering for gene expression during the estrous cycle in equine endometrium (Figure III-9).

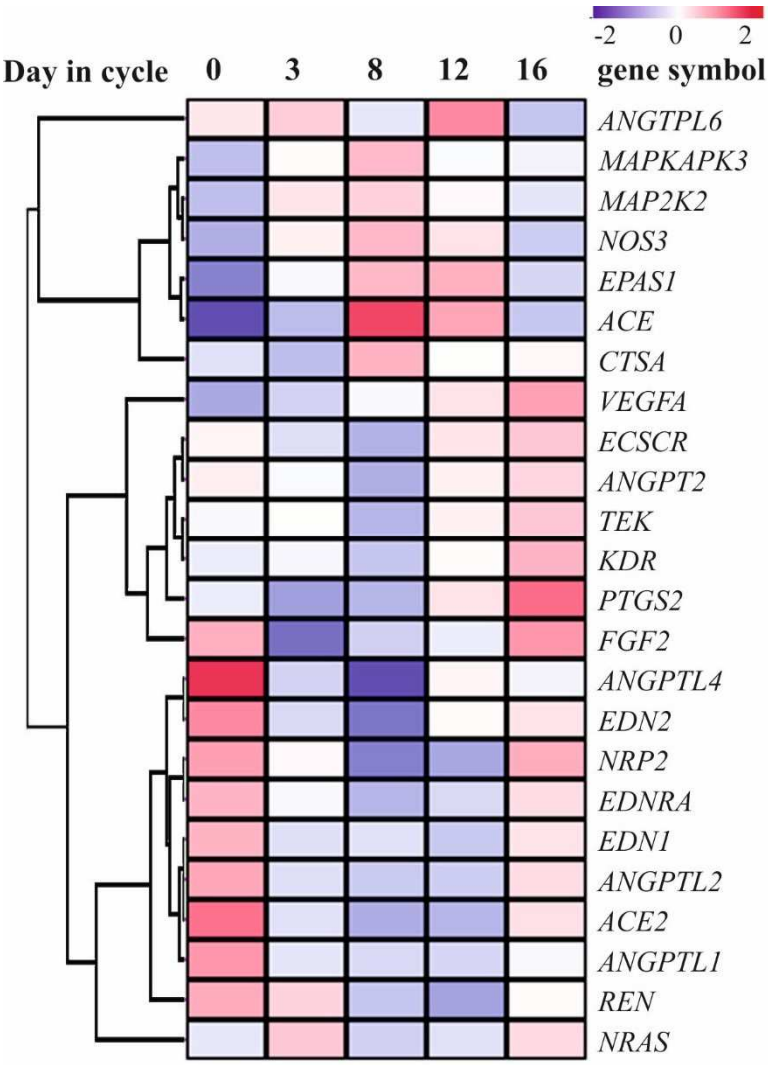

Figure III-9: Graphical illustration of mRNA expression profiles of genes related to 'angiogenesis', 'blood circulation' and 'vasculature development'. Heatmap was established using MeV software (V 4.9.0). Color scale is from 4-fold lower (log2-fold=-2) than the mean (blue) to 4-fold higher (log2-fold=2) than the mean (red). Graphic was edited using CorelDraw X6 software.

Most of the genes showed up-regulation during the estrus phase (17 out of 24 genes). Angiopoietin-like 6 (*ANGPTL6*) showed highest expression on day 3 and on day 8. During luteal phase 6 genes were up-regulated. Two of these genes (mitogen-activated protein kinase 2, *MAP2K2* and nitric oxide synthase 3, *NOS3*) showed already up-regulation on day 3, highest expression on day 8 and slightly expression on day 12. Angiotensin I converting enzyme (*ACE*) and endothelial PAS domain protein 1 (*EPAS1*) were up-regulated on day 8 and on day 12.

3.2. Microarray analysis of porcine endometrium during the estrous cycle

3.2.1. Heatmap

The normalized dataset (differentially expressed genes from Significance analysis of microarrays (SAM)) was used for calculation of pairwise distances and drawing a heatmap (Figure III-10). The heatmap clearly demonstrates a homogenous group clustering of samples collected on day 0, day 3, day 6 and day 12. Samples collected on day 18 were clearly more heterogenous with two samples (D18S25 and D18S26) separated from the other 4 samples in this group.

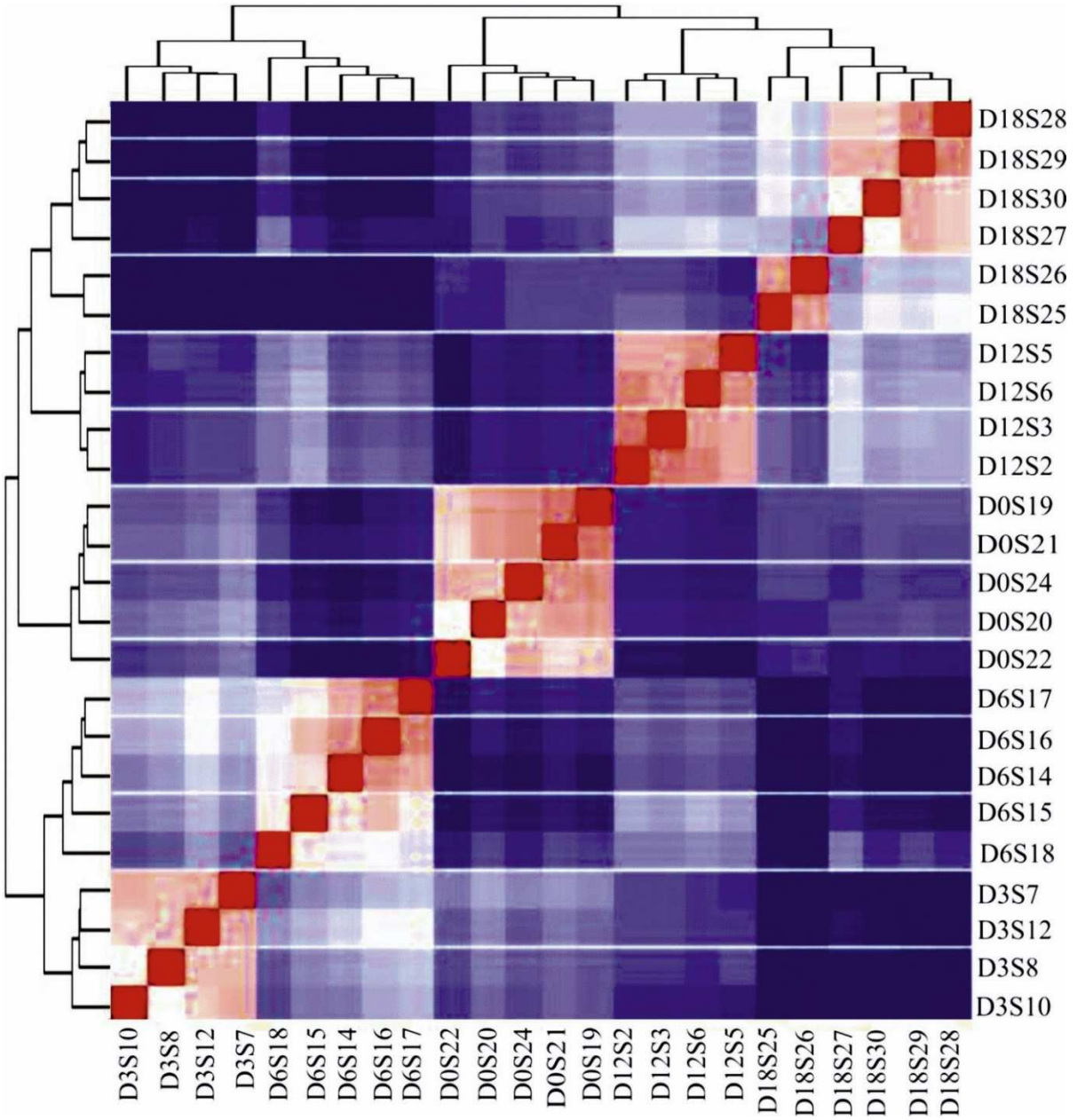

Figure III-10: Heatmap of pairwise distances from porcine microarray data set. One sample is represented by one column that demonstrates the distance to all samples (including itself) with red for distance = 0 and dark blue for the highest observed distance. Illustration was edited with CorelDraw X6 software. D-day, S-sow.

3.2.2. Clustering of similar mRNA expression profiles (MeV/SOTA)

For the identification of differentially expressed genes, the data set was analyzed using the same bioinformatics tools as for the equine data set. The microarray probes represented 9,275 different genes/transcripts as listed in supplementary data. A cluster analysis based on similarities in gene expression during the estrous cycle was performed using corresponding software (MeV, SOTA algorithm) (Figure III-11-see next page).

Eight major expression profiles have been established. The first Cluster (1244 genes) shows mRNAs with highest levels at estrus (day 0) and very low levels during metestrus, diestrus and preestrus. In the second Cluster (849 genes) highest mRNA expression levels were observed in the phase from day 0 to day 3. Cluster 3 (897 genes) contained genes with highest mRNA expression on day 3 with increased levels on day 0 and lowest expression levels during late luteal phase. Messenger RNA levels in Cluster 4 (3163 genes) showed highest number of genes in total. In this Cluster, levels started to decrease on day 12 and were lowest on day 18 and day 0. The highest mRNA levels in Cluster 5 (421 genes) spanned from day 6 to day 12 with low increase on day 18 and showed low levels on day 0 and day 3. In Cluster 6 (448 genes) mRNA expression profiles showed highest levels on day 12 and minor levels on day 6 and day 18. Messenger RNA levels in Cluster 7 (421 genes) were higher from day 12 to day 18 and showed lowest expression during estrus (day 0). The last Cluster (Cluster 8) contained 1109 genes. Their mRNA levels were very low on day 6 and showed highest expression from day 18 to day 0.

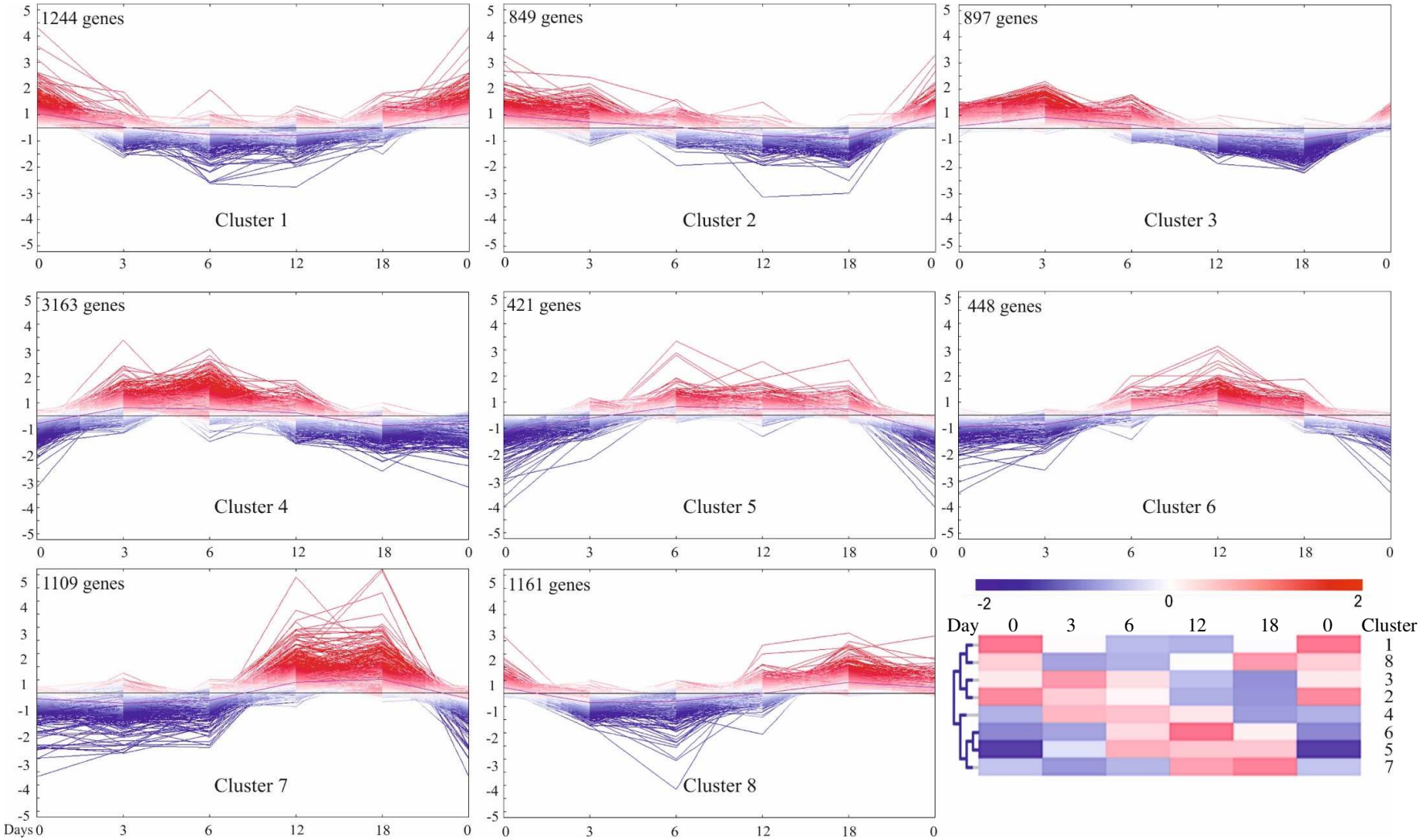

Figure III-11: Clustering of genes with similar gene expression profiles in porcine endometrium during the estrous cycle. Calculation of mean centered expression values (normalized value of one time point minus mean of normalized values of all 5 time points) revealed relative gene expression levels during the estrous cycle for the differentially expressed genes. MeV software (SOTA version 4.8.1) was used to obtain clusters of genes with similar expression profiles. The SOTA dendrogram (bottom right) shows the similarity between clusters and mean expression changes. Vertical axis is in log2 scale and shows the deviation from the mean expression during the estrous cycle. Horizontal axis shows the day of the estrous cycle. Graphic was edited with CorelDraw X6 software.

3.2.3. Functional annotation clustering

The characterization of molecular functions and biological processes over-represented during different phases of the porcine estrous cycle was performed using functional annotation clustering (DAVID) for the clusters of genes with similar expression profiles that were obtained by SOTA clustering. The results revealed numerous significant annotation clusters of related functional categories representing distinct over-represented processes on different times during the cycle (Figure III-12-see next page).

In Clusters 1 and 2 (highest levels on day 0 and from day 0 to day 3) processes related to 'collagens', 'immune response' and 'cell adhesion' were highly over-represented. In addition, genes assigned to the category 'angiogenesis' and 'vasculature' were over-represented in cluster 1. This category, interestingly, showed three peaks in numbers of genes during the cycle: on day 0, from day 3 to day 6 and from day 12 to day 18. Specifically for Cluster 3 (highest expression levels on day 3) categories related to 'mitosis', 'cell cycle' and 'chromosome' showed highest numbers of genes. Functions and processes, such as metabolic processes (lipids, fatty acid, glucose), secretory processes (vesicles, endoplasmic reticulum, Golgi apparatus) and cell junctions showed numerous genes with highest mRNA expression during early luteal phase (SOTA cluster 4, highest level from day 3 to day 6). 'Lipid metabolism' was over-represented in cluster 5 (highest mRNA expression from day 6 to day 12) and with the second highest number of genes in Cluster 6 (highest level on day 12). For Cluster 8 (representing genes with highest expression on day 18) genes assigned to categories such as 'collagens', and 'immune response' were over-represented (see supplementary data).

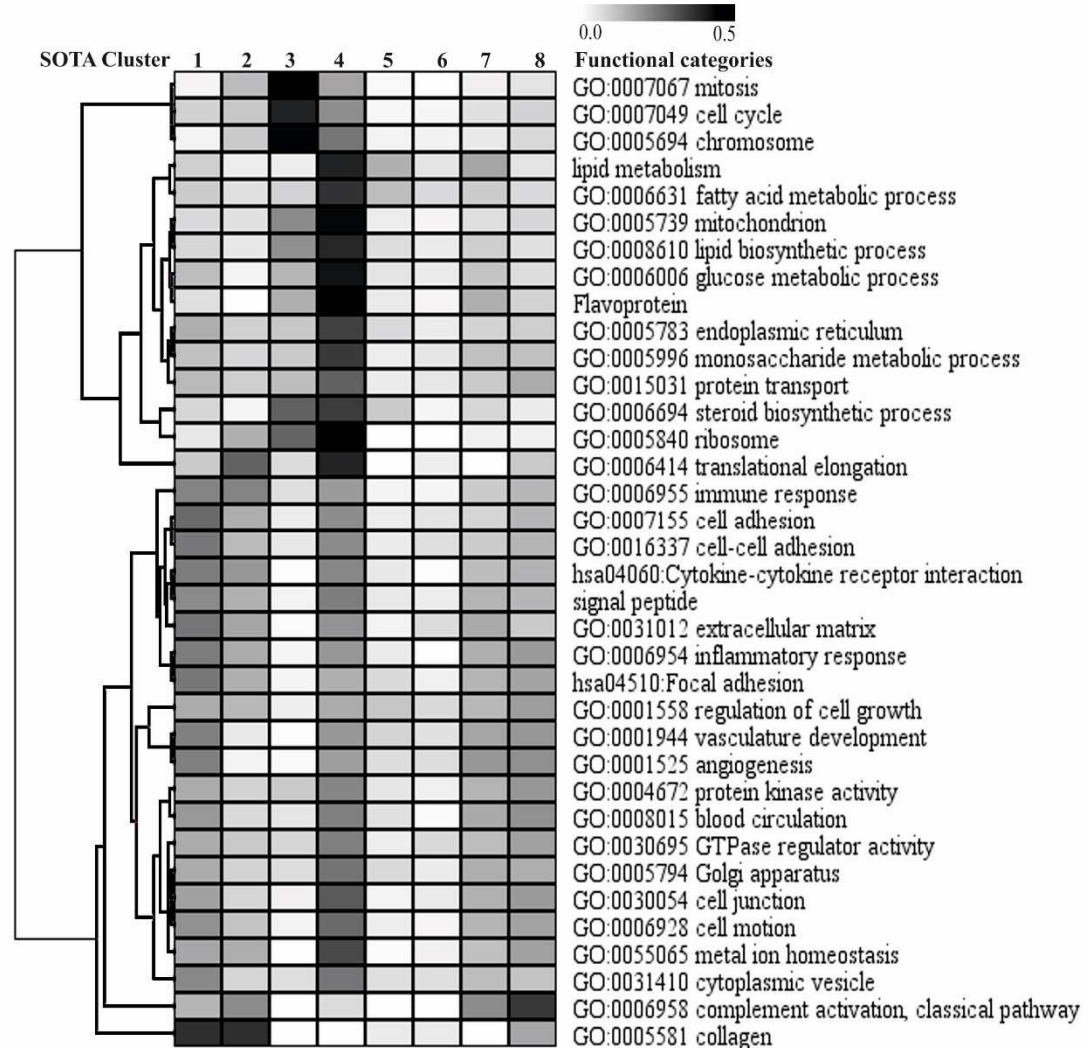

Figure III-12: Heatmap with selected functional categories/terms during the porcine estrous cycle. Functional terms over-represented during distinct phases of the estrous cycle were selected from DAVID functional annotation clustering analysis. Numbers of genes assigned to these functional terms (in rows) are shown for each SOTA cluster (in columns) as percentage of the number of all differentially expressed genes assigned to a term (white = 0 %; black = 50 %). SOTA-Cluster with highest gene expression: 1- on day 0, 2-from day 0 to day 3, 3- on day 3, 4-from day 3 to day 6, 5- from day 6 to day 12, 6- on day 12, 7-from day 12 to day 18 and 8- on day 18. Graphic was edited using CorelDraw X6 software.

3.2.4. Genes related to prostaglandin metabolism and signaling and to steroid hormone signaling

As for the analysis of the equine estrous cycle, genes assigned to prostaglandin metabolism and signaling and to steroid hormone signaling were selected from the DEG's and used for a clustering analysis. Genes were obtained from corresponding Gene Ontology categories (www.geneontology.org), search in the Entrez Gene database (www.ncbi.nlm.nih.gov/gene) and in the literature. For steroid hormone signaling, only selected genes were used, e.g. classical and non-classical hormone receptors and related receptors and some genes encoding steroid hormone metabolic enzymes (Figure III-13-see next page).

Estrogen receptor 1 mRNA (*ESR1*) showed a very similar profile to progesterone receptor mRNA (*PGR*) and interleukin 1B (*IL1B*) with highest levels on day 0 and total down regulation during the luteal phase, whereas G protein-coupled estrogen receptor 1 mRNA (*GPER*) showed highest expression from day 6 to day 12. Progesterone receptor membrane component 1 and 2 (*PGRMC1, PGMRC2*) mRNAs showed slightly different expression changes during the cycle

compared to one another; *PGRMC1* showed highest mRNA level from day 6 to day 18 while *PGRMC2* mRNA was highest expressed only on day 6. Messenger RNA levels of prostaglandin E synthase (*PTGES)* showed highest mRNA level on day 12 of the estrous cycle in contrast to prostaglandin D synthetase 2 and prostaglandin E synthetase 3 *(PTGD2, PTGES3*) which showed lowest levels during the luteal phase. PTGE receptor mRNAs (*PTGER2, PTGER3, PTGER4*) showed completely different expression profiles. Prostaglandin-endoperoxide synthase 2 (prostaglandin G/H synthase and cyclooxygenase, *PTGS2*) showed high expression on day 12 and day 18. Additionally, prostaglandin-endoperoxide synthase 1 (prostaglandin G/H synthase and cyclooxygenase, *PTGS1*) showed highest mRNA expression on day 0. The prostaglandin F receptor (*PTGFR*) and its negative regulator (*PTGFRN*) showed contrary expression profiles; *PTGFR* is up-regulated during luteal phase while *PTGFRN* is down-regulated during this time in reproductive cycle. *OXTR* was highly expressed on day 18, respectively.

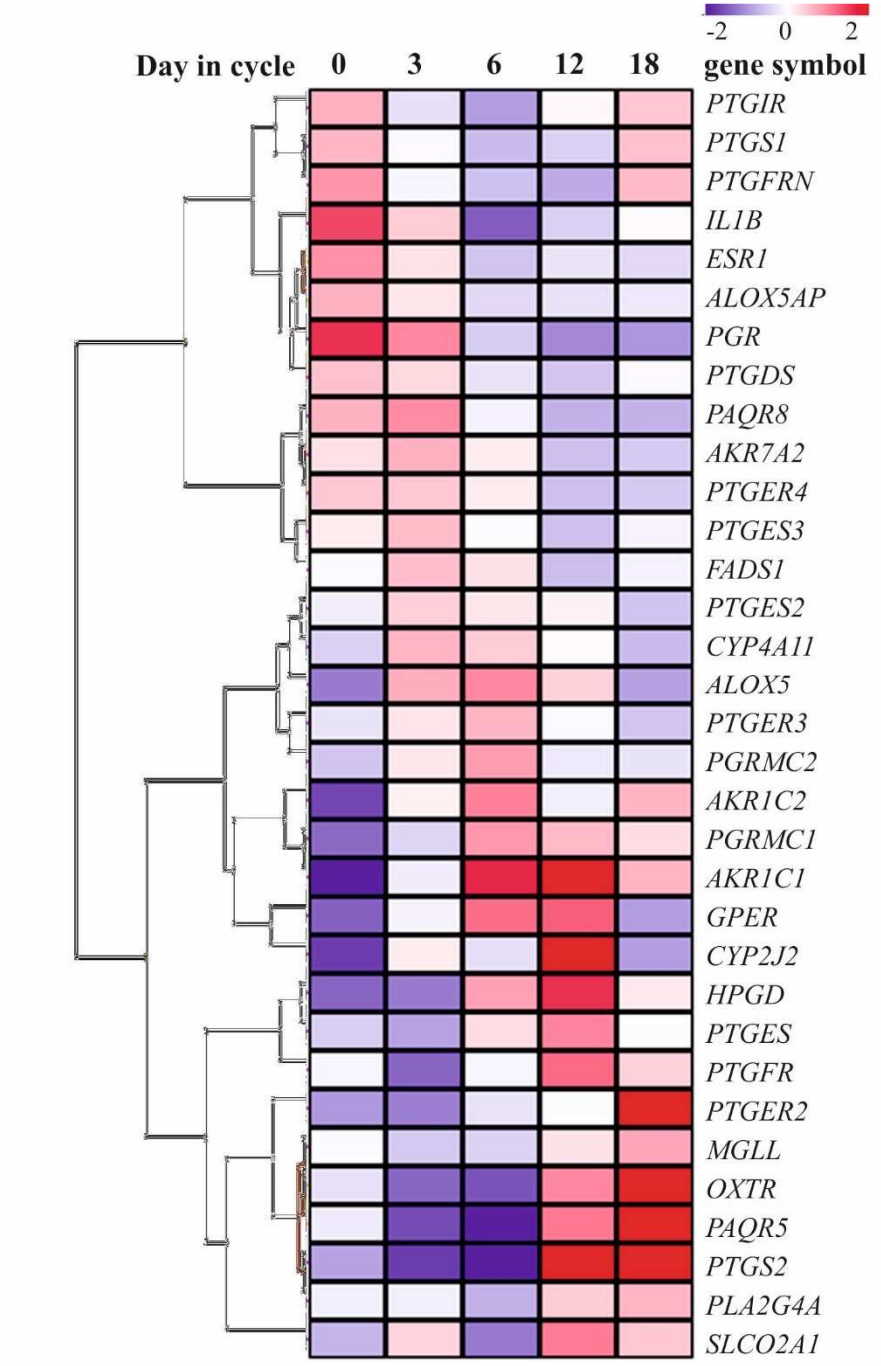

Figure III-13: Graphical illustration of genes related to prostaglandin metabolism and signaling and steroid hormone signaling. Relative expression values of differentially expressed genes matching this candidate list were subjected to hierarchical clustering for gene expression during the estrous cycle in porcine endometrium (MeV software, version 4.8.1). Color scale is from 4-fold lower (log2-fold=-2) than the mean (blue) to 4-fold higher (log2-fold= 2) than the mean (red). Graphic was edited using CorelDraw X6 software.

3.2.5. Genes related to 'regulation of apoptosis'

An expression heatmap for genes related to 'regulation of apoptosis' is shown in Figure III-14. For apoptosis signaling, candidate genes were found using www.wikipathways.com.

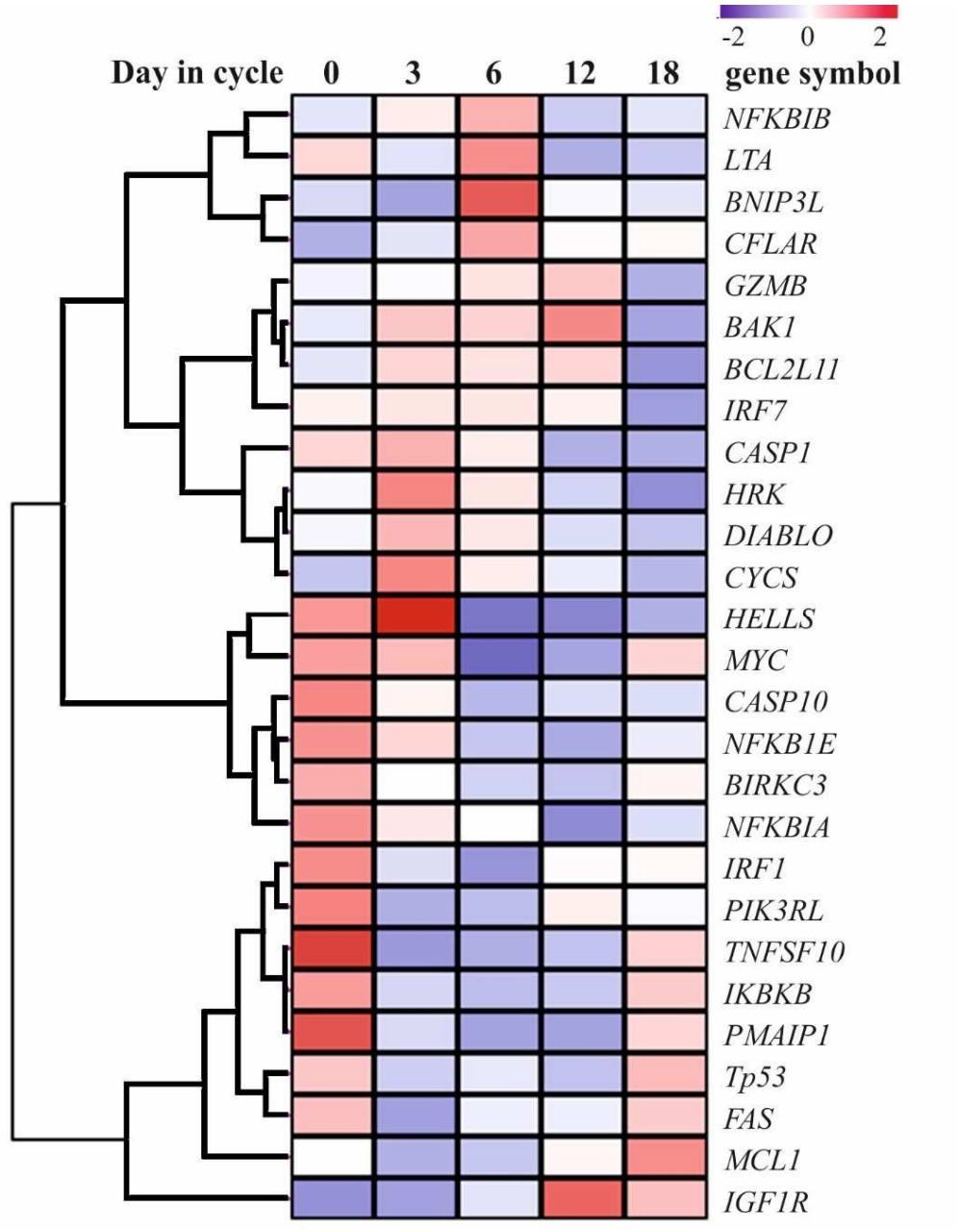

Figure III-14: Heatmap of expression profiles during the estrous cycle in porcine endometrium for genes related to 'regulation of apoptosis'. Relative expression values of differentially expressed genes matching this candidate list were subjected to hierarchical clustering for gene expression (MeV software, version 4.8.1). Color scale is from 4-fold lower (log2-fold=-2) than the mean (blue) to 4-fold higher (log2-fold=2) than the mean (red). Graphic was edited using CorelDraw X6 software.

Several functional categories for the regulation of apoptotic functions were found as over-represented for the genes with highest mRNA concentrations during the estrus phase (14 out of 24 genes in total for the category 'regulation of apoptosis'),e.g., the nuclear factor of kappa light polypeptide gene enhancer in B-cells 1A and E (*NFKB1A, NFKB1E*) and caspase 10 apoptosis-related cystein peptidase (*CASP10*). Four of these genes showed earlier or later up-regulation; helicase, lymphoid specific (*HELLS*) and myelocytomatosis oncogene, (*MYC*) show up-regulation during metestrus also whereas Fas cell surface death receptor (*Fas)*, and myeloid cell leukemia sequence 1 (*MCL1)* show earlier up-regulation on day 18 and insulin-like growth factor 1 receptor (*IGFR1)* was already up-regulated on day 12. Four genes related to regulation of apoptosis showed highest mRNA expression on day 3; cytochrome c, somatic (*CYCS*), IAP-binding mitochondrial protein (*DIABLO*), hara-kiri BCL2 interacting protein (contains only BH3 domain) (*HRK*), and caspase 1, apoptosis-related cysteine peptidase (*CASP1*) with slightly up-regulation on day 6. During the early luteal phase, 4 genes showed highest mRNA expression (BCL2/adenovirus E1B interacting protein 3-like (*BNIP3L)* the nuclear factor of kappa light polypeptide gene enhancer in B-cells 1B (*NFKB1B*), CASP8 and FADD-like apoptosis regulator (*CFLAR*) and lymphotoxin alpha (*LTA*)).The remaining genes showed diverse regulation throughout metestrus and diestrus.

3.2.6. Genes related to angiogenesis, blood circulation and vasculature development

In addition to genes involved in steroid hormone signaling and regulation of apoptosis, genes involved in ‘angiogenesis’, ‘blood circulation’ and ‘vasculature development’ were obtained as highly over-represented during the estrous cycle. These genes were identified by comparison to corresponding Gene Ontology categories, search in the Entrez Gene, WikiPathways, KEGG database, and literature. Relative expression values of differentially expressed genes matching this candidate list were subjected to hierarchical clustering for gene expression during the estrous cycle (Figure III-15). During preestrus, angiopoietin 2 (*ANGPT2*), angiopoietin-like 4 (*ANGPTL4*), endothelial PAS domain protein 1 (*EPAS1*), kinase insert domain protein receptor (*KDR*), nitric oxide synthase 3 (endothelial cell) (*NOS3*), tyrosine kinase, endothelial (*TEK*), and vascular endothelial growth factor A (*VEGFA*) showed up-regulation with slightly higher regulation of mRNA on day 12. Following estrus, angiopoietin-like 6 (*ANGPTL6*) shows over-expression on day 3 and on day 8. During luteal phase several genes showed highest mRNA expression e.g. mitogen-activated protein kinase kinase 1 *(MAP2K1),* nitric oxide synthase 3 (endothelial cell), *NOS3*), angiotensin I converting enzyme 2 (*ACE2*), and endothelial PAS domain protein 1 (*EPAS1*).

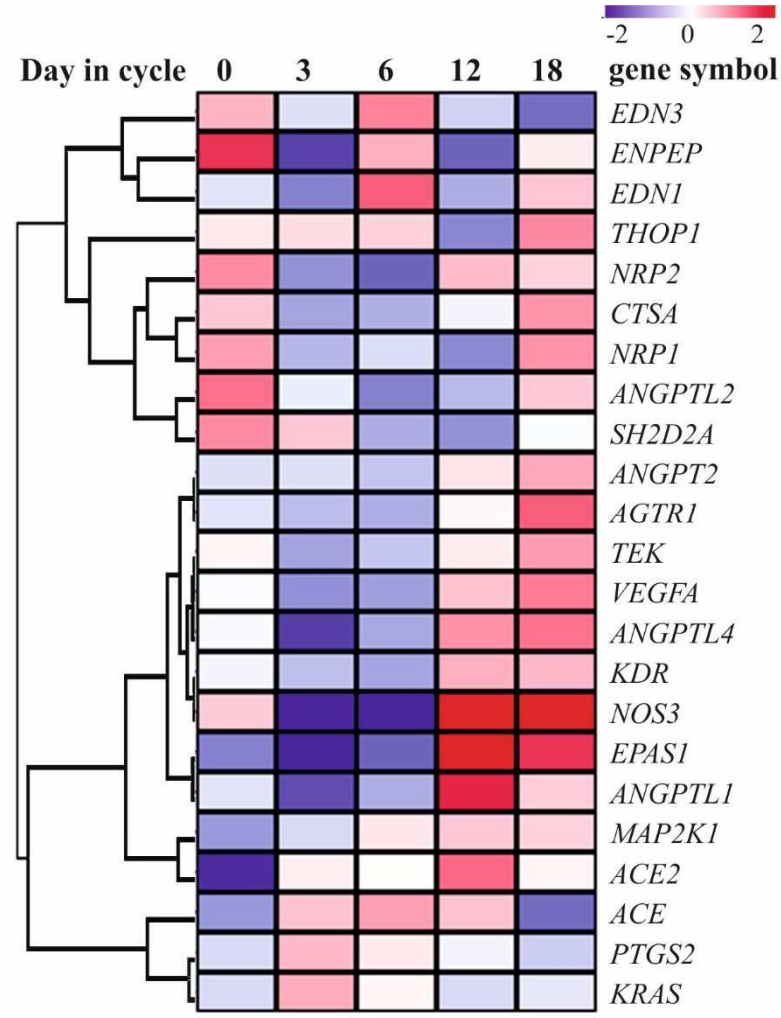

Figure III-15: Messenger RNA expression profiles of genes related to 'angiogenesis', 'blood circulation' and 'vasculature development' in porcine endometrium. Heatmap was established using MeV software (V 4.9.0). Color scale is from 4-fold lower (log2-fold=-2) than the mean (blue) to 4-fold higher (log2-fold=2) than the mean (red). Graphic was edited using CorelDraw X6 software

3.3. Validation of microarray data by the use of quantitative real-time RT-PCR (qPCR)

Microarray results were exemplarily confirmed with the analysis of selected genes by quantitative real-time RT-PCR (qPCR). The genes were selected based on the results of the clustering of similar expression profiles. Primers were designed with the NCBI Primer Blast-tool (http://www.ncbi.nlm.nih.gov/tools/primer-blast/index.cgi?LINK_LOC=BlastHome) based on the accession number of the original target sequence of the microarray probe. All gene symbols, Entrez IDs, Accession No's and sequences of used primers are shown in Tables II-1a, b and II-2. The length of all primers were between 18 and 25 nt, with GC content ranging from 30 % to 70 % and the melting temperature (Tm value) was between 59° C and 61° C. Amplicon length ranged from 80 to 200 bp. Primer pairs were selected separated by at least one intron on the corresponding genomic DNA. Genes were selected as representatives from functional annotation clustering (DAVID) and by literature. For some of the analyzed genes t-test p-values for the qPCR results were not significant ($p > 0.05$) due to variations in expression between animals of the same cycle stage. To confirm specificity of qPCR products and to verify product length and quantity of product/transcript, the samples were first purified with microdialysis and afterwards analyzed with an Agilent 2100 Bioanalyzer and sequenced.

3.3.1. Analysis of selected genes (*Equus caballus*)

Agarose gel electrophoresis was used to analyze PCR products obtained for equine samples. Results showed one clear product at an annealing temperature of 60°C only for 11 out of 22 oligonucleotide primer pairs. Remaining 11 pairs were run again at an annealing temperature of 62°C, 64°C and 68°C. For the following genes one specific product was obtained for the annealing temperature of 60°C: *ABCA1, ANXA3, CDK4, CXCR4, ERGIC1, ERP29, INHBA, MCM7, PGRMC1, SERPING1, SNRPA* and *SPP1* and could verify the microarray results. In addition, for the following genes a specific product was observed at an annealing temperature of 64°: *ACTB, COL1A1, RNA18S, RPL7, RPS27A, SLC25A22* and *UBB* which are shown in Figure III-16. *COL1A1* and *UBB* showed the same results during estrous cycle as microarray data. The primer pairs still yielding diverse products/transcripts were run again with an annealing temperature of 68° (*CDH16* and *GAPDH*). Product length, annealing temperature and melting point of all oligonucleotides are summarized in Table III-6. *H3F3A* showed a fluctuating pattern during the cycle and the microarray results could not be validated using qPCR technique. Furthermore, results showed an increase of actin B (*ACTB)* on day 3 with slightly increased expression on day 0 that could be verified with qPCR but did not reach statistical significance in the statistical analysis (data not shown) Messenger RNA profiles for *CDH16* and *H3F3A* showed higher expression on day 0 for 'vsn' value compared to the qPCR analysis but within relatively slight deviation. Analysis for *ERGIC1* showed lower expression on day 3 for 'vsn'-values. *GAPDH* was higher expressed on day 0 and lower on day 3 according to qPCR vs. microarray. Additionally, *RPL7* showed up-regulation for qPCR analysis on day 8 and down-regulation for microarray data vice versa for *SLC25A22* mRNA expression. *RPS27a* analysis revealed different almost contrary results for all times during the estrous cycle. Results for the remaining 14 genes were in very good agreement between analyses (Figure III-17).

Gene Symbol [1]	Product size [base pair]	Annealing temperature [°C] [2]	Melting point [°C] [3]
ABCA1	156	60	81.5
ACTB	132	64	87.4
ANXA3	145	60	79.4
CDH16	140	68	85.4
CDK4	163	60	85.5
COL1A1	185	64	87.5
CXCR4	125	60	79.3
ERGIC1	172	60	83.5
ERP29	171	60	80
GAPDH	138	68	82
H3F3A	146	68	83.5
INHBA	196	60	80.4
MCM7	189	60	82.5
PGRMC1	197	60	85
RPL7	137	64	82
RPS27a	156	64	76
SERPING1	92	60	81
SNRPA	200	60	75
SLC25A22	161	64	85.5
SPP1	82	60	77.7
UBB	86	64	76.9

Table III-VI: Annealing temperature, melting point and product length for qPCR.Table shows a summary for

equine qPCR analysis. [1] official Gene Symbol, [2] and [3] provided by software.

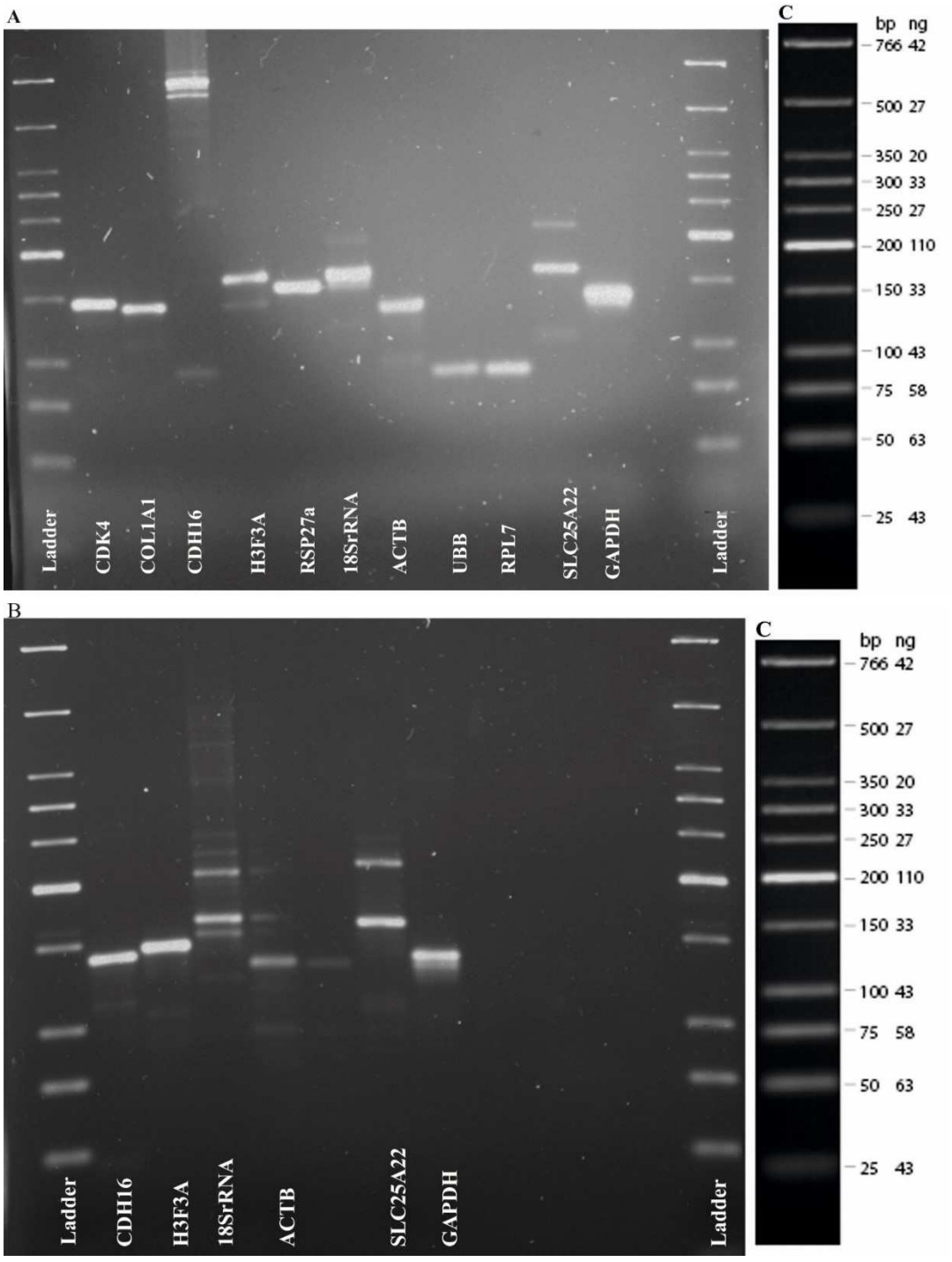

Figure III-16: Agarose analyses of qPCR products. A) gel shows results after qPCR with annealing temperature of 64°C, B) gel shows results after qPCR with annealing temperature of 68°C. C) N3233 New England BioLabs Low molecular weight marker. bp-base pair.

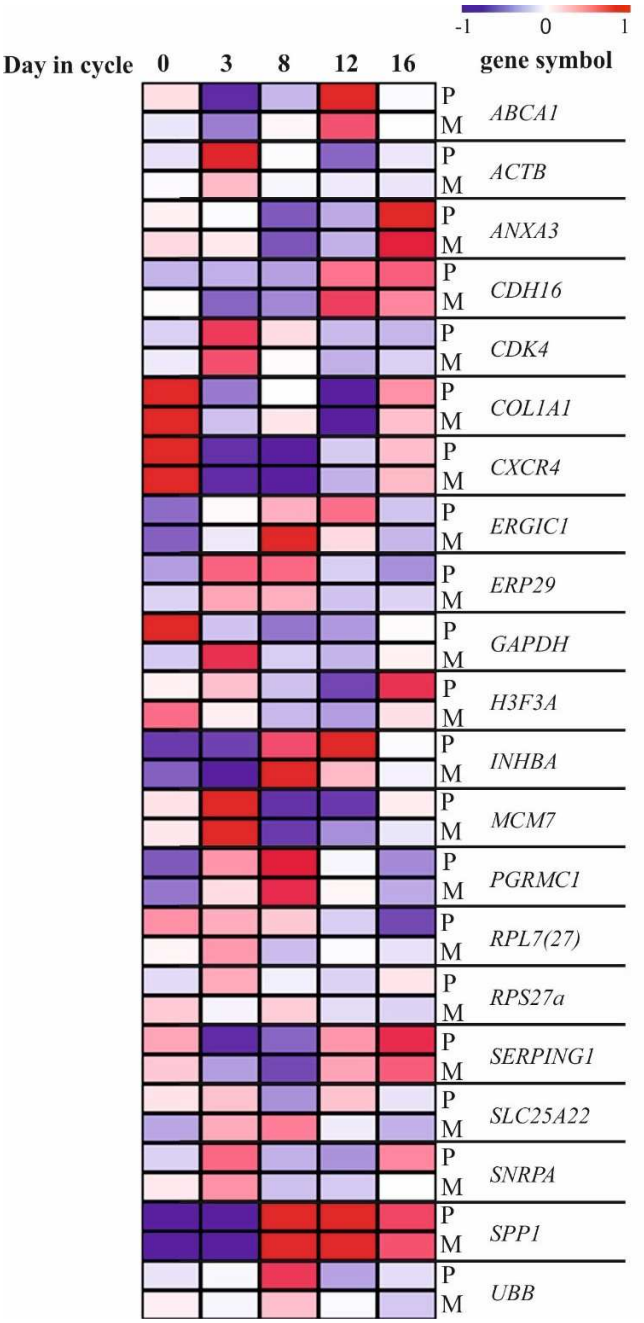

Figure III-17: Correlation of microarray and qPCR data of equine analysis. Relative expression levels were calculated (vsn value of one time point minus mean vsn values of all 5 time points; Mean Ct-values of all 5 time points minus Ct-value of one time point) and shown as a heatmap (MeV software, version 4.9.0. Color scale is from 2-fold lower (log2-fold=-1) than the mean (blue) to 2-fold higher (log2-fold=1) than the mean (red). Figure was edited using CoreDraw X6 Software. M–microarray, P-qPCR.

3.3.2. Analysis of selected genes (*Sus scrofa*)

Heatmap (Figure III-18) shows results of quantitative real-time PCR (qPCR) of selected genes. Fifteen genes were selected for validation by qPCR. *ANXA7* showed higher expression on day 3 in qPCR analysis compared to microarray data. *BAALC* was still up-regulated on day 18 according to qPCR compared to microarray results. *CXCR4*, *PGF* and *SERPING1* showed different expression for qPCR and microarray on day 0 and on day 3 and *COL1A1* showed different expression values on day 3 as well as *FGFR1*. Remaining genes were in very good agreement between results of the different techniques. Table III-7 summarizes annealing temperature and product size for the selected primer pairs used for quantitative real-time PCR

(qPCR) analysis.

Gene Symbol[1]	Product size [bp]	Annealing temperature [°C]	Gene Symbol[1]	Product size [bp]	Annealing temperature [°C]
ABCA1	161	60	*H3F3A*	200	60
ANXA7	102	60	*PGF*	155	60
BAALC	162	60	*SERPING1*	137	60
CCNE1	182	60	*SNRPA*	121	60
CDK4	113	60	*SPP1*	134	60
COL1A1	118	60	*TIMP-3*	155	60
CXCR4	80	60	*UBB*	142	60
FGFR1	86	60			

Table III-VII: Product size and annealing temperature for qPCR.Summary of porcine qPCR analysis is shown. [1] official gene symbol.Bp-basepair, °C-celcius.

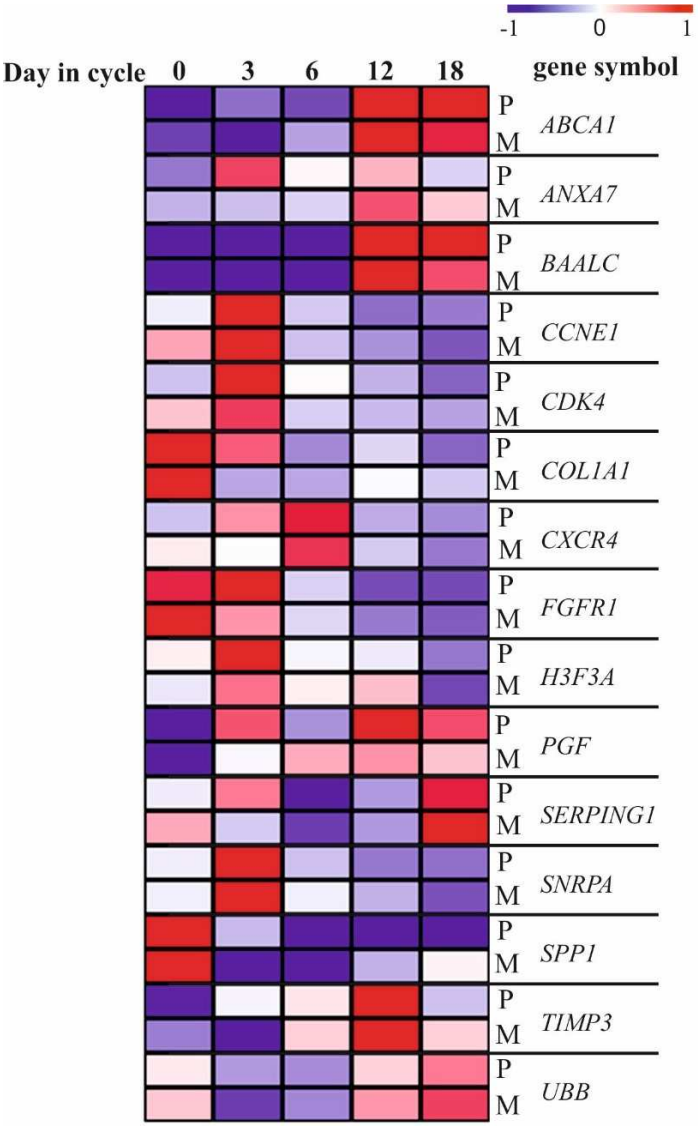

Figure III-18: Correlation of microarray and qPCR data of porcine analysis. Heatmap (MeV software, version 4.9.0) demonstrates the correlation of microarray data and qPCR data of porcine samples. Relative expression levels were calculated (normalized value of one time point minus mean normalized values of all 5 time points; mean Ct-values of all 5 time points minus Ct-value of one time point). Color scale is from 2-fold lower (log2-fold=-1) than the mean (blue) to 2-fold higher (log2-fold=1) than the mean (red). Figure was edited using

CoreDraw X6 Software. M–microarray, P-qPCR.

4. Comparison of gene expression profiles during the equine and the porcine estrous cycle

To make a statistical relevant statement regarding the comparison of expression profiles between equine and porcine endometrium, the significance of the correlation of gene expression profiles during the estrous cycle was further determined. All significant positively and negatively correlated genes were analyzed in relation to the SOTA clustering. Additionally, functional annotation clustering was performed using DAVID bioinformatics tool to show distinct molecular and biological processes as over-represented in each cluster compared.

4.1. Significance of correlation between differentially expressed genes in both species

In total, the comparison of the datasets revealed approx. 1862 genes/transcripts referred to as differentially expressed in both species. The comparison provided 690 genes as positively correlated ($p<0.05$) and 151 genes as negatively correlated ($p<0.05$). The calculation and list of genes can be found in supplementary data. An illustration summarizing bioinformatics analyses of distinct molecular functions and biological processes of positively and negatively correlated genes is shown in Figure III-19 and 20.

4.1.1. Relation of positively correlated genes to SOTA clustering analyses

The 690 genes that were assigned as significantly positive correlated were analyzed according to the cluster analysis (SOTA cluster) of both species (Table III-8).

A total number of 48 genes were up-regulated on day 0 (Cluster 1-*Eca*, Cluster 1-*Ssc*) in both species. 15 genes clustered together on day 0 in equine expression profiling and showed high mRNA expression from day 0 to day 3 (Cluster 2) in the pig. Additionally, 15 genes were up-regulated on day 18 (Cluster 8) in the pig and on day 0 in the mare concurrently. Only 3 genes were up-regulated on day 3 (Cluster 3) in the pig and on day 0 in the mare. 14 genes assigned as up-regulated in Cluster 1 (*Ssc*) were up-regulated from day 0 to day 3 (Cluster 2) in the mare and 21 genes were already up-regulated on day 16. Only 2 genes showed highest mRNA levels on day 3 in the mare. 34 genes showed highest mRNA levels from day 0 to day 3 (Cluster 2-*Eca*, Cluster 2-*Ssc*) in both species. 35 genes were up-regulated on day 3 in the pig and from day 0 to day 3 in the mare at the same time. Additionally, out of 9 genes that were up-regulated from day 0 to day 3 in the mare, 7 genes were clustered together in cluster 4 and 2 genes showed up-regulation in cluster 8 in the pig. Comparison of mRNA expression on day 3 (Cluster 3-*Eca*, Cluster 3-*Ssc*) in both species revealed 107 genes as up-regulated, which is the highest amount of genes clustering together. Of 173 genes that were up-regulated on day 3 in the mare, 29 genes showed highest mRNA levels from day 0 to day 3, 33 genes were up-regulated during early luteal phase and 4 genes showed higher mRNA profiles during estrus phase in the pig. Vice versa, of 154 genes that were assigned as up-regulated on day 3 in the pig, only 9 genes showed later increase of expression during the estrous cycle in the mare. 44 genes of positive correlation were clustered together from day 3 to day 8 in the mare and from day 3 to day 6 in the pig (Cluster 4-*Eca*, Cluster 4–*Ssc*). Whereas only 8 genes were additionally up-regulated in the mare, 135 genes were up-regulated in the pig at this time during cycle; 67 genes were up-regulated on day 8, 28 genes showed highest mRNA expression from day 8 to day 12 and 40 genes were up-regulated earlier in equine estrous cycle concurrently. During diestrus, the analysis revealed 11 genes as up–regulated in both species (Cluster 5-*Eca*, Cluster5–*Ssc*). 19 genes showed highest mRNA expression later in the equine cycle. Cluster 6 of both species (from day 8 to day 12-*Eca*, on day 12-*Ssc*) showed 10 genes as up-regulated. Additionally, 30 genes showed earlier up-regulation and 4 genes were up-regulated later in time during porcine

estrous cycle. From 19 genes that were assigned as up-regulated on day 12 in the pig, 11 genes were up-regulated from day 12 to day 16, 2 genes showed highest mRNA on day 16 and 6 genes were clustered together related to day 8 in the mare. In Cluster 7 a total number of 33 genes and in Cluster 8 a total number of 47 genes showed higher mRNA levels in both species. Twelve genes were up-regulated in cluster 7 in the mare and in cluster 8 in the pig at the same time. Eighteen genes were up-regulated in cluster 7 in the pig and in cluster 8 in the mare concurrently.

			Equus caballus								
	SOTA		1	2	3	4	5	6	7	8	total
	SOTA	Day in cycle	0	0-3	3	3-8	8	8-12	12-16	16	
Sus scrofa	1	0	48	14	2	0	0	0	0	21	85
	2	0-3	15	34	29	1	0	1	0	0	80
	3	3	3	35	107	7	2	0	0	0	154
	4	3-6	0	7	33	44	67	28	0	0	179
	5	6-12	0	0	0	0	11	11	6	2	30
	6	12	0	0	0	0	6	10	11	2	29
	7	12-18	0	0	0	0	0	4	33	18	55
	8	18	15	2	2	0	0	0	12	47	78
total			81	92	173	52	86	54	62	90	690

Table III-8: Overview of significantly positive correlated genes in relation to cluster analyses. SOTA cluster: all expression cluster obtained from the analysis of all genes found as differentially expressed during the equine and porcine estrous cycle (MeV analysis).Genes: number of significant positive correlated ($p<0.05$) genes as assigned to both expression cluster, grey background-genes as up-regulated in both species in the same cluster number, brown background-more than 10 genes clustered together. D-day.

4.1.2. Relation of negatively correlated genes to SOTA clustering analyses

150 genes were assigned as negatively correlated ($p<0.05$) and analyzed in relation to SOTA clustering analyses (Table III-9).

Most of the genes showed negative correlation on day 0 (Cluster 1) in each species (separately) and during the luteal phase. 62 genes were up-regulated from day 3 to day 6 in the pig whereof 22 genes showed up-regulation in cluster 1 (highest level on day 0) and 36 genes were up-regulated in cluster 8 (highest level on day 16) in the mare. From 29 genes that were up-regulated on day 0 in the pig, 12 genes were up-regulated on day 8 and 11 genes showed up-regulation from day 8 to day 12 in the mare concurrently.

Sus scrofa	*Equus caballus*										
	SOTA		1	2	3	4	5	6	7	8	total
	SOTA	Day in cycle	0	0-3	3	3-8	8	8-12	12-16	16	
	1	0	0	0	1	1	12	11	4	0	29
	2	0-3	0	0	0	1	1	7	7	0	16
	3	3	0	0	2	0	0	4	2	1	9
	4	3-6	22	1	0	0	0	0	3	36	62
	5	6-12	3	3	0	0	0	0	0	1	7
	6	12	3	1	0	0	0	0	0	0	4
	7	12-18	0	1	2	2	0	0	0	0	5
	8	18	0	1	0	6	6	6	0	0	19
		total	28	7	5	10	19	28	16	37	**151**

Table III-9: Overview of significantly negative correlated genes in relation to cluster analyses. SOTA cluster: all expression cluster obtained from the analysis of all genes found as differentially expressed during the equine and porcine estrous cycle (MeV analysis).Genes: number of significant negative correlated ($p<0.05$) genes as assigned to both expression cluster, brown background-more than 10 genes clustered together. D-day.

4.2. Functional annotation clustering

4.2.1. Analysis of positive correlated genes

The characterization of molecular functions and assigned biological processes as over-represented during different phases of the equine and porcine estrous cycle was performed using functional annotation clustering (DAVID) for the clusters of genes with similar expression profiles that have been obtained by SOTA clustering and genes as significant positive and negative correlated in both species. Two heatmaps based on the frequency pattern (numbers of genes on different cycle stages) during the reproductive cycle were plotted for graphical illustration of the processes over-represented during distinct phases of the porcine and the equine estrous cycle. This graphical illustration is demonstrated in Figure III-19 and 20. Selected functional categories were clustered according to their frequency patterns achieved in functional annotation clustering for each dataset (list of significant positive and negative correlated differentially expressed genes

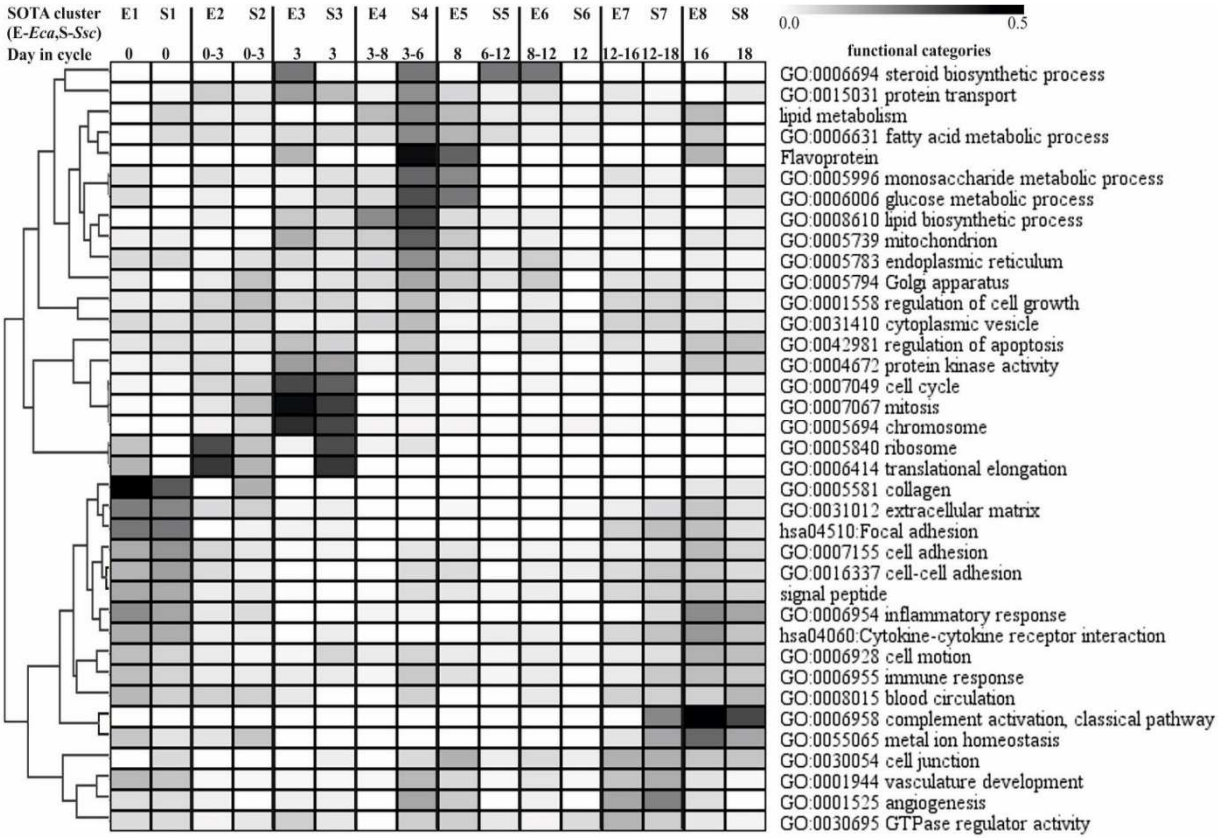

Figure III-19: DAVID functional annotation clustering of all significantly positive correlated genes in both species throughout the cycle. Functional terms over-represented during distinct phases of the estrous cycle were selected from DAVID functional annotation clustering analysis. Numbers of genes assigned to these functional terms (in rows) are shown for each SOTA cluster (in columns) as percentage of the number of all differentially expressed genes assigned to a term (white = 0%; black = 50%). Graphic was edited using MeV and CorelDraw X6 software.

Genes with highest mRNA levels on day 0 (Clusters E1 and S1) clustered together in the functional groups related to terms such as 'collagens', 'extracellular matrix', 'focal adhesion' and 'translational elongation'. Cluster E1 showed, in addition, the categories 'inflammatory response' and 'ribosomes' as over-represented. S1 showed lower expression of genes related to the category 'collagens' in comparison to E1. Clusters E2 and S2 represent highest mRNA expression levels from day 0 to day 3 and showed genes as over-represented by the categories 'translational elongation' and 'ribosome'. Altogether, most expression values of cluster S2 showed lower expression values than of E2 except for the category 'collagens'. Specifically for clusters E3 and S3 (highest expression levels on day 3) categories related to 'cell-cycle', 'mitosis' and 'chromosome' showed highest numbers of genes. Additionally, cluster E3 showed highest expression for the functional term 'steroid biosynthetic process'. The biological terms 'Flavoprotein', 'protein transport', 'mitochondrion', 'glucose and monosaccharide metabolism' and 'lipid metabolism' were over-represented in cluster S4 (highest level from day 3 to day 6). Cluster E4 (highest level from day 3 to day 8) showed 'lipid metabolism' as the only category that was over-represented. Interestingly, the expression in cluster S5 (highest level from day 6 to day 12) and cluster E6 (highest level from day 8 to day 12) showed similar over-representation represented by functional term 'steroid biosynthetic process' other than the clusters S5 and E5 (highest level on day 8). Cluster S6 (highest level on day 12) showed slightly over-representation for 'GTPase regulator activity'. Cluster E7 (highest level from day 12 to day 16) and S7 (highest level from day 12 to day 18) showed the term 'angiogenesis', 'GTPase regulator activity' and 'cell junction' as highly represented. Clusters E8 (highest level on day 16) and S8 (highest level on day 18) revealed highest mRNA expression for genes assigned to

categories as ‘cytokine-cytokine receptor interaction’ and ‘complement activation, classical pathways’

4.2.2. Analysis of negatively correlated genes

Cluster E1 revealed highest mRNA expression for the categories ‘focal adhesion’, ‘extra cellular matrix’ and ‘fatty acid and lipid metabolism’ whereas cluster S1 showed highest representation for the biological terms ‘glucose and monosaccharide metabolism’ and ’protein transport’. Negative correlated genes showed over-representation for ‘monosaccharide metabolic process’ in cluster S2 but no representation for cluster E2. The functional categories ‘collagens’ and ‘cell junctions’ showed over-representation in E5 and S8. Cluster E3 and S3 revealed highest representation for the category ‘mitosis’, cell-cycle’ and ‘chromosome’. The categories ‘angiogenesis’ and ‘vasculature development’ showed over-representation in cluster E5 and S8, respectively. Most of the functional terms as over-represented in cluster S4 showed same deviation for cluster E8. The clusters E5, S6 and E6 revealed only very low expression for all functional categories as well as cluster E2. Negative correlation showed over-representation for genes assigned to the biological term ’extracellular matrix’ in cluster E1 and S4.The category ‘translational elongation’ showed no negative significant regulation at all.

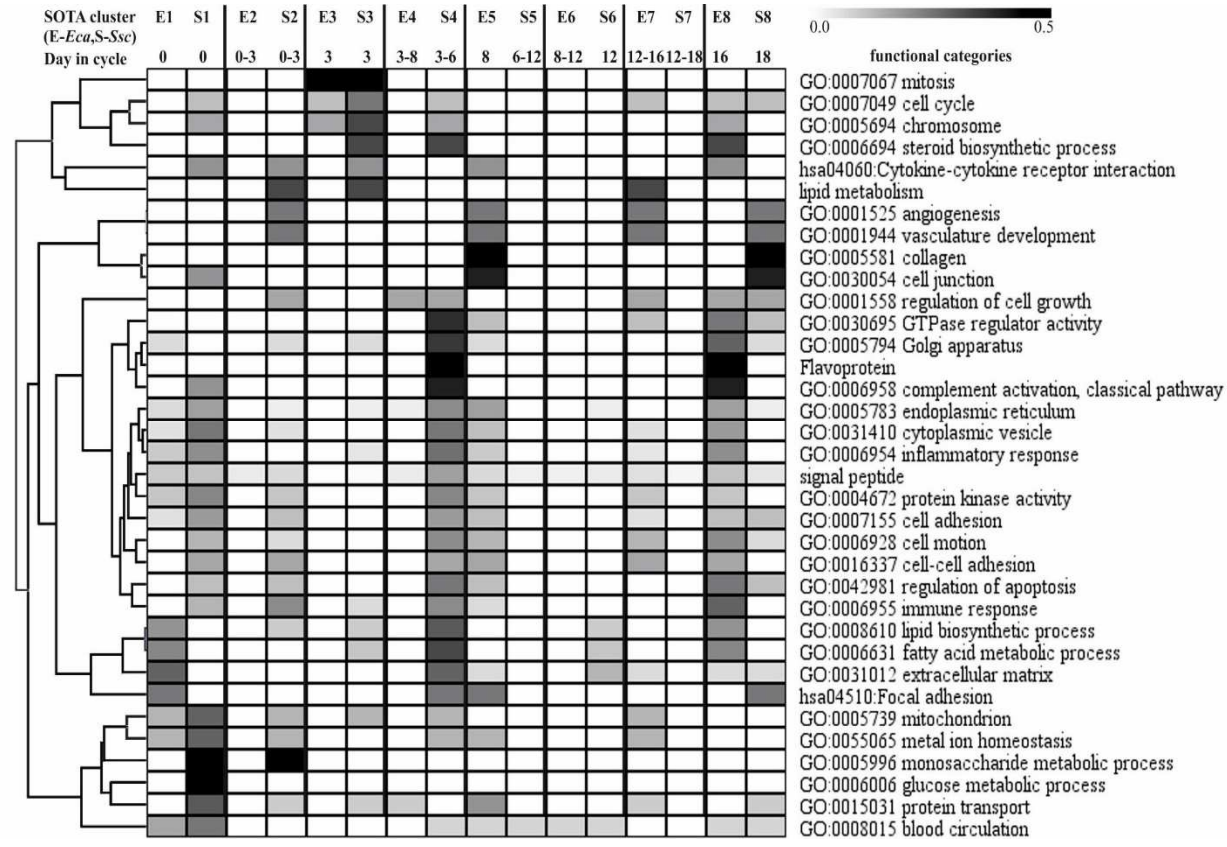

Figure III-20: Representation of selected functional categories of all negative correlated genes in both species throughout the cycle. Functional terms over-represented during distinct phases of the estrous cycle were selected from DAVID functional annotation clustering analysis. Numbers of genes assigned to these functional terms (in rows) are shown for each SOTA cluster (in columns) as percentage of the number of all differentially expressed genes assigned to a term (white = 0 %; black = 50 %). Graphic was edited using MeV and CorelDraw X6 software.

4.2.3. Comparison to dynamic gene expression changes during the estrous cycle in bovine endometrium (Mitko, 2008)

4.2.3.1. Positively correlated genes

In this analysis the list of differentially expressed genes from the study of the bovine endometrium (Mitko et al.,'08) was compared to the list of significant positive and significant negative correlating genes from the equine and porcine correlation analysis. The analysis revealed a total number of 33 genes/transcripts as positively correlated in the equine and porcine endometrium and regulated during the estrous cycle in the bovine endometrium.

Three genes related to the term 'collages' were regulated in all three species: *COL1A2, COL3A1,* and *COL4A1*. In the mare and the pig all three genes show highest expression on day 0 only in the bovine endometrium *COLA41* shows up-regulation during preestrus. In addition, the comparison of the transcriptome analysis in all three species revealed an up-regulation of the immune-related genes that are involved in the complement system (classical pathway), namely complement component genes *C1R* and the C1 inhibitor *SERPING1* (Bauersachs et al.,'06, Klein et al.,'06). Slightly correlative expression differences were found within the immune-related genes complement component 1, r subcomponent (*C1R*) and serpin peptidase inhibitor, clade G (C1 inhibitor), member 1 (*SERPING1*). In porcine endometrium both genes showed mRNA up-regulation during preestrus (day 18) as in equine endometrium (day 16). Other than that, the mRNA expression of *C1R* and *SERPING1* in bovine endometrium showed earlier up-regulation on day 12.

4.2.3.2. Negatively correlated genes

As with the analysis of significant positive genes, in this analysis the list of differentially expressed genes from the study of the bovine endometrium (Mitko et al.,'08) was compared to the list of significant negative correlating genes from the equine and porcine correlation analysis. The analysis revealed a total number of 7 genes/transcripts as negative correlated in the equine and porcine endometrium and regulated during the estrous cycle in the bovine endometrium: *COL5A3* (collagen, type V, alpha 3), *GM2A* (GM2 ganglioside activator), *MGP* (matrix Gla protein), *NEU1* (sialidase 1 (lysosomal sialidase)), *PDIA4* (protein disulfide isomerase family A, member 4), *TMSB10* (thymosin beta 10) and *TNC* (tenascin C).

IV. DISCUSSION

The present thesis provides new insights into the gene expression changes in equine and porcine endometrium during the estrous cycle and the analysis and interpretation of similarities and differences between these species. Since a comparison between species of different mammalian groups can be used for the identification of genes related to common and species-specific mechanisms for establishment and maintenance of pregnancy (Bauersachs et al., 2012) and the regulation of the reproductive cycle, data sets obtained in the gene expression analysis of equine and porcine endometrium were analyzed in this regard. Furthermore, a comparison of significantly correlated genes in both species to dynamic gene expression changes in the bovine endometrium throughout the cycle provided additional insights into interactions and characteristics during distinct stages of the estrous cycle.

At first, limitations of the comparison between the investigated mammalian species regarding differences in sample collection, endocrine regulation of the estrous cycle, e.g., profiles of progesterone concentration levels and methodic analysis, is debated. Then gene expression in the equine and porcine endometrium in relation to their particular biological function during distinct events throughout the cycle is discussed, respectively. These consolidated findings are compared to one another and discussed in detail referring to distinct reproductive events. At last, significant gene expression throughout species during the estrous cycle is analyzed.

1. Comparative methodology

1.1. Comparison between the analysis of equine and porcine endometrium

1.1.1. Sample collection, plasma P4 concentration and tissue composition

According to the changes in steroid hormone concentrations and corresponding endometrial structural and functional changes, the estrous cycle is divided into four different stages; estrus, metestrus, diestrus and preestrus corresponding to ovulatory, early luteal, mid luteal and follicular phase. Equine biopsy samples were collected on day 16 for beginning of estrus and on day 0 as the time shortly after ovulation (two times during estrus phase with low P4 concentrations). In addition, for the luteal phase, three times were selected for sample collection; day 3 for the early luteal phase with P4 concentrations on the rise, day 8 for the mid luteal phase (diestrus-highest P4 concentration) and day 12 for the late luteal (decreasing P4 concentrations). For porcine endometrial samples, collection was performed on day 0 for the time around ovulation (low P4 concentrations), respectively. The samples collected on day 18 (assumingly the time for the beginning of estrus and therefore low P4 concentrations) showed higher concentrations of P4 and should be considered as samples collected during late luteal phase. Biopsy samples collected on day 3 represent metestrus, the time during the reproductive cycle when P4 concentrations start to increase. For the luteal phase, sample collection was performed on two different times; day 6 for the early luteal phase and day 12 for diestrus (high P4 concentrations). Precise timing of sample collection was controlled by routinely monitoring follicular development and ovulation by daily transrectal palpation and ultrasound examination in case of equine samples and by rehousing of pigs and induction of ovulation and post mortem evaluation of ovary status for porcine samples.

Furthermore, determination of P4 concentration, as the key hormone which prepares the endometrium for establishment and maintenance of pregnancy, was performed to confirm timing of sample collection. The analysis of equine blood samples was in agreement with the expected P4 concentrations as described throughout literature. The blood samples for some pigs

slaughtered on day 18 showed higher levels of P4 concentrations than expected on this time during the cycle but showed decreasing levels compared to day 12. One of the animals in this group showed an extremely high number of corpora lutea (*pl.* Corpus luteum) (D18S28 with 22 CL's) in the left ovary resulting in the peripheral progesterone concentration of 42.8 ng/ml. This value is almost three times higher than the P4 concentrations of 3 other animals in this group. In addition, the group of day 18 samples was the most heterogeneous among all. However, the progression of P4 concentrations throughout the analyzed stages (except day 18) of the estrous cycle was consistent and in good agreement with the literature and the samples were further processed. The higher P4 concentrations on day 18 in porcine blood samples could have an impact on the comparison of gene expression during this time with the mare and is kept in mind until further parts of this discussion.

As reviewed in Ulbrich et al. (Ulbrich et al., 2012), in addition to collection from defined stages, the performance of tissue sampling itself needs to be standardized to ensure i) short times for tissue or cell recovery and sampling (instability of RNA), ii) similar times for all biological replicates and iii) collection of representative tissue samples. Therefore, sample collection procedures were carried out in very strictly manner and described in detail in the protocol. Equine endometrial biopsy samples were collected from five cycling mares at five times during the estrous cycle. To avoid effects of a previous biopsy collection on gene expression, no more than two biopsy samples were taken during the same cycle with an interval of at least 15 days. Sample collection procedures are recorded in the dissertation of Dr. ved. med. M. Merkl. The collection of the samples was also performed by Dr. vet. med. M. Merkl. The biopsy samples were taken transcervical, meaning a relatively 'blind' operation. Therefore, every second slice of each sample was used for quantitative stereology for the analysis of tissue composition. Sample collection from porcine endometrium was performed from 30 different female gilts at five different times during the estrous cycle. For each time point six animals were slaughtered and post-mortem sample collection and evaluation of ovaries was carried out. Since tissue sampling was performed on the opened uterine horns it could be performed in a controlled way, and additional analysis of tissue composition (quantitative stereology) was not necessary. Other than for equine samples, three endometrial tissue samples were taken from each uterine horn (left and right): proximal (i.e. towards the corpus=front), intermedial (middle) and distal (back). All tissue samples were immediately transferred into vials containing RNAlater. Since pooling of tissue samples from the same animal can be used to reduce variations of tissue composition in case of complex tissues, three samples from one uterine horn were pooled (equal amounts of total RNA).

1.1.2. Quality of the isolated RNA

The process from collected tissue samples to isolated total RNA comprises many steps that can have influences on the quantity of the results. Therefore, control of RNA quality and purity is a crucial step in guaranteeing integer stable RNA and receiving meaningful results in gene expression profiling experiments. The quantity and purity of isolated RNA was determined using a spectrophotometer. In our laboratory the NanoDrop-1000 spectrophotometer was used which enables highly accurate analyses of small sample volumes with remarkable reproducibility and, therefore, eliminates the need for cuvettes and capillaries without losing fractions of the sometimes precious and valuable RNA samples (see product descriptions in web). RNA samples should be non-degraded or fragmented and free of protein, genomic DNA, nucleases, and enzymatic inhibitors. The purity of RNA was tested by determining the ratio of the absorption at 260 and 230 nm which indicates the presence of contaminants like chaotropic salts. This ration should not be lower than 2.1. Furthermore, the 260/280-nm ratio indicates contamination with DNA, proteins and phenol (2.0 for pure RNA at neutral pH). The most impure sample (D6S13-b) was rejected for further analysis. In general, neglectable amounts of

chemically degraded RNA are common due to thawing and freezing of samples for several times. For even more certainty about the quality of the isolated RNA, RNA integrity was analyzed using fluidic chip technology. All samples showed good RNA integrity with slightly better porcine (RINs: 7.9-10.0) than equine (RINs :6.8–9.4) quality estimations. Taken together the isolated total RNA showed very good quality for the assignment of further analysis and was comparable between equine and porcine endometrium.

1.1.3. Microarray analyses

Microarray analysis of equine samples was performed with Agilent Horse genome arrays comprising a 'Quick Amp Labeling Kit (one-color)' and for porcine samples with Agilent Swine genome array and the 'Low Input Quick Amp Labeling Kit (one-color)'. Except for labeling, all other steps were performed by the use of the same Agilent kits and the same technical equipment. Both Agilent array experimental designs used in this study were 4x44k arrays, meaning there are 4 array areas on each slide with respectively 44,000 oligonucleotide probes. As already mentioned, the distribution of the porcine samples of the same time point on the slides was not in a random manner. For equine biopsy samples, different samples from different mares and different times were loaded on each slide for hybridization to avoid bias from technical variation. Unfortunately, the distribution on the slides for porcine samples was according to sample numbers which were from D0 through D18. Therefore a bias derived from technical deviances cannot be completely excluded.

1.1.4. Statistical analysis of microarray data and functional annotation clustering

Microarrays simultaneously measure transcript abundance for tens of thousands of genes in a cell population or tissue sample. The measurement is performed by quantitation of the fluorescence intensities of labeled sample cRNA that has hybridized to probes on the array. Statements about the relative abundance of a gene transcript in these samples can be made by comparing the corresponding fluorescence intensities. Due to variations in sample treatment and labeling efficiency the fluorescence intensities have an inter-array variation. For optimal comparison, appropriate calibration is necessary, which is also called 'normalization'. Numerous methods exist for normalization (basic processing) of microarray gene expression data. These methods can have an important effect on the final analysis outcome. Therefore, it is crucial to use methods, which are appropriate for a given dataset in order to assure the validity and reliability of expression data analysis. 'Variance Stabilization and normalization' (BioConductor package VSN) (Huber**,** 2002) is a method that incorporates data calibration, an intensity-dependent error model and data transformation. It is intended to lead to a measure of differential expression which is independent of the mean intensity. 'Vsn' assumes that less than half of the genes on the array are differentially expressed across the experiment. The analysis of the 4x44k Horse Genome microarrays was first performed by filtering processed signal intensities, that had been generated by Feature Extraction Software 10.7.3.1, in MS Excel based on the 'Is well above background' flag. The filter threshold was detection in 4 of 5 samples in at least one of the five experimental groups for equine samples. For the analysis of 4x44k Porcine Genome microarray, the processed signals were obtained in the same way as for equine samples. Filtering the processed signal intensities, in MS Excel, was based on the 'Is well above background' flag with a filter threshold detection in 3 of 4 samples, 4 of 5 samples and 5 of 6 samples per group. Due to the fact that more than 60 % of the porcine genes on the array were differentially expressed, the 'vsn'-BioConductor package could not be used for this experiment. This is why '75th percentile' normalization of the filtered signals was calculated by dividing the processed signals by the 75th percentile of each sample in MS Excel and log2 transformation and then multiplying by the mean of 75th percentiles of each sample. Altogether, bioinformatics analysis revealed 4.996 differentially expressed genes for equine samples and 5.325 known

differentially expressed genes for porcine samples. A heatmap based on pair-wise distances (BioConducter package 'geneplotter') was generated for quality control of each dataset. Significance analysis was performed using the SAM function of the 'siggenes' package (BioConducter, multiclass) for both experimental projects with different false discovery rates (equine data-1%, porcine data 0.1%). Most likely sample composition can have strong influence on microarray findings based on different mRNA concentration changes in different cell types. According to pronounced differences in progesterone concentration on day 18 in porcine samples, it was not surprising that those samples showed clustering closer to day 12 with highest P4 concentration other than to day 0 as expected. Altogether, the analysis of sample correlation (pairwise distances of microarray data sets) showed grouping of samples according to the different phases of the cycle.

Annotation data can be downloaded and therefore updated e.g. at the Agilent homepage. In addition, data from genome sequencing projects of different genomes are available through a number of genome browsers and genome project databases. To improve the annotation (assignment to known horse and human genes), BLAT and BLAST analyses were performed using Ensembl and UCSC genome browsers and NCBI BLAST to assigned equine genes and human putative orthologous genes, Entrez Gene identifiers and the corresponding gene information. All of the probes of the porcine microarray were mapped against the whole genome and porcine tanscripts using Bowtie and further the output sequences (primary accession) were blasted against human genes using UniGene, TIGR, and RefSeq data bases. Due to the enormous number of differentially expressed transcripts/probes and less available annotation data in databases, the improvement of the annotation provided by Agilent for porcine differentially expressed genes could not be performed in such a good quality as compared to the equine data set (9295 probe ID's but only 7560 Hsa Entrez Gene ID's). Although the technical basis already existed, the major hurdle was incomplete gene annotation, particularly for the pig. Furthermore, the knowledge of orthologous genes between mammalian species is also far from complete but it is needed for a reliable cross-species analysis to get a unique gene identifier for comparison of gene expression data. According to Bauersachs and Wolf (Bauersachs et al., 2012) gene symbols cannot be used as unique identifiers, since official gene symbols are still not available for all porcine and equine genes (only locus IDs). One possibility could be to assign putative human orthologous genes and use human Entrez Gene identifiers as a unique identifier. On the basis of these orthologous genes, gene expression data could be compared more directly. However, this task is complicated by duplicated genes, highly similar genes in closely related members of a gene family, incomplete genome sequences or assemblies, incomplete annotation, and the presence of genes specific for different mammalian groups (Bauersachs et al., 2012).

However, the genes obtained from the analyses were classified according to similarities of their gene expression profiles during the estrous cycle (MeV software version 4.7.1/SOTA algorithm). This revealed 8 clusters of major expression profiles for highest mRNA levels at different times during the estrous cycle in both species. Furthermore, for investigating differentially expressed genes in relation to their over-representation of distinct functional terms DAVID Functional Annotation Clustering (online-tool) was performed for the obtained gene clusters. This analysis revealed a number of similar but also many different biological terms as over-represented during comparable stages of the equine and porcine reproductive cycle.

1.1.5. Validation of microarray data

In general, results should be validated by additional experiments. Such validation was performed using quantitative real-time RT-PCR (qPCR). According to Zhang (Zhang et al., 2012) gene expression analysis requires the use of reference genes consistently expressed under

various conditions. Furthermore, the use of housekeeping genes (HKG) as internal controls for quantitative real-time PCR (qPCR) studies of gene expression is based on the assumption of their inherent stability (Sadek et al., 2012). Both studies suggested actin beta (*ACTB)* for HKG, and further on Zhang found H3 histone, family 3A (*H3F3A)* as the most suitable gene for accurate normalization. Microarray data showed that mRNA expression of *H3F3A* followed an extreme regulated pattern during the equine and the porcine cycle and could not be used as a reference gene with stable expression during the estrous cycle. Furthermore, results of equine data showed an increase of actin B (*ACTB)* on day 3 (verified with qPCR analysis), but did not reach statistical significance (q-value = 0.15, threshold q-value = 0.01). Researchers found that even house-keeping genes such as ß-actin and glyceraldehyde-3-phosphate dehydrogenase (*GAPDH*) are up-regulated in endometrium by estradiol (L'Horset et al., 1990). *GAPDH* showed highest expression on day 0 (qPCR analysis) and highest expression on day 3 (microarray analysis) during equine estrous cycle. However, analyses in both species revealed ubiquitin B (*UBB)* as the best 'HKG' candidate. In addition, several genes were selected as representatives for typical expression profiles during the estrous cycle. The results for qPCR of equine samples confirmed results from microarray analysis within 12 out of 22 genes chosen. The aberration within the remaining genes could be a reflection of technical issues. The transcription of RNA samples into cDNA provides the most important and also most critical step in the qPCR process regarding sample-to-sample variation. First-strand cDNA was synthesized for all samples, starting from 1 µg of total RNA with the Sprint™ RT Complete-Double PrePrimed Kit. Unfortunately, there is no simple method to measure the efficiency of reverse transcription of RNA into cDNA. Besides, the mechanical handling of a total volume of 20 µl for each sample can be difficult as well. The stripes provided by the company show synthetic lids that might not close properly. Due to multiple using and therefore thawing of samples, the water could partially sublimate. Another contributing factor in such distribution of Ct-values may be the functionality of primers that were used. Sometimes primers are derived from predicted sequences that might not represent the real existing transcripts. Due to the lack of validated annotation data, several oligonucleotides for equine samples had to be tested by changing annealing temperatures of qPCR or even changing primer designs (*GAPDH, RPL7, SLC25A22* - data only shown for final primer pair). Additionally, the selection of UBB as candidate for house-keeping gene might have been a suboptimal choice. Altogether, despite some technical inaccuracy and bias in bioinformatics analysis, the results of qPCR analysis were overall in accordance with the microarray analysis for equine and porcine experiments.

1.2. Comparison to the study of bovine mRNA expression profiles in endometrium during the estrous cycle (Mitko, 2008)

According to Mitko et al (Mitko, 2008), the bovine tissue samples used in their study were collected on day 18 from heifers which had already low P4 concentrations (shortened cycle) for beginning of estrus and on day 0 as the time around ovulation (two time points during estrus phase), for metestrus, samples collection was performed on day 3.5 and for the luteal phase two times were chosen for sample collection; day 12 (diestrus) with highest P4 concentration and day 18 from heifers with still higher P4 concentrations (normal cycle). After collection further procedures (samples storing, RNA isolation etc.) were performed according to manufactures instruction as it was carried out in the present study. The timing of sample collection was controlled by observation of sexual behavior (i.e. toleration, sweating, vaginal mucus) and ultrasound-guided follicle monitoring. In order to determine P4 concentrations, blood samples were taken. In this regard the procedures were similar.

Microarray analysis was performed using a custom cDNA array, the BOE (bovine oviduct and endometrium) cDNA array version 1. The generation of this array is explained in detail by Bauersachs and coworkers (Bauersachs et al., 2007) and can be summarized as follows: the

array covered approx. 950 different genes that were annotated based on comparisons to common data base sequences. The human orthologous genes were also identified to obtain more information regarding gene function. Although the bovine genome array from Affymetrix was available, the BOE array had the advantage that it is enriched for genes which were found to be differentially expressed during the most important physiological stages of this tissue. Furthermore, the relatively small number of represented genes on the BOE array circumvents many problems of data evaluation and processing and keeps costs down. The background was subtracted with provided software (lowest grid dot) and raw data were normalized applying the BioConductor package ‚vsn' (Huber**,** 2002). Microarray results in this study were validated using qPCR methods as described earlier (Ulbrich et al.**,** 2004).

Altogether the results in this study can be used for comparison of results with the present study to identify changes in dynamic gene expression throughout species but with some limitations. On the one hand, the BOE array data used in the study of Mitko et al. was limited to a comparison of differential gene expression during estrus and diestrus phase. On the other hand, a comparable time point during the bovine cycle representing early luteal phase is missing in the analysis performed by Mitko et al. Both the equine as well as the porcine microarray analysis showed 8 major expression profiles throughout the estrous cycle including early luteal phase and preestrus. Therefore, the genes found to have a significant correlation (positive and negative) in equine and porcine endometrium were compared to the differentially expressed genes revealed from bovine endometrium (by Mitko et.al.) throughout the estrous cycle.

2. Exploration of differentially expressed genes throughout the estrous cycle

The results of both studies of endometrial gene expression changes agree well with cyclic changes of steroid hormones and findings from histological analysis. Although gene expression changes are mainly regulated by the interplay of the ovarian steroid hormones E2 and P4, the 'wave-like' dynamics of gene expression changes (8 major clusters (MeV/SOTA analysis) in each species) demonstrate an intricate fluctuating network of regulation throughout the cycle. In addition to gene expression profiling, specific gene functions and biological processes (bioinformatics analysis of the clusters of genes with similar expression profiles) confirmed dynamic gene expression changes in the endometrium in distinct phases during the estrous cycle, respectively.

2.1. Messenger RNA expression profiles in the endometrium during the equine estrous cycle

All differentially expressed genes in the equine endometrium that are discussed in this part are summarized in supplementary Table VIII-I. The table shows *Hsa* gene ID, *Hsa* gene symbol and mRNA expression on D0, D3, D8, D12 and D16, q-values (achieved from microarray analysis) and results of SOTA clustering analysis.

2.1.1. Genes with highest mRNA expression during estrus

Cytokines include chemokines, interferons, interleukins, lymphokines and tumor necrosis factor and are regulatory proteins secreted by immune cells and other immune component cells acting in a paracrine and autocrine manner. The analysis of equine endometrial expression during estrus phase (low P4 concentration; from day 16 to day 0) revealed a very huge number of genes representing the cytokine family; the chemokine (C-C motif) ligand family (*CCL2, CCL3L3, CCL5, CCL8, CCL13, CCL15, CCL21*), the chemokine (C-X-C motif) ligand family (*CXCL1, CXCL5, CXCL6, CXCL9, CXCL10, CXCL16, CXCL17*) and the interleukin family (*IL8, IL15, IL32, IL34*), attractors for almost all types of immune cells, such as monocytes,

macrophages, dendritic cells, neutrophils, B-cells, T-cells, and natural killer cells (Gebhardt et al., 2012). Furthermore, in reproductive biology, chemokines have been implicated in crucial processes such as ovulation, menstruation, embryo implantation, parturition and pathological processes such as preterm delivery, HIV infection, endometriosis and ovarian hyperstimulation syndrome (Cocchi et al., 1995, Simon et al., 1995). Results were confirmed by the analysis of functional annotation clustering that revealed several categories for immune system functions (e.g. inflammatory response, immune response) as over-represented during this time in cycle. Additionally, mRNA expression of the chemokine (C-C motif) receptor (*CCR9*) and three genes representing the chemokine (C-X-C motif) receptors (*CXCR1*, *CXCR4* and *CXCR7*) were up-regulated during estrus. Results from qPCR analysis confirmed the expression pattern for *CXCR4* showing highest mRNA levels on day 0 and lowest during the luteal phase. Furthermore, the mRNA expression of the interleukin *IL8* (highest level on day 16, higher levels on day 0) is in good agreement with results of the recent study by Fumuso et al. (Fumuso et al., 2007) which observed up-regulation of this gene in the endometrium of mares in estrus compared to diestrus. The functions of interleukins are wide spread throughout all kinds of tissue and species. So far, interleukins have been demonstrated to stimulate prostaglandin production in the endometrium in many species besides the mare (Kotwika et al., 1999, Krzymowski, 1990, Soede, 1997, Virolainen et al., 2005. , Waclawik, 2011). Moreover, most recent studies showed an up-regulation of endometrial interleukin 1 alpha (*IL1A)* and interleukin 6 (*IL6)* mRNA expression during the follicular phase of the equine estrous cycle, as well as their promotion of endometrial cell proliferation and also that E2 enhanced their support of PG production (Szostek et al., 2014). However, results in this study revealed no detection of neither *IL-1α* nor *IL-6* in the equine endometrium but its receptor interleukin 1 receptor, type 1 (*IL1R1*) showed highest expression on day 16.

Phospholipase A2 is an essential enzyme for the release of the arachidonic acid from the cell membrane which is the starting molecule of the biosynthesis of prostaglandins. Annexins, a family of intracellular proteins with calcium–dependent phospholipid binding properties, can affect many components of the inflammatory reaction by inhibition of phospholipase A2 and suppression of neutrophil and monocyte migration (Gerke V., 2002). Data showed up-regulation of *ANXA3* mRNA on day 16 (microarray and qPCR) and down-regulation during the luteal phase. However, Mitko et al. (Mitko, 2008) found a number of genes such as lectin galactoside-binding soluble 1 (*LGALS1)*, tenascin C (*TNC*), osteonectin (*SPARC)*, proprotein convertase subtilisin/kexin type 5 (*PCSK5)*, gastrin releasing peptide (*GRP*), annexin A2 (*ANXA2*) and nephroblastoma overexpressed gene (*NOV*) as up-regulated during estrus in bovine endometrium, which have been described as positively involved in the regulation of the process ‘invasive growth’. The decreased mRNA levels of these genes during the luteal phase may be associated with the regulation of non-invasive implantation in cattle and in mares. Out of this group of genes, results of microarray analysis of equine endometrium revealed higher expression of *TNC*, *SPARC,* and *NOV* on day 0 during equine estrous cycle. The increased mRNA concentrations of genes coding for specific surface antigens indicates infiltration and activation of the endometrium with immune cells during estrus, respectively. Continuatively, researchers assumed that cytokines may play a role in local changes, such as angiogenesis, cell proliferation, and other processes taking place in the endometrium (Szostek et al., 2014). This statement is verified by the findings of the functional terms ‘angiogenesis’, ‘blood circulation’ and ‘vasculature’ as over-represented during this time in cycle. Several genes with highest mRNA levels during the estrus phase that were found as assigned to members of the angiopoietin system (angiopoietin 2, *ANGPT2*; angiopoietin-like 1, 2 and 4, *ANGPTL1*, *ANGPTL2, ANGPTL4;* TEK tyrosine kinase, *TEK*), the VEGF system (neuropilin 2, *NRP2*, kinase insert domain receptor (*KDR,* also known as *VEGFR2*)), genes related to endothelial cell regulation (endothelins 1 and 2, *EDN1/EDN2*; the receptor for EDN1, endothelin receptor type

A, *EDNRA*; endothelial cell surface expressed chemotaxis and apoptosis regulator, *ECSCR*), angiotensin I converting enzyme (peptidyl-dipeptidase A) 2 (*ACE2*), and fibroblast growth factor 2 (basic) (*FGF2*) were found as up-regulated during estrus (data published in (Gebhardt et al., 2012). The over-representation of these genes is a sign for increased growth that occurs during ovulatory phase and of vascular changes which could be related to the observation that 'inflammatory response' genes are over-represented during the same time, since inflammatory responses and vascular responses are tightly connected (Saban et al., 2010). In addition, up-regulation of a number of angiogenic factors by E2 was shown in sheep (Johnson et al., 2006).

The immune response can be divided into two types: innate (non-adaptive or non-specific) and adaptive or specific immune response (Dalin et al., 2004). The complement cascade is part of the innate immune response which contributes to the elimination of cellular antigens. Three biochemical pathways are known to activate the complement system: the classical complement pathway, the alternative complement pathway, and the lectin pathway. Results of DAVID functional annotation clustering revealed the category 'complement activation, classical pathway' as over-represented on day 16 during the equine estrous cycle. The complement cascade mediates a series of biologic reactions, which include increased vascular permeability, chemotaxis, opsonization prior to phagocytosis, activation of membrane lipases, and lysis of target organisms. Complement activity as well as isolation of complement cleavage products have been demonstrated in the equine reproductive tract (Asbury et al., 1982, Watson et al., 1987a). Four genes assigned to the complement cascade were found as up-regulated in equine endometrium: complement component 3 (*C3*), complement component 4 binding protein, alpha and beta (*C4BPA*, *C4BPB*), complement component 1, r subcomponent (*C1R*), complement component 7 (*C7*) and serpin peptidase inhibitor, clade G (C1 inhibitor), member 1 (*SERPING1*). *SERPING1*, encoding a protein known as C1 inhibitor, regulates complement pathway activation and blocks the activity of plasma kallikrein and the activated form of factor XII in blood (Davis, 2008). These two proteins participate in the production of bradykinin, which promotes inflammation by increasing vascular permeability. However, Hayashi et al (Hayashi et al., 2011) showed that SERPING1 may suppress inflammation promoted by bradykinin but in bovine ovarian follicles. Klein et al. (Klein et al., 2006) suggested that the up–regulation of *SERPING1* mRNA in the bovine uterine glandular and luminal epithelial cells on day 18 during pregnancy could be a mechanism to protect the embryo against an attack from the maternal immune system in case of pregnancy. In addition, five genes representing the superfamily of the SERPINs (*SERPINA1*, *SERPINA5*, *SERPINE1*, *SERPINE2* and *SERPINI1*), which are involved in inflammation processes and other processes like fibrinolysis, coagulation, cell mobility, cellular differentiation and apoptosis, were found to be up-regulated during estrus phase. Regarding the fact that the group of SERPINs is further separated e.g. SERPINA14 is represented in a limited group of species (Padua et al., 2010) and only little is known about their potential functions during the estrous cycle further analyses are necessary. The inflammatory process involves chemokine-initiated recruitment of polymorphonuclear neutrophils (PMNs) and other inflammatory cells to the area of insult, leading to the removal of pathogens and resolution of inflammation (Parham, 2005). Complement products as well as leukotriene B4 (LTB4), prostaglandin E (PGE), and prostaglandin F2alpha (PGF2a) may all serve as chemoattractants for polymorphonuclear neutrophils (PMNs) in the uterus (Lees et al., 1986, Watson et al., 1987a, b). The genes with highest expression levels during estrus clearly indicate that the endometrium prepares for uterine clearance needed during and after mating which is probably further triggered by spermatozoa and components of the seminal plasma (Troedsson, 2001) leading for example to influx of PMNs into the uterine lumen (Troedsson, 1999). Although the mares used in this study were not inseminated, the corresponding immune-related genes (inflammatory response, cytokine-cytokine receptor interaction, complement and coagulation cascades, innate immune response) were up-regulated during estrus, which is

probably caused by effects of estrogen in preparation for the shock of intrauterine insemination in the mare (Gebhardt et al., 2012). Besides, the findings indicate a reconstruction at the end of the estrous cycle to prepare the endometrium for the onset of a new cycle.

Furthermore, several genes with highest mRNA concentrations during estrus were related to 'extracellular matrix (ECM)' and the process of 'focal adhesion' (adhesion of cells to ECM): e.g. three representatives of the matrix metallopeptidase family (*MMP3, MMP9* and *MMP28*). Matrix metalloproteinase (MMPs) are calcium- and zinc-dependent proteases (peptidases) believed to be responsible for degradation and reorganization of ECM in tissues (Nagase et al., 2006). In addition MMPs are involved in laminitis, osteoarthritis, recurrent airway obstruction, skin wounds repair, degenerative diseases of the central nervous system, ulcerative keratitis, cancer (Clutterbuck et al., 2010) and equine endometriosis (Walter et al., 2005). In relation to the term ECM, the functional term 'collagens' (e.g. 19 genes) was found as over-represented during estrus. A decrease in collagen fibers has been observed during the pre-implantation phase in bovine endometrium in a recent study (Yamada et al., 2002) which is in line with the lower mRNA levels of collagen genes (e.g. *COL1A1*) at diestrus. Microarray data revealed highest expression of *COL1A1* on day 0 which was confirmed by qPCR experiments. The mRNA expression profile of these genes and the results of the study from Yamada et al. (Yamada et al., 2002) suggest a complex regulation of the ECM remodeling in the endometrium during the estrous cycle.

As the endometrial changes during estrus are mainly controlled by estradiol, the large number of genes related to estrogen metabolism and signaling is coherent at this time during the estrous cycle. Besides, *FGF9* has been described as one of the mediators of estrogen signaling in the endometrium (Tsai et al., 2002). In case of pregnancy, *FGF9* mRNA has been found as increased in pregnant endometrium by Merkl et al. (microarray 9-fold, qPCR 8-fold up-regulated in day 12 pregnant endometrium (Merkl et al., 2010)) and has been described as an autocrine endometrial stromal growth factor induced by E2 in human endometrial stroma (Tsai et al., 2002). Induction of FGF9 expression by PGE2 through the EP3 receptor was also demonstrated in human endometrium (Chuang et al., 2006). Microarray analysis revealed highest mRNA expression of prostaglandin E receptor 3 (*PTGER3* (subtype EP3)) on day 0 which is in good agreement as well as highest *FGF9* mRNA concentration on day 16 and on day 0 following serum E2 levels. In addition, the mRNAs of two estrogen related receptors, estrogen-related receptor alpha (*ESRRA*) and estrogen-related receptor gamma (*ESRRG*) were also found as differentially expressed during the estrous cycle. *ESRRG* showed lowest expression levels on day 3 and highest levels on day 0, and *ESRRA* had lowest levels on day 0 and highest on day 8 and slightly over-expressed on day 16. Estrogen-related receptors are a subfamily of orphan nuclear receptors closely related to the classical estrogen receptors and have been shown to share target genes, co-regulatory proteins, etc. with classical ESRs and can influence the estrogenic response (Giguere, 2002). Although ESRRs lack identified natural ligands (orphan nuclear receptor), binding and activation by phytoestrogens have been shown (Hirvonen, 2011).

In addition, several genes related to PG metabolism and signaling showed up-regulation throughout the cycle. Prostaglandin E receptor 4 *(PTGER4 (*subtype EP4*))*, phospholipase A2, group IVA (*PLA2G4A,* cytosolic, calcium dependent), and solute carrier organic anion transporter family, member 2A1 (*SLCO2A1*, PG transporter) showed highest mRNA concentrations on days 16 and day 0. In contrast, Merkl et al. (Merkl et al., 2010) found all four genes to be increased on day 12 in pregnancy of equine endometrium compared to non-pregnant controls indicating a shift from maternal to a possible conceptus derived E2 induction. In case of pregnancy, conceptus mobility is at maximum between days 11 and days 14 after ovulation. It is apparent that localized myometrial contractions provide the driving force that literally

squeeze the vesicle around the uterine lumen (Cross et al., 1988, Ginther, 1984). In addition, Stout and Allen (Stout, 2001) postulated a possible role of PGE and PGF2a in intrauterine migration of the equine conceptus as both prostaglandins are known to have potent actions on smooth muscle activation. As non-pregnant endometrium shows mRNA expression of two receptors of PGE as up-regulated in this time period, a possible preparation of the uterus for eventual pregnancy is reasonable. PGF2a can be produced directly from PGH2 by aldo-keto reductase family 1 members B1 and C3 (AKR1B1 and AKR1C3) and can be synthesized via PGE2 by the action of the enzymes carbonyl reductase 1 (CBR1), AKR1C1 and AKR1C2 or by reduction of PGD2 by AKR1C3 (Catalano et al., 2011, Dozier et al., 2008). Following biosynthesis, $PGF_{2\alpha}$, exerts its function through the G protein coupled receptor PTGFR (Abramovitz et al., 2000), preferentially. Our data showed highest expression of *AKR1C1* on day 12 during the equine estrous cycle as luteolysis is about to start while its receptor, prostaglandin F receptor (*PTGFR,*also known as *FP)* was highly expressed on day 3.

As reported, endometrial stimulation with high-dose of E2 increased myometrial oxytocin receptor density in human uterus (Richter et al., 2003) and furthermore, oxytocin and certain prostaglandins have been demonstrated to stimulate uterine contractility via different mechanisms (Turnbull, 1971). Increased expression of prostaglandin-endoperoxide synthase 2 (*PTGS2*), also known as cyclooxygenase 2 (*COX2*), was found in uterine epithelial cells on day 15 of the cycle, whereas increase of endometrial *PTGS2* expression was inhibited in pregnant mares Our data showed increased mRNA expression of *PTGS2* on day 16 when luteolysis is in process. Aurich (Aurich, 2011) suggested an important role of COX2 in pulsatile secretion of oxytocin within the onset of luteolysis in the mare which is in good agreement to results of the present study as oxytocin, prepropeptide (*OXT*) showed highest expression on day 0, higher expression during the luteal phase and lowest on day 16 following E2 concentrations. The importance of physical clearance as an part of the uterine defense system was suggested in studies using fluid accumulation in the uterus following experimentally induced endometritis in susceptible mares (Allen et al., 1988, LeBlanc et al., 1989, Troedsson, 1999)Furthermore, recent investigations suggest an important role of PGF2a in this physical clearance, as myometrial contractions are regulated by PGF2a together with oxytocin in mares (Asbury et al., 1982, Goddard et al., 1985). This has been clarified by Cadario and coworkers (Cadario et al., 1995) who used phenylbutazone to inhibit PGF2a induced myometrial contractions and observed a delayed clearance of radiocolloids from the uteri of reproductively normal mares. Equine endometrial secretory cells produce, store and secrete oxytocin and are thus most likely involved in stimulating and maintaining uterine contractility (Bae et al., 2003). The secretory activity of the endometrium during estrus together with increased myometrial activity contributes to uterine clearance mechanisms that void uterine infection (Aurich, 2011). Data indicate a role of endometrial OXT in uterine contractility stimulated by E2 as well. Altogether, the complex regulation of genes involved in PG metabolism and signaling suggests an important role of the corresponding genes in the regulation of the estrous cycle.

The results of dynamic gene expression during the estrus phase indicate a relation of genes involved in ‘immune system function’ with the ‘vasculature’ and ‘angiogenesis’ of endometrial tissue involving ECM remodeling and complex tissue reconstruction and beginning of cell proliferation.

2.1.2. Genes with highest mRNA expression during early luteal phase

Cyclic changes in the endometrium are a complex process governed by the interplay of several signaling pathways that critically regulate cell growth and proliferation. Tissue maintenance is an ongoing process in which progenitor cells differentiate into various cell types to perform specialized functions while the undifferentiated cells are then removed without affecting

neighboring cells and overall tissue structure (Medh et al., 2000), thereby maintaining steady state kinetics via low rate apoptosis that complements mitosis (Roberto da Costa et al., 2007). Several studies regarding cyclic pattern in cell proliferation and apoptosis in the uterine endometrium in relation to ovarian steroid hormone secretion in humans (Harada et al., 2004, Jones et al., 1998) and animal species, such as pigs (Kaeoket et al., 2001, Okano et al., 2007, Wasowska et al., 2001), mice (Sato et al., 1997), dogs (Chu et al., 2002), rats (Lai et al., 2000), hamsters (Sandow et al., 1979) and in rabbits (Nawaz et al., 1987) have been published. In addition, few studies (Aupperle et al., 2000, Gerstenberg et al., 1999, Roberto da Costa et al., 2007) have been performed analyzing the role of apoptosis and cell proliferation in the regulation of endometrial changes during the equine estrous cycle. Gilbert and coworkers (Gilbert, 1992) found, by counting mitotic figures that most luminal epithelial cells divide in late estrus, whereas most glandular epithelial cells divide on day 4 of diestrus in the mare endometrium. Moreover, latter researcher have been the first to suggest that luminal and glandular epithelial cells should be regarded as functionally distinct cell populations since they show different cyclic responses (Gilbert, 1992). Results of the study by Roberto da Costa (Roberto da Costa et al., 2007) support this argument as they observed higher proliferation during the luteal phase in glandular and luminal cells but not in the stroma (superficial and deep). DAVID functional annotation clustering revealed biological categories such as 'cell-cycle', 'mitosis' and 'chromosome' as over-represented following estrus. In addition, cyclin-dependent kinase 4 (*CDK4*) mRNA showed highest level on day 3 during the cycle (microarray and qPCR data). Cell proliferation and apoptosis are hormone-dependent physiological processes involved in endometrial growth and regression (Roberto da Costa et al., 2007). A huge number of factors control the initiation of physiological cell turnover and apoptosis, including the cellular environment, growth factors, cytokines and hormones, which can act in an autocrine, paracrine and endocrine manner (Kayisli et al., 2002). Results of the study by Roberto da Costa (Roberto da Costa et al., 2007) demonstrated higher active caspase-3 in stromal cells being significantly higher in the follicular phase than during luteal phase but no significant differences in LE and sGE. In mammalian cells, activation of caspase-3 has been shown to occur through two major apoptotic pathways which are initiated by the Fas ligand complex and cytochrome c (Hengartner, 2000). The gene expression profiling showed several genes related to regulation of apoptosis as over-represented throughout the cycle. In order to understand the interaction of these genes and their products, further detailed studies of dynamic gene expression changes in the endometrium related to the regulation to apoptosis should be performed in the field of research of equine reproduction.

During the estrous cycle, the endometrium releases oxytocin-induced luteolytic pulses of PGF that result in functional and structural regression of the ovarian corpus luteum (CL), termed luteolysis (Spencer, 2004). The mechanism that develops in the endometrial LE and sGE requires sequential effects of progesterone, estradiol, and oxytocin, acting through their respective receptors (Spencer et al., 2002, Spencer, 1996). Several studies in ovine endometrium observed increased expression for all three respective receptors at estrus (Spencer et al., 1995a, Wathes et al., 1993) stimulated by estrogen levels that peak from the ovulatory Graafian follicle. Following estrus, progesterone levels increase and act via PGR to block expression of estrogen and oxytocin receptor in the endometrial LE and sGE which are therefore not detected during most of diestrus (days 5 to 11) in the ovine estrous cycle (McCracken, 1980). Microarray analysis revealed highest mRNA expression of *PGR* from day 0 to day 3 and endometrial mRNA concentration for estrogen receptor 1 (*ESR1*) from day 16 to day 3 in the equine cycle. This is additionally in agreement with the results of Hartt et al. who found highest mRNA levels on days 0, 17 and 20 of the estrous cycle, but did not investigate day 3 (Hartt, 2005). Receptors for both steroid hormones exist in the luminal and glandular epithelium and stroma of the equine endometrium. The expression of the progesterone receptor gene (*PGR)* in

equine endometrium decreases during the luteal phase particularly in luminal and glandular epithelium (Hartt**,** 2005). However, the study by Spencer et al. in sheep suggested a rapid increase in expression of estrogen receptor on day 13 followed by oxytocin receptor on day 14 in LE and sGE following the loss of PGR block (Spencer et al.**,** 1995b). This increase could not be detected in the present study in equine endometrium for *ESR1* but the mRNA expression of *ESRRG* showed a similar profile. In addition, the study by Starbuck (Starbuck**,** 1998) found high oxytocin receptor expression on day 14 of the equine estrous cycle. The oxytocin receptor (*OXTR)* showed highest mRNA expression from day 12 to day 16 during the estrous cycle but did not reach statistical significance (q-value 0.05, threshold q-value 0.01). As already mentioned, oxytocin, prepropeptide (*OXT*) mRNA change was found during the equine estrous cycle. Equine endometrial secretory cells produce, store and secrete oxytocin and are thus most likely involved in stimulating and maintaining uterine contractility (Bae et al.**,** 2003). In addition to a role of oxytocin in myometrial activity in context with uterine clearance data suggest a storage of endometrial oxytocin prepropeptide during early luteal phase and release at the onset of PG synthesis and therefore a role in the mechanism in equine luteolysis. In addition, G protein-coupled estrogen receptor (*GPER)* showed a profile similar to *ESR1* mRNA with highest levels on day 3 as in human endometrium where *GPER* expression is also regulated during the cycle with highest mRNA levels during the proliferative phase (Plante et al.**,** 2012). Moreover, several studies (Tomanelli et al.**,** 1991, Watson**,** 1992) showed that the concentration of both E2 and P4 receptor proteins in the mare endometrium increased at estrus and early luteal phase and decreased in the mid and late luteal phase. Similar to sheep, results from horse suggest that expression of estrogen and progesterone receptor is positively regulated by circulating levels of estrogen and negatively by progesterone, respectively (Hartt**,** 2005).

Altogether, the expression patterns of these selected genes involved in steroid hormone signaling indicate a complex regulation of E2 effects on the endometrium starting on day 0 and persisting to day 3 during the estrous cycle. Furthermore, less up-regulation of genes related to estrogen signaling during the late luteal phase are in contrast to a possible interaction with ovarian FSH (second FSH peak). Besides, detailed studies of dynamic temporal and spatial gene expression changes have to be performed to understand the interaction of genes related to steroid hormone signaling and metabolism and their respective receptors - especially the role of endometrial oxytocin regulation in the equine endometrium – and the connection to cell proliferation pattern and apoptosis, respectively.

2.1.3. Genes with highest mRNA expression during luteal phase

Highest mRNA concentrations for genes coding for enzymes involved in fatty acid metabolism, such as acyl-CoA synthetases, acyl-CoA dehydrogenase (*ACADL*), carnitine palmitoyltransferases, acetyl-CoA acyltransferase 2 (*ACAA2*), acetyl-CoA carboxylase beta (*ACACB*), enoyl-CoA delta isomerase 2 (*ECI2*), hydroxyacyl-CoA dehydrogenase/3-ketoacyl-CoA thiolase/enoyl-CoA hydratase (trifunctional protein), beta subunit (*HADHB*), and ELOVL fatty acid elongase 5 (*ELOVL5*) were observed during this time of the estrous cycle. Both adiponectin receptors 1 and 2 (*ADIPOR1, ADIPOR2*) of the adipocytokine signaling pathway were found as expressed. Expression of *ADIPOR1* and *ADIPOR2* was also described in murine and human endometrium during the time of implantation and in pre-implantation endometrium, respectively (Evans et al.**,** 1997, Knox**,** 2005). The increased fatty acid synthesis suggests a need for provisioning of the preattachment equine conceptus (in case of pregnancy) with essential fatty acids and retinoids. Suire et al. (Suire**,** 2001) suggested that equine uterocalin (official name and symbol: P19 lipocalin, P19) binds fatty acids and lipids and transports them to the conceptus. The mRNA expression profile of P19, coding for one of the major, progesterone-dependent proteins secreted into the uterine lumen of the mare (Crossett et al.**,** 1998) was similar to those genes involved in fatty acid metabolism with highest expression

during luteal phase and lowest on day 0 of the estrous cycle. Furthermore, fatty acids are, substrates in prostaglandin synthesis. Effects of P4 during the time of highest P4 levels are mainly mediated via stromal cells that still express PGR (Fortune et al., 2001) and via other types of non-classical progesterone receptors such as progesterone receptor membrane component 1 and 2 (*PGRMC1, PGRMC2*) (Signoret, 1970). *PGRMC1* belongs to the membrane–associated progesterone receptor (*MAPR*) protein family which is widespread in eukaryotes and involved in regulating numerous biological functions (Cahill, 2007). PGRMC1 expression has been demonstrated in several female reproductive tissues in different mammalian species (Luciano, 2011). The analysis of *PGRMC1* mRNA expression in the uterus revealed a down-regulation from the proliferative (i.e. epithelial cell cycle progression, mucosal edema and angiogenesis) to the secretory (i.e., mitosis blockade, cellular differentiation and mucosal secretion) phase of the human menstrual cycle (Geisert et al., 1994). Despite the dynamic regulation of PGRMC1 in the human endometrium, PGRMC1 expression does not change during the estrous cycle in the cow, respectively (Luciano, 2011). Data for equine endometrium showed highest mRNA expression of *PGRMC1* during the luteal phase. Additionally, several studies indicated that progesterone mediates an anti-apoptotic action through PGRMC1 but in the ovary (Mansouri et al., 2008, Peluso et al., 2006).

In addition to genes related to steroid-hormone signaling, genes with highest levels on days 8 and 12 were predominantly related to protein secretion as indicated by functional categories, such as ‘protein transport’, ‘endoplasmic reticulum’ and ‘Golgi apparatus’, to signaling processes and to metabolic processes, such as ‘monosaccharide metabolic process’ and ‘lipid metabolism’. Specifically, genes involved in ‘fatty acid metabolism’, ‘adipocytokine signaling pathway’, ‘PPAR signaling pathway’, and ‘glycerophospholipid metabolism’ were found in the expression clusters with highest mRNA levels during this time of the estrous cycle. The functions of the genes involved in protein secretion, signaling, metabolic processes during this phase of the cycle indicate that the equine endometrium prepares for the support of embryo growth and development (data published in (Gebhardt et al., 2012). Highly significant over-representation of molecular functions and biological processes related to cell proliferation for genes with highest mRNA levels on day 3 and highest expression levels of “supportive” genes with functions related to protein secretion and nutrient supply during the luteal phase of the estrous cycle is in good agreement with results of a recent study of asynchronous embryo transfer that showed a relatively wide period of time for the establishment of pregnancy in the mare (Adams, 1999). In this regard, the situation in equids seems to be different compared to ruminants, where an adequate timing of P4-regulated changes in the endometrium is the prerequisite for normal embryo development and conceptus elongation (Fortune, 1994, Morales, 2000).

The genes for nitric oxide synthase 3 (NOS3), angiotensin I converting enzyme (peptidyl-dipeptidase A) 1 (Genbacev et al., 2003), angiotensinogen (Gilles et al., 2003), angiomotin (*AMOT*) angiopoietin-like 6 (*ANGPTL6*), and endothelial PAS domain protein 1 (*EPAS1*) showed their highest mRNA levels during diestrus. Differential expression of NOS3 protein was described in human endometrial vessels with highest expression in the early secretory phase (Sayasith et al., 2007). Renin stimulates the cleavage of angiotensinogen to angiotensin which is subsequently cleaved into peptides with either vasodilator or vasoconstrictor activities by angiotensin-converting enzymes (see KEGG pathway ko04614 Renin-angiotensin system) (Ginther et al., 2008). Interestingly, mRNA coding for *ACE2* that produces vasodilators from angiotensin I and II was highest at estrus, whereas mRNA coding for ACE that produces the potent vasopressor angiotensin II was highest on day 8 of the estrous cycle. Studies of uterine blood flow in cyclic mares found highest blood flow on days 0 and 10/11 (Alexander et al., 1982, Aurich et al., 1995) which correlates with the observation that the genes in this study

related to the functional terms ‘blood circulation’ and ‘angiogenesis’ were predominantly found in the expression clusters with highest mRNA concentrations during estrus and in expression clusters with highest mRNA concentrations on days 8 or 12. The comparison to studies of gene expression during the time around maternal recognition of pregnancy (MRP) (Merkl et al., 2010, Tortonese et al., 2001) shows that expression of similar genes is induced during estrus and on days 12 and 14 of pregnancy indicating a specific induction of those genes by the presence of the conceptus, probably by conceptus estrogens. Additionally to genes involved in mentioned signaling pathways, secreted phosphoprotein 1 (*SPP1,* also known as osteopontin) mRNA was found as up-regulated during the luteal phase. Since *SPP1* is an extracellular matrix/adhesion molecule that is up-regulated in the pregnant uterus of all mammals examined to date (White et al., 2005) and only little is known about its regulation during the reproductive cycle in non-pregnant animals, the up-regulation and thereby the function of *SPP1* in this context remains unclarified. In mice uteri *SPP1* is up-regulated during estrus However, White et al. (White et al., 2005) supported the hypothesis that SPP1 has functions in implantation and placentation of mammalian species especially in the pig. Additionally, Yoo et al. (Yoo et al., 2006) suspected an anti-apoptotic role of *SPP1* but in the neonate. Results in Figure IV-1.

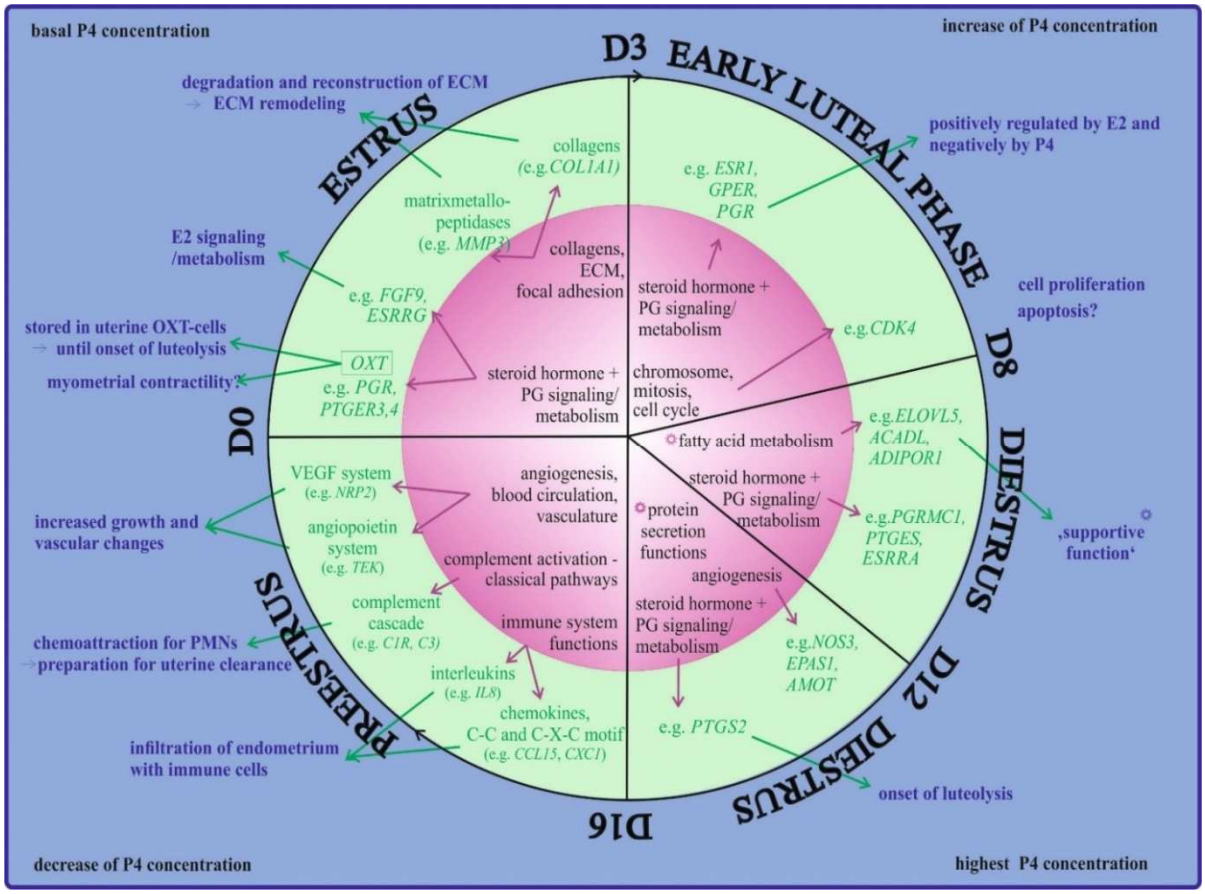

Figure IV-1: Summary of the results from the analysis of equine endometrium during the estrous cycleThe equine estrous cycle is 21 days in length and the day of ovulation is defined as D0. The main phases of the cycle and the analyzed days (D0, D3, D8, D12, D16-exterior lettering) are shown. Progesterone (P4) concentration during the particular phase is given in each corner. Internal circle (pink) shows over-represented biological functions during the specific phases of the estrous cycle achieved from DAVID functional annotation clustering analysis. External circle (green) represents single genes or groups represented by several genes with highest mRNA expression during the corresponding time of the estrous cycle. Blue area demonstrates conclusions (potential connection to changes in endometrium). Connection between events are demonstrated with arrows. *ACADL*-acyl-Coenzyme A dehydrogenase, long chain, *ADIPOR1*-adiponectin receptor 1, *AMOT*-angiomotin *C1R*-complement component 1, r subcomponent, *C3*-complement component 3, *CDK4*-cyclin dependent kinase 4, ECM-extracellular matrix, e.g.-for example, *ELOVL5*-ELOVL fatty acid elongase 5, EPAS1-endothelial PAS domain protein 1, *ESR1*-estrogen

receptor 1, *ESRRA,G*-estrogen-related receptor alpha, gamma, *FGF9*-fibroblast growth factor 9, *GPER*- G protein-coupled estrogen receptor, *NOS3*-nitric oxide synthase 3 (endothelial cells), *NRP2*-neuropilin 2, *OXT*-oxytocin, *PGRMC1*-progesterone receptor membrane component 1, *PGR*-Progesterone receptor, PMN-polymorphnuclear neutrophils, *PTGER3,4*-prostaglandin receptor 3 and 4, *PTGES*-prostaglandin E synthase, *PTGS2*-prostaglandin-endoperoxide synthase 2, *TEK*-TEK tyrosine kinase, endothelial

2.2. Messenger RNA expression profiles in the endometrium during the porcine estrous cycle

Supplemental Table VIII-III summarizes all differentially expressed genes in the porcine endometrium that are discussed in this part. The table shows *Hsa* gene ID, *Hsa* gene symbol and mRNA expression on D0, D3, D6, D12 and D18, q-values (achieved from microarray analysis) and the number of Cluster from SOTA clustering analysis. In addition a summary of the results is shown in Figure IV-2.

2.2.1 Genes with highest mRNA expression during estrus

Dynamic changes in the uterine endometrium are a type of homeostasis and are associated with proliferation and exclusion of cells. Apoptosis plays a major role during development and is also involved in the homeostasis of the uterus that involves various hormones and cytokines. Additionally, it has been defined for the human uterus that it is a mechanism by which uterine luminal epithelium and glands degenerate in the absence of embryonic factors and regenerate in a cycling fashion through the cycle (Dery et al., 2003). Furthermore, it was demonstrated in hamster and rat uterine epithelium during the estrous cycle by electron microscopy, that numerous epithelial cells undergo apoptosis at estrus (Sandow et al., 1979). The number of different cell types involved in apoptotic cell death exhibits a scientific challenge that has not been completely clarified yet. Several factors such as nitric oxide synthase (*NOS*) (Tschugguel et al., 1999), tumor necrosis factor-alpha (*TNFa*) (Tabibzadeh, 1995), Fas (TNF receptor superfamily, member 6) (*Fas)* (Harada et al., 2004) and interleukin-1 (*IL1*) (Tanaka et al., 1998) are known to induce apoptosis in epithelial cells of the human endometrium. In addition, ovarian hormone withdrawal may play a key role in the regulation of endometrial apoptosis (Rotello et al., 1992, Slayden et al., 1993). As for the expression of *TNFa* in the estrous cycle in the mouse, no or only slight expression of *TNFa* mRNA was observed in uterine tissues during preestrus, estrus, and early luteal phase, but the expression increased in the late luteal phase (Roby, 1994). Microarray data showed genes coding for *IL1ß* as up-regulated on day 0, nitric oxide synthase 3 (*NOS3*, endothelial cell) and 1 (*NOS1,* neuronal) and *TNF* as up-regulated on day 18 as well as *Fas (*TNF receptor superfamily, member 6*)* with highest mRNA expression from day 18 to day 0 during the cycle in pigs. In accordance to the results from microarray analysis, DAVID functional annotation clustering revealed the category 'regulation of apoptosis' as over-represented during the estrus phase in porcine endometrium. Small nuclear ribonucleoprotein polypeptide A (*SNRPA)* is an important gene which had been reported to function in binding stem loop II of U1 snRNA and may be involved in coupled pre-mRNA splicing and the polyadenylation process. Recently many reports described that *SNRPA* is associated with the regulation of apoptosis (Degen et al., 2000, Hof et al., 2005). Detailed function of SNRPA in this context has to be clarified. Microarray data for *SNRPA* mRNA was validated by qPCR analysis showing highest expression on day 3. Moreover, results of a recent study of endometrial gene analysis in non-pregnant and pregnant sows on day 14 after ovulation (Østrup et al., 2010) revealed 22 genes assigned to the biological term 'apoptosis' (15 up- and 7 genes down-regulated in pregnant endometrium) which is in good agreement to the study of Samborski et al.(Samborski et al., 2013) that showed genes related to the 'regulation of apoptosis' as over-represented on day 14 in pregnant pigs. Results in the latter study showed characteristic pro-apoptotic genes like BCL2-antagonist/killer 1 (*BAK1*), BCL2/adenovirus E1B 19kDa interacting protein 3 (*BNIP3*), caspases 1 (intrinsic pathway) and 10 (extrinsic

pathway) (*CASP1*, *CASP10*), *Fas* and tumor necrosis factor (ligand) superfamily, member 10 (*TNFSF10/TRAIL*) as well as anti-apoptotic genes B-cell CLL/lymphoma 2 family (*BCL2A1, BCL2L14*), baculoviral IAP repeat containing 3 (*BIRC3*), and CASP8 and FADD-like apoptosis regulator (*CFLAR*) to be increased in pregnant endometrium among others. The present microarray results in cyclic porcine endometrium showed the genes coding for *CASP10*, *TNFSF10* and *BIRC3* with highest mRNA levels on day 0, *Fas* as up-regulated from day 18 to day 0 and *CASP1* as highly expressed on day 3 during the cycle among others, respectively. The similarity in gene expression analysis between pregnant (D14) and cycling (D0) pigs could be due to elevated estrogen levels around estrus and estrogen signaling of the conceptus in case of pregnancy. Okano et al. (Okano et al**.,** 2007) have investigated the morphological features and occurrence of apoptosis in the porcine endometrium during the estrous cycle with main focus on surface epithelium (SE), glandular epithelium (GE) and stroma cells. The results in this study clearly showed a peak of apoptosis at estrus which may be explained by the exclusion of many cells from the epithelium from preestrus to the early luteal phase by programmed cell death. Thus apoptosis was suppressed in the epithelium in accordance to the high levels of progesterone from the functional corpora lutea, and the surface epithelium remained in a low columnar or cuboidal state. Okano and coworkers further suggested that apoptosis frequently switches from the surface epithelium to the stromal cells during estrus (Okano et al**.,** 2007). The expression patterns of genes assigned to 'regulation of apoptosis' indicate a complex rearrangement of cells including cell death and proliferation in the porcine endometrium during this time of the estrous cycle. However, the relationship between apoptosis and uterine function in the pig has not been fully analyzed yet. In order to understand the interaction of these genes and their products, further detailed studies of dynamic protein expression and localization of expression in different endometrial compartments have to be performed.

Blood levels of estrogen reach a peak during estrus phase which is rapidly followed by a marked surge of progesterone during the early luteal phase. Estrogens regulate growth, development, and behavior associated with reproduction. As already mentioned, one pivotal effect of estrogen is its regulation of estrogen receptor 1 (ESR1) and progesterone receptor (PGR) gene expression. The presence of these specific receptors is the primary determinant of tissue responsiveness to steroid hormones (Webb et al**.,** 1992); estrogen up-regulates both receptors, whereas progesterone inhibits ESR1 expression and has a negative effect on PGR expression in epithelial cells (Spencer et al**.,** 1996). During the ovine estrous cycle, ESR1 and PGR abundance increases as levels of estrogen rise in the circulation (Koligian et al**.,** 1977, Ott et al**.,** 1993). The observed mRNA expression pattern for estrogen receptor 1 (*ESR1*) in the porcine endometrium during the estrous cycle are in good agreement to latter statement; highest expression on day 0, decrease on day 3 and lowest expression during the luteal phase. In porcine endometrium, mRNA for one estrogen-related receptors that have been shown to share target genes, co-regulatory proteins, etc. with classical ESRs and are able to influence the estrogenic response (Giguere**,** 2002), estrogen-related receptor beta (*ESRRB*), was differentially expressed with highest expression on day 3. As already mentioned binding and activation by phytoestrogens have been shown (Hirvonen**,** 2011) for estrogen-related receptors although ESRRs lack identified natural ligands (orphan nuclear receptor). Furthermore, the actions of progesterone on tissues are controlled through interaction with the progesterone receptor (PGR), which has been characterized as a ligand activated transcription factor that functions to regulate gene expression (Pru et al**.,** 2013). In the pig, *PGR* mRNA and protein decrease in the uterine luminal epithelium during the first week of the estrous cycle (Mathew et al**.,** 2011). Results of a recent study showed further down-regulation in *PGR* as less pronounced in the uterine glandular epithelium and occurrence within the endometrial stroma or within the myometrium (Geisert et al**.,** 1994). In addition, PGR down-regulation in the pig uterus is initiated by day 8 and is completed by day 12 in both cyclic and pregnant animals (Geisert et

al., 1994, Persson et al., 1997). Microarray data in this study are in good agreement as they showed down-regulation of *PGR* mRNA after day 0 with lowest level on day 12. Cellular mechanisms that control the down-regulation itself, however, are largely unknown.

During the estrous cycle and the establishment of pregnancy, endometrial cells undergo rapid growth and differentiation, extracellular matrix (ECM) break down and remodeling (Curry et al., 2001, Yamada et al., 2002). These changes in the endometrium are partly modulated by the expression of the matrix metalloproteinase system, a disintegrin and metalloproteinase with thrombospondin motif (ADAMTS)-1 and extracellular matrix metalloproteinase inducer (EMMPRIN) in coordination with ovarian steroids (Mishra et al., 2010). In accordance with DAVID functional annotation which revealed the biological term 'extracellular matrix' as over-represented (starting on day 0 and continuing to day 3), several genes representing the matrix metalloproteinase (MMP) family *(MMP2, MMP7, MMP12,* and *MMP14* - highest mRNA on day 0 and *MMP11, MMP17,* and *MMP25* – highest mRNA from day 0 to day 3) were found as highly expressed during this time in cycle. The MMP family consists of more than 20 related proteolytic enzymes which include four comprehensive classes: collagenases, gelatinases, stromelysins, and membrane-type enzymes (MT-MMPs). These proteinases exhibit common features such as i) synthesis of the MMPs as preproenzymes that are secreted as inactive pro-MMPs, ii) activation of the latent zymogen in the extracellular space, iii) recognition and cleavage of the ECM by the catalytic domain, and iv) inhibition of MMP action in the extracellular environment by both serum-borne and tissue-derived metalloproteinase inhibitors (TIMPs) (as reviewed in (Curry et al., 2001). The collagenases (i.e., MMP-1, MMP-8, and MMP-13) are able to catalyze a crucial cleavage of collagens which changes the stability and solubility properties. Conspicuously in this context, none of these MMPs were found as differentially expressed in the porcine endometrium. In addition, the functional category 'collagens' was over-represented starting from estrus and continuing till metestrus. Several genes showed highest mRNA expression assigned to this category on day 0 (*COL1A1, COL1A2, COL3A1, COL4A1, COL5A1, COL12A1*, and *COL 17A1*) and from day 0 to day 3 (*COL4A5, COL4A6, COL5A2, COL6A3, COL7A1, COL14A1*, and *COL15A1*) in the endometrium of the pig. The results from qPCR analysis validated highest mRNA expression of the gene *COL1A1* on day 3. As noted above, the activity of the MMPs in the extracellular space is controlled by MMP inhibitors referred to as tissue inhibitors of metalloproteinases (TIMPs). TIMPs 1-4 have been shown to be involved in the maintenance of balanced ECM remodeling. In general, far less tissue remodeling occurs during the estrous cycle exhibited by many mammalian species compared to primates. Therefore, in the uterus of domesticated animals, only moderate expression of MMPs and their interaction with TIMPs has been observed compared to more robust expression during the tissue-loss and -repair processes that are the hallmark of the menstrual cycle (Curry et al., 2001). Some studies analyzing the cyclic changes of MMP mRNA expressions during the estrous cycle, e.g. in rodents have been performed (Rudolph-Owen et al., 1997, Woessner, 1996) showing *MMP-2*, *MMP-7*, and *MMP-11* as highly expressed during preestrus and estrus. Furthermore, the expression profile of the MMP system and their interaction with their inhibitors in the uterus of domestic species, including the cow (Maj et al., 1997) and sheep (Salamonsen et al., 1995) were reported only in association with the tissue dynamics of pregnancy. In this regard results of the study from Ulbrich et al. indicated a TIMP-2 involvement in very early local maternal recognition of pregnancy (Ulbrich et al., 2011) in cattle. In addition, studies in gene expression in bovine endometrium during the estrous cycle indicated a stimulation of TIMP-2 by progesterone (Bauersachs et al., 2005, Hampton et al., 1995). In ovine endometrium, TIMP2 mRNA (1·0 kb transcript) abundance has been shown to be stimulated by P4 and to be increased on day 10 of the cycle (Hampton et al. 1995). Microarray data showed up-regulation of *TIMP-3* mRNA expression on day 12 (validated by qPCR analysis) and of *TIMP2* mRNA from day 12 to day

18 during the porcine estrous cycle confirming a stimulation by P4. Furthermore, estrogens, interferons (IFNs), and prolactin (PRL) have the potential to interact with P4 to influence synthesis of *SPP1* (secreted phosphoprotein 1- commonly referred to as osteopontin (OPN) and formerly known as bone sialoprotein 1, early T-lymphocyte activation 1) in the GE (Craig et al., 1991). In addition, increases in transcription of the *OPN* gene may be induced by interleukin-1 beta (*IL-1ß*), transforming growth factor beta-1 (*TGFß1*), fibroblast growth factor (*FGF*), tumor necrosis factor alpha (*TNFa*), interferon gamma (*IFNγ*), and 1,25-dihydroxy vitamin D3 (Mukherjee et al., 1995, Omigbodun et al., 1997, Rittling et al., 1997, Safran et al., 1998). Its expression is regulated in LE by estrogens but whether estrogens act directly on LE or indirectly through another uterine factor still remains unknown. The conservation across various forms of placentation suggests that *SPP1* provides functions that are basic to pregnancy establishment and maintenance (White et al., 2005). Additionally, Burghardt and coworkers (Burghardt et al., 2002) showed that *SPP1* is a component of the ovine and porcine histotroph which is characterized by a complex temporal and spatial pattern of uterine and conceptus secretions involving immune, epithelial and stromal cells. It is further found that these events are orchestrated to contribute to conceptus attachment and implantation and, conclusively, hypothesized that OPN has potential influence on the events of implantation and subsequent placental development. To date no published data exist on the role of OPN during the reproductive cycle. Microarray data showed highest mRNA expression level for *SPP1* on day 0 (validated by qPCR analysis) in non-pregnant pigs. In general, OPN binds primarily to $\alpha_v ß_3$ integrin heterodimers by its Arg-Gly-Asp (RGD) sequence, however, other *OPN* receptors have been described; the integrin heterodimers $\alpha_v ß_1$, $\alpha_v ß_5$, and $\alpha_v 8 ß_1$ have affinities for the RGD motif of OPN that are similar to $\alpha_v ß_3$ (Denda et al., 1998, Hu et al., 1995) and OPN contains a cryptic binding sequence recognized by the $\alpha_v 9 ß_1$ integrin heterodimer (Smith et al., 1996). Several genes coding for integrins (20 genes) were found as differentially expressed throughout the porcine cycle; most showed highest levels during estrus but only one integrin alpha v with no specific ß subunit - integrin, alpha V (*ITGAV*-vitronectin receptor, alpha polypeptide, antigen CD51). It was also demonstrated in sheep that OPN contains a Gly-Leu (GL) sequence which is indicative of those that are susceptible to cleavage by various MMPs. Indeed, commercial substrates for MMP 2 and MMP 7 activity contain this sequence (Pro-Leu- Gly-Leu) and substrates for MMP 1, 3, 8 and 9 all contain variations on the x-y-Gly-z motif (Salamonsen et al., 1995). Johnson and coworkers summarized and defined the functions of OPN (as reviewed in (Johnson et al., 2003) as i) an ECM molecule that mediates cell-cell and cell-matrix adhesion and communication, ii) a cytokine that can exhibit pro-inflammatory properties (e.g., macrophage/monocyte and T-cell recruitment and stimulation of cytokine production), anti-inflammatory actions (e.g., inhibition of inducible nitric oxide production and MMP-2 expression), and effects on tissue repair at sites of inflammatory responses, and iii) an intracellular protein associated with hyaluronan-CD44-ERM (ezrin/radixin/moesin) attachement complex in migrating cells. In domestic animals, there is a delay between blastocyst hatching from the zona pellucida and conceptus attachment to the uterine epithelium, and this is referred to as the pre-implantation stage. The ability of blastocysts to adhere to a variety of cell types and extracellular matrix (ECM) components and of the normally noninvasive pig blastocyst to invade and form a syncytium when placed on an ectopic site (Samuel et al., 1972) supports the concept of uterine control of implantation. However, during the pre-receptive, non-adhesive stage, uterine epithelial cells are known to exhibit an abundant surface glycoprotein, mucin 1 (Bowen et al., 1996, Burghardt et al., 2002) (Muc-1, cell surface associated) that diminishes during the receptive phase in most mammals including the pig. Bowen and coworkers (Bowen et al., 1996) showed *Muc-l* staining on the apical surface of porcine endometrial epithelium as maximal at estrus (Day 0) and on Day 4, but decreased to non-detectable levels by Day 10 in both cyclic and pregnant gilts. The microarray data showed

highest mRNA expression of *Muc-1* on day 0 and lowest during the luteal phase of the porcine cycle. In addition, DAVID functional annotation clustering revealed the biological terms 'cell adhesion' and 'cell-cell adhesion' as over-represented during estrus. Furthermore, the accessibility of integrin receptors to their ligands may be controlled by the cyclic pattern of anti-adhesive glycoproteins such as MUC1 which may constitute a barrier to invasiveness on the LE in pigs and sheep. Available evidence indicates that the implantation adhesion cascade in these species is initiated following down-regulation of MUC1 (Bowen et al., 1996, Burghardt et al., 2002, Johnson, 2001). As a multiparous animal, the pig usually ovulates more than one follicle during one cycle, which is why the porcine endometrium must provide more structural flexibility. A sophisticated balance between the MMPs and their inhibitors is necessary to allow remodeling of the ECM while limiting the site and extent of proteolysis. A more accurate understanding of the role that MMPs and TIMPs play as regulators of growth, cellular differentiation, and specialized tissue function is crucial to fully comprehend all aspects of ovarian and uterine physiology (Curry et al., 2001) and the morphological regulation pattern during the estrous cycle, respectively. Results of gene expression patterns suggest a role of *OPN* in ECM remodeling in the cycling pigs and a possible interaction with *Muc-1* and other unknown interacting partners contributing from uterine pre-receptive to receptive stage. The expression pattern clearly indicate a positive effect of estrogen signaling on both genes. Hence, the function and regulation of *SPP1* and interacting partners such as *Muc*-1 and integrins is a very complex field, further analysis has to be performed.

2.2.2. Genes with highest mRNA expression during metestrus

Following estrus, estradiol that is suggested to lead to a pro-inflammatory response within the uterus (Tibbetts et al., 1999) decreases and progesterone which creates an anti-inflammatory environment by regulating the expression of various cytokines (Park et al., 2011) increases. Several genes related to the biological categories 'immune response' and 'inflammatory response' showed highest mRNA concentrations during the estrous cycle (D0, D3 and D6) in the porcine endometrium. These genes mainly represented the chemokine (C-C motif) ligand family (*CCL3L3, CCL5, CCL8, CCL11, CCL17, CCL21, CCL26, CCL27, CCL28*) and the chemokine (C-C motif) receptors (*CCR1, CCR2, CCR4, CCR5, CCR7, CCR 9, CCR10*), the chemokine (C-X-C motif) ligand family (*CXCL2, CXCL3, CXCL4, CXCL6, CXCL9, CXCL10, CXCL11, CXCL17*) and the chemokine (C-X-C motif) receptor (*CXCR3, CXCR4*, *CXCR6*). Microarray data of C-X-C chemokine receptor type 4 (*CXCR4*) confirm biological functional terms and processes with slightly deferment results in qPCR analysis. In addition to chemokines, some representatives of the interleukin family (*IL1ß*, *IL4, IL5, IL6, IL7, IL8, IL10, IL15, IL16, IL18*) and theirs respective receptors (*IL2RB* (interleukin-2 receptor subunit beta-like), *IL4R*, *IL6R*, *IL7R, IL17RE* (interleukin-17 receptor E-like), *IL21R* (interleukin-21 receptor-like), *IL22RA1* (interleukin 22 receptor, alpha 1)) showed higher mRNA concentrations on D0, D3 and D6 during the estrous cycle. In women, interleukins (IL11 and IL15) were demonstrated to stimulate the proliferation of human natural killer (NK) cells and cytokine production by these cells and can affect the proliferation and differentiation of T helper cells within the uterus (Dimitriadis et al., 2002, Okada et al., 2000). Besides, NK cells are suggested to play a role during pregnancy (Kaeoket et al., 2001). To date the role of NK cells in the porcine endometrium during the estrous cycle is not clarified, and neither published study exist about the specific role of the immune system during the estrous cycle. In addition to categories assigned to immune functions, the biological terms 'cell-cycle', 'mitosis' and 'chromosome' were found as over-represented during this time in cycle. In this regard, microarray data showed the gene cyclin E1 (*CCNE1)* and cyclin dependent kinase 4 (*CDK4*) as highest expressed on day 3 (both genes were validated by qPCR analysis). Supposedly there is a connection between cell proliferation pattern and 'immune-sytem' functions since the NK

cells in the pig are present in the uterine stroma and infiltrate the surface and glandular epithelium during early diestrus.

As already noted, fibroblast-growth factor 9 (*FGF9*) has been described as one of the mediators of estrogen signaling in the endometrium (Tsai et al., 2002). The results of the study by Østrup et al (Østrup et al., 2010) showed that *FGF9* up-regulation in pregnant porcine endometrium might be stimulated by the conceptus, whereas its receptor *FGFR3* is down-regulated. In contrast, *FGF9* mRNA concentration in the cycling porcine endometrium was highest on day 3 during the cycle and its receptor (*FGFR3*) was up-regulated during luteal phase. Additionally, *FGF9* was identified previously as a growth factor in human endometrium. The localization is, however, different. In pigs, the strongest staining for FGF9 was observed at the apical domain of the glandular epithelial cells (Østrup et al., 2010) in humans, glandular epithelium only expresses the gene at low levels (Tsai et al., 2002). The expression patterns of FGF9 and its receptor (*FGFR3*) suggest that these genes not only play a role involved in pregnancy but during the estrous cycle as well. Furthermore, fibroblast-growth factor receptor 1 *(FGFR1)* mRNA expression was up-regulated from day 0 to day 3 during the porcine reproductive cycle (validated by qPCR analysis). The study of Agas et al. (Agas et al., 2013) showed that PGF2a acts as a strong mitogenic and survival agent on osteoblasts, and these effects are mediated, at least in part, by the binding of fibroblast growth factor-2 (FGF-2) to the specific receptor FGFR1. Although FGF-2 was identified in endometrial epithelium, stroma and myometrium of gilts during the estrous cycle, no regulative changes were detected (Wollenhaupt et al., 2004). Finally in this context, it has been shown that estrogens produced by porcine conceptuses bind to *ESR1* in the LE to induce the maximal levels of *FGF7* expression observed on day 12 of pregnancy (Ka et al., 2007). In addition, Samborski (Samborski et al., 2013) and coworkers found decreased expression of *FGF7* in day 14 pregnant endometrium that agrees with the negative effect of long-term estradiol treatment on FGF7 expression, which were found in neonatal ovine endometrium (Hayashi et al., 2005). Furthermore, higher expression of FGF7 in porcine endometrium on day 12 of pregnancy and after E2 treatment of endometrial explants from day 9 of the estrous cycle was observed (Ka et al., 2000). The latter group suggested an indication of a specific role of the growth factor FGF7 particularly during the time of conceptus elongation between days 10 and 12 in pregnancy. FGF-7 is known to be involved in differentiation, and morphogenesis via binding to the transmembrane tyrosine kinase receptor FGFR2IIIb (Ornitz et al., 1996). Microarray data revealed higher expression of *FGF-7* and *FGFR2* from day 12 to day 18 which is in correlation to findings of recent studies (Ka et al., 2000, Wollenhaupt et al., 2005) and suggests a P4 dependent expression in non-pregnant sows. The results of gene expression patterns of the fibroblast-growth factors and their respective receptors indicates a steroid hormone-dependent signaling shift; estrogen signaling during estrus phase and conceptus signaling in case of pregnancy during luteal phase. Altogether, the complex regulation of genes involved in steroid hormone signaling suggests an important role of the corresponding genes in the regulation of endometrial functions during the estrous cycle. The results in this study suggest an estrogen induced immune answer in regard to cell proliferation and degeneration involved in remodeling of the endometrium.

2.2.3 Genes with highest mRNA expression during the luteal phase

Not only the endometrium but also blastocysts in many species, including mouse (Marshburn et al., 1990), rat (Parr et al., 1988), rabbit (Dey et al., 1980), sheep (Hyland et al., 1982) cow (Lewis et al., 1982), human (Holmes et al., 1980) and pig (Davis et al., 1983) appear to have the capacity of transforming arachidonic acid into its biological active derivatives via PG G/H synthase enzyme (*PGHS*) pathway, resulting in the production of PGE2 and PGF2a. Our results of the microarray analysis showed increased expression of prostaglandin E receptor 4 gene (*PTGER4*) already shortly after ovulation and prostaglandin E receptor 3 gene (*PTGER3)*

during early luteal phase, while prostaglandin E receptor 2 gene (*PTGER2*), phospholipase A2-like, group IVA (*PLA2G4A*), solute carrier organic anion transporter family, member 2A1 (*SLCO2A1, PG* transporter) and the prostaglandin F receptor (*PTGFR*) were up-regulated during the luteal phase. It has been found during the time around luteolysis, when PGF2a pulses in venous blood are high, that COX-1 and -2 expression in porcine endometrium (Ashworth et al., 2006) as well as the expression of PGF synthase (Waclawik et al., 2006) significantly decrease on days 16 to 20 in the cycle. These data confirm that the higher PGF2a peaks in venous blood during luteolysis do not result from the ongoing intensified synthesis and secretion of PGF2a. Furthermore, it was suggested that this finding could be a result of degeneration of endometrial cells from which PGF2a is released, as well as the excretion of tissue fluid containing proteins binding PG's and their metabolites, which takes place during uterine contraction (Krzymowski et al., 2008). Microarray data showed that cyclooxygenase-2 (*COX-2*, also known as prostaglandin-endoperoxide synthase (*PTGS*)) was up-regulated starting on day 12 continuing to day 18 indicating an interaction of these genes with uterine contraction but no analysis was performed measuring PGF2a concentration in venous blood. The peak of COX-2 expression could therefore be within day 12 and day 18 of the estrous cycle since the day of luteolysis (D14) was not analyzed. In addition, results of a recent study showed a significant increase in endometrial *PTGS2* mRNA in the endometrial LE from day 10 to day 18 of the estrous cycle and early pregnancy, where it is optimally placed to possibly mediate placentation in pigs (Kraeling et al., 1985). Latter researchers hypothesized that the increased expression of *PTGS2* in the uterine LE is temporally associated with the loss of the progesterone receptor (PGR) from the uterine LE (Geisert et al., 1994) and further suggested a possible induction through activation of the NFkB pathway which has been detected in the human endometrium (Page et al., 2002). In the pig uterus oxytocin receptor (*OXTR*) was expressed in greatest abundance on luminal epithelial cells, whereas stromal cells possessed the least amount of receptors (Boulton et al., 1996). Oxytocin receptors have been characterized on the endometrium of cyclic pigs (Whiteaker et al., 1994) and on the myometrium from a late pregnant sow (Soloff et al., 1974). Microarray analysis of the porcine endometrium revealed higher expression of *OXTR* mRNA from day 12 to day 18 and highest on day 18 of the estrous cycle indicating a role in the regulation of luteolysis in the pig. Altogether, gene expression of genes related to PG and steroid hormone metabolism and signaling was clearly highest during luteal phase.

In the uterus, spatiotemporal synthesis and secretion of various growth factors, cytokines, lipid mediators and transcription factors triggered by steroid hormones are thought to play an important role in uterine function. The process of angiogenesis and regulation of blood flow plays also an important role in the context of endometrial remodeling during the estrous cycle (Bauersachs et al., 2008). Vascular endothelial growth factor (VEGF) has emerged as an important regulator of angiogenesis (Wollenhaupt et al., 2004). The latter research group found endometrial VEGF as sensitive to P4 signaling in the pig. Microarray data of this study are in good agreement since *VEGFA* mRNA was up-regulated during luteal phase. In addition, neuropeptide Y (*NPY*) is a potent angiogenic factor as well as a stimulator of vascular smooth muscle proliferation (Abe et al., 2007) and was found as up-regulated from day 6 to day 12 in porcine cycle. The bovine proenkephalin (*PENK*) mRNA, which is increased during diestrus, was found to be up-regulated in the rat endometrium during secretory phase (Jin et al., 1988) and also positively regulated by progesterone in the endometrium of mice (Cheon et al., 2002). For this gene the mRNA pattern is similar in ruminant species and rodents, but different in primates. Microarray data for porcine endometrium showed *PENK* as up-regulated during diestrus. Furthermore, the receptor for endothelial cell regulation 1 (*EDN1*) and angiotensin I converting enzyme (peptidyl-dipeptidase A, *ACE*) were found as highly expressed from day 3 to day 6. Messenger RNA levels were highest for members of the angiopoietin system TEK

(tyrosine kinase, *TEK*), leucyl/cystinyl aminopeptidase (*LNPEP*), type-1 angiotensin II receptor-like (*AGTR1*), cathepsin A (*CTSA*) and angiotensinogen-like (*AGT*) which codes for the progenitor of angiotensin II (a potent vaso-constrictor) and was described to regulate feto-placental angiogenesis in the ovine placenta (Zheng et al., 2005) on day 18 of the porcine estrous cycle. Wollenhaupt further found that one of the two receptors for VEGF (*VEGF-R2*) is only increased after the treatment with both steroid hormones. This would demand the interaction with conceptus estrogen signaling during early pregnancy when P4 is elevated. In addition, the results of this work showed up-regulation of VEGF system (a co-receptor for VEGF, neuropilin 1 and 2, *NRP1* and *NRP2*), thimet oligopeptidase 1 (*THOP1*) and glutamyl aminopeptidase (aminopeptidase A, *ENPEP*) but during estrus phase. Following estrus, endothelin 3 (*EDN3*) and the rennin-binding protein (*RENBP*) showed highest expression from day 0 to day 3. However, most of the genes assigned to the biological category 'angiogenesis' and 'vasculature' in the pig showed fluctuating profiles: their highest mRNA concentrations were found during estrus, from day 3 to day 6 but also on day 18. This also indicates a more or less independency in signaling from either steroid hormones, or at least, when both E2 and P4 are necessary for activation, an interaction with conceptus estrogens.

Several research groups (Hammond et al., 1993, Mukku et al., 1985, Watson et al., 1996) stated that one mechanism for steroid hormones to exert their mitogenic effects on the ovary and the uterus might be by stimulating the epidermal growth factor receptor (EGF-R) system (Hammond et al., 1993). Wollenhaupt (Wollenhaupt et al., 2004) found EGF-R to be distributed in glandular and stromal cells in the porcine endometrium and significantly increased concentration within preestrus compared to luteal phase during the reproductive cycle. The results of microarray analysis of the porcine endometrium showed an up-regulation of epidermal growth factor (*EGF*), receptor tyrosine-protein kinase erb-3-like and erbB-4-like (*ERBB3*, *ERBB4*) and erbb2 interacting protein (*ERBB2IP*) mRNAs from day 12 to day 18 during the estrous cycle. Furthermore, results of latter study showed an independence of EGF-R activation from steroid hormones because of no difference in tyrosine phophorylation status of the EGFR-R protein on days 12 and days 20 in ovarieectomized pigs. Altogether, more detailed studies are required to identify the role of steroid hormone signaling in relation to the EGF-R system in the porcine endometrium.

2.2.4 Genes with highest mRNA expression during late luteal phase

Steroid hormones are important regulators of reproductive physiology in domestic animals. Both estradiol and progesterone mediate dramatic changes in the endometrium during the estrous cycle. As already noted, the samples collected on day 18 (assumingly the time for the beginning of estrus and therefore low P4 concentrations) showed higher concentrations of P4 and should be considered as samples collected during late luteal phase. DAVID functional annotation clustering revealed the biological category 'complement activation, classical pathway' as over-represented on day 18. Furthermore, microarray analysis showed five genes related to this category as highly expressed; clusterin (also known as apolipoprotein J, *CLU*), complement component 1,s subcomponent (*C1s*), complement component 1,r subcomponent (*C1R*), complement component 6 (*C6*) and *SERPING1*. Role and function of the complement cascade in the pig endometrium were not analyzed to date but were already discussed (2.1.1) in regard of gene expression during the estrous cycle in equine endometrium. The up-regulation in porcine endometrium clearly indicates an involvement of P4 in the complement cascade activity.

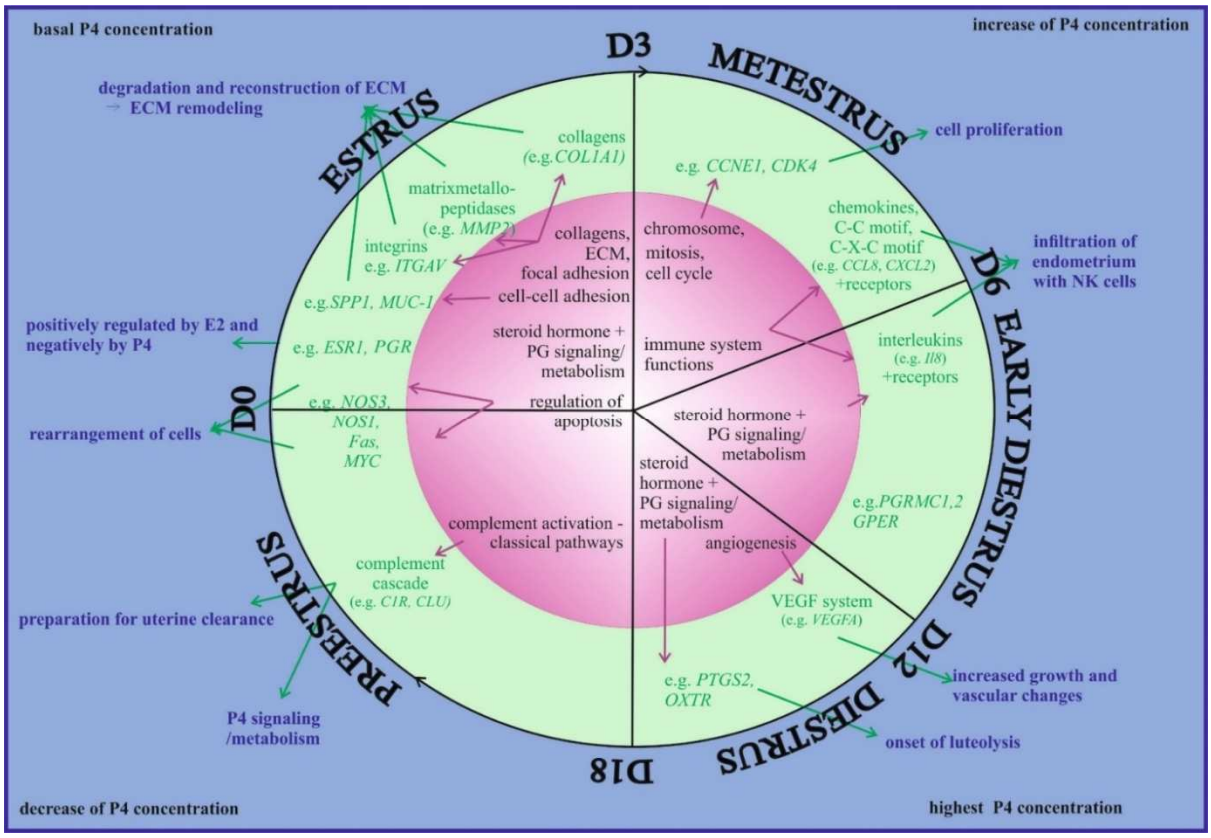

Figure IV-2: Summary of the results from the analysis of porcine endometrium during the estrous cycle The porcine estrous cycle is illustrated as black circle (cycle in length is 21 days; from D0 to D0 which is defined as the day of ovulation) with main phases and the analyzed days (D0, D3, D6, D12, D18-external lettering). Progesterone (P4) concentration during the particular phase is given in each corner. Over-represented biological functions during the specific phases of the estrous cycle-achieved from DAVID functional annotation clustering analysis-are represented in internal circle (pink). External circle (green) shows single genes or groups represented by several genes with highest mRNA expression during the time in estrous cycle. Conclusions about potential connection with function of the endometrium are demonstrated in blue area. Connection between events are demonstrated with arrows. *CCNE1*-cyclin E1, *CDK4*-cyclin dependent kinase 4, ECM-extracellular matrix, e.g.- for example, *ESR1*-estrogen receptor 1, gamma, Fas- Fas (TNF receptor superfamily member 6), *GPER*- G protein-coupled estrogen receptor, *ITGAV*-integrin alpha 5, *MUC-1*-mucin 1, MYC-v-myc avian myelocytomatosis viral oncogene homolog, NK-natural killer cells, NOS1,3- nitric oxide synthase 1 and 3, *OXTR*-oxytocin receptor, *PGRMC1,2*-progesterone receptor membrane component 1 and 2, SPP1- secreted phosphoprotein 1 (osteopontin), *PGR*-progesterone receptor, PMN-polymorphnuclear neutrophils, *PTGS2*- prostaglandin-endoperoxide synthase 2, *PTGER3,4*-prostaglandin receptor 3 and 4, *VEGFA*-vascular endothelial growth factor A2.3

2.3. Messenger RNA expression profiles in the endometrium during equine and porcine estrous cycle

So far the present study revealed widespread gene expression changes in equine and porcine endometrium during the estrous cycle involving a total number of approx. 14271 genes. These gene expression changes were associated with molecular pathways and gene networks that describe ECM remodeling and other processes, e.g., immune response and changes in vasculature. Given these results, it is crucial to investigate whether these changes in gene expression are common or species-specific. Therefore a correlation analysis was performed which showed approx. 1862 genes/transcripts referred to as differentially expressed (listed in supplementary data) in both species out of which 841 genes showed significant correlation ($p<0.05$). A total number of 691 genes showed positive and 150 genes showed negative correlation. Figure IV-3 summarizes the results of the correlation analysis.

2.3.1 Genes with highest mRNA expression during preestrus (low P4 levels)

The phase immediately preceding estrus or the end of luteal phase is characterized by basal plasma P4 concentration. In the mare, preestrus begins around day 16 (also referred to as estrus phase) which corresponds more or less to day 18 (also referred to as late luteal phase) in the pig. Comparing the genes assigned to Clusters 8 (highest mRNA expression on day 16 and on day 18, respectively) in both analyses one have to keep in mind, that the P4 concentration of blood samples from day 18 in the pig were still relatively high.

A total number of 47 genes (positively correlated) were up-regulated in both species during this time in the cycle. The functional annotation clustering analysis revealed biological terms such as 'cytokine-cytokine receptor interaction', 'cell adhesion', 'complement activation-classical pathway' and 'inflammatory response' as over-represented. For example, *SERPING1* and *CR1* were found as highly expressed in both species during this time. Both genes might be functioning in the context of 'immune system' – as already discussed – as well as the category 'complement activation-classical pathway' since the complement activation is one key component of the innate inflammatory response. In addition to inducing inflammation, the complement system plays a major role in protecting against infection and killing diseased cells (Morris et al., 2009). Most SERPINs inactivate serine proteases and some cysteine proteases, and play a functional role in diverse biological processes including fibrinolysis, coagulation, inflammation, cell mobility, cellular differentiation and apoptosis (Hayashi et al., 2011, Law et al., 2006). *SERPING1* is also discussed to be collagen binding and therefore debated to take action in the ECM remodeling process in the bovine follicle (Hayashi et al., 2011). Since the functional category 'extracellular matrix' showed minor over-representation during this time of the cycle in both species an involvement in ECM remodeling of *SERPING1* is reasonable but remains suspicious and further studies in this regard are needed. In addition, SERPINH1 (serpin peptidase inhibitor, clade H, member 1), also known as HSP47, was described as collagen-binding protein of the endoplasmic reticulum involved in collagen processing and secretion (Nagata, 1996). Microarray data showed up-regulation for *SERPINH1* mRNA from day 0 to day 3 in the pig but no regulation in the mare. In the study of Yip and coworkers, many genes of the 'complement and coagulation cascade' showed lower level of expression in the estrus than in the proestrus during the estrous cycle in mice (Yip et al., 2013). The authors found that mRNA expression of *C3* was elevated in proestrus compared to estrus which is because E2 stimulates the synthesis of *C3*, whereas simultaneous or delayed administration of P4 inhibits its synthesis (Hasty et al., 1994). Nevertheless, microarray data from this study showed highest expression of *C3* from day 3 to day 6 in the pig and on day 16 in the mare. Interestingly, functional annotation revealed – as already mentioned – terms such as 'complement activation, classical pathway' and 'immune response' as over-represented categories with negative correlation; both terms were over-represented in the mare on day 16 but during the early luteal phase in the pig. Vice versa, the categories 'collagen' and 'cell junction' showed over-representation in the pig on day 18 but on day 8 in the mare. These findings contradict the statements of general inhibitory P4 steroid-hormone signaling on *C3* (Hasty et al., 1994).

2.3.1. Genes with highest mRNA expression during estrus

Positively correlated genes assigned to Clusters 1 (highest mRNA expression on day 0) summarized a number of 48 genes and the genes clustered together in Clusters 2 (highly expressed from day 0 to day 3) during the estrous cycle summarized a number of 34 genes. Functional annotation clustering of these genes revealed the biological terms 'extracellular region', 'collagens' and 'focal adhesion' as over-represented during this time. Four genes were assigned to the collagen family *(COL1A2, COL3A1, COL4A1,* and *COL5A1; CL1A1* did not show significant correlation; r=0.59 and p-value=0.07). In addition, *COL4A5, COL4A6* and

COL7A1 were differentially expressed in both species but increased on different times in the cycle: on day 0 in the mare and from day 0 to day 3 in the pig. Furthermore, the functional terms 'cell adhesion' and 'cell-cell adhesion' were found as over-represented during this time in the estrous cycle. The ADAM metallopeptidase domain 12 and 22 *(ADAM12, ADAM22)* mRNAs were found to be assigned to these categories. Additionally, ADAM metallopeptidase with thrombospondin type 1 motif, 19 (*ADAMTS19*) was found as up-regulated in both species; on day 0 in the pig and from day 0 to day 3 in the mare. Members of this family are membrane-anchored proteins and have been implicated in a variety of biological processes involving cell-cell and cell-matrix interactions, including fertilization, muscle development and neurogenesis which indicates a relation to ECM remodeling that is processing at this time in cycle. As already mentioned, ECM turnover and homeostasis is controlled, in part, by the interplay of a specific class of proteolytic enzymes known as the matrix metalloproteinases (MMPs) and their inhibitors (TIMPs-tissue-derived metalloproteinase inhibitors) (as reviewed in (Curry et al., 2003). Several members of both families showed highest mRNA levels during the estrus phase in the mare and in porcine endometrium but only one representative of the family, namely *MMP11*, was differentially expressed in both species but was excluded by statistics (p-value = 0.31). This clearly indicates a species-specific regulation of ECM remodeling on single gene basis. Probably, in connection with increased, species-specific ECM synthesis, genes relevant for protein folding and secretion were found as enriched during estrus. The biological category 'ribosome' and 'translation elongation' showed over-representation from day 0 to day 3 in both species and additionally on day 3 in the pig. Nine genes coding for ribosomal proteins (*RPL18, RPL22, RPL29, RPL36AL, RPLP2, RPS10 RPS15, RPSA* and *RPSAP58*) showed highest mRNA expression from day 0 to day 3 in the mare and up-regulation on day 3 in the pig. *RPL8* and *RPS18* mRNA were increased from day 0 to day 3 in both species. In addition to functional categories related to ECM remodeling, the functional term 'inflammatory response' was over–represented on day 0. Two representative genes assigned to this category and coding for the chemokine family (C-X-C motif) *CXCL6* and *CXCL8* were found as up-regulated in both species on day 0. The chemokine (C-X-C motif) ligand 9 *(CXCL9)* showed highest mRNA expression on day 0 in the mare and from day 0 to day 3 in the pig.

Estrogen, acting through its receptor ERα (also known as ESR1), is a critical regulator of uterine endometrial epithelial proliferation. Although the dynamic communication between endometrial stromal and epithelial cells is considered to be an important component in this process, key molecular players in particular compartments remain poorly defined (Pabona et al., 2009). Even though both species showed mRNA expression of *ESR1* in the endometrium during the estrus phase (on day 0 in the pig and on day 3 in the mare) but statistical correlation analysis of mRNA levels did not reach significant importance (correlation r=0.41, p-value=0.24). In addition, Kruppel-like factor 9 (KLF9) (a member of the Kruppel-like family of mammalian zinc finger-containing transcription factors and previously designated basic transcription element binding protein-1 (BTEB1)) is debated (Dang et al., 2000) to function as a co-regulator of steroid hormone receptor signaling in the uterine endometrium (Zhang et al., 2002). P4 together with estrogen and uterine-associated growth factors coordinates cellular proliferation, differentiation, and apoptosis in a temporal- and spatial-specific manner by binding to its nuclear receptor PGR (Tsai et al., 1994) which is expressed and regulated distinctly in the epithelial and stromal compartments of the uterus (Tibbetts et al., 1998). Microarray results of this study showed highest mRNA expression of *KLF9* in Clusters 8. Results of a recent study by Zhang and co-workers (Zhang et al., 2002) implicate KLF9 as a PGR-interacting partner *in vitro* and suggest a novel mechanism by which progesterone regulates the expression of its target genes in uterine epithelial cells during pregnancy. Zhang and coworkers further postulated an interaction between *KLF9* and *HOXA10* in this context and showed that *HOXA10* directly regulates *KLF9* expression in porcine endometrial epithelial

cells. *HOXA10* has been shown to be expressed in the adult murine (Taylor et al., 1997), canine (Guo et al., 2009), primate (Godbole et al., 2007), human (Taylor et al., 1997) and porcine uteri (Blitek et al., 2010). In pigs, HOXA10 protein was localized in the luminal and glandular epithelium, stroma and blood vessels of the endometrium but also in the myometrium of the uterus (Blitek et al., 2010). Furthermore, increased expression of *HOXA10* in response to E2 alone or in the presence of P4 was observed in the endometrium collected on day 9 after estrus of the porcine estrous cycle (Blitek et al., 2010). In addition, it was suggested that the activity of *HOXA10* and *HOXA13* may contribute to the differentiation and growth of myocytes during the peri-implantation period in pregenant pigs and may be involved in the morphological and ultrastructural adaptation of the myometrium to pregnancy (Franczak et al., 2014). *HOXA10* was contained in Clusters 1 and *PGR* in Clusters 2 which clearly agrees with the suggested estrogen action on *HOXA10* expression. In addition, the interaction between *KLF9* and *HOXA10* and *PGR* signaling seems temporally delayed but common in distinct phases.

Antagonism of estrogenic effects by androgens in the uterus (Leiva et al., 1991), mammary gland (Zhou et al., 2000) and sexual receptivity (Blasberg et al., 1998) have been described in rats or humans. In pigs, the primary circulating androgen is androstenedione (A4), which serves as the principal substrate for E1 synthesis (Simpson et al., 2001). Androgens are also synthesized and secreted locally by the porcine myometrium during both early pregnancy and luteolysis (Franczak, 2008). Kowalski and coworkers (Kowalski et al., 2004) suggested co-regulatory roles of *AR* and *ESR1* in endometrial gene expression and cell proliferation and further suggested that androgens may also functionally interact with the *PGR*-mediated program of endometrial gene expression. Results in this study showed *AR* and, as mentioned above, *PGR* as up-regulated (found in Clusters 2) verifying recent statement.

2.3.2 Genes with highest mRNA expression on day 3 (increasing P4 levels)

The results of the comparative analysis revealed a total number of 107 genes with positive correlation assigned together in Clusters 3 (highest mRNA expression on day 3). Tissue remodeling, mitotic activity, and DNA synthesis are accompanied by extensive cell proliferation, as indicated by the highest mRNA expression of several genes assigned to DNA replication and cell division. For example, cyclin dependent kinases 1 and 4 (*CDK1, CDK4*), cyclin B1, B2 and D1 (*CCNB1, CCNB2, CCND1*), 4 genes representing cell division cycle 6, 20, 24 and A3 (*CDC6, CDC20, CDC45, CDCA3*) and 5 genes encoding centromere proteins (*CENPE, CENPF, CENPL, CENPM, CENPN*) showed up-regulation on this day, as well as *SNRPA*, respectively. In addition, genes encoding many minichromosome maintenance complex component proteins (*MCM3*, *MCM4*, *MCM6* and *MCM10*) were up-regulated which help initiate DNA replication and are also involved in replication elongation (Forsburg, 2004). Functional annotation clustering revealed terms such as ‘cell cycle’, ‘mitosis’ and ‘chromosome’ to be over-represented during this time in cycle. At the cellular level, calcium controls a wide variety of cellular functions, e.g., cell growth, proliferation, and cell death (Clapham, 2007). Maintenance of calcium balance in the uterus is also critically important for many physiological functions, e.g. smooth muscle contraction during embryo implantation (Choi et al., 2011a). Expression of the calcium regulatory molecules in the uterine endometrium has been reported in several species; e.g. transient receptor potential vanilloid type 6 (*TRPV6)* in the uterine endometrium during the estrous cycle and pregnancy in rats (Kim et al., 2006) and mice (Lee et al., 2007) and during the menstrual cycle in humans (Yang et al., 2011) and calbindin-D9k (*S100G)* in the uterine endometrium during the estrous cycle and pregnancy in mice (Warembourg et al., 1987), rats (Tatsumi et al., 1999) and pigs (Krisinger et al., 1995). Microarray data showed highest level of mRNA expression of *TRPV6* in Clusters 7 and *S100G* in Clusters 3 in both species during the estrous cycle. The *TRPV6* transcript was highly expressed at estrus during the murine estrous cycle, implying that it might be involved in a

specific uterine function such as Ca^{2+} transport (Lee et al., 2007). In contrast, *TRPV6* transcripts in the rat uterus were highly expressed at diestrus (Kim et al., 2006). Both transient receptor potential vanilloid types 5 and 6 (TRPV5, 6) manage the influx of extracellular calcium ions into the epithelial cells which are then transported by calcium transport proteins, calbindin-D9k (S100G) and calbindin-D28k (CALB1), to the basolateral side of the epithelial cells. Subsequently, intracellular calcium ions are extruded to the outside of epithelial cells by sodium/calcium exchanger 1 (SLC8A1) (Choi et al., 2011b). *SLC8A1* showed highest mRNA level on day 0 in both species but correlation did not reach statistical significance (correlation r=0.48, p-value=0.16). Taken together, these results indicate that uterine *TRPV6*, *S100G* and *SLC8A1* are regulated differently during the estrous cycle. In the pig and the mare, calcium influx seems to start during late luteal phase which is in good agreement indicating P4 influence as compared to pregnancy. In addition and contributing the P4 influence, both genes coding for transient receptor potential vanilloid types 5 and 6 (*TRPV5, 6*) were up-regulated on day 12 in pregnant mares (Merkl et al., 2010).

2.3.4 Genes with highest mRNA levels during diestrus (highest P4 levels)

Diestrus is defined as the time during the estrous cycle with highest P4 levels. In the pig diestrus is around day 12 (Cluster 6) and in the mare around day 8 (Cluster 5). A total number of only 6 genes (namely Acetoacetyl-COa synthetase (*AACS*), dermatopontin (*DPT*), glutathione S-transferase mu 4 (*GSTM4*), rhophilin, Rho GTPase binding (*RHPN2*), structural maintenance of chromosome 6 (*SMC6*) and zinc finger and BTB domain containing 7B (*ZBTB7B*)) were up-regulated during these phases in the estrous cycle in both species. This low number of genes with positive correlation during diestrus indicates a species-specific gene expression and, in this regard, regulated changes of the endometrium that are dependent on P4 concentration in different ways. Furthermore, only 19 genes showed negative correlation, i.e., were up-regulated in diestrus in the mare (Cluster 5) and regulated in different phases in porcine cycle (6 genes on day 18 and 12 genes in day 0). Vice versa, 4 genes were found as up-regulated in diestrus in the pig (Cluster 6) which showed up-regulation during the cycle in the mare at estrus.

The transition phase from metestrus (around day 3) to diestrus (highest P4 levels) revealed a higher number of correlated genes. Genes clustering together in Clusters 4 (highest mRNA levels from day 3 to day 6 in the pig and from day 3 to day 8 in the mare) revealed 44 genes as positively correlated. Functional annotation clustering showed over-representation for the categories ‘lipid metabolism’, ‘fatty acid metabolism process’, ‘lipid biosynthetic process’ and ‘monosaccheride metabolic process’ during this time. Lipid metabolism appears in three of the top 5 networks, suggesting its importance as a metabolic process in uterine physiology (Killeen et al., 2014) which coincides with increased fatty acid catabolism (Mahendroo et al., 1999). Fatty acids are essential precursors to steroids and eicosanoids, metabolites necessary for normal ovarian and uterine function (Bazer et al., 1994). Furthermore, fatty acid supplementation positively influences reproductive performance. Increased fatty acid synthase (*FASN)* would be favorable to deliver the required fatty acid for the assembly of new cell membranes, modification of DNA transcriptional machinery and hormone production during the estrous cycle. Therefore, the up-regulation of *FASN* mRNA during estrus would be expected. Nevertheless, mRNA expression of *FASN* was highest in Clusters 4 in both species. The cellular metabolism is a well-represented process in the secretory phase of the human estrous cycle. Apolipoprotein D (*APOD*) is a multifunctional transporter involved in both lipid metabolism and the transport of cholesterols. The activation of its expression detected in most studies is consistent with the activation of lipid metabolism in the mid secretory phase (as reviewed in (Aghajanova et al., 2008). These findings are in good agreement with functional annotation clustering and mRNA expression of *APOD* (did not reach correlation significance r=-0.18).

Correlation analysis of gene expression revealed 11 genes as positively correlated assigned to Clusters 5 (highest mRNA expression on day 8 in the mare and from day 6 to day 12 in the pig). Progesterone receptor membrane component 1 (*PGRMC1*) mRNA profiles showed up-regulation in these phases and down-regulation during estrus in both species. Additional members of steroid hormone metabolism and signaling as well as members of prostaglandin metabolism showed negatively correlation; *PTGFR* showed up-regulation from day 12 to day 18 in the pig and from day 3 to day 8 in the mare, and *PTGER3* showed highest mRNA level from day 3 to day 6 in the pig.

2.3.5 Genes with highest mRNA level during late luteal phase (decreasing P4 level)

Following luteolysis P4 levels decrease to lowest levels during late luteal phase which is represented by genes assigned to Clusters 7 (highest mRNA level from day 12 to day 18 in the pig and from day 12 to day 16 in the mare). In both species luteolysis takes place within the timespan (around days 14/15). A total number of 33 genes were positively correlated during this time in the estrous cycle (Clusters 7). A recent study has demonstrated that on days 15 to 16 of the estrous cycle in pigs, cytokine action, steroidogenesis and prostaglandin synthesis take place in the myometrial tissue (Franczak**,** 2008). Nevertheless, in equine and porcine endometrial tissue 'angiogenesis', 'vasculature development' and 'blood circulation' were over-represented during this time in the estrous cycle. A critical element of tissue growth and development is the growth of new blood vessels, also known as angiogenesis (Lee et al.**,** 2010). Generally, angiogenesis plays an active role in endometrial function, as well as growth of ovarian follicles and CL during the reproductive cycle. In a highly dynamic tissue such as the endometrium, angiogenesis is necessary for the provision of nutrients (Killeen et al.**,** 2014). This study showed highest mRNA expression of vascular endothelial growth factor A (*VEGFA*) during late luteal phase in both species. *VEGF* is a factor that plays a pivotal role in the promotion of blood vessel formation under physiological and pathological conditions (Xiong et al.**,** 1998). Furthermore, macrophages are known to produce a variety of angiogenic factors. Activated macrophages have the unique capacity to influence the angiogenic process, that is, by extracellular matrix remodeling or induction of endothelial cell chemotaxis and proliferation. The experiments of the study by Kaczmarek (Kaczmarek et al.**,** 2013) indicate increased expression of VEGF that coincided with increased macrophage infiltration of the superficial endometrium and endometrial stroma. Since the study of the latter research group is based on inseminated pigs and to the actual knowledge macrophages infiltrate the equine and the porcine endometrium during preestrus and estrus, the results in this study contradict the statement. Additionally, it is postulated that PGs participate in the local increase of endometrial vascular permeability, as well as angiogenesis but during implantation. PGE2 up-regulates vascular endothelial growth factor (VEGF) in a number of tissues including the uterus (Lopes et al.**,** 2006). In addition, the results showed significant up-regulation of the prostaglandin-endoperoxide synthase 2 (*PTGS2*) in Clusters 7. This clearly indicates a common onset of luteolysis in both species. The correlation between angiogenesis, vasculature and PG signaling involvement requires more detailed investigations. All genes that are discussed in this part are summarized in Supplemental Table VIII-IV.

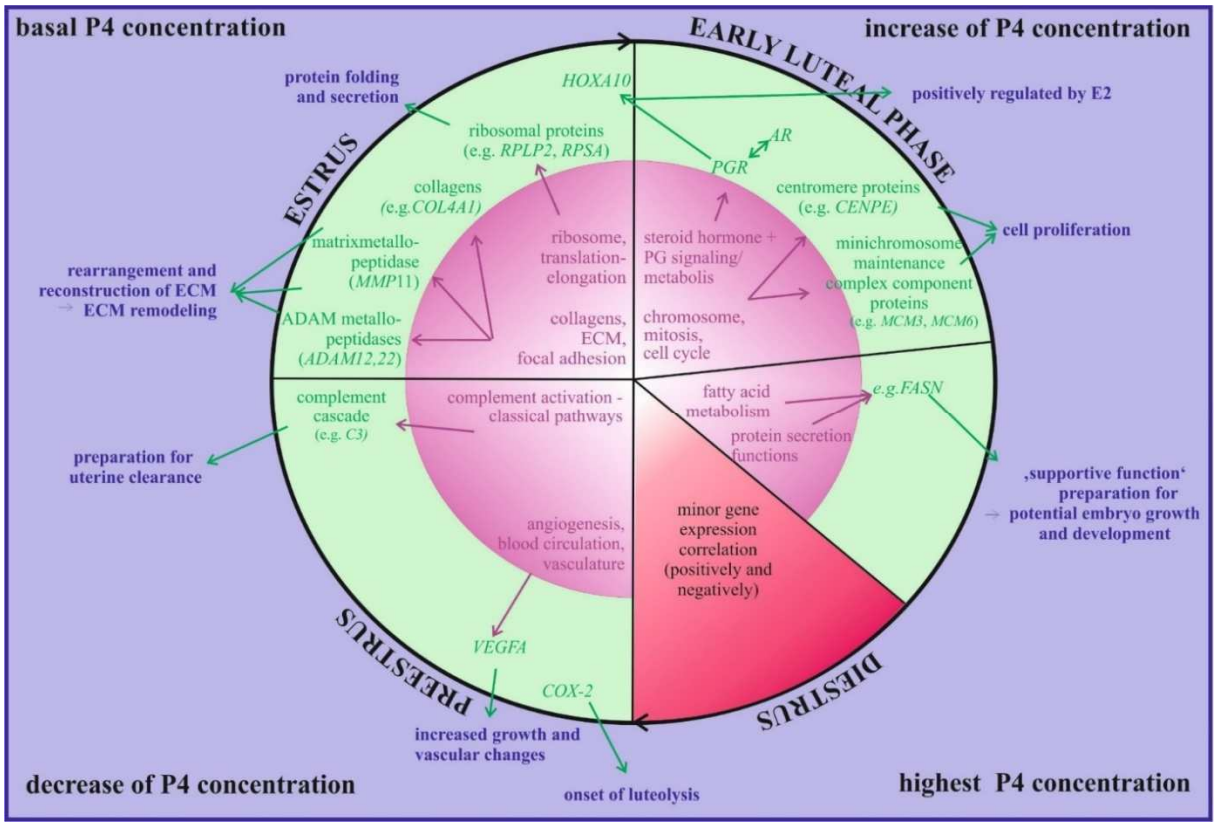

Figure IV-3 shown on next page. Summary of results from the correlation analysis. Phases of estrous cycle are illustrated as black circle (cycle duration is 21 days; from D0 to D0)-Estrus, early luteal phase, diestrus and preestrus. Progesterone (P4) concentration during the particular phase is given in each corner. Over-represented biological functions of genes with positively correlated expression during specific phases of the estrous cycle – obtained from DAVID functional annotation clustering analysis – are represented in the internal circle (pink). External circle (green) shows positively correlated genes or groups represented by several genes with highest mRNA expression during this time in estrous cycle. Conclusions about potential connection with the function of endometrium are shown in the blue area. Connection between events are demonstrated with arrows. *AR*-androgen receptor, ECM-extracellular matrix, *FASN*-fatty acid synthase, *HOXA10*-homeobox A 10, *PGR*-progesterone receptor, *PTGS2*-prostaglandin-endoperoxide synthase 2, *VAGFA*-vascular endothelial growth factor A.

2.4 Messenger RNA expression profiles in the endometrium during the bovine, equine and porcine estrous cycle

The comparison of published data from bovine endometrium (Mitko**,** 2008) with comparable phases of the porcine and equine endometrium during the estrous cycle revealed several genes as differentially expressed across species. The analysis was performed on the basis of assigned putative human orthologous genes and revealed 33 genes as positively and 7 genes/transcripts as negatively correlated in equine, porcine and bovine endometrium supplementary Table VIII-V during the estrous cycle. These numbers are relatively low but the dataset from bovine endometrium contained only 230 DEGs.

Similar to the mare endometrium which showed highest *ESR1* mRNA expression on day 3 during estrous cycle, the bovine endometrial mRNA concentration for *ESR1* was increased on day 3.5. In the pig, mRNA concentrations are highest on day 0 and slightly increased on day 3 (no statistical significance achieved). This agrees well with the changes during the ovulatory phase that are mainly controlled by estradiol (E2). Results indicate similar interactions in estrogen signaling during the estrus phase. In addition, genes related to the family of collagens were highest during estrus in all three species: *COL1A2, COL3A1,* and *COL4A1*. Due to ECM remodeling and thus edematization the highly represented genes related to collagens during estrus are in agreement. A number of genes with slightly higher mRNA levels at estrus were

found to be in the context of the biological term ‚cell adhesion' (e.g. focal adhesion). Genes coding for ECM proteins and components of the cytoskeleton, which are linked via paxillin, are involved in this process (Mitko**,** 2008). A possible candidate for the regulation of cytoskeleton proteins is polo-like kinase 2 (*PLK2*), also known as serum-inducible kinase (*SNK*). *PLK2* has been shown to play a role in the remodeling of synapses via phosphorylation of spine-associated Rap guanosine triphosphatase-activating protein (SPAR), a postsynaptic actin regulatory protein, leading to the degradation of SPAR (Pak et al.**,** 2003). *PLK2* could play a similar role in the modulation of actin filament polymerization in the endometrium (Mitko**,** 2008). Data showed up-regulation for *PLK2* from preestrus to estrus in all three species.

Furthermore, the transcriptome analysis of endometrium of all three species revealed an up-regulation of the immune-related genes that are involved in the complement system (classical pathway), namely complement component genes *C1R* and the C1 inhibitor *SERPING1* (Bauersachs et al.**,** 2006, Klein et al.**,** 2006). Slightly correlative expression differences were found within the immune-related genes complement component 1, or subcomponent (*C1R*) and serpin peptidase inhibitor, clade G (C1 inhibitor), member 1 (*SERPING1*). In porcine endometrium both of them showed mRNA up-regulation from day 18 to day 0 as in equine endometrium. But the mRNA in equine transcriptome analysis is slightly earlier on day 12. Other than that, the mRNA expression of *C1R* and *SERPING1* in bovine endometrium showed up-regulation on day 12 and 18 but not on day 0. Differences in endometrial gene expression changes between different mammals are probably related to specific histological changes in the endometrium during the cycle (Bauersachs et al.**,** 2012).

Altogether, the exploration of gene expression during the cycle in both species showed common regulation in three of the four phases; during estrus, metestrus (early luteal phase) and preestrus As for diestrus, correlation showed only a minority of positively regulated genes indicating species-specific gene expression changes during this time of the reproductive cycle. Although, the functional annotation analysis of the endometrial gene expression during bovine estrous cycle revealed the same biological terms as over-represented during distinct phases the analysis of gene expression on the basis of single genes revealed only minor similarities. This indicates common functionality but species-specific gene expression.

3. Conclusion and forecast

In conclusion, this study provides a holistic view on the quantitative changes in transcript levels during the estrous cycle in equine and porcine endometrium. Microarray analysis identified numerous genes as differentially expressed throughout the estrous cycle in both species. Furthermore, with focus on specific functional categories and biological processes in relation to dynamic gene expression profiles, results pinpoint the molecular reflections of important physiological changes in the cyclic endometrium with regard to the crucial role of this tissue for successful reproduction. However, detailed and clear functions of many of these genes, especially with respect to the many interactions in reproductive processes, are still unknown. Furthermore, the comparison of results between species showed many species-specific gene expression changes especially during diestrus but also common characteristics for distinct phases in both species.

Results of this study provide the basis for an in-depth analysis of individual genes or particularly interesting components of molecular regulation of endometrial changes during the estrous cycle, respectively. In addition, the comparison to dynamic gene expression changes in bovine endometrium indicates an adaptation of endometrial gene expression to specific differences in cyclic endometrial dynamics.

This study provides an explorative analysis that can be used as a basis for further hypothesis-

driven investigation in reproduction of domestic animals. Future studies could investigate even more stages during the distinct phases of the reproductive cycle using a similar approach to provide a more detailed view of dynamic gene expression changes. Furthermore, the optimal way for comparison of datasets from different species would be the determination of one-to-one orthologous genes based on sequence similarities and location in the genome. However, results of other groups showed differences in responses to hormonal control and signals of the embryo between different compartments. Since this study only investigated tissues that contained all compartments, namely LE, GE, blood vessels and stroma, further investigation should be performed on separated tissue samples to increase the spatial resolution of gene expression.

V. SUMMARY

Analysis and comparison of dynamic mRNA expression changes in the equine and porcine endometrium during the estrous cycle

The endometrium (mucosa of the uterus) exhibits morphological and functional changes during the estrous cycle which are mainly regulated by the interplay of the ovarian steroid hormones estradiol (E2) and progesterone (P4). According to the changes in hormone concentration the estrous cycle can be divided into four different phases: estrus (low P4 level), metestrus (P4 level on the rise), diestrus (highest P4 level) and preestrus (decreasing P4 level) corresponding to ovulatory, early luteal, mid luteal and follicular phase.

In order to study the response of the equine and the porcine endometrium to the changing hormonal environment during the estrous cycle at the transcriptome level, transcriptome-wide microarray analyses were performed. Therefore, endometrial biopsy samples were collected from five different mares and endometrial tissue samples after slaughter of 30 different sows on five different time points during the estrous cycle. To determine plasma P4 concentrations blood samples were collected when the corresponding endometrial sample was taken.

For equine samples the bioinformatics analysis revealed 4.996 differentially expressed genes and 5.325 differentially expressed genes for porcine samples. To obtain detailed information about gene expression profiles and co-regulation of genes during the estrous cycle, the differentially expressed genes were clustered together based on similarities in mRNA expression profiles. In addition, a comparative analysis of both datasets was performed to achieve more insights into the species-specific or common gene expression changes. This analysis revealed 841 genes as significantly positive and negative correlated in both species, respectively. To characterize the differentially expressed genes of individual expression clusters in relation to their potential biological functions DAVID functional annotation clustering analysis (online-tool) was performed. Expression of selected equine and porcine genes was validated using quantitative real-time PCR (qPCR).

The data from functional annotation analysis revealed biological processes such as ‘extra cellular matrix (ECM)’ and ‘collagens’ during estrus, ‘cell cycle’ and ‘mitosis’ during metestrus, terms related to ‘secretory activity and metabolism’ and ‘protein transport’ during diestrus and ‘cytokine-cytokine receptor interaction’, ‘coagulation cascades’ and ‘inflammatory response’ during following preestrus as over-represented in equine endometrium. During porcine estrus, the functional categories ‘extra cellular matrix (ECM)’ and ‘collagens’ showed over-representation, and during metestrus, the categories ‘cell cycle’ and ‘mitosis’ respectively. The biological processes related to immune system functions (e.g. ‘immune response’, ‘inflammatory response’) showed over-representation during early until mid diestrus, and the process ‘regulation of apoptosis’ was over-represented during following preestrus in porcine endometrium. Functional annotation clustering of correlated genes (positive and negative) showed common biological terms as over-represented such as ‘extracellular matrix’ and ‘collagens’ during estrus and ‘cell-cycle’ and ‘mitosis’ during metestrus but also revealed differences especially during luteal phase, respectively. In addition, the comparison of the genes with significant correlation to gene expression profiles in the bovine endometrium (Mitko**,** 2008) revealed even more species-specific genes expression profiles.

Altogether, the results of this study show species-specific preparation for the support of potential embryo growth and development and active infiltration of the endometrium with immune cells as well as remodeling of endometrial cells during the luteal phase and preestrus. Furthermore, the reconstruction of the tissue (ECM remodeling) during estrus and active cell proliferation during early luteal phase suggest a common characteristic throughout species.

VI. ZUSAMMENFASSUNG

Untersuchungen und Vergleich der mRNA Expressionsprofile im Endometrium der Stute und der Sau während des Sexualzyklus

Das Endometrium (Gebärmutterschleimhaut) durchläuft morphologische und funktionale Änderungen während des Sexualzyklus, welche hauptsächlich durch die Interaktion der ovariellen Steroidhormone Östradiol (E2) und Progesteron (P4) reguliert werden. An Hand der sich ändernden Hormonkonzentrationen wird der Sexualzyklus in vier verschiedene Phasen eingeteilt: Östrus (niedrige P4-Konzentration), Metöstrus (ansteigende P4-Konzentration), Diöstrus (höchste P4-Konzentration) und Pröstrus (sinkende P4-Konzentration). Der Diöstrus wird auch als Gelbkörperphase oder Lutealphase bezeichnet.

Um die Änderungen der Gebärmutterschleimhaut der Stute und der Sau in Reaktion auf die sich verändernde hormonelle Umgebung auf Trankriptomebene zu untersuchen, wurden trankriptom-weite Mikroarray-Analysen durchgeführt. Hierfür wurden von fünf verschiedenen Stuten Endometrium-Biopsieproben und 30 verschiedenen Jungsauen Endometrium-Proben nach Schlachtung an fünf unterschiedlichen Tagen während des Zyklus entnommen. Zusätzlich wurden die Progesteronkonzentrationen über genommene Blutproben bestimmt.

Die bioinformatischen Analysen der Expressionsdaten der Stute ergaben 4.996 und die beim Schwein 5.325 Gene als differentiell exprimiert. Für eine detaillierte Analyse der Genexpression und des Koregulationsverhaltens der Gene während des Sexualzyklus wurden die differentiell exprimierten Gene basierend auf den Expressionsveränderungen der Transkripte in sogenannte Cluster mit ähnlichen Expressionsprofilen eingeteilt. Zusätzlich wurde eine Vergleichsanalyse durchgeführt, um genauere Informationen über speziesspezifische bzw. generelle Genexpressionsprofile im Zyklusverlauf zu erhalten. Diese Analyse ergab 841 Gene mit signifikant positiv bzw. negativ korrelierenden Expressionsprofilen. Zur Charakterisierung der biologischen Funktionalität einzelner Gengruppen der individuellen Cluster wurde eine funktionelle Annotation mittels DAVID (online Software) durchgeführt. Die Expression einzelner ausgewählter Gene wurde mittels qPCR validiert.

Die Ergebnisse der Funktionsanalyse der Stute ergaben charakteristische biologische Prozesse als überrepräsentiert, wie zum Beispiel die Kategorien „extrazelluläre Matrix“ und „Kollagene“ während des Östrus und die biologischen Prozesse „Zellzyklus“ und „Mitose“ während des Metöstrus. Die biologischen Funktionen „Proteintransport“ und Prozesse, die „sekretorische Aktivität und Stoffwechsel“ beschreiben, waren vor allem unter den Genen mit erhöhter Expression während der Gelbkörperphase überrepräsentiert. Im darauf folgenden Proöstrus fielen biologische Prozesse auf, die mit dem Immunsystem zusammen hängen („Immunantwort“, „Zytokin-Zytokinrezeptor Interaktionen“ etc.). Während des Östrus beim Schwein zeigten ebenfalls die Kategorien „extrazelluläre Matrix“ und „Kollagene“ und während des Metöstrus die biologischen Prozesse „Zellzyklus“ und „Mitose“ erhöhte Repräsentanz. Während der frühen bis zur späten Gelbkörperphase waren zum Beispiel die Prozesse überrepräsentiert, die das Immunsystem vertreten und im folgenden Proöstrus der Prozess der „Regulation der Apoptose“. Dementsprechend ergab die weitere Funktionsanalyse der korrelierenden Gene (positiv und negativ) die bei beiden Spezies verbreiteten, biologischen Kategorien wie „Extrazelluläre Matrix“ und „Kollagene“ als stark repräsentiert während des Östrus und „Zellzyklus“ und „Mitose“ während des Metöstrus, aber auch speziesspezifische Unterschiede, vor allem während der Gelbkörperphase. Weiterhin zeigte ein Vergleich mit der Genexpressionsanalyse des bovinen Endometriums während des Sexualzyklus (Mitko**,** 2008) weitere speziesspezifische Expressionsprofile auf.

Die Ergebnisse dieser Arbeit zeigen eine artenspezifische Vorbereitung der Gebärmutterschleimhaut auf die Unterstützung von Wachstum und Entwicklung des Embryos und eine aktive Infiltrierung durch Immunzellen sowie den aktiven Umbau endometrialer Zellen

während der Gelbkörperphase und dem Proöstrus. Desweiteren weisen der Umbau der extrazellulären Matrix während des Östrus und die aktive Zellproliferation während des Metöstrus hingegen auf eine allgemein verbreitete Charakteristik hin.

VII. REFERENCES

Abe, et al. 2007: NPY and NPY receptors in vascular remodeling. Curr Top Med Chem, Vol: 7

Abramovitz, et al. 2000: The utilization of recombinant prostanoid receptors to determine the affinities and selectivities of prostaglandins and related analogs. Biochim Biophys Acta, Vol: 1483

Adams 1999: Comparative patterns of follicle development and selection in ruminants. J Reprod Fertil Suppl, Vol: 54

Agas, et al. 2013: Prostaglandin F2alpha: a bone remodeling mediator. J Cell Physiol, Vol: 228

Aghajanova, et al. 2008: Uterine receptivity to human embryonic implantation: histology, biomarkers, and transcriptomics. Semin Cell Dev Biol, Vol: 19

Alexander, et al. 1982: Radioimmunoassay and in-vitro bioassay of serum LH throughout the equine oestrous cycle. J Reprod Fertil Suppl, Vol: 32

Allen, et al. 1988: Cyclical accumulation of uterine fluid in mares with lowered resistance to endometritis. Vet Rec, Vol: 122

Arai, et al. 2013: Remodeling of bovine endometrium throughout the estrous cycle. Anim Reprod Sci, Vol: 142

Asbury, et al. 1982: Factors affecting phagocytosis of bacteria by neutrophils in the mare's uterus. J Reprod Fertil Suppl, Vol: 32

Ashworth, et al. 2006: Expression of porcine endometrial prostaglandin synthase during the estrous cycle and early pregnancy, and following endocrine disruption of pregnancy. Biol Reprod, Vol: 74

Aupperle, et al. 2000: Cyclical endometrial steroid hormone receptor expression and proliferation intensity in the mare. Equine Vet J, Vol: 32

Aurich 2011: Reproductive cycles of horses. Animal Reproduction Science, Vol: 124

Aurich, et al. 1995: Effects of gonadal steroids on the opioid regulation of LH and prolactin release in ovariectomized pony mares. J Endocrinol, Vol: 147

Bae, et al. 2003: A light microscopic and ultrastructural study on the presence and location of oxytocin in the equine endometrium. Theriogenology, Vol: 60

Bauersachs, et al. 2007: Technical note: Bovine oviduct and endometrium array version 1: a tailored tool for studying bovine endometrium biology and pathophysiology. J Dairy Sci, Vol: 90

Bauersachs, et al. 2008: Transcriptome studies of bovine endometrium reveal molecular profiles characteristic for specific stages of estrous cycle and early pregnancy. Exp Clin Endocrinol Diabetes, Vol: 116

Bauersachs, et al. 2005: Gene expression profiling of bovine endometrium during the oestrous cycle: detection of molecular pathways involved in functional changes. J Mol Endocrinol, Vol: 34

Bauersachs, et al. 2006: Embryo-induced transcriptome changes in bovine endometrium reveal species-specific and common molecular markers of uterine receptivity. Reproduction, Vol: 132

Bauersachs, et al. 2012: Transcriptome analyses of bovine, porcine and equine endometrium during the pre-implantation phase. Anim Reprod Sci, Vol: 134

Bazer, et al. 1994: Pregnancy recognition in ruminants, pigs and horses: Signals from the trophoblast. Theriogenology, Vol: 41

Bigsby 1991. Reciprocal Tissue Interactions in Morphogenesis and Hormonal Responsiveness of the Female Reproductive Tract. *In:* Lavia (ed.) *Cellular Signals Controlling Uterine Function.* Boston, MA: Springer US.

Blasberg, et al. 1998: Inhibition of Estrogen-Induced Sexual Receptivity by Androgens: Role

of the Androgen Receptor. Hormones and Behavior, Vol: 34
Blatchley, et al. 1971: Identification of prostaglandin F2-alpha in the utero-ovarian blood of guinea-pig after treatment with oestrogen. Nature, Vol: 230
Blitek, et al. 2010: Effect of steroids on HOXA10 mRNA and protein expression and prostaglandin production in the porcine endometrium. J Reprod Dev, Vol: 56
Boerboom, et al. 2004: Expression of key prostaglandin synthases in equine endometrium during late diestrus and early pregnancy. Biol Reprod, Vol: 70
Boulton, et al. 1996: Changes in content of mRNA encoding oxytocin in the pig uterus during the oestrous cycle, pregnancy, at parturition and in lactational anoestrus. J Reprod Fertil, Vol: 108
Bowen, et al. 1996: Spatial and temporal analyses of integrin and Muc-1 expression in porcine uterine epithelium and trophectoderm in vivo. Biol.Reprod., Vol: 55
Burghardt, et al. 2002: Integrins and extracellular matrix proteins at the maternal-fetal interface in domestic animals. Cells Tissues Organs, Vol: 172
Cadario, et al. 1995: Relationship between prostaglandin and uterine clearance of radiocolloid in the mare. Biol. Reprod. Mono, Vol: 1
Cahill 2007: Progesterone receptor membrane component 1: an integrative review. j steroid Biochem Mol Biol, Vol: 105
Caldwell, et al. 1972: The effects of exogenous progesterone and estradiol on prostaglandin F levels in ovariectomized ewes. Prostaglandins, Vol: 1
Castracane, et al. 1975: The effect of estrogen and progesterone on uterine prostaglandin biosynthesis in the ovariectomized rat. Biol Reprod, Vol: 13
Catalano, et al. 2011: Comprehensive expression analysis of prostanoid enzymes and receptors in the human endometrium across the menstrual cycle. Mol Hum Reprod, Vol: 17
Cheon, et al. 2002: A genomic approach to identify novel progesterone receptor regulated pathways in the uterus during implantation. Mol.Endocrinol., Vol: 16
Choi, et al. 2011a: Regulation and molecular mechanisms of calcium transport genes: do they play a role in calcium transport in the uterine endometrium? J Physiol Pharmacol, Vol: 62
Choi, et al. 2011b: Regulation of S100G Expression in the Uterine Endometrium during Early Pregnancy in Pigs. Asian Australas. J. Anim. Sci, Vol: 25
Chomczynski, et al. 2006: The single-step method of RNA isolation by acid guanidinium thiocyanate-phenol-chloroform extraction: twenty-something years on. Nat Protoc, Vol: 1
Chu, et al. 2002: Apoptosis of endometrial cells in the bitch. Reprod Fertil Dev, Vol: 14
Chuang, et al. 2006: Prostaglandin E2 induces fibroblast growth factor 9 via EP3-dependent protein kinase Cdelta and Elk-1 signaling. Mol Cell Biol, Vol: 26
Clapham 2007: Calcium signaling. Cell, Vol: 131
Clutterbuck, et al. 2010: Matrix metalloproteinases in inflammatory pathologies of the horse. Vet J, Vol: 183
Cocchi, et al. 1995: Identification of RANTES, MIP-1 alpha, and MIP-1 beta as the major HIV-suppressive factors produced by CD8+ T cells. Science, Vol: 270
Corner 1921: Cyclic changes in the ovaries and uterus of the sow, and their relation of the mechanism of implantation. . Contr. Embryol, Vol: 13
Craig, et al. 1991: The murine gene encoding secreted phosphoprotein 1 (osteopontin): promoter structure, activity, and induction in vivo by estrogen and progesterone. Gene, Vol: 100
Crawford, et al. 1987: Effects of topical PGF2 alpha on aqueous humor dynamics in cynomolgus monkeys. Curr Eye Res, Vol: 6
Cross, et al. 1988: Uterine contractions in nonpregnant and early pregnant mares and jennies as determined by ultrasonography. J Anim Sci, Vol: 66
Crossett, et al. 1998: Transfer of a uterine lipocalin from the endometrium of the mare to the

developing equine conceptus. Biol Reprod, Vol: 59
Croy, et al. 2009: Comparison of immune cell recruitment and function in endometrium during development of epitheliochorial (pig) and hemochorial (mouse and human) placentas. Placenta, Vol: 30 Suppl A
Cunha, et al. 1985: Stromal-epithelial interactions in adult organs. Cell Differ, Vol: 17
Curry, et al. 2001: Cyclic changes in the matrix metalloproteinase system in the ovary and uterus. Biol Reprod, Vol: 64
Curry, et al. 2003: The matrix metalloproteinase system: changes, regulation, and impact throughout the ovarian and uterine reproductive cycle. Endocr Rev, Vol: 24
Dalin, et al. 2004: Immune cell infiltration of normal and impaired sow endometrium. Anim Reprod Sci, Vol: 82-83
Dang, et al. 2000: The biology of the mammalian Kruppel-like family of transcription factors. Int J Biochem Cell Biol, Vol: 32
Davis 2008: Biological activities of C1 inhibitor. Mol Immunol, Vol: 45
Davis, et al. 1983: Prostaglandins in swine blastocysts. Biol Reprod, Vol: 28
Degen, et al. 2000: The fate of U1 snRNP during anti-Fas induced apoptosis: specific cleavage of the U1 snRNA molecule. Cell Death Differ, Vol: 7
Denda, et al. 1998: Identification of osteopontin as a novel ligand for the integrin alpha8 beta1 and potential roles for this integrin-ligand interaction in kidney morphogenesis. Mol Biol Cell, Vol: 9
Dennis, et al. 2003: DAVID: Database for Annotation, Visualization, and Integrated Discovery. Genome Biol, Vol: 4
Dery, et al. 2003: Regulation of Akt expression and phosphorylation by 17beta-estradiol in the rat uterus during estrous cycle. Reprod Biol Endocrinol, Vol: 1
Dey, et al. 1980: Prostaglandin synthesis in the rabbit blastocyst. Prostaglandins, Vol:
Dimitriadis, et al. 2002: Interleukin 11 advances progesterone-induced decidualization of human endometrial stromal cells. Mol Hum Reprod, Vol: 8
Dozier, et al. 2008: Two pathways for prostaglandin F2 alpha synthesis by the primate periovulatory follicle. Reproduction, Vol: 136
Evans, et al. 1997: Selection of the dominant follicle in cattle occurs in the absence of differences in the expression of messenger ribonucleic acid for gonadotropin receptors. Endocrinology, Vol: 138
Fabian. 1960. *Zum zyklischen Verhalten vornehmlich der Höhe des Endometriums beim Schwein.*
Ford 1982: Control of uterine and ovarian blood flow throughout the estrous cycle and pregnancy of ewes, sows and cows. Journal of animal science, Vol: 2
Ford, et al. 1979: Blood flow to uteri of sows during the estrous cycle and early pregnancy: local effect of the conceptus on the uterine blood supply. Biol Reprod, Vol: 21
Ford, et al. 1977: Role of estradiol-17 beta and progesterone in regulating constriction of ovine uterine arteries. Biol Reprod, Vol: 17
Forde, et al. 2011: Changes in the endometrial transcriptome during the bovine estrous cycle: effect of low circulating progesterone and consequences for conceptus elongation. Biol Reprod, Vol: 84
Forsburg 2004: Eukaryotic MCM proteins: beyond replication initiation. Microbiol Mol Biol Rev, Vol: 68
Fortune 1994: Ovarian follicular growth and development in mammals. Biology of Reproduction, Vol: 50
Fortune, et al. 2001: Differentiation of dominant versus subordinate follicles in cattle. Biol Reprod, Vol: 65
Franczak 2008: Endometrial and myometrial secretion of androgens and estrone during early

pregnancy and luteolysis in pigs. Reprod Biol, Vol: 8
Franczak, et al. 2014: Transcriptomic analysis of the myometrium during peri-implantation period and luteolysis--the study on the pig model. Funct Integr Genomics, Vol: 14
Fumuso, et al. 2007: Immune parameters in mares resistant and susceptible to persistent post-breeding endometritis: effects of immunomodulation. Vet Immunol Immunopathol, Vol: 118
Garrett, et al. 1988: Evidence for maternal regulation of early conceptus growth and development in beef cattle. J Reprod Fertil, Vol: 84
Gebhardt, et al. 2012: Exploration of global gene expression changes during the estrous cycle in equine endometrium. Biol Reprod, Vol: 87
Geisert, et al. 1994: Immunocytochemical localization and changes in endometrial progestin receptor protein during the porcine oestrous cycle and early pregnancy. Reprod Fertil Dev, Vol: 6
Genbacev, et al. 2003: Trophoblast L-selectin-mediated adhesion at the maternal-fetal interface. Science, Vol: 299
Gerke V. 2002: Annexins:From structure to function. Physiol Rew., Vol: 82
Gerstenberg 1999: Cell proliferation patterns in the equine endometrium throughout the non-pregnant reproductive cycle. J Reprod Fertil, Vol: 116
Gerstenberg, et al. 1999: Cell proliferation patterns in the equine endometrium throughout the non-pregnant reproductive cycle. J Reprod Fertil, Vol: 116
Giguere 2002: To ERR in the estrogen pathway. Trends Endocrina Metab, Vol: 13
Gilbert 1992: Cyclical changes in equine endometrial histology. (Abstract). Proceedings of the 12th International Conference on Animal Reproduction, Vol:
Gilles, et al. 2003: Transactivation of vimentin by beta-catenin in human breast cancer cells. Cancer Res., Vol: 63
Ginther 1984: Intrauterine movement of the early conceptus in barren and postpartum mares. Theriogenology, Vol: 21
Ginther, et al. 2008: Dynamics of the Equine Preovulatory Follicle and Periovulatory Hormones: What's New? Journal of Equine Veterinary Science, Vol: 28
Godbole, et al. 2007: Regulation of homeobox A10 expression in the primate endometrium by progesterone and embryonic stimuli. Reproduction, Vol: 134
Goddard, et al. 1985: Genital tract pressures in mares II. Changes induced by oxytocin and prostaglandin F(2)alpha. Theriogenology, Vol: 24
Goff 2004: Steroid hormone modulation of prostaglandin secretion in the ruminant endometrium during the estrous cycle. Biol.Reprod., Vol: 71
Groothuis, et al. 2007: Estrogen and the endometrium: lessons learned from gene expression profiling in rodents and human. Hum Reprod Update, Vol: 13
Guo, et al. 2009: Expression and hormonal regulation of Hoxa10 in canine uterus during the peri-implantation period. Reprod Domest Anim, Vol: 44
Hakhuyan, et al. 2009: Identification of Differentially Expressed Genes in the Uterine Endometrium on Day 12 of the Estrous Cycle and Pregnancy in Pigs. Molecular Reproduction & Development, Vol: 76
Hammond, et al. 1993: The effect of growth factors on the proliferation of human endometrial stromal cells in culture. Am J Obstet Gynecol, Vol: 168
Hampton, et al. 1995: Tissue inhibitors of metalloproteinases in endometrium of ovariectomized steroid-treated ewes and during the estrous cycle and early pregnancy. Biol.Reprod., Vol: 53
Harada, et al. 2004: Apoptosis in human endometrium and endometriosis. Hum Reprod Update, Vol: 10(1)
Hartt 2005: Temporal and spatial associations of oestrogen receptor alpha and progesterone receptor in the endometrium of cyclic and early pregnant mares. Reproduction, Vol: 130

Hasty, et al. 1994: Hormonal regulation of complement components and receptors throughout the menstrual cycle. Am J Obstet Gynecol, Vol: 170
Hayashi, et al. 2005: Estrogen disruption of neonatal ovine uterine development: effects on gene expression assessed by suppression subtraction hybridization. Biol Reprod, Vol: 73
Hayashi, et al. 2011: Differential gene expression of serine protease inhibitors in bovine ovarian follicle: possible involvement in follicular growth and atresia. Reproductive Biology and Endocrinology, Vol: 9
Hengartner 2000: The biochemistry of apoptosis. Nature, Vol: 407
Hirvonen 2011: Transcriptational activity of estrogen-related receptor gamma (ERRgamma) is stimulated by the phytoestrogen equo. j steroid Biochem Mol Biol, Vol: 123(1-2)
Hof, et al. 2005: Autoantibodies specific for apoptotic U1-70K are superior serological markers for mixed connective tissue disease. Arthritis Res Ther, Vol: 7
Holmes, et al. 1980: Evidence of prostaglandin involvement in blastocyst implantation. J Embryol Exp Morphol., Vol: 55
Hu, et al. 1995: A biochemical characterization of the binding of osteopontin to integrins alpha v beta 1 and alpha v beta 5. J Biol Chem, Vol: 270
Huber 2002: Variance stabilization applied to microarray data calibration and to the quantification of differential expression. Bioinformatics, Vol: 18 Suppl 1
Hyland, et al. 1982: Prostaglandin production by ovine embryos and endometrium in vitro. J Reprod Fertil, Vol: 65
Hyttel, et al. 2010. Essentials of domestic animal embryology. Saunder Elsevier.
Jabbour, et al. 2006: Endocrine regulation of menstruation. Endocr Rev, Vol: 27
Jin, et al. 1988: Estrous cycle- and pregnancy-related differences in expression of the proenkephalin and proopiomelanocortin genes in the ovary and uterus. Endocrinology, Vol: 122
Johnson 2001: Muc-1, integrin, and osteopontin expression during the implantation cascade in sheep. Biol Reprod, Vol: 65
Johnson, et al. 2003: Osteopontin: roles in implantation and placentation. Biol Reprod, Vol: 69
Johnson, et al. 2006: Effects of estradiol-17beta on expression of mRNA for seven angiogenic factors and their receptors in the endometrium of ovariectomized (OVX) ewes. Endocrine, Vol: 30
Johnson, et al. 1997: Effects of ovarian steroids on uterine growth, morphology, and cell proliferation in ovariectomized, steroid-treated ewes. Biol Reprod, Vol: 57
Jones, et al. 1998: Apoptosis and bcl-2 expression in normal human endometrium, endometriosis and adenomyosis. Hum Reprod, Vol: 13
Ka, et al. 2007: Regulation of expression of fibroblast growth factor 7 in the pig uterus by progesterone and estradiol. Biol Reprod, Vol: 77
Ka, et al. 2000: Keratinocyte growth factor: expression by endometrial epithelia of the porcine uterus. Biol Reprod., Vol: 62
Kaczmarek, et al. 2013: Seminal plasma affects prostaglandin synthesis and angiogenesis in the porcine uterus. Biol Reprod, Vol: 88
Kaeoket, et al. 2001: The sow endometrium at different stages of the oestrous cycle: studies on morphological changes and infiltration by cells of the immune system. Anim Reprod Sci, Vol: 65
Kayisli, et al. 2002: Uterine chemokines in reproductive physiology and pathology. Am J Reprod Immunol, Vol: 47
Kenney 1978: Cyclic and pathologic changes of the mare endometrium as detected by biopsy, with a note on early embryonic death. J Am Vet Med Assoc, Vol: 172
Killeen, et al. 2014: Global gene expression in endometrium of high and low fertility heifers

during the mid-luteal phase of the estrous cycle. BMC Genomics, Vol: 15
Kim, et al. 2006: Differential expression of uterine calcium transporter 1 and plasma membrane Ca2+ ATPase 1b during rat estrous cycle. Am J Physiol Endocrinol Metab, Vol: 291
Klein 2010: Transcriptional profiling of equine endometrium during the time of maternal recognition of pregnancy. Biol Reprod, Vol: 83
Klein, et al. 2006: Monozygotic twin model reveals novel embryo-induced transcriptome changes of bovine endometrium in the preattachment period. Biol Reprod, Vol: 74
Knox 2005: Recruitment and selection of ovarian follicles for determination of ovulation rate in the pig. Domest Anim Endocrinol, Vol: 29
Koligian, et al. 1977: Progesterone inhibition of estrogen receptor replenishment in ovine endometrium. Biol Reprod, Vol: 17
Kotwika, et al. 1999: Effect of an oxytocin antagonist on prostglandin F2alpha secretion and the course of luteolysis in sows. Acto Veterinaria Hungarica, Vol: 4
Kowalski, et al. 2004: Uterine androgen receptors: roles in estrogen-mediated gene expressionand DNA synthesis. Biol Reprod, Vol: 70
Koziorowski 1988: Counter current transfer of polypeptide hormones from uterus to ovary in gilts using insulin as a model. Acta Physiol Pol, Vol: 39
Kraeling, et al. 1985: Inhibition of pregnancy with indomethacin in mature gilts and prepuberal gilts induced to ovulate. Biol Reprod, Vol: 32
Krisinger, et al. 1995: Porcine calbindin-D9k gene: expression in endometrium, myometrium, and placenta in the absence of a functional estrogen response element in intron A. Biol Reprod, Vol: 52
Krzymowski 1982: A subovarian exchange mechanism for the countercurrent transfer of ovarian steroid hormones in the pig. J Reprod Fertil, Vol: 65
Krzymowski 1990: Uterine and ovarian countercurrent pathways in the control of ovarian function in the pig. . J. Reprod. Fertil., Vol: 40 (Suppl.)
Krzymowski 2004: The oestrous cycle and early pregnancy--a new concept of local endocrine regulation. Vet J, Vol: 168
Krzymowski, et al. 2008: The role of the endometrium in endocrine regulation of the animal oestrous cycle. Reprod Domest Anim, Vol: 43
L'horset, et al. 1990: 17 beta-estradiol stimulates the calbindin-D9k (CaBP9k) gene expression at the transcriptional and posttranscriptional levels in the rat uterus. Endocrinology, Vol: 127
Lai, et al. 2000: Expression of proliferating cell nuclear antigen in luminal epithelium during the growth and regression of rat uterus. J Endocrinol, Vol: 166
Law, et al. 2006: An overview of the serpin superfamily. Genome Biol, Vol: 7
Leblanc, et al. 1989: Uterine clearance mechanisms during the early postovulatory period in mares. Am J Vet Res, Vol: 50
Lee, et al. 2007: Uterine TRPV6 expression during the estrous cycle and pregnancy in a mouse model. Am J Physiol Endocrinol Metab, Vol: 293
Lee, et al. 2010: Analysis of nuclear high mobility group box 1 (HMGB1)-binding proteins in colon cancer cells: clustering with proteins involved in secretion and extranuclear function. J Proteome Res, Vol: 9
Lees, et al. 1986: Eicosanoids and equine leucocyte locomotion in vitro. Equine Vet J, Vol: 18
Leiser, et al. 1988: Normal cyclical morphology of the endometrium and ovary of swine. Tierarztl Prax, Vol: 16
Leiva, et al. 1991: Complement C3 synthesis, peroxidase activity and eosinophil chemotaxis in the rat uterus: Effect of estradiol and testosterone. Molecular and Cellular Endocrinology, Vol: 81
Lewis, et al. 1982: Metabolism of arachidonic acid in vitro by bovine blastocysts and endometrium. Biol Reprod, Vol: 27

Loeffler, et al. 2013. Anatomie und Physiologie der Haustiere. Ulmer.
Lopes, et al. 2006: Transcriptional regulation of uterine vascular endothelial growth factor during early gestation in a carnivore model, Mustela vison. J Biol Chem, Vol: 281
Luciano 2011: Expression of progesterone receptor membrane component-1 in bovine reproductive system during estrous cycle. European journal of histochemistry : EJH, Vol: 55
Mahendroo, et al. 1999: The parturition defect in steroid 5alpha-reductase type 1 knockout mice is due to impaired cervical ripening. Mol Endocrinol, Vol: 13
Maj, et al. 1997: Activity of 72-kDa and 92-kDa matrix metalloproteinases in placental tissues of cows with and without retained fetal membranes. Placenta, Vol: 18
Mansouri, et al. 2008: Alterations in the expression, structure and function of progesterone receptor membrane component-1 (PGRMC1) in premature ovarian failure. Hum Mol Genet, Vol: 17
Marshburn, et al. 1990: Immunohistochemical localization of prostaglandin H synthase in the embryo and uterus of the mouse from ovulation through implantation. Mol Reprod Dev, Vol: 25
Mathew, et al. 2011: Uterine progesterone receptor expression, conceptus development, and ovarian function in pigs treated with RU 486 during early pregnancy. Biol Reprod, Vol: 84
Mccracken 1973: The physiological role of prostaglandin F2alpha in corpus luteum regression. Adv.Biosci., Vol: 9
Mccracken 1980: Hormone receptor control of prostaglandin F2 alpha secretion by the ovine uterus. Adv Prostaglandin Thromboxane Res, Vol: 8
Mccracken J. 1999: Luteolysis: a neuroendocrine-mediated event. Physiol Rev, Vol: 79
Medh, et al. 2000: Hormonal regulation of physiological cell turnover and apoptosis. Cell Tissue Res, Vol: 301
Mehlhorn, et al. 1975: Studies on improving the fertility of aged sows. 2. Results of histological studies on the structure of the endometrium in aged sows during estrous cycle. Arch Exp Veterinarmed, Vol: 29
Merkl, et al. 2010: Microarray analysis of equine endometrium at days 8 and 12 of pregnancy. Biol Reprod, Vol: 83
Mishra, et al. 2010: Expression of extracellular matrix metalloproteinase inducer (EMMPRIN) and its related extracellular matrix degrading enzymes in the endometrium during estrous cycle and early gestation in cattle. Reprod Biol Endocrinol, Vol: 8
Mitko 2008: Dynamic changes in messenger RNA profiles of bovine endometrium during the oestrous cycle. Reproduction, Vol: 135
Morales 2000: Different pattern of structural luteolysis in the human corpus luteum of menstruation. Human Reproduction, Vol: 5
Morel 2008. Equine Reproductive Physiology, Breeding and Stud Management.
Morris, et al. 2009: Genetic variation in complement component 2 of the classical complement pathway is associated with increased mortality and infection: a study of 627 patients with trauma. J Trauma, Vol: 66
Mukherjee, et al. 1995: Interaction of osteopontin with fibronectin and other extracellular matrix molecules. Ann N Y Acad Sci, Vol: 760
Mukku, et al. 1985: Regulation of epidermal growth factor receptor by estrogen. J Biol Chem, Vol: 260
Nagase, et al. 2006: Structure and function of matrix metalloproteinases and TIMPs. Cardiovasc Res, Vol: 69
Nagata 1996: Hsp47: a collagen-specific molecular chaperone. Trends Biochem Sci, Vol: 21
Narumiya, et al. 1999: Prostanoid receptors: structures, properties, and functions. Physiol Rev, Vol: 79
Nawaz, et al. 1987: Hormonal regulation of cell death in rabbit uterine epithelium. Am J Pathol,

Vol: 127
Nelson, et al. 2001: Estrogen production and action. J AM Acad Dermatol, Vol: 45 (3Suppl)
Okada, et al. 2000: Expression of interleukin-15 in human endometrium and decidua. Molecular Human Reproduction, Vol: 6
Okano, et al. 2007: Apoptosis in the porcine uterine endometrium during the estrous cycle, early pregnancy and post partum. J Reprod Dev, Vol: 53
Omigbodun, et al. 1997: Progesterone regulates osteopontin expression in human trophoblasts: a model of paracrine control in the placenta? Endocrinology, Vol: 138
Ornitz, et al. 1996: Receptor specificity of the fibroblast growth factor family. J Biol Chem, Vol: 271
Østrup, et al. 2010: Differential endometrial gene expression in pregnant and nonpregnant sows. Biol Reprod, Vol: 83
Ott, et al. 1993: Changes in progesterone and oestrogen receptor mRNA and protein during maternal recognition of pregnancy and luteolysis in ewes. J Mol Endocrinol, Vol: 10
Pabona, et al. 2009: Nuclear receptor co-regulator Krüppel-like factor 9 and prohibitin 2 expression in oestrogen-induced epithelial cell proliferation in the mouse uterus. J Endocrinol, Vol: 200
Padua, et al. 2010: Evolution and function of the uterine serpins (SERPINA14). Am J Reprod Immunol, Vol: 64
Page, et al. 2002: Expression of nuclear factor kappa B components in human endometrium. J Reprod Immunol, Vol: 54
Pak, et al. 2003: Targeted protein degradation and synapse remodeling by an inducible protein kinase. Science, Vol: 302
Parham 2005. The Immune System. Garland Science Publishing, New York.
Park, et al. 2011: Hormonal regulation of uterine chemokines and immune cells. Clin Exp Reprod Med, Vol: 38
Parr, et al. 1988: Immunohistochemical localization of prostaglandin synthase in the rat uterus and embryo during the peri-implantation period. Biol Reprod, Vol: 38
Peltoniemi, et al. 1995: Effect of chronic treatment with a GnRH agonist (Goserelin) on LH secretion and early pregnancy in gilts. Animal Reproduction Science, Vol: 40
Peluso, et al. 2006: Progesterone Membrane Receptor Component 1 Expression in the Immature Rat Ovary and Its Role in Mediating Progesterone's Antiapoptotic Action. Endocrinology, Vol: 147
Persson, et al. 1997: Insulin-like growth factor-I in the porcine endometrium and placenta: localization and concentration in relation to steroid influence during early pregnancy. Anim Reprod Sci, Vol: 46
Plante, et al. 2012: G protein-coupled estrogen receptor (GPER) expression in normal and abnormal endometrium. Reprod Sci, Vol: 19
Prakash, et al. 1987: Development of a sensitive enzymeimmunoassay (EIA) for progesterone determination in unextracted bovine plasma using the second antibody technique. J Steroid Biochem, Vol: 28
Prehn 1963: Messungen am Uterus des nulliparen Schweines im mittleren Postoestrum und späten Interoestrum. Zbl. Vet. Med., Vol:
Pru, et al. 2013: PGRMC1 and PGRMC2 in uterine physiology and disease. Front Neurosci, Vol: 7
Richter, et al. 2003: Immunohistochemical reactivity of myometrial oxytocin receptor in extracorporeally perfused nonpregnant human uteri. Arch Gynecol Obstet, Vol: 269
Riegel J. 2002: Anatomie des Pferdes. Vol: Band 1
Rittling, et al. 1997: Osteopontin expression in mammary gland development and tumorigenesis. Cell Growth Differ, Vol: 8

Roberto Da Costa, et al. 2007: Caspase-3-mediated apoptosis and cell proliferation in the equine endometrium during the oestrous cycle. Reprod Fertil Dev, Vol: 19
Roby 1994: Mouse endometrial tumor necrosis factor-alpha messenger ribonucleic acid and protein: localization and regulation by estradiol and progesterone. Endocrinology, Vol: 135
Rotello, et al. 1992: Characterization of uterine epithelium apoptotic cell death kinetics and regulation by progesterone and RU 486. Am J Pathol., Vol: 140(2)
Rudolph-Owen, et al. 1997: Coordinate expression of matrix metalloproteinase family members in the uterus of normal, matrilysin-deficient, and stromelysin-1-deficient mice. Endocrinology, Vol: 138
Rüsse 1998. Lehrbuch der Embryologie der Haustiere. PAREY.
Saban, et al. 2010: Neuropilin-VEGF signaling pathway acts as a key modulator of vascular, lymphatic, and inflammatory cell responses of the bladder to intravesical BCG treatment. Am J Physiol Renal Physiol, Vol: 299
Sadek, et al. 2012: Variation in stability of housekeeping genes in endometrium of healthy and polycystic ovarian syndrome women. Hum Reprod, Vol: 27
Safran, et al. 1998: Modulation of osteopontin post-translational state by 1, 25-(OH)2-vitamin D3. Dependence on Ca2+ influx. J Biol Chem, Vol: 273
Salamonsen, et al. 1995: Matrix metalloproteinases and their tissue inhibitors at the ovine trophoblast-uterine interface. J Reprod Fertil Suppl, Vol: 49
Samborski, et al. 2013: Deep sequencing of the porcine endometrial transcriptome on day 14 of pregnancy. Biol Reprod, Vol: 88
Samuel, et al. 1972: The ultrastructure of pig trophoblast rransplanted to an ectopic site in the uterine wall. J Anat, Vol: 113
Sandow, et al. 1979: Hormonal control of apoptosis in hamster uterine luminal epithelium. Am J Anat., Vol: 156
Sasaki, et al. 2005: Influence of prostaglandin F2α and its analogues on hair regrowth and follicular melanogenesis in a murine model. Experimental Dermatology, Vol: 14
Sato, et al. 1997: Apoptotic cell death during the estrous cycle in the rat uterus and vagina. Anat Rec, Vol: 248(1)
Sayasith, et al. 2007: Cloning of equine prostaglandin dehydrogenase and its gonadotropin-dependent regulation in theca and mural granulosa cells of equine preovulatory follicles during the ovulatory process. Reproduction, Vol: 133
Schermer 1999. Confocal scanning microscopy in microarray detection. *In:* Press (ed.) *DNA microarrays - a practical approach.* Oxford.
Schoon, et al. 1992: Uterusbiopsien als Hilfsmittel für Diagnose und Prognose von Fertilitätsstörungen. Pferdeheilk, Vol: 8
Sidler, et al. 1986. *Das normale zyklische Geschehen in Endometrium des Schweines. Eine histologische, transmissions und rasterelectronenmikroskopische Untersuchung*. . Klinik für Nutztiere der Universität, Bern, Switzerland,.
Signoret 1970: Reproductive behaviour of pigs. J. Reprod. Fertil., Vol: 11(Suppl.),
Simon, et al. 1995: Interleukin-1 system crosstalk between embryo and endometrium in implantation. Hum Reprod, Vol: 10 Suppl 2
Simpson, et al. 2001: Tissue-specific estrogen biosynthesis and metabolism. Ann N Y Acad Sci, Vol: 949
Slayden, et al. 1993: Estrogen action in the reproductive tract of rhesus monkeys during antiprogestin treatment. Endocrinology, Vol: 132(4)
Smith, et al. 1996: Osteopontin N-terminal domain contains a cryptic adhesive sequence recognized by alpha9beta1 integrin. J Biol Chem, Vol: 271
Soede 1997: Expression of oestrus and timing of ovulation in pigs. J. Reprod. Fertil., Vol: 52 (Suppl.)

Soede, et al. 2011: Reproductive cycles in pigs. Anim Reprod Sci, Vol: 124
Soloff, et al. 1974: Characterization of a proposed oxytocin receptor in the uterus of the rat and sow. J Biol Chem, Vol: 249
Spencer 1996: tau-Interferon: pregnancy recognition signal in ruminants. Proc Soc Exp Biol Med, Vol: 213
Spencer 2004: Progesterone and placental hormone actions on the uterus: insights from domestic animals. Biology of reproduction, Vol: 71
Spencer, et al. 1995a: Temporal and spatial alterations in uterine estrogen receptor and progesterone receptor gene expression during the estrous cycle and early pregnancy in the ewe. Biol Reprod, Vol: 53
Spencer, et al. 1996: Ovine interferon tau suppresses transcription of the estrogen receptor and oxytocin receptor genes in the ovine endometrium. Endocrinology, Vol: 137
Spencer, et al. 2002: Biology of progesterone action during pregnancy recognition and maintenance of pregnancy. Front Biosci, Vol: 7
Spencer, et al. 1995b: Ovine interferon-tau regulates expression of endometrial receptors for estrogen and oxytocin but not progesterone. Biol Reprod, Vol: 53
Starbuck 1998: Endometrial oxytocin receptor and uterine prostaglandin secretion in mares during the oestrous cycle and early pregnancy. J Reprod Fertil, Vol: 113
Steinbach, et al. 1970: Cyclical Phenomena in the Female Genital Tract of Swine—Histological Observations. Journal of Animal Science, Vol: 30
Stout 2001: Role of prostaglandins in intrauterine migration of the equine conceptus. Reproduction, Vol: 121
Stroband, et al. 1986: The ultrastructure of the uterine epithelium of the pig during the estrous cycle and early pregnancy. Cell Tissue Res, Vol: 246
Suire 2001: Uterocalin, a lipocalin provisioning the preattachment equine conceptus: fatty acid and retinol binding properties, and structural characterization. Biochem J, Vol: 356
Szostek, et al. 2014: Interleukins affect equine endometrial cell function: modulatory action of ovarian steroids. Mediators Inflamm, Vol: 2014
Tabibzadeh 1995: Site and menstrual cycle-dependent expression of proteins of the tumour necrosis factor (TNF) receptor family, and BCL-2 oncoprotein and phase-specific production of TNF alpha in human endometrium. Hum Reprod. , Vol: 10(2)
Tanaka, et al. 1998: Enhancement of apoptotic susceptibility by interleukin-1 beta in human endometrial epithelial cells. Gynecol Endocrinol, Vol: 12(5)
Tatsumi, et al. 1999: Expression of calcium binding protein D-9k messenger RNA in the mouse uterine endometrium during implantation. Mol Hum Reprod, Vol: 5
Taylor, et al. 1997: A conserved Hox axis in the mouse and human female reproductive system: late establishment and persistent adult expression of the Hoxa cluster genes. Biol Reprod, Vol: 57
Tibbetts, et al. 1999: Progesterone via its receptor antagonizes the pro-inflammatory activity of estrogen in the mouse uterus. Biol Reprod, Vol: 60
Tibbetts, et al. 1998: Mutual and intercompartmental regulation of estrogen receptor and progesterone receptor expression in the mouse uterus. Biol Reprod, Vol: 59
Tomanelli, et al. 1991: Soluble oestrogen and progesterone receptors in the endometrium of the mare. J Reprod Fertil Suppl, Vol: 44
Tortonese, et al. 2001: The equine hypophysis: a gland for all seasons. Reprod Fertil Dev, Vol: 13
Troedsson 1999: Uterine clearance and resistance to persistent endometritis in the mare. Theriogenology, Vol: 52
Troedsson 2001: Interaction between equine semen and the endometrium: the inflammatory response to semen. Anim Reprod Sci, Vol: 68

Tsai, et al. 1994: Molecular mechanisms of action of steroid/thyroid receptor superfamily members. Annu Rev Biochem, Vol: 63
Tsai, et al. 2002: Fibroblast growth factor-9 is an endometrial stromal growth factor. Endocrinology, Vol: 143
Tschugguel, et al. 1999: Elevation of inducible nitric oxide synthase activity in human endometrium during menstruation. Biol Reprod. , Vol: 60(2)
Tuckey, et al. 2002: Transfer of cholesterol between phospholipid vesicles mediated by the steroidogenic acute regulatory protein (StAR). J Biol Chem, Vol: 277
Tunon 1995: Ultrastructure of the secretory endometrium during oestrus in young maiden and foaled mares. Equine Vet J, Vol: 27
Turnbull 1971: Myometrial contractility in pregnancy and its regulation. Proc R Soc Med, Vol: 64
Tusher 2001: Significance analysis of microarrays applied to the ionizing radiation response. Proc Natl Acad Sci U S A, Vol: 98
Ulbrich, et al. 2012: Transcriptational profiling to address molecular determinants of endometrial receptivity-Lessons from studies in livestock species. Methods, Vol:
Ulbrich, et al. 2011: Bovine endometrial metallopeptidases MMP14 and MMP2 and the metallopeptidase inhibitor TIMP2 participate in maternal preparation of pregnancy. Mol Cell Endocrinol, Vol: 332
Ulbrich, et al. 2004: Hyaluronan in the bovine oviduct--modulation of synthases and receptors during the estrous cycle. Mol Cell Endocrinol, Vol: 214
Virolainen, et al. 2005. : Plasma progesterone concentration depends on sampling site in pigs. . Anim. Reprod., Vol: 86
Vogel, et al. 1973: Der Formenzyklus der Uterindriisen der Stute im Vergleich zu dem anderer Säugetiere und des Menschen. Anatomia, Histologia, Embryologia, Vol: 2
Waclawik 2011: Novel insights into the mechanisms of pregnancy establishment: regulation of prostaglandin synthesis and signaling in the pig. Reproduction, Vol: 142
Waclawik, et al. 2010: Oxytocin and tumor necrosis factor alpha stimulate expression of prostaglandin E2 synthase and secretion of prostaglandin E2 by luminal epithelial cells of the porcine endometrium during early pregnancy. Reproduction, Vol: 140
Waclawik, et al. 2006: Molecular cloning and spatiotemporal expression of prostaglandin F synthase and microsomal prostaglandin E synthase-1 in porcine endometrium. Endocrinology, Vol: 147
Walter, et al. 2005: Matrix metalloproteinase 2 (MMP-2) and tissue transglutaminase (TG 2) are expressed in periglandular fibrosis in horse mares with endometrosis. Histol Histopathol, Vol: 20
Warembourg, et al. 1987: Analysis and in situ detection of cholecalcin messenger RNA (9000 Mr CaBP) in the uterus of the pregnant rat. Cell Tissue Res, Vol: 247
Wasowska, et al. 2001: Apoptotic cell death in the porcine endometrium during the oestrous cycle. Acta Vet Hung, Vol: 49
Watanabe 2002: Prostaglandin F synthase. Prostaglandins & Other Lipid Mediators, Vol: 68–69
Wathes, et al. 1993: Localization of oestradiol, progesterone and oxytocin receptors in the uterus during the oestrous cycle and early pregnancy of the ewe. J Endocrinol, Vol: 138
Watson 1992: Progesterone and estrogen receptor distribution in the endometrium of the mare. Theriogenology, Vol: 38
Watson, et al. 1996: Regulation of epidermal growth factor receptor synthesis by ovarian steroids in human endometrial cells in culture. J Reprod Fertil, Vol: 107
Watson, et al. 1987a: Cellular and humoral defence mechanisms in mares susceptible and resistant to persistent endometritis. Vet Immunol Immunopathol, Vol: 16

Watson, et al. 1987b: Influence of arachidonic acid metabolites in vitro and in uterine washings on migration of equine neutrophils under agarose. Res Vet Sci, Vol: 43
Webb, et al. 1992: The limits of the cellular capacity to mediate an estrogen response. Mol Endocrinol, Vol: 6
Weber 1980: Renal prostaglandins, kidney function and essential hypertension. Contrib Nephrol, Vol: 23
White, et al. 2005: Steroid regulation of cell specific secreted phosphoprotein 1 (osteopontin) expression in the pregnant porcine uterus. Biol Reprod, Vol: 73
Whiteaker, et al. 1994: Detection of functional oxytocin receptors on endometrium of pigs. Biol Reprod, Vol: 51
Woessner 1996: Regulation of matrilysin in the rat uterus. Biochem Cell Biol, Vol: 74
Wollenhaupt, et al. 2005: Regulation of endometrial fibroblast growth factor 7 (FGF-7) and its receptor FGFR2IIIb in gilts after sex steroid replacements, and during the estrous cycle and early gestation. J Reprod Dev, Vol: 51
Wollenhaupt, et al. 2004: Expression of epidermal growth factor receptor (EGF-R), vascular endothelial growth factor receptor (VEGF-R) and fibroblast growth factor receptor (FGF-R) systems in porcine oviduct and endometrium during the time of implantation. J.Reprod.Dev., Vol: 50
Woody, et al. 1967: Effect of exogenous progesterone on estrous cycle length. J Anim Sci, Vol: 26
Xiao, et al. 1998: Differential effects of oestradiol and progesterone on proliferation and morphology of cultured bovine uterine epithelial and stromal cells. Journal of Reproduction and Fertility, Vol: 112
Xiong, et al. 1998: Production of vascular endothelial growth factor by murine macrophages: regulation by hypoxia, lactate, and the inducible nitric oxide synthase pathway. Am J Pathol, Vol: 153
Yamada, et al. 2002: The dynamic expression of extracellular matrix in the bovine endometrium at implantation. J.Vet.Med.Sci., Vol: 64
Yang, et al. 2011: Coexpression and estrogen-mediated regulation of TRPV6 and PMCA1 in the human endometrium during the menstrual cycle. Mol Reprod Dev, Vol: 78
Yip, et al. 2013: Changes in mouse uterine transcriptome in estrus and proestrus. Biol Reprod, Vol: 89
Yoo, et al. 2006: Osteopontin regulates renal apoptosis and interstitial fibrosis in neonatal chronic unilateral ureteral obstruction. Kidney Int, Vol: 70
Youngs 2001: Factors influencing the success of embryo transfer in the pig. Theriogenology, Vol: 56
Zhang, et al. 2006: Importance of uterine cell death, renewal, and their hormonal regulation in hamsters that show progesterone-dependent implantation. Endocrinology, Vol: 147
Zhang, et al. 2012: Evaluating a set of reference genes for expression normalization in multiple tissues and skeletal muscle at different development stages in pigs using quantitative real-time polymerase chain reaction. DNA Cell Biol, Vol: 31
Zhang, et al. 2002: Direct interaction of the Kruppel-like family (KLF) member, BTEB1, and PR mediates progesterone-responsive gene expression in endometrial epithelial cells. Endocrinology, Vol: 143
Zheng, et al. 2005: Angiotensin II regulation of ovine fetoplacental artery endothelial functions: interactions with nitric oxide. J Physiol, Vol: 565
Zhou, et al. 2000: Testosterone inhibits estrogen-induced mammary epithelial proliferation and suppresses estrogen receptor expression. The FASEB Journal, Vol: 14

VIII. SUPPLEMENTAL MATERIAL

Target accession number[1]	Hsa Entrez Gene ID[2]	Hsa Gene symbol[3]	Hsa Gene description[4]	D0	D3	D8	D12	D16	q.value[5]	SOTA cluster[6]
DN511209; ENSECAT00000002458	59272	*ACE2*	angiotensin I converting enzyme (peptidyl-dipeptidase A) 2	1.15	-0.23	-0.62	-0.58	0.28	0.0004	1
ENSECAT00000011365	9068	*ANGPTL1*	angiopoietin-like 1	0.88	-0.21	-0.30	-0.32	-0.05	0.0088	1
XM_001501670	23452	*ANGPTL2*	angiopoietin-like 2	0.76	-0.26	-0.42	-0.40	0.31	0.0002	1
CX601805; ENSECAT00000020044	51129	*ANGPTL4*	angiopoietin-like 4	1.58	-0.35	-1.26	0.12	-0.10	0.0003	1
ENSECAT00000026830	6359	*CCL15*	chemokine (C-C motif) ligand 15	0.97	-0.70	-0.24	-0.42	0.39	0.0006	1
AY246812	414062	*CCL3L3*	chemokine (C-C motif) ligand 3-like 3	1.18	-0.65	0.02	-0.23	-0.33	0.0013	1
ENSECAT00000003108	10803	*CCR9*	chemokine (C-C motif) receptor 9	0.84	-0.45	-0.52	0.09	0.03	0.0067	1
CX595027;CX602717; CX604282; ENSECAT00000010157	7373	*COL14A1*	collagen, type XIV, alpha 1	1.29	-0.56	-0.55	-0.85	0.66	0.0007	1
ENSECAT00000020087; ENSECAT00000020883	1277	*COL1A1*	collagen, type I, alpha 1	1.13	-0.31	0.12	-1.21	0.27	0.0001	1
ENSECAT00000026976; ENSECAT00000026981	1278	*COL1A2*	collagen, type I, alpha 2	1.10	-0.48	0.17	-0.98	0.19	0.0002	1
ENSECAT00000010653	81578	*COL21A1*	collagen, type XXI, alpha 1	2.10	-0.34	-0.86	-1.23	0.33	0.0000	1
ENSECAT00000018719	84570	*COL25A1*	collagen, type XXV, alpha 1	0.73	-0.13	-0.33	-0.42	0.15	0.0053	1
CX595082	1280	*COL2A1*	collagen, type II, alpha 1	0.57	0.15	-0.26	-0.17	-0.29	0.0090	1
ENSECAT00000026766; ENSECAT00000026771	1281	*COL3A1*	collagen, type III, alpha 1	1.03	-0.29	0.26	-1.26	0.26	0.0001	1
ENSECAT00000022446	1282	*COL4A1*	collagen, type IV, alpha 1	0.51	-0.43	-0.15	-0.44	0.50	0.0007	1
ENSECAT00000007919	1285	*COL4A3*	collagen, type IV, alpha 3 (Goodpasture antigen)	0.39	-0.70	0.35	-0.43	0.40	0.0071	1
ENSECAT00000000945	1287	*COL4A5*	collagen, type IV, alpha 5	0.97	-0.10	-0.32	-0.56	0.01	0.0001	1
ENSECAT00000023228	1288	*COL4A6*	collagen, type IV, alpha 6	0.82	-0.17	-0.15	-0.32	-0.18	0.0024	1
CX602562; ENSECAT00000013712	1289	*COL5A1*	collagen, type V, alpha 1	0.77	-0.38	0.03	-0.62	0.21	0.0018	1
ENSECAT00000011989	1290	*COL5A2*	collagen, type V, alpha 2	0.42	-0.32	0.24	-0.47	0.14	0.0057	1
CX603428	1291	*COL6A1*	collagen, type VI, alpha 1	0.89	-0.01	-0.27	-0.47	-0.15	0.0003	1
CX605460	1292	*COL6A2*	collagen, type VI, alpha 2	0.81	0.14	-0.42	-0.25	-0.28	0.0016	1
ENSECAT00000022862	1293	*COL6A3*	collagen, type VI, alpha 3	1.06	0.18	-0.71	-0.82	0.30	0.0002	1
ENSECAT00000012001	646300	*COL6A4P2*	collagen, type VI, alpha 4 pseudogene 2	1.37	-0.17	-0.65	-0.40	-0.16	0.0001	1

ENSECAT00000013001	1294	*COL7A1*	collagen, type VII, alpha 1	0.82	-0.13	-0.39	-0.24	-0.06	0.0023	1
CX594651; ENSECAT00000025116	1299	*COL9A3*	collagen, type IX, alpha 3	0.96	-0.25	0.20	-0.58	-0.33	0.0008	1
ENSECAT00000012809	2919	*CXCL1*	chemokine (C-X-C motif) ligand 1 (melanoma growth stimulating activity, alpha)	1.87	-0.15	-1.30	-1.47	1.05	0.0001	1
NM_001081886	6374	*CXCL5*	chemokine (C-X-C motif) ligand 5	1.98	-0.70	-1.20	-1.27	1.19	0.0000	1
BI961602	6372	*CXCL6*	chemokine (C-X-C motif) ligand 6 (granulocyte chemotactic protein 2)	2.84	-0.61	-1.88	-2.33	1.99	0.0000	1
EU438776	4283	*CXCL9*	chemokine (C-X-C motif) ligand 9	0.93	-0.31	-0.05	-0.40	-0.17	0.0038	1
XM_001490737	3577	*CXCR1*	chemokine (C-X-C motif) receptor 1	1.17	-1.24	-0.11	0.26	-0.07	0.0098	1
ENSECAT00000003720	7852	*CXCR4*	chemokine (C-X-C motif) receptor 4	2.48	-0.94	-1.47	-0.37	0.30	0.0000	1
ENSECAT00000012106	1906	*EDN1*	endothelin 1	0.64	-0.25	-0.23	-0.42	0.26	0.0042	1
NM_001081823	1907	*EDN2*	endothelin 2	0.99	-0.31	-1.00	0.05	0.27	0.0019	1
ENSECAT00000020976	1909	*EDNRA*	endothelin receptor type A	0.63	-0.06	-0.58	-0.31	0.31	0.0011	1
ENSECAT00000012792	146433	*IL34*	interleukin 34	0.49	0.06	-0.51	-0.02	-0.02	0.0054	1
BI961791; NM_001083951	3576	*IL8*	interleukin 8	0.89	-0.22	-0.60	-1.07	1.00	0.0019	1
ENSECAT00000004954	79148	*MMP28*	matrix metallopeptidase 28	0.40	-0.14	-0.31	0.24	-0.19	0.0075	1
NM_001082495	4314	*MMP3*	matrix metallopeptidase 3 (stromelysin 1,	2.24	-0.73	-1.22	-1.29	1.01	0.0000	1
NM_001111302	4318	*MMP9*	matrix metallopeptidase 9 (gelatinase B, 92kDa gelatinase, 92kDa type IV collagenase)	1.38	0.11	-0.97	-0.36	-0.17	0.0004	1
ENSECAT00000024697	4856	*NOV*	nephroblastoma overexpressed gene	0.76	0.09	-0.78	-0.18	0.11	0.0007	1
AF076673	5020	*OXT*	oxytocin, prepropeptide	0.47	-0.15	0.21	0.11	-0.64	0.0089	1
ENSECAT00000014888	5733	*PTGER3*	prostaglandin E receptor 3 (subtype EP3)	0.98	-0.27	-1.12	-0.22	0.63	0.0002	1
ENSECAT00000015356	5265	*SERPINA1*	serpin peptidase inhibitor, clade A (alpha-1 antiproteinase, antitrypsin), member 1	1.57	-0.13	-1.73	-1.77	2.06	0.0001	1
NM_001114533	5265	*SERPINA1*	serpin peptidase inhibitor, clade A (alpha-1 antiproteinase, antitrypsin), member 1	1.69	-0.07	-1.96	-1.88	2.21	0.0001	1
ENSECAT00000026755	5104	*SERPINA5*	serpin peptidase inhibitor, clade A (alpha-1 antiproteinase, antitrypsin), member 5	0.48	0.17	-0.43	-0.34	0.12	0.0062	1
DN510302	6678	*SPARC*	secreted protein, acidic, cysteine-rich (osteonectin)	0.77	-0.42	-0.17	-0.48	0.29	0.0001	1
ENSECAT00000019034	3371	*TNC*	tenascin C	1.61	-0.35	-1.47	-1.48	1.69	0.0000	1
NM_001081772	2099	*ESR1*	estrogen receptor 1	0.18	0.69	-0.22	-0.93	0.28	0.0054	2
ENSECAT00000019888	2254	*FGF9*	fibroblast growth factor 9 (glia-activating factor)	0.83	0.36	-0.30	-1.06	0.17	0.0008	2
AF053141; ENSECAT00000012266	5241	*PGR*	progesterone receptor	0.62	0.39	-0.04	-0.74	-0.24	0.0043	2

ENSECAT00000027031	1019	*CDK4*	cyclin-dependent kinase 4	-0.10	0.69	0.03	-0.38	-0.23	0.0061	3
ENSECAT00000001020	2852	*GPER*	G protein-coupled estrogen receptor 1	0.07	0.73	-0.30	-0.63	0.13	0.0020	3
NM_001081806	5737	*PTGFR*	prostaglandin F receptor (FP)	-0.03	0.70	0.39	-0.20	-0.85	0.0007	4
ENSECAT00000016007	33	*ACADL*	acyl-CoA dehydrogenase, long chain	-0.68	-0.04	0.91	0.02	-0.22	0.0010	5
ENSECAT00000009814	51094	*ADIPOR1*	adiponectin receptor 1	-0.84	0.14	0.37	0.47	-0.13	0.0002	5
ENSECAT00000016893	79602	*ADIPOR2*	adiponectin receptor 2	-1.00	0.05	0.88	0.76	-0.69	0.0001	5
ENSECAT00000015567	60481	*ELOVL5*	ELOVL fatty acid elongase 5	-0.78	0.09	0.61	0.39	-0.31	0.0015	5
ENSECAT00000016651	2101	*ESRRA*	estrogen-related receptor alpha	-0.48	-0.17	0.56	-0.13	0.22	0.0055	5
DN509190; ENSECAT00000009911	10857	*PGRMC1*	progesterone receptor membrane component 1	-0.63	0.16	0.82	0.05	-0.41	0.0003	5
ENSECAT00000020544	10449	*ACAA2*	acetyl-CoA acyltransferase 2	-0.37	-0.28	0.18	0.49	-0.02	0.0018	6
ENSECAT00000018172	32	*ACACB*	acetyl-CoA carboxylase beta	-0.62	-0.28	0.76	0.11	0.03	0.0090	6
ENSECAT00000000590	10455	*ECI2*	enoyl-CoA delta isomerase 2	-0.92	-0.34	1.21	0.63	-0.56	0.0000	6
DN511229	3032	*HADHB*	hydroxyacyl-CoA dehydrogenase/3-ketoacyl-CoA thiolase/enoyl-CoA hydratase (trifunctional protein), beta subunit	-0.11	-0.25	0.54	0.13	-0.31	0.0029	6
NM_001082509	*100034213	**P19*	*P19 lipocalin	-2.54	-0.61	1.61	1.34	0.20	0.0000	6
NM_001081908	1645	*AKR1C1*	aldo-keto reductase family 1, member C1 (dihydrodiol dehydrogenase 1; 20-alpha (3-alpha)-hydroxysteroid dehydrogenase)	-0.56	-0.47	-0.65	1.46	0.22	0.0014	7
ENSECAT00000018317	6696	*SPP1*	secreted phosphoprotein 1	-1.46	-2.02	1.18	1.62	0.68	0.0000	7
ENSECAT00000017044	285	*ANGPT2*	angiopoietin 2	0.15	-0.04	-0.60	0.13	0.36	0.0075	8
ENSECAT00000019790	306	*ANXA3*	annexin A3	0.17	0.10	-0.77	-0.38	0.88	0.0010	8
ENSECAT00000023112	715	*C1R*	complement component 1, r subcomponent	0.05	-0.52	-0.38	0.32	0.53	0.0052	8
ENSECAT00000007684; ENSECAT00000008036	718	*C3*	complement component 3	1.01	-0.46	-1.46	-0.05	0.95	0.0015	8
ENSECAT00000014288	722	*C4BPA*	complement component 4 binding protein, alpha	-0.48	-1.26	-0.68	-0.09	2.51	0.0001	8
ENSECAT00000023700	722	*C4BPA*	complement component 4 binding protein, alpha	-0.11	-0.78	-0.26	-0.12	1.28	0.0005	8
XM_001492512	725	*C4BPB*	complement component 4 binding protein, beta	-0.36	-1.24	-0.15	-0.21	1.95	0.0004	8
ENSECAT00000013161	730	*C7*	complement component 7	-0.18	-0.73	-0.63	0.11	1.42	0.0003	8
ENSECAT00000025665	6357	*CCL13*	chemokine (C-C motif) ligand 13	0.24	-0.69	-0.38	0.74	0.09	0.0053	8
NM_001081931	6347	*CCL2*	chemokine (C-C motif) ligand 2	0.02	-0.59	-0.24	-0.50	1.31	0.0005	8
ENSECAT00000014867	6366	*CCL21*	chemokine (C-C motif) ligand 21	0.56	-0.53	-0.29	-0.29	0.54	0.0050	8
NM_001081863	6352	*CCL5*	chemokine (C-C motif) ligand 5	0.31	-0.17	-0.64	0.28	0.21	0.0029	8
NM_001081864	6355	*CCL8*	chemokine (C-C motif) ligand 8	-0.06	-0.28	-0.56	0.23	0.66	0.0070	8

ENSECAT00000027086	1303	*COL12A1*	collagen, type XII, alpha 1	0.27	-1.09	-0.23	0.09	0.95	0.0001	8
ENSECAT00000019794	1305	*COL13A1*	collagen, type XIII, alpha 1	0.10	-0.09	-0.48	-0.27	0.74	0.0075	8
ENSECAT00000008760	1308	*COL17A1*	collagen, type XVII, alpha 1	0.54	-0.91	-0.61	0.74	0.25	0.0020	8
ENSECAT00000020647	1295	*COL8A1*	collagen, type VIII, alpha 1	0.56	-0.94	-0.91	-0.33	1.62	0.0000	8
ENSECAT00000019475	58191	*CXCL16*	chemokine (C-X-C motif) ligand 16	0.48	-0.06	-0.87	-0.35	0.80	0.0004	8
ENSECAT00000000643	284340	*CXCL17*	chemokine (C-X-C motif) ligand 17	0.03	-0.48	-0.81	-0.03	1.29	0.0004	8
CX605159	57007	*CXCR7*	chemokine (C-X-C motif) receptor 7	0.30	-0.53	-0.59	0.27	0.56	0.0015	8
ENSECAT00000018689	641700	*ECSCR*	endothelial cell-specific chemotaxis regulator	0.12	-0.26	-0.59	0.23	0.49	0.0014	8
XM_001489561	2104	*ESRRG*	estrogen-related receptor gamma	0.70	-0.73	-0.58	0.15	0.45	0.0010	8
ENSECAT00000015464	2247	*FGF2*	fibroblast growth factor 2 (basic)	0.68	-1.04	-0.38	-0.14	0.89	0.0005	8
ENSECAT00000015025	3600	*IL15*	interleukin 15	0.52	-0.96	-0.52	0.28	0.68	0.0001	8
NM_001081794	3554	*IL1R1*	interleukin 1 receptor, type I	0.16	-0.54	-0.38	-0.05	0.81	0.0062	8
XM_001499705	9235	*IL32*	interleukin 32	0.50	-0.49	-0.45	-0.18	0.61	0.0011	8
AY246709	3791	*KDR*	kinase insert domain receptor (a type III receptor tyrosine kinase)	-0.16	-0.07	-0.45	0.05	0.63	0.0073	8
NM_001081843	5321	*PLA2G4A*	phospholipase A2, group IVA (cytosolic, calcium-dependent)	0.70	0.21	-1.35	-0.78	1.22	0.0000	8
ENSECAT00000011519	5734	*PTGER4*	prostaglandin E receptor 4 (subtype EP4)	0.39	-0.54	-0.59	0.07	0.67	0.0003	8
NM_001081775	5743	*PTGS2*	prostaglandin-endoperoxide synthase 2 (prostaglandin G/H synthase and cyclooxygenase)	-0.15	-0.74	-0.57	0.26	1.19	0.0073	8
ENSECAT00000011379	710	*SERPING1*	serpin peptidase inhibitor, clade G (C1 inhibitor), member 1	0.24	-0.46	-0.82	0.39	0.65	0.0002	8
ENSECAT00000010346	5274	*SERPINI1*	serpin peptidase inhibitor, clade I (neuroserpin), member 1	0.68	-0.29	-1.44	-0.40	1.45	0.0000	8
DN507993	6578	*SLCO2A1*	solute carrier organic anion transporter family, member 2A1	0.16	-0.44	-0.40	-0.16	0.84	0.0010	8
ENSECAT00000018137	7010	*TEK*	TEK tyrosine kinase, endothelial	-0.05	0.01	-0.58	0.14	0.48	0.0055	8

Table VIII-I: List of differentially expreseed genes in equine endmetrium (only genes that are mentioned in this study are shown).[1] Target Accession number supplied by databases [2] Gene Identifier supplied by NCBI ,[3] Official Gene Symbol, [4] Gene descrition supplied by databases), analyzed days during the cycle, [5]q-value achieved from microarray analysis and [6]SOTA clustering number.* no official human orthologous gene (*Eca* Entrez gene ID, *Eca* Gene symbol and *Eca* gene description are shown).

Day in cycle	Date	Animal-ID	CL (shape and number) left	CL (shape and number) right	Time left	Time right	additional comments
Day 0	08.05.2007	D0S19	8 larger follicles	5	7:27-7:35	7:39-7:45	oedematized mucosa, no liquid right side
		D0S20	5 smaller follicles	10	7:48-7:53	7:57-8:02	1 Ovulation right side
		D0S21	6	4	8:04-8:10	8:16-8:22	oedematized mucosa,
		D0S22	11 relatively large	6	8:28-8:33	8:38-8:44	oedematized mucosa
		D0S23	11 relatively large	14	8:49-8:54	8:59-9:04	oedematized mucosa,
		D0S24	5	2 large, many smaller	9:08-9:14	9:18-9:23	oedematized m
Day 3	10.04.2007	D3S07	7	4	7:30-7:48	7:40-7:50	Very, very small
		D3S08	8	5	7:58-8:08	8:10-8:18	Very, very small
		D3S09	11 very bloody	4	8:22-8:34	8:37-8:41	Very, very small, endometrium extremely blooded
		D3S10	8	7	8:45-8:51	8:57-9:03	Very, very small, endometrium extremely blooded
		D3S11	11	10	9:14-9:20	9:29-9:34	Very, very small
		D3S12	3	7	9:38-9:43	9:52-9:56	Very, very small
Day 6	01.05.2007	D6S13	5	7 very small (1 extreme large Follicle)	7:23-7:31	7:36 -7:41	very small uterus, extremely blooded, not sure if day 0
		D6S14	5	6	7:50-7:57	8:04-8:10	very small uterus, extremely blooded, not sure if day 0
		D6S15	4	7	8:15-8:22	8:24-8:30	uterus extremely good blooded
		D6S16	6	9	8:35-8:43	8:46-8:51	-
		D6S17	6	5	8:57-9:02;	9:06-9:12	Ok
		D6S18	5	6	9:14-9:19	9:24-9:30	Ok
Day 12	03.04.2007	D12S1	21	23	7:42-7:45	7:50-8:00	Ok
		D12S2	9	11	8:12-8:15	8:25-8:30	Ok
		D12S3	13	6	8:40-8:43	8:50-8:56	Ok
		D12S4	5(0.5cm)	-	9:05-9:07	9:15-9:23	100 small follicles (1mm) 5 large Follicles left side (2cm), many follicles right
		D12S5	9 (1 extreme large Follicle)	ca. 100 small follicles (2-3mm)	9:32-9:35;	9:45-9:48	Endometrium extremely blooded
		D12S6	Data missing	Data missing	9:56-10:02	10:05-10:12	OK

Day 18	03.07.2007	D18S25	3 large, many smaller	10, many smaller	7:28-7:32	7:42-7:44	liquid pink, oedematized mucosa
		D18S26	8 C.L.(little bit larger)	7	7:58-8:02	8:12-8:15	liquid pink, oedematized mucosa
		D18S27	9 large	_	8:27- 8:29	8:288:41	liquid pink, oedematized mucosa
		D18S28	22	_	8:53-8:50	9:01-9:04	liquid pink, oedematized mucosa
		D18S30	5	7	9:35-9:38	9:42-9:45	liquid pink, oedematized mucosa

Table VIII-II: Sample collection protocol for porcine endometrium tissue samples. Three samples (front, middle and back) of each unterine horn (left and right) were collected from six sows (S07-S30) on five times during the cycle (D0, D3, D6, D12, D18). Protocol shows CL (shape and number) in left and right ovaries, the time (beginning and end) of sample collection and includes all comments (sample condition and collection procedure). S-Saw, D-days, CL-corpus luteum.

Target accession number[1]	**Hsa Entrez Gene ID[2]**	**Hsa Gene symbol[3]**	**Hsa Gene description[4]**	**D0**	**D3**	**D6**	**D12**	**D18**	**q.value[5]**	**SOTA-Cluster[6]**
NM_214181	330	*BIRC3*	baculoviral IAP repeat containing 3	0.72	0.02	-0.38	-0.48	0.12	0.0007	1
NM_001161640	843	*CASP10*	caspase 10,apoptosis-related cysteine peptidase	1.02	0.12	-0.58	-0.28	-0.28	0.0000	1
TC467326	843	*CASP10*	caspase 10, apoptosis-related cysteine peptidase	1.08	0.38	-0.82	-0.42	-0.22	0.0000	1
NM_001001621	1230	*CCR1*	chemokine (C-C motif) receptor 1	1.58	-0.22	-0.67	-0.52	-0.17	0.0000	1
NM_001001618	1234	*CCR5*	chemokine (C-C motif) receptor 5	0.92	0.02	-0.28	-0.98	0.32	0.0001	1
ENSSSCT00000004952	1303	*COL12A1*	collagen,type XII,alpha 1	2.22	-0.28	-0.98	-1.88	0.92	0.0000	1
ENSSSCT00000004955	1303	*COL12A1*	collagen, type XII, alpha 1	2.08	-1.12	-0.92	-0.82	0.78	0.0000	1
XM_001927036	1303	*COL12A1*	collagen,type XII,alpha 1	2.00	-0.15	-1.05	-1.20	0.40	0.0000	1
XM_001929444	1308	*COL17A1*	collagen,type XVII,alpha 1	2.88	-0.22	-3.42	-0.12	0.88	0.0000	1
ENSSSCT00000019137	1277	*COL1A1*	collagen,type I,alpha 1	1.13	-0.42	-0.42	-0.02	-0.27	0.0000	1
ENSSSCT00000019139	1277	*COL1A1*	uncharacterized LOC100738213	1.30	-0.80	-0.40	-0.40	0.30	0.0000	1
ENSSSCT00000016699	1278	*COL1A2*	collagen,type I,alpha 2	1.40	-0.70	-0.50	-0.40	0.20	0.0000	1
CK450104	85301	*COL27A1*	collagen,type XXVII,alpha 1	1.60	-0.10	-0.30	-0.80	-0.40	0.0000	1
EW423756	85301	*COL27A1*	collagen alpha-1(XXVII) chain-like;collagen, type XXVII, alpha 1	1.54	-0.16	-0.66	0.34	-1.06	0.0006	1
TC407931	1281	*COL3A1*	collagen, type III, alpha 1	1.08	-1.02	-0.12	-0.22	0.28	0.0000	1
CK453450	1282	*COL4A1*	collagen alpha-1(IV) chain-like	0.98	-0.72	-0.12	-0.82	0.68	0.0006	1
XM_001925656	1282	*COL4A1*	collagen alpha-1(IV) chain-like	0.96	-0.58	-0.60	-0.28	0.48	0.0001	1
NM_001014971	1289	*COL5A1*	collagen,type V,alpha 1	1.43	-0.54	-0.54	-0.21	-0.14	0.0000	1
NM_001009580	6387	*CXCL12*	chemokine (C-X-C motif) ligand 12	0.94	-0.26	-0.66	-0.06	0.04	0.0008	1

ENSSSCT00000003385	284340	*CXCL17*	chemokine (C-X-C motif) ligand 17	3.98	0.58	-2.22	-2.62	0.28	0.0000	1
NM_001001861	2920	*CXCL2*	chemokine (C-X-C motif) ligand 2	2.42	-0.08	-1.98	0.27	-0.63	0.0001	1
NM_213876	6372	*CXCL6*	alveolar macrophage-derived chemotactic factor-II	5.24	-0.46	-1.56	-1.86	-1.36	0.0000	1
TC444818	6372	*CXCL6*	alveolar macrophage-derived chemotactic factor-II	3.94	-0.56	-1.06	-1.26	-1.06	0.0000	1
NM_214017	2028	*ENPEP*	glutamyl aminopeptidase (aminopeptidase A)	1.58	-1.32	0.68	-1.12	0.18	0.0001	1
NM_214220	2099	*ESR1*	estrogen receptor 1	0.94	0.27	-0.56	-0.26	-0.39	0.0000	1
CO987406	2099	*ESR1*	estrogen receptor 1	0.98	0.18	-0.82	0.18	-0.52	0.0005	1
TC497409	2099	*ESR1*	estrogen receptor 1	1.04	0.14	-0.66	-0.36	-0.16	0.0000	1
NM_214041	3586	*IL10*	interleukin 10	0.78	-0.12	-0.62	-0.52	0.48	0.0000	1
NM_214390	3600	*IL15*	interleukin 15	1.76	-0.34	-0.59	-0.69	-0.14	0.0000	1
AK233260	3600	*IL15*	interleukin 15	2.48	-0.72	-0.62	-1.62	0.48	0.0000	1
NM_213997	3606	*IL18*	interleukin 18 (interferon-gamma-inducing factor)	0.85	-0.05	-0.65	-0.40	0.25	0.0001	1
NM_214055	3553	*IL1B*	interleukin 1,beta	1.44	0.44	-1.46	-0.46	0.04	0.0002	1
TC465413	3566	*IL4R*	interleukin 4 receptor	0.40	0.10	-0.70	-0.30	0.50	0.0001	1
NM_001083932	3685	*ITGAV*	integrin,alpha V (vitronectin receptor,alpha polypeptide,antigen CD51)	0.66	-0.54	-0.04	-0.44	0.36	0.0006	1
CK453646	4012	*LNPEP*	leucyl/cystinyl aminopeptidase	0.62	-0.38	-0.48	-0.38	0.62	0.0002	1
NM_001099938	4321	*MMP12*	matrix metallopeptidase 12 (macrophage elastase)	3.56	-0.74	-0.84	-1.04	-0.94	0.0000	1
NM_214239	4323	*MMP14*	matrix metallopeptidase 14 (membrane-inserted)	1.10	-0.30	-0.60	-0.30	0.10	0.0000	1
NM_214192	4313	*MMP2*	matrix metallopeptidase 2 (gelatinase A,72kDa gelatinase,72kDa type IV collagenase)	0.64	-0.51	-0.41	0.09	0.19	0.0001	1
TC454140	4313	*MMP2*	matrix metallopeptidase 2 (gelatinase A; 72kDa gelatinase; 72kDa type IV collagenase)	0.74	-0.56	-0.46	0.04	0.24	0.0000	1
TC438862	8829	*NRP1*	neuropilin 1	0.82	-0.58	-0.28	-0.88	0.92	0.0002	1
NM_214023	6696	*SPP1*	secreted phosphoprotein 1	3.56	-1.99	-1.07	-0.32	-0.19	0.0000	1
TC512863	6696	*SPP1*	secreted phosphoprotein 1	1.62	-0.98	-0.48	-0.78	0.62	0.0001	1
BI338261	6696	*SPP1*	secreted phosphoprotein 1	2.86	-1.14	-1.44	-0.04	-0.24	0.0000	1
BF441912	7064	*THOP1*	thimet oligopeptidase 1	0.20	0.30	0.40	-0.90	0.00	0.0008	1
DV229960	7124	*TNF*	tumor necrosis factor	1.12	-0.18	-0.38	-0.48	-0.08	0.0000	1
NM_001024696	8743	*TNFSF10*	tumor necrosis factor (ligand) superfamily,member 10	1.51	-0.79	-0.64	-0.49	0.41	0.0000	1
TC445342	8743	*TNFSF10*	tumor necrosis factor ligand superfamily member 10-like	1.24	-1.06	-0.36	0.04	0.14	0.0001	1
*16724	8743	*TNFSF10*	tumor necrosis factor (ligand) superfamily, member 10	1.28	-0.32	-0.52	-0.32	-0.12	0.0000	1
NM_001129946	6352	*CCL5*	chemokine (C-C motif) ligand 5	0.96	0.61	-0.24	-0.49	-0.84	0.0000	2

AK233548	6352	*CCL5*	chemokine (C-C motif) ligand 5	1.08	0.48	-0.22	-0.52	-0.82	0.0002	2
ENSSSCT00000019288	6355	*CCL8*	chemokine (C-C motif) ligand 8	0.78	0.78	0.28	-1.32	-0.52	0.0000	2
NM_001164515	6355	*CCL8*	chemokine (C-C motif) ligand 8	0.60	0.50	0.30	-0.80	-0.60	0.0001	2
DN100836	898	*CCNE1*	cyclin E1	0.58	1.08	-0.52	-0.72	-0.42	0.0001	2
AJ945293	729230	*CCR2*	chemokine (C-C motif) receptor 2	1.02	0.52	-0.38	-0.58	-0.58	0.0000	2
ES445357	1233	*CCR4*	chemokine (C-C motif) receptor 4	1.60	0.60	-0.40	-0.80	-1.00	0.0000	2
NM_001001532	1236	*CCR7*	chemokine (C-C motif) receptor 7	1.22	-0.28	0.32	-0.48	-0.78	0.0000	2
ENSSSCT00000006580	7373	*COL14A1*	collagen,type XIV,alpha 1	0.30	0.10	0.28	0.27	-0.94	0.0005	2
XM_001925576	1306	*COL15A1*	collagen; type XV; alpha 1	1.15	0.31	0.27	-0.71	-1.03	0.0000	2
ENSSSCT00000005921	1306	*COL15A1*	collagen,type XV,alpha 1	1.15	0.08	0.31	-0.52	-1.02	0.0001	2
TC456033	1287	*COL4A5*	collagen,type IV,alpha 5	0.80	-0.50	0.40	-0.30	-0.40	0.0000	2
ENSSSCT00000013747	1287	*COL4A5*	collagen,type IV,alpha 5	0.98	-0.32	0.18	-0.12	-0.72	0.0000	2
ENSSSCT00000013746	1288	*COL4A6*	collagen alpha-6(IV) chain-like	1.06	-0.04	-0.14	-0.24	-0.64	0.0000	2
NM_001105289	1290	*COL5A2*	collagen,type V,alpha 2	1.19	-0.01	-0.01	-0.46	-0.71	0.0000	2
BG383121	1290	*COL5A2*	collagen, type V, alpha 2	1.08	-0.12	0.08	-0.42	-0.62	0.0000	2
AY368623	1290	*COL5A2*	collagen, type V, alpha 2	0.96	0.06	-0.14	-0.24	-0.64	0.0000	2
XM_001928087	1293	*COL6A3*	collagen,type VI,alpha 3	1.27	-0.25	-0.32	0.04	-0.74	0.0001	2
ENSSSCT00000017779	1293	*COL6A3*	collagen,type VI,alpha 3	0.96	-0.14	0.06	-0.04	-0.84	0.0002	2
ENSSSCT00000017780	1293	*COL6A3*	collagen,type VI,alpha 3	1.20	0.00	-0.20	0.10	-1.10	0.0005	2
TC483186	1294	*COL7A1*	collagen, type VII, alpha 1	1.20	0.10	0.20	-0.90	-0.60	0.0000	2
ENSSSCT00000012432	1294	*COL7A1*	similar to alpha 1 type VII collagen	1.19	0.09	0.25	-1.01	-0.51	0.0000	2
NM_001008691	3627	*CXCL10*	chemokine (C-X-C motif) ligand 10	1.69	0.19	-0.56	-0.21	-1.11	0.0000	2
NM_001128491	6373	*CXCL11*	chemokine (C-X-C motif) ligand 11	3.06	0.56	-0.74	-1.04	-1.84	0.0000	2
ENSSSCT00000015634	9547	*CXCL14*	chemokine (C-X-C motif) ligand 14	0.90	1.50	-0.50	-1.20	-0.70	0.0007	2
NM_001114289	4283	*CXCL9*	chemokine (C-X-C motif) ligand 9	1.96	0.36	-0.54	-0.64	-1.14	0.0000	2
NM_001001623	10663	*CXCR6*	chemokine (C-X-C motif) receptor 6	1.54	0.54	-0.36	-1.06	-0.66	0.0000	2
NM_001098582	1908	*EDN3*	endothelin 3	0.64	-0.26	1.04	-0.36	-1.06	0.0001	2
XM_001928678	2260	*FGFR1*	fibroblast growth factor receptor 1	1.22	0.42	-0.28	-0.68	-0.68	0.0000	2
TC439806	2260	*FGFR1*	fibroblast growth factor receptor 1	1.18	0.48	-0.32	-0.72	-0.62	0.0000	2
ENSSSCT00000017223	2260	*FGFR1*	fibroblast growth factor receptor 1	0.81	0.46	0.01	-0.39	-0.89	0.0002	2
CF359055	50615	*IL21R*	interleukin-21 receptor-like	1.10	0.40	0.50	-1.60	-0.40	0.0001	2

XM_001929445	4320	*MMP11*	matrix metallopeptidase 11 (stromelysin 3)	0.44	-0.06	0.14	0.04	-0.56	0.0007	2
ENSSSCT00000011032	4320	*MMP11*	matrix metallopeptidase 11 (stromelysin 3)	0.72	0.12	-0.28	-0.28	-0.28	0.0002	2
BI338397	4326	*MMP17*	matrix metallopeptidase 17 (membrane-inserted)	1.00	-0.20	0.30	-0.40	-0.70	0.0003	2
TC504067	64386	*MMP25*	matrix metalloproteinase-25-like	1.18	0.38	0.08	-1.02	-0.62	0.0000	2
CF792385	5241	*PGR*	progesterone receptor	1.16	1.16	-0.44	-0.14	-1.74	0.0001	2
NM_001166488	5241	*PGR*	progesterone receptor	1.60	1.00	-0.50	-1.10	-1.00	0.0000	2
TC492417	5241	*PGR*	progesterone receptor	1.28	1.18	-0.52	-0.92	-1.02	0.0000	2
DB792958	5734	*PTGER4*	prostaglandin E2 receptor EP4 subtype-like	0.48	0.48	0.18	-0.62	-0.52	0.0003	2
NM_213900	5973	*RENBP*	renin binding protein	0.74	-0.36	0.44	-0.06	-0.76	0.0000	2
EU681268	6366	*CCL21*	chemokine (C-C motif) ligand 21	0.00	1.70	0.70	-0.70	-1.70	0.0004	3
*12017	414062	*CCL3L3*	chemokine (C-C motif) ligand 3-like 1	0.18	0.58	-0.32	-0.02	-0.42	0.0008	3
XM_001924034	2826	*CCR10*	chemokine (C-C motif) receptor 10	0.28	0.78	0.28	-0.42	-0.92	0.0000	3
ENSSSCT00000006725	1019	*CDK4*	cyclin-dependent kinase 4	0.26	0.76	-0.24	-0.34	-0.44	0.0002	3
ENSSSCT00000004588	2254	*FGF9*	fibroblast growth factor 9 (glia-activating factor)	0.26	0.76	0.26	-1.44	0.16	0.0004	3
TC498977	6626	*SNRPA*	small nuclear ribonucleoprotein polypeptide A	-0.08	1.32	-0.08	-0.38	-0.78	0.0000	3
AK236306	7064	*THOP1*	thimet oligopeptidase 1	0.13	0.93	-0.07	-0.57	-0.42	0.0000	3
NM_001033015	1636	*ACE*	angiotensin I converting enzyme (peptidyl-dipeptidase A) 1	-0.78	0.52	0.82	0.52	-1.08	0.0001	4
BW967338	6356	*CCL11*	CCL11	-0.66	1.04	0.74	0.14	-1.26	0.0000	4
DB794536	6361	*CCL17*	chemokine (C-C motif) ligand 17	-0.60	0.60	0.60	0.40	-1.00	0.0000	4
NM_001003922	10850	*CCL27*	chemokine (C-C motif) ligand 27	-0.26	0.24	0.54	0.14	-0.66	0.0001	4
NM_001024695	56477	*CCL28*	chemokine (C-C motif) ligand 28	-0.94	1.86	2.76	-0.14	-3.54	0.0000	4
NM_001001619	729230	*CCR2*	chemokine (C-C motif) receptor 2	0.30	0.50	0.20	0.00	-1.00	0.0001	4
NM_001001624	10803	*CCR9*	chemokine (C-C motif) receptor 9	-0.52	0.58	0.78	0.58	-1.42	0.0000	4
AK238923	7852	*CXCR4*	chemokine (C-X-C motif) receptor 4	0.04	-0.06	0.84	-0.26	-0.56	0.0009	4
TC499070	400935	*IL17REL*	putative interleukin-17 receptor E-like	-1.58	-0.28	2.72	0.42	-1.28	0.0001	4
NM_214399	3569	*IL6*	interleukin 6 (interferon,beta 2)	-0.92	2.28	-0.02	-1.12	-0.22	0.0010	4
CF359271	5179	*PENK*	proenkephalin	-1.72	0.58	0.68	2.48	-2.02	0.0004	4
NM_213882	1906	*EDN1*	endothelin 1	-0.22	-0.92	1.28	-0.62	0.48	0.0003	5
ENSSSCT00000000163	7078	*TIMP3*	tissue inhibitor of metalloproteinase-3	-0.68	-0.78	0.12	1.22	0.12	0.0005	6
CF367219	185	*AGTR1*	type-1 angiotensin II receptor-like	-0.22	-0.52	-0.62	0.08	1.28	0.0002	7
NM_214020	1950	*EGF*	epidermal growth factor	-0.98	-1.15	-0.95	3.25	-0.18	0.0000	7

TC414631	2066	*ERBB4*	receptor tyrosine-protein kinase erbB-4-like	-0.22	-0.92	-0.92	0.78	1.28	0.0001	7
EH009240	2252	*FGF7*	fibroblast growth factor 7	-1.36	-3.36	-2.66	3.04	4.34	0.0000	7
ENSSSCT00000005134	2252	*FGF7*	fibroblast growth factor 7;keratinocyte growth factor-like	-1.44	-3.24	-2.34	2.96	4.06	0.0000	7
NM_001099924	2263	*FGFR2*	fibroblast growth factor receptor 2	-0.98	-1.45	-0.45	2.02	0.85	0.0000	7
BX924155	2261	*FGFR3*	fibroblast growth factor receptor 3-like	0.18	-0.52	-1.62	1.78	0.18	0.0001	7
NM_214027	5021	*OXTR*	oxytocin receptor	-0.64	-1.94	-2.54	0.86	4.26	0.0000	7
TC415136	5021	*OXTR*	oxytocin receptor	0.04	-0.86	-0.56	1.14	0.24	0.0007	7
TC444315	5321	*PLA2G4A*	cytosolic phospholipase A2-like	-0.16	-0.16	-0.76	0.44	0.64	0.0006	7
TC429092	5321	*PLA2G4A*	cytosolic phospholipase A2-like	-0.22	-0.72	-1.12	0.98	1.08	0.0000	7
ENSSSCT00000005548	5732	*PTGER2*	prostaglandin E receptor 2 subtype EP2	-0.98	-1.18	-0.28	0.02	2.42	0.0002	7
XM_001928689	5732	*PTGER2*	prostaglandin E receptor 2 subtype EP2	-1.56	-1.11	-1.11	0.49	3.29	0.0000	7
FJ750950	5737	*PTGFR*	prostaglandin F receptor (FP)	-0.10	-1.40	-0.80	1.45	0.85	0.0000	7
TC469578	5737	*PTGFR*	prostaglandin F receptor (FP)	-0.24	-1.04	-0.24	0.26	1.26	0.0003	7
NM_214059	5737	*PTGFR*	prostaglandin F receptor (FP)	-0.10	-1.40	-0.10	1.20	0.40	0.0003	7
DY437619	5743	*PTGS2*	prostaglandin-endoperoxide synthase 2 (prostaglandin G/H synthase and cyclooxygenase)	-0.28	-1.38	-2.18	1.12	2.72	0.0000	7
NM_214321	5743	*PTGS2*	prostaglandin-endoperoxide synthase 2 (prostaglandin G/H synthase and cyclooxygenase)	-0.88	-1.73	-3.28	2.07	3.82	0.0000	7
NM_001145985	7077	*TIMP2*	TIMP metallopeptidase inhibitor 2	-1.22	-1.92	-2.12	1.68	3.58	0.0000	7
TC450358	7077	*TIMP2*	TIMP metallopeptidase inhibitor 2	-1.10	-1.80	-1.90	1.80	3.00	0.0000	7
XM_001924659	183	*AGT*	angiotensinogen-like	0.31	-0.97	-2.34	-0.67	3.66	0.0000	8
ENSSSCT00000011150	183	*AGT*	angiotensinogen-like	-0.22	-0.32	-1.62	-0.02	2.18	0.0002	8
ENSSSCT00000012803	185	*AGTR1*	type-1 angiotensin II receptor-like	-0.08	-0.48	-0.58	0.02	1.12	0.0002	8
ENSSSCT00000000733	715	*C1R*	complement component 1,r subcomponent	0.60	-0.30	-1.00	-0.50	1.20	0.0001	8
NM_001005349	716	*C1S*	complement component 1,s subcomponent	0.66	-0.34	-1.09	-0.54	1.31	0.0002	8
ENSSSCT00000000735	716	*C1S*	complement component 1,s subcomponent	0.92	-0.58	-1.28	-0.78	1.72	0.0000	8
TC413063	716	*C1S*	complement component 1,s subcomponent	1.06	-0.44	-1.34	-0.74	1.46	0.0000	8
NM_001097449	729	*C6*	complement component 6;complement component C6-like	1.32	-1.78	-0.58	0.82	0.22	0.0000	8
NM_213971	1191	*CLU*	clusterin	1.94	-1.46	-2.06	-0.16	1.74	0.0000	8
ENSSSCT00000008134	5476	*CTSA*	cathepsin A	0.50	-0.70	-0.60	-0.10	0.90	0.0000	8
XM_001927652	2065	*ERBB3*	erb-b2 receptor tyrosine kinase 3	-0.18	-1.08	-0.88	0.02	2.12	0.0000	8
NM_213839	355	*FAS*	Fas (TNF receptor superfamily,member 6)	0.56	-0.74	-0.14	-0.14	0.46	0.0001	8

NM_001105291	4012	*LNPEP*	leucyl/cystinyl aminopeptidase	0.56	-0.64	-0.44	-0.34	0.86	0.0001	8
CF790427	4012	*LNPEP*	leucyl/cystinyl aminopeptidase	0.52	-1.08	-0.38	0.02	0.92	0.0000	8
ENSSSCT00000007146	4582	*MUC1*	mucin 1,cell surface associated	1.31	-1.84	-1.49	1.21	0.81	0.0000	8
NM_214295	4846	*NOS3*	nitric oxide synthase 3 (endothelial cell)	0.44	-0.56	-0.66	-0.46	1.24	0.0000	8
TC475132	4846	*NOS3*	nitric oxide synthase 1 (neuronal)	1.48	-2.42	-7.32	3.68	4.58	0.0000	8
BG610210	4846	*NOS3*	nitric oxide synthase 1 (neuronal)	0.30	-2.70	-4.10	3.00	3.50	0.0000	8
TC410747	8828	*NRP2*	neuropilin-2-like	0.98	-0.82	-1.12	0.58	0.38	0.0000	8
NM_001123194	710	*SERPING1*	serpin peptidase inhibitor,clade G (C1 inhibitor),member 1	0.37	-0.26	-0.86	-0.49	1.24	0.0004	8
TC407865	710	*SERPING1*	serpin peptidase inhibitor, clade G (C1 inhibitor), member 1	0.58	-0.52	-1.02	-0.52	1.48	0.0001	8
AJ961798	6578	*SLCO2A1*	solute carrier organic anion transporter family, member 2A1	-0.04	-0.24	-1.14	0.26	1.16	0.0000	8
ENSSSCT00000005647	7010	*TEK*	TEK tyrosine kinase,endothelial	0.12	-0.71	-0.45	0.19	0.85	0.0000	8
DY424396	7010	*TEK*	TEK tyrosine kinase, endothelial	0.10	-1.20	-0.40	0.30	1.20	0.0000	8

Table VIII-III: List of differentially expressed genes in the porcine endometrium (only genes that are discussed in this study are shown). List provides; Target Accession Number from Agilent mircoarray software, Hsa Entrez Gene ID, Hsa Gene symbol, Hsa Gene description; relative gene expression levels (normalized value of one time point minus mean of normalized values of all 5 time points (D0, D3, D6, D12, D18); q-value, SOTA cluster (Self-organizing tree algorithm of MeV software (version 4.8.1) was used to obtain groups of genes with similar expression profiles. D-day, Ssc-*Sus scorfa*, Hsa-*Homo sapiens,* ID-identifier.

Hsa Entrez Gene ID[1]	**Hsa Gene symbol[2]**	***Sus scrofa***						***Equus caballus***						**positive correlation r[4]**	**p-value[5]**
		D0	**D3**	**D6**	**D12**	**D18**	**SOTA cluster[3]**	**D0**	**D3**	**D8**	**D12**	**D16**	**SOTA cluster[3]**		
8038	*ADAM12*	0.68	-0.72	-0.12	-0.12	0.28	1	1.16	-0.10	-0.61	-0.86	0.41	1	0.68	0.030
1278	*COL1A2*	1.40	-0.70	-0.50	-0.40	0.20	1	1.10	-0.48	0.17	-0.98	0.19	1	0.83	0.003
1281	*COL3A1*	1.08	-1.02	-0.12	-0.22	0.28	1	1.03	-0.29	0.26	-1.26	0.26	1	0.67	0.036
1282	*COL4A1*	0.98	-0.72	-0.12	-0.82	0.68	1	0.51	-0.43	-0.15	-0.44	0.50	1	0.99	0.000
1289	*COL5A1*	1.43	-0.54	-0.54	-0.21	-0.14	1	0.77	-0.38	0.03	-0.62	0.21	1	0.78	0.008
6372	*CXCL6*	5.24	-0.46	-1.56	-1.86	-1.36	1	2.84	-0.61	-1.88	-2.33	1.99	1	0.72	0.020
3206	*HOXA10*	0.94	-0.36	-0.06	-0.36	-0.16	1	0.75	-0.17	-0.33	-0.58	0.33	1	0.81	0.004
171019	*ADAMTS19*	2.02	-0.58	0.12	-0.88	-0.68	1	1.23	0.00	-0.57	-0.77	0.12	2	0.81	0.005
1287	*COL4A5*	0.80	-0.50	0.40	-0.30	-0.40	2	0.97	-0.10	-0.32	-0.56	0.01	1	0.65	0.043
1288	*COL4A6*	1.06	-0.04	-0.14	-0.24	-0.64	2	0.82	-0.17	-0.15	-0.32	-0.18	1	0.93	0.000
1294	*COL7A1*	1.20	0.10	0.20	-0.90	-0.60	2	0.82	-0.13	-0.39	-0.24	-0.06	1	0.74	0.015
4283	*CXCL9*	1.96	0.36	-0.54	-0.64	-1.14	2	0.93	-0.31	-0.05	-0.40	-0.17	1	0.83	0.003
367	*AR*	0.64	-0.03	0.07	-0.26	-0.43	2	0.51	0.00	-0.02	-0.56	0.07	2	0.71	0.021

5241	*PGR*	1.16	1.16	-0.44	-0.14	-1.74	2	0.62	0.39	-0.04	-0.74	-0.24	2	0.65	0.040
6132	*RPL8*	0.46	0.46	0.06	-0.64	-0.34	2	0.45	0.26	-0.12	-0.30	-0.29	2	0.92	0.000
4172	*MCM3*	1.54	1.94	-0.96	-1.06	-1.46	2	0.17	1.01	-0.52	-0.46	-0.21	3	0.87	0.001
6147	*RPL23A*	0.21	0.31	0.46	-0.54	-0.44	3	0.54	0.03	0.03	-0.17	-0.43	1	0.64	0.048
4175	*MCM6*	0.46	1.06	0.16	-0.64	-1.04	3	0.49	1.50	-1.03	-0.74	-0.21	2	0.68	0.030
6141	*RPL18*	0.25	0.49	0.52	-0.65	-0.61	3	0.45	0.34	0.03	-0.37	-0.45	2	0.85	0.002
6146	*RPL22*	0.11	0.65	0.45	-0.52	-0.69	3	0.41	0.30	-0.03	-0.41	-0.27	2	0.76	0.012
6159	*RPL29*	0.22	0.59	0.45	-0.58	-0.68	3	0.54	0.40	-0.01	-0.45	-0.48	2	0.84	0.002
6166	*RPL36AL*	0.06	0.76	0.36	-0.44	-0.74	3	0.63	0.11	0.14	-0.44	-0.45	2	0.64	0.047
6181	*RPLP2*	0.32	0.42	0.22	-0.68	-0.28	3	0.48	0.09	0.07	-0.38	-0.26	2	0.85	0.002
6204	*RPS10*	0.23	0.73	0.59	-0.65	-0.89	3	0.58	0.05	0.02	-0.27	-0.39	2	0.64	0.045
6209	*RPS15*	0.04	0.64	0.64	-0.56	-0.76	3	0.36	0.45	0.02	-0.31	-0.52	2	0.81	0.005
3921	*RPSA*	0.44	0.84	0.14	-0.96	-0.46	3	0.55	0.47	-0.28	-0.54	-0.20	2	0.87	0.001
388524	*RPSAP58*	0.31	0.82	0.26	-0.76	-0.63	3	0.52	0.62	-0.40	-0.56	-0.17	2	0.76	0.011
891	*CCNB1*	1.52	3.02	-0.08	-1.98	-2.48	3	0.39	2.20	-0.54	-1.52	-0.52	3	0.89	0.001
9133	*CCNB2*	1.30	2.50	-0.20	-1.40	-2.20	3	0.47	2.65	-0.38	-1.83	-0.91	3	0.91	0.000
595	*CCND1*	0.18	1.08	-0.22	-0.72	-0.32	3	0.05	0.93	-0.45	-0.52	0.00	3	0.94	0.000
991	*CDC20*	1.44	3.14	0.14	-1.36	-3.36	3	0.47	2.58	-0.50	-1.28	-1.26	3	0.91	0.000
8318	*CDC45*	0.15	1.20	-0.70	-0.40	-0.25	3	0.17	2.72	-1.03	-1.56	-0.31	3	0.96	0.000
990	*CDC6*	0.40	1.40	-0.40	-0.50	-0.90	3	-0.51	2.11	-0.44	-0.93	-0.25	3	0.82	0.004
83461	*CDCA3*	1.58	2.78	-0.12	-1.72	-2.52	3	0.42	2.59	-0.46	-1.72	-0.84	3	0.90	0.000
983	*CDK1*	1.39	2.89	-0.21	-1.41	-2.66	3	0.41	2.64	-0.48	-2.03	-0.54	3	0.83	0.003
1019	*CDK4*	0.26	0.76	-0.24	-0.34	-0.44	3	-0.10	0.69	0.03	-0.38	-0.23	3	0.87	0.001
1062	*CENPE*	-0.58	1.52	0.37	0.02	-1.33	3	0.23	1.72	-0.34	-1.12	-0.49	3	0.65	0.042
1063	*CENPF*	0.34	1.34	0.54	-1.26	-0.96	3	-0.05	2.39	-0.24	-1.49	-0.60	3	0.88	0.001
91687	*CENPL*	0.56	1.26	-0.44	-0.54	-0.84	3	0.20	1.58	-0.73	-0.65	-0.41	3	0.93	0.000
79019	*CENPM*	0.24	1.24	-0.46	0.04	-1.06	3	0.11	1.64	-0.63	-0.83	-0.29	3	0.78	0.008
55839	*CENPN*	0.90	2.70	-0.50	-0.90	-2.20	3	0.19	1.74	-0.38	-1.05	-0.51	3	0.89	0.001
4173	*MCM4*	1.02	2.22	-0.88	-1.08	-1.28	3	0.23	1.32	-0.68	-0.69	-0.19	3	0.92	0.000
795	*S100G*	0.70	2.55	-0.25	-0.35	-2.65	3	-0.04	1.26	0.65	-0.88	-0.99	3	0.81	0.004
6626	*SNRPA*	-0.08	1.32	-0.08	-0.38	-0.78	3	-0.12	1.11	-0.30	-0.62	-0.06	3	0.86	0.002
55388	*MCM10*	-0.14	0.86	0.16	-0.14	-0.74	4	-0.09	1.53	-0.50	-0.89	-0.05	3	0.66	0.039

2194	*FASN*	-0.25	1.00	0.90	-0.85	-0.80	4	-0.98	1.10	0.64	-0.34	-0.43	4	0.84	0.003
10857	*PGRMC1*	-1.36	-0.43	0.87	0.61	0.31	5	-0.63	0.16	0.82	0.05	-0.41	5	0.70	0.025
5743	*PTGS2*	-0.9	-1.7	-3.3	2.1	3.8	7	-0.15	-0.74	-0.57	0.26	1.19	7	0.94	0.000
55503	*TRPV6*	-1.42	-1.42	-0.02	-0.22	3.08	7	-2.02	-0.98	0.66	1.27	1.07	7	0.69	0.028
7422	*VEGFA*	-0.03	-0.83	-0.73	0.52	1.07	7	-0.65	-0.35	-0.06	0.26	0.80	7	0.74	0.014
715	*C1R*	0.60	-0.30	-1.00	-0.50	1.20	8	0.05	-0.52	-0.38	0.32	0.53	8	0.66	0.037
687	*KLF9*	0.49	-0.73	-0.72	-0.02	0.98	8	0.13	-0.31	-0.40	0.12	0.46	8	0.97	0.000
710	*SERPING1*	0.37	-0.26	-0.86	-0.49	1.24	8	0.24	-0.46	-0.82	0.39	0.65	8	0.75	0.012
5733	*PTGER3*	-0.26	0.24	0.64	-0.06	-0.56	4	0.98	-0.27	-1.12	-0.22	0.63	1	-0.90	0.000
718	*C3*	-1.02	0.58	1.18	0.48	-1.22	4	1.01	-0.46	-1.46	-0.05	0.95	8	-0.96	0.000
5737	*PTGFR*	-0.10	-1.40	-0.80	1.45	0.85	7	-0.03	0.70	0.39	-0.20	-0.85	4	-0.83	0.003

Table VIII-IV: List of differentially expressed genes in equine and porcine endometrium (ony genes that are discussed int his study). Calculation of correlation coefficience (correl r), t-value and p-value of positive and negative correlated genes is demontrated in list.

Hsa Entrez Gene ID	**Hsa Gene symbol**	***Sus scrofa***						***Equus caballus***						***Bos taurus***				
		D0	**D3**	**D6**	**D12**	**D18**	**SOTA-Cluster**	**D0**	**D3**	**D8**	**D12**	**D16**	**SOTA cluster**	**D18P4L**	**D0**	**D3.5**	**D12**	**D18P4H**
715	*C1R*	0,60	-0,30	-1,00	-0,50	1,20	2	0,05	-0,52	-0,38	0,32	0,53	1	-0,21	-0,75	0,15	0,22	0,59
1278	*COL1A2*	1,40	-0,70	-0,50	-0,40	0,20	2	1,10	-0,48	0,17	-0,98	0,19	1	0,11	0,7	0,23	-0,38	-0,66
1281	*COL3A1*	1,08	-1,02	-0,12	-0,22	0,28	3	1,03	-0,29	0,26	-1,26	0,26	1	0,26	0,68	-0,01	-0,27	-0,66
1282	*COL4A1*	0,98	-0,72	-0,12	-0,82	0,68	3	0,51	-0,43	-0,15	-0,44	0,50	3	0,45	0,33	-0,17	-0,21	-0,41
2099	*ESR1*	0,94	0,27	-0,56	-0,26	-0,39	4	0,18	0,69	-0,22	-0,93	0,28	7	0,14	-0,04	0,69	-0,48	-0,31
10769	*PLK2*	0,86	-1,64	-1,14	0,46	1,46	1	-0,02	0,03	-0,59	-0,05	0,63	3	0,61	0,71	0,26	-0,95	-0,63
710	*SERPING1*	0,37	-0,26	-0,86	-0,49	1,24	3	0,24	-0,46	-0,82	0,39	0,65	3	-0,27	-0,77	-0,28	0,78	0,54

Table VIII-V: List of differentially expressed genes in all three species (only genes are shown that are discussed in this study . Comparison of significant positive and negative correlated genes from equine and porcine endometrium were compared to the list of differentially expressed genes in bovine estrous cycle (Mitko, 2008).P4L-low levels of progesterone, P4H-higher level of progesterone.

IX. ACKNOWLEDGEMENTS

In the following lines the people that have been supporting and encouraging the successful completion of this research work are gratefully acknowledged. However, I am aware of the fact that there are many more and these words cannot express the gratitude and respect I feel for all of those.

At first, I like to take this opportunity to thank the people who provided scientific support to make this work possible. Thank you to Priv.-Doz. Dr. Stefan Bauersachs who not only offered me a welcome in his research group and was very helpful in providing information and assisting during the process of this study but also helped sponsoring this study and introduced me to Prof. Dr. Eckhard Wolf.

I must thank Dr. Helmut Blum and Prof. Dr. Eckhard Wolf who gave me the unique opportunity to use the excellent research facilities in their lab.

Thanks you to Prof. Dr. Rolf Mansfeld, Prof. Dr. Heidrun Potschka and Prof. Dr. Christina Hölzel, for examining this scientific study.

My sincere thanks go to all group members of LAFUGA Genomics for scientific discussion, advice and continuous appreciated support, among them Karin Gross who introduced me to the secrets of Microarray-Analysis, Andrea Klannert for her ‚Sanger-sequencing performance' and Paul Setzermann for the help in bioinformatics analysis. In the context of sample collection, I further like to express greatest thanks to the staff members of the Bavarian principal and state stud of Schwaiganger for providing and housing the mares and Dr. Maximilliane Merkl for taking the equine biopsy samples used in this study. Thanks to Dr. Barbara Kessler and Christian Erdle for taking care of purchasing, housing and treatment of the sows/gilts and the staff members of the abbatoir in Grub. In addition, thanks to Dr. Herbach and Dr. Kempter for their support within quantitative stereology.

I would like to acknowledge the help and valuable ideas and suggestions from Dr. Dorothee Lange. Special thanks are addressed to Elisabeth Aberl for technical support and to Sylvia Hornig.

In addition, my special thanks go to following institutions for financial support and funding: BMBF/compemdium, ReproZentrum, LAFUGA, and the Ludwig-Maximillians Universität (LMU).

Last but by no means least, I like to thank Marga Gebhardt and Elisabeth Mieke